Geophysical Monitoring for Climatic Change

No. 8

Summary Report 1979

U.S. DEPARTMENT OF COMMERCE

NATIONAL OCEANIC AND ATMOSPHERIC ADMINISTRATION

ENVIRONMENTAL RESEARCH LABORATORIES

Bob Grau

Geophysical Monitoring for Climatic Change No. 8

Summary Report 1979

Gary A. Herbert, Editor

December 1980

Boulder, Colorado

U.S. DEPARTMENT OF COMMERCE
Philip M. Klutznick, Secretary

National Oceanic and Atmospheric Administration
Richard A. Frank, Administrator

Environmental Research Laboratories
Joseph O. Fletcher, Acting Director

NOTICE

Mention of a commercial company or product does not constitute an endorsement by NOAA Environmental Research Laboratories. Use for publicity or advertising purposes of information from this publication concerning proprietary products or the tests of such products is not authorized.

CONTENTS

ACRONYMS AND ABBREVIATIONS

AFGL	Air Force Geophysical Laboratory, Hanscom Air Force Base, Mass.
APCL	Atmospheric Physics and Chemistry Laboratory, Boulder, Colo. (NOAA)
ARL	Air Resources Laboratories, Washington, D.C. (NOAA)
BRW	Barrow Observatory, Barrow, Alaska (GMCC)
CAF	Clean Air Facility, South Pole Observatory, Antarctica (GMCC)
CSRIO	Commonwealth Scientific and Industrial Research Organization, Australia
DOE	U.S. Department of Energy
EDIS	Environmental Data and Information Service, Washington, D.C. (NOAA)
EML	Environmental Measurements Laboratory, U.S. Department of Energy, New York, N.Y.
EPA	Environmental Protection Agency
G.E.	General Electric
ICDAS	instrument controlled data acquisition system
LBL	Lawrence Berkeley Laboratory
LST	Local standard time
MLO	Mauna Loa Observatory, Mauna Loa, Hawaii (GMCC)
MPI	Max Planck Institute, Mainz, Germany
NARL	Naval Arctic Research Laboratory, Barrow, Alaska
NIP	normal incidence pyrheliometer
NOAA	National Oceanic and Atmospheric Administration, U.S. Dept. of Commerce
NRC	National Research Council
NSF	National Science Foundation, Washington, D.C.
NWS	National Weather Service, Washington, D.C. (NOAA)
OGC	Oregon Graduate Center, Beaverton, Ore.
SIO	Scripps Institution of Oceanography, La Jolla, Calif.
SMO	Samoa Observatory, American Samoa (GMCC)
SPO	South Pole Observatory, Antarctica (GMCC)
SRL	Smithsonian Institution Radiation Biology Laboratory
SUNYA	State University of New York at Albany
URI	University of Rhode Island, Kingston, R.I.
WMO	World Meteorological Organization, Geneva, Switzerland

FOREWORD

The invention of instruments and measurement techniques to document the courses of meteorological elements was not an accomplishment sufficient unto itself. It was recognized long ago that although the diurnal and seasonal cycles of many elements are reasonably predictable in a general sense, in detail and precise magnitude they are highly variable and sensitive to local environmental circumstances--circumstances that could compromise the detection of significantly representative long term trends. To minimize or stabilize local influences, an observatory system was established similar to the Kew Observatory in England in the 18th century and the Abbe Observatory in Ohio and the Mt. Weather Observatory in Virginia. The sites were selected in rural or park-land settings, relatively free from drastic local environmental deterioration. However, the intensive urbanization in the decades about the turn of this century and the shifting of many observing sites, for economic reasons, to more urbanized locations near governmental office buildings downgraded the environments surrounding sites. Many observatory sites were shifted to airports in the 1930's to accommodate the expanding aviation industry and to provide information for day-to-day forecasting, but such sites had minimal utility for meteorological research.

In the late 1950's monitoring programs, inspired by the activities connected with the International Geophysical Year, intensified attention on atmospheric composition (e.g., CO_2 and O_3). At about this time, the late Dr. Harry Wexler and others began to significantly upgrade the Mauna Loa program. But until well into the 1960's little concern was directed toward long term climatic changes or trends except on geological time periods or by temporary and spatially limited aberrations caused by natural phenomena such as volcanic eruptions. Then three developments pointed out that not only was an important climatic change perhaps in progress, but also that human activities could be contributing factors:

(1) Data were published indicating a world-wide downward trend in surface air temperature, at least in the Northern Hemisphere. This trend in the late 1930's followed an upward trend that had been persisting from before the turn of the century.

(2) The atmospheric CO_2 levels on Mauna Loa showed a definite upward annual trend.

(3) Turbidity data indicated that the aerosol loading of the atmosphere might be on the upswing and playing an important role in the energy balance of the earth-atmosphere system.

Although questions about the sign and magnitude of factors (1) and (3) were hotly debated, the discussions directed attention to the need for reliable long term data on human impact on climate and atmospheric composition, and the magnitude of climatic change.

Concern in the United States crystallized in 1970 with the Study of Man's Impact on the Global Environment and an assessment and recommendations for action. An Expert Task Group, formed by the World Meteorological Organization, proposed guidelines and criteria for establishing a baseline global atmospheric monitoring network by national weather services. These recommendations were echoed in 1972 and 1973 by a task group of the International Council of Scientific Unions.

This Summary Report 1979 describes the Geophysical Monitoring for Climatic Change (GMCC) program, which has operated for eight years. The siting of the four observatories, the scientific data, and resulting studies meet the fundamental objectives of global atmospheric monitoring to the greatest extent that geographic circumstances and human ingenuity can achieve. Particular credit must be given to D. H. Pack, whose tireless dedication and creative inspiration were so instrumental in the successful genesis of GMCC. Tribute should also be given to the on-site scientific staffs who work in extreme conditions mostly in barren settings devoid of any aura of romanticism which their exotic place-names imply.

Robert A. McCormick
Former Director of the Meteorology Laboratory
Air Resources Laboratories, NOAA

GEOPHYSICAL MONITORING FOR CLIMATIC CHANGE

NO. 8

Summary Report 1979

1. SUMMARY

The most significant change in the GMCC operational program in 1979 was the initiation of 10 additional CO_2 flask sampling stations. Flask sampling was previously conducted at 3 maritime locations in addition to the 4 GMCC baseline stations. Most of the 10 new stations are located at coastal sites in the tropics and polar zones. The flask analysis calibration procedure was converted from Co_2-in-N_2 to CO_2-in-air as of January 1979.

Continuous measurement of CO_2 and aerosol scattering at four wavelengths, using a nephelometer, was begun at the South Pole station at the end of 1978 and continued throughout 1979. Other measurement programs operated without serious interruption throughout the year.

Only minor changes and improvements were made to the stations. The main concern involved the future of the Barrow station because of the pending shutdown of the Naval Arctic Research Laboratory. The staff began locating alternate power, repair facilities, and housing. At the Mauna Loa Observatory the main concern was the temperature oscillations induced by air conditioner cycling. A 5-yr lease agreement was negotiated with the local chief in Samoa.

A filter collection system was installed at the Barrow station to make possible the determination of the mass of the carbonaceous aerosols. The analysis is performed by H. Rosen of the University of California. Early results show that graphitic carbon makes up a significant part of the arctic haze, and because of its optical absorptivity, it may cause a significant contribution to the radiative energy budget.

At MLO a new cooperative measurement program to observe the chemical composition of aerosols was initiated. By considering the times when the flow is free of local contamination, changes in sources can be evaluated. The filter will be analyzed by W. H. Zoller of the University of Maryland.

2. OBSERVATORY REPORTS

2.1 Mauna Loa

2.1.1 Facilities

The following modifications to the Mauna Loa facilities were effected in 1979:

(1) Ultraviolet pyranometer no. 10232 was replaced by no. 12350 on 31 January.

(2) Pyrheliometer filter wheel no. 13911 was replaced by no. 13910 on 26 January.

(3) Equipment for a cooperative program with W. Zoller, University of Maryland, was installed 12 February.

(4) Pyranometer no. 12560 was replaced by no. 12502 on 11 April.

(5) The 5/8-in ruby rod in the lidar was replaced by a 3/8-in rod on 24 April.

(6) A new main frame for the ICDAS computer was installed in early April.

(7) A new dew cell was placed in operation on 25 May.

(8) The nitrogen dioxide analyzer was returned to Boulder in mid-June because the program was suspended in April.

(9) The filter heads and cartridges of the EML directions wind sampling equipment were replaced with modified versions in May.

(10) A special clean bench for changing University of Maryland filters was installed on 22 June.

(11) A millipore deionized water still and an Aerochemetric wet-dry precipitation collector were delivered to MLO in June.

(12) The central air conditioner at the main observatory was modified in July to give more stable temperatures in the building.

(13) The 3-M copier in the Hilo office was replaced by a Xerox 2600 on 1 October.

(14) The polarizing radiometer system, acquired on a 5-yr loan from the University of California, Davis, was delivered to MLO on 19 November.

(15) The gust recorder scale was changed from knots to miles per hour during December.

(16) Room 205 of the Federal Building, Hilo, was assigned to MLO on 17 December.

(17) Special museum display cabinets built for MLO by Hilo Community College were delivered to room 205 on 21 December.

(18) Equipment for a cooperative program with T. Cahill, University of California, Davis, was installed on 29 December.

2.1.2 Programs

Table 1 lists the programs carried out at MLO during 1979. Brief status reports on the principal programs follow.

Carbon Dioxide

The URAS-2 and Applied Physics nondispersive infrared gas analyzers used for monitoring carbon dioxide concentration were operated continuously without major problems during 1979.

Pairs of GMCC glass flasks used for collecting CO_2 air samples were exposed weekly at MLO and Cape Kumukahi, and pairs of 5-ℓ flasks were exposed for SIO on alternate weeks at the same locations. Two methods were used interchangeably for filling flasks at the observatory. The normal method, which used a small, hand operated aspirator, was replaced on alternate weeks by pumping air into the flasks from the air flow system of the URAS-2 analyzer. In the latter method, the measured flask concentration could be corroborated by data taken simultaneously with the analyzer.

Outgassing from the volcanic caldera at the summit of Mauna Loa was recorded occasionally in the CO_2 measurements. Such outgassing occurred mainly between midnight and 8 a.m. local time during a downslope wind flow regime on the mountain. The monthly frequency of occurrence of the outgassing recorded in 1979 was as follows:

	J	F	M	A	M	J	J	A	S	O	N	D
No. of days	5	15	12	9	16	13	10	9	10	11	6	5
Percent of days	16%	43%	39%	30%	52%	43%	32%	29%	33%	35%	20%	16%

The average frequency (32%), the same as for 1978, is somewhat lower than the 42% and 43% that occurred in 1976 and 1977 after the July 1975 eruption of Mauna Loa.

Atmospheric Ozone

Total ozone in the atmospheric column was measured three times a day, on approximately 260 days during 1979. In addition, a special series of total ozone measurements was conducted for 2 months during the summer. Concentration of ozone in air near the surface was monitored continuously with Dasibi and ECC ozone meters.

Atmospheric Aerosols

The aerosol monitoring programs continued with only minor interruptions during the year. The principal parameters of the measurements are volume scattering coefficient of the air and concentration of condensation nuclei in the air.

Table 1.--Summary of monitoring programs at Mauna Loa in 1979

Monitoring Program	Instrument	Sampling frequency	Remarks
Gases			
Carbon dioxide	URAS-2 infrared gas analyzer	Continuous	
Carbon dioxide	Evacuated glass flasks	Weekly	Mountain and seacoast
Surface ozone	Electrochemical concentration cell	Continuous	
Surface ozone	Dasibi ozone meter	Continuous	
Total ozone	Dobson spectrophotometer	Discrete	3 meas. weekdays; 0 weekends
Fluorocarbons	Pressurized flasks	Weekly	
Aerosols			
Stratospheric aerosols	Lidar	Weekly	694.3 nm, 1 J
Condensation nuclei	Pollak CN counter	Discrete	5 meas. weekdays; 0 weekends
Condensation nuclei	G.E. CN counter	Continuous	
Optical properties	4-wavelength nephelometer	Continuous	Wavelengths 450, 550, 700, 850 nm
Solar radiation			
Global irradiance	4 Eppley pyranometers	Continuous	Cutoff filters at 280, 390, 530, 695 nm
Ultraviolet irradiance	Eppley ultraviolet pyranometer	Continuous	Wavelength range 295 to 385 nm
Direct beam irradiance	Eppley pyrheliometer	Continuous	Wavelength range 280 to 3,000 nm
Direct beam irradiance	Eppley pyrheliometer with filters	Discrete	Cutoff filters at 280, 530, 630, 695 nm
Direct beam irradiance	Eppley 13-channel pyrheliometer	Continuous	
Meteorology			
Maximum temperature	Maximum thermometer	Daily	
Minimum temperature	Minimum thermometer	Daily	
Ambient temperature	Thermistor	Continuous	
Ambient temperature	Hygrothermograph	Continuous	At MLO and Kulani Mauka
Dew point temperature	Dew point hygrometer	Continuous	
Relative humidity	Hygrothermograph	Continuous	At MLO and Kulani Mauka
Total precipitable water	Faskett infrared hygrometer	Continuous	
Pressure	Electronic pressure transducer	Continuous	
Pressure	Microbarograph	Continuous	
Precipitation	Rain gage, 8-in	Daily	At MLO
Precipitation	Rain gage, 8-in	2 wk^{-1}	At Kulani Mauka
Precipitation	Rain gage, tipping bucket	Continuous	
Windspeed	Anemometer	Continuous	
Wind direction	Wind vane	Continuous	
Precipitation chemistry			
Acidity of rainwater	pH meter	Discrete	Rainwater collections at 6 sites
Conductivity of water	Conductivity bridge	Discrete	
Chemical components	Ion chromatograph	Discrete	
Cooperative programs			
Carbon dioxide (SIO)	Infrared analyzer (Applied Physics)	Continuous	
	Evacuated flasks	8 mo^{-1}	Mountain and seacoast
Carbon monoxide (MPI)	Special system	Continuous	Chemical reaction with HgO
Surface SO_2 (EPA)	Chemical bubbler system	Every 12 days	
Total surface particulates (DOE)	High volume filter	Continuous	Dependent on wind direction
Total surface particulates (EPA)	High volume filter	Every 12 days	
Atmospheric electricity (APCL/NOAA)	Field mill, air conductivity meter, surface antenna	Continuous	
Stratospheric aerosols (AFGL)	Twilight photometer	Continuous	
Ultraviolet radiation (Temple Univ.)	Ultraviolet radiometer	Continuous	Radiation responsible for sunburning of skin
Precipitation collection (DOE)	Wet-dry Health & Safety Lab collector	Continuous	
Precipitation collection (EPA)	Misco model 93	Continuous	
Precipitation collection (Univ. of Paris)	Likens funnel collector	2 wk^{-1}	
Precipitation collection (IAEA, Vienna, Austria)	Likens funnel collector	2 wk^{-1}	
Atmospheric aerosols (Univ. of Md.)	Nuclepore and quartz filters	Continuous	Day-night discrimination
Atmospheric aerosols (Florida State Univ.)	Special filters	Continuous	
Atmospheric aerosols (Univ. of Calif.)	Nuclepore filters and impactors	Night only	Installed in late December

Lidar Observations

In contrast to most MLO programs, the lidar program was less than successful during 1979. It is thought, however, that any clouds of volcanic ash in the stratosphere could have been detected had they occurred. The Biomation component of the system was returned to the factory for repairs on two occasions, and the power output of the laser was always low and erratic. The operation was so marginal that in September a major refurbishing of the system was deemed necessary for reliable operation. Consequently, a new ruby rod was purchased and the old one repolished, the Pockels cell was checked and repolished, new mirrors were purchased, and a new flash lamp was installed. Because of extensive repairs, the system was not in operation during the last 4 months of the year, but measurements were expected to begin again early in 1980.

Solar Radiation

Solar radiation measurements continued without essential problems throughout 1979. The 13-channel pyrheliometer was in operation all year, but it is without calibration. Efforts to get Eppley Laboratories to refurbish and recalibrate one unit for use at MLO were not successful, so at present only relative flux values are available for the instrument.

Meteorological Parameters

Temperature, pressure, wind, and other meteorological parameters were monitored routinely with few problems. A new dew cell for dew point measurements, installed in February, operated the remainder of the year. An occasional ambiguity of 180° in wind direction resulting from a defective winding in one of the synchro units of the wind vane was corrected in late December, and at the same time the unit of wind speed for the recorder was changed from knots to miles per hour.

Precipitation Chemistry

The program continued in 1979 with few changes. A Kauai water collection site was added to investigate the effects of an island with no active volcano. A reverse osmosis deionizing water still was installed to improve rainwater analyses on the DIONEX chromatograph. Besides improving the quality of the water, the unit is semi-automatic, so that clean water is always on hand for solution preparation, labware cleaning, and plasticware cleaning.

Fluorocarbons (Halocarbons)

This low effort program continued in 1979 without difficulty. Weekly air samples taken at the observatory were shipped to the Boulder laboratory for analysis.

Cooperative Programs

Most cooperative programs listed in table 1 were continued through 1979 without major difficulties. A modified procedure for the acceptance of cooperative projects was instituted in 1979. Since a written project plan is now required, better control of the experiment and more consistent relations with the cooperators are expected.

Carbon monoxide measurements (MPI): This program was continued until mid-October, when the equipment failed. Repairs were not attempted because the German scientists were expecting to replace the outmoded system with a new one early in 1980.

Arosol collections (Fla. State Univ.; Univ. of Md.; Univ. of Calif., Davis): Three types of aerosol collectors were installed by cooperators during 1979. A traveling orifice in a small filter device from Florida State University causes particles to be laid down in a 5-in-long streak over a 2-wk period. In a more elaborate installation from the University of Maryland, two pumps fitted with Nuclepore and quartz filters are operated at night, and a third with a Nuclepore filter operates during the day; the time discrimination is an attempt to separate out particles from upslope and downslope wind regimes. The third aerosol collector is a hybrid filter-impactor device from the University of California, Davis. The aerosol samples from all installations are analyzed by the respective Principal Investigators for the chemical composition of the particles.

A 10-channel photometer and a corona meter were operated for several days in April by G. Shaw of the University of Alaska.

A 1-yr study of the chemistry of precipitation in the vicinity of Kilauea Volcano by D. Harding was completed during March 1979. This study was sponsored by the National Research Council (NRC) associateship program.

A second NRC associate, A. Dittenhoefer, began a 1-yr project at MLO on the chemistry of aerosols during early December 1979.

Measurements of sulfur dioxide (EPA): No changes were made in operational procedures during 1979. The unit functioned normally during sampling intervals. Analytical techniques may be updated at the central laboratory in Honolulu to alleviate temperature related problems.

Collection of atmospheric particulates (EPA): The high volume samples were run continuously to collect total particulates. No changes of equipment were made during the year, and no particular problems were encountered.

Precipitation chemistry (EPA): Monthly precipitation samples were sent to the EPA laboratory in North Carolina.

Precipitation chemistry (DOE): The wet-dry fallout samplers operated normally throughout 1979, and samples were mailed monthly to New York.

Collection of atmospheric particulates (DOE): The only equipment change during the year was the provision of a different type of manifold to which the filters do not adhere. This greatly simplifies filter changes. One interesting observation is that the nighttime filters, used during the predominantly downslope flow regime (2100 to 0600 LST), were generally cleaner than those of the daytime upslope flow regime (0600 to 2100). This is the reverse of the prevailing situation during much of 1978 but corresponds to observations in previous years.

ICDAS Data Acquisition System

Two significant changes of the ICDAS system were made during 1979. In February a modified control program (BOSS 79001) was put into operation, and a new carbon dioxide control board was installed. These improvements increased system

reliability and greatly reduced the possibility of rapid loss of carbon dioxide reference gas during computer failure. In April a NOVA 1220 computer chassis with a linear power supply was installed, reducing electrical noise and improving quality of the analog signals.

The main problems with the data acquisition system during 1979 were system outages caused by sporadic rewinding of the tape and a rash of thunderstorms during the fall months that burned out electronic components and caused system downtime periods.

2.2 Barrow

2.2.1 Facilities

The lidar observatory wanigan was completed and located in August 1979. However, as the winter progressed drifting snow caused by the wanigan's proximity to other buildings caused access problems and may force consideration of another location.

The Thomas E. DeFoor Memorial Walkway from the station to the tower, aerosol platform, and Dobson dome was completed in September. The walkway, named in honor of the former station chief, saves many wet and boggy steps in the summertime.

Hut 164 at NARL (Naval Arctic Research Laboratory) was obtained for housing GMCC staff. Previously, single members lived in the main lab building, at greater cost to GMCC.

Extensive renovation work on the station road was completed in August. A binder mixture of gravel and clay was spread to harden and stabilize the road's surface, with satisfactory results.

2.2.2 Programs

Programs carried out at BRW during 1979 are listed in table 2.

Several modifications were made to the ICDAS system in 1979. The NOVA mainframe was upgraded with a linear power supply and installed in April, and a new multiplexer was installed in July. The magnetic tape drive, adapter, and associated NOVA control board were exchanged for those from the Boulder prototype station to try to cure a spurious tape drive reversal problem that still persists on a very intermittent basis. Environmental causes are being investigated.

A cooperative project to investigate carbonaceous particles in the atmosphere was initiated with Lawrence Berkeley Laboratory in October. Filter samples are run for 4 days and then sent to LBL for analysis.

Two programs were terminated in 1979: the NOAA/Aeronomy Lab NO_2 project in May and operation of GMCC's ECC ozone meter in June.

The University of Rhode Island sampling sector controller, which runs URI's high volume samplers only when the wind is from the clean sector, was installed in December.

Table 2.--Summary of sampling programs at Barrow in 1979

Monitoring program	Instrument	Sampling frequency
Gases		
Carbon dioxide	URAS-2T infrared analyzer	Continuous
	Glass flask pairs	1 pair wk^{-1}
Surface ozone	Dasibi ozone meter	Continuous
Halocarbons	Flask samples	1 pair wk^{-1}
Total ozone	Dobson spectrophotometer	3 day^{-1}
Aerosols		
Condensation nuclei	G.E. CN counter	Continuous
	Pollack counter	Discrete
Optical properties	4-wavelength nephelometer	Continuous
Solar radiation		
Global spectral irradiance	4 Eppley pyranometers with Q1, GG22, OG1 and RG8 filters	Continuous
Direct spectral irradiance	Eppley normal incidence pyrheliometer with filter wheel	Discrete
Turbidity	Eppley sunphotometer	Discrete
Meteorology		
Air temperature	Thermistor	Continuous
	Hygrothermograph	Continuous
Relative humidity	Dew point hygrometer	Continuous
	Sling psychrometer	Discrete
Air pressure	Transducer	Continuous
	Microbarograph	Continuous
	Mercurial barometer	Discrete
Wind (speed and direction)	Bendix aerovane	Continuous
Ground temperature	Thermistor	Continuous
Precipitation chemistry		
pH and conductivity	Wide mouth polyethylene collector (samples analyzed at MLO)	Discrete
	Collection of snow on tundra (samples analyzed at MLO)	2 mo^{-1}
Cooperative programs		
Total surface particulates (DOE/ELM)	High volume sampler	Continuous
Arctic haze particulates (URI)	High volume samplers	Continuous
	Radon monitors	Discrete
Global radiation (SRL)	Eppley pyranometers	Continuous
	Temple Univ. sunburning meter	Continuous
CO_2 sampling (SIO)	Flask samples	2 sets mo^{-1}
Precipitation gage (Soil Conservation Service)	Wyoming shielded precipitation gage	2 readings mo^{-1}
Carbonaceous particles (Lawrence Berkeley Lab.)	High volume sampler	Continuous
	Surface snow samples	2 mo^{-1}

2.3 Samoa

2.3.1 Facilities

No major additions to the Samoa GMCC facility were made during 1979. The lease agreement was renegotiated between NOAA and High Chief Iuli Togi for the land on which the GMCC facility is located. N. Stiewig from Research Support Services arrived on the island during January and negotiated the new settlement. A unique feature of the renegotiation was lump sum advance payment, which was used to construct a Samoa style guest house for the Iuli family in Tula village. Construction was begun in November 1979 and completed in early 1980. The structure has been useful and practical for the Iuli family and Tula village. N. Stiewig's role in suggesting this plan and incorporating it in the lease documentation and payment schedule is gratefully acknowledged. Local individuals involved in the renegotiation were High Chief Iuli Togi, Lt. Governor Tufele Lia, who signed the document approving the communal land lease between NOAA and High Chief Iuli (all communal land leases must be approved by the Governor's office and the local attorney general's office), L. Richmond, assistant to the Governor, and Tauivi Tuinei, attorney for the Iuli family. This renegotiation is binding for the next 5-yr period.

2.3.2 Programs

Table 3 lists the programs carried out at SMO during 1979. Status reports on the principal programs follow.

Trace Gases

Carbon Dioxide: Continuous CO_2 analyzer data were significantly improved in February 1979 when the polyethylene sample line system was modified, resulting in index values more in agreement with those obtained in hand aspirated flasks exposed in the vicinity of the actual polyethylene line intake. To eliminate recurrence of what appeared to be diffusion effects on the polyethylene line, an aluminum sample line was installed in May 1979 and became the primary sample line. Coinciding with the new air line installation, a special CO_2 flask sampling program was initiated to more thoroughly document air line effects. Thus, twice weekly flask samplings were begun. A sampling consisted of four flasks, two hand aspirated near the air line intake at the point and two using the through-the-analyzer procedure. Long term records of the closure between these two kinds of flask pairs should establish integrity of the air intake system data set.

Surface Ozone: The Samoa ECC sensor was operational all year; however, difficulties were experienced with the Dasibi unit that required servicing off the island. Data from approximately 3 months of Dasibi operation are missing for the year, from early May until early August.

Total Ozone (Dobson): Regular daily observations were maintained all year.

CO_2 Flask Sampling: Regular weekly samplings were maintained all year plus special extra samplings each week for air line checks.

Halocarbon Sampling: A weekly sampling schedule was maintained all year.

Cooperative Trace Gas Programs: The Oregon Graduate Center (OGC) halocarbon monitoring equipment functioned all year. In addition, a second gas chromatograph for monitoring CH_4, CO, and CO_2 was installed during September 1979.

Table 3.--Summary of sampling programs at Samoa in 1979

Monitoring program	Instrument	Sampling frequency
Gases		
Carbon dioxide	URAS-2T NDIR analyzer	Continuous
	Evacuated glass flasks	Discrete
Surface ozone	Electrochemical concentration cell	Continuous
	Dasibi ozone meter	Continuous
Total ozone	Dobson spectrophotometer #42	Discrete
Fluorocarbons	Flask sampling	1 wk^{-1}
Aerosols		
Condensation nuclei	G.E. CN counter	Continuous
	Pollak CN counter	Discrete
Scattering properties (surface air)	4-wavelength nephelometer	Continuous
Atmospheric turbidity	Volz sunphotometer	Discrete
Solar radiation		
Global spectral irradiance	4 Eppley pyranometers with quartz, GG22, OG1, RG8 filters	Continuous
Direct spectral irradiance	Eppley NIP with filter wheel (OG1, RG2, RG8)	Discrete
	Eppley NIP/equatorial mount combination	Continuous
Meteorology		
Temperature (air)	Thermistor	Continuous
	Thermograph	Continuous
	Psychrometer	Discrete
	Max.-min. thermometers	Discrete
Temperature (soil)	Thermistor	Continuous
Temperature (dew point)	Thermistor with LiCl dew cell	Continuous
Relative humidity	Hygrothermograph	Continuous
Wind (speed and direction)	Bendix aerovane	Continuous
Pressure	Transducer (capacitance type)	Continuous
	Microbarograph	Continuous
	Mercurial barometer	Discrete
Precipitation chemistry		
pH and conductivity	Orion pH meter Beckman conductivity bridge Samples sent to MLO for further analysis on ion chromatograph	Discrete
Cooperative programs		
CH_4, CO, CO_2 (OGC)	Carle gas chromatograph	Discrete 3 h^{-1}
Atmospheric Lifetime Experiment fluorocarbon program (OGC)	H-P 5840A gas chromatograph	Discrete 1 h^{-1}
Rain collection (DOE/EML)	Wet-dry collectors	Continuous
Rain collection (EPA)	Misco collector	Continuous

Aerosols

The GMCC GECNC functioned continuously all year except for a few minor breakdowns and repair-maintenance eqisodes. The Pollak functioned properly all year also. Major problems developed in the Samoa nephelometer unit, however, and it was returned to Boulder in January for checkout and repair. After its return in late March, its performance was somewhat better, but deterioration began again and a major problem seemed to involve the PM tube cooling system. Therefore, in September, the unit was again returned to the United States for modification so that PM tube cooling could be eliminated. The unit should be back in operation in 1980.

Solar Radiation

GMCC sensors were online continuously all year. The NIP filter wheel was returned to Boulder in March to measure its transmission characteristics and returned after tests were completed. GMCC solar radiation program traveling standards were received in June, and intercomparisons with SMO GMCC sensors were performed. Deterioration of filter domes for the Samoa pyranometers continues to be a problem, particularly for the RG8 and OG1 units.

Meteorology Sensors

The GMCC Aerovane transmitter synchro was replaced in October after it was discovered that the original synchro rotor winding was open. In consequence, wind direction signals intermittently differed by 180° from true wind direction. Receipt of replacement bobbens for the LiCl dew cell was delayed, resulting in the sensor being offline from August until December, when spare bobbens finally arrived.

Precipitation Collection

DOE/EML wet-dry collectors: One of the two collectors failed during December. A 2-yr summary of the DOE/EML analysis of Samoa GMCC samples from the wet-dry collectors was published during the year, covering the period from April 1976 through March 1978 (Bogen et al., 1980).

2.4 South Pole

2.4.1 Facilities

The GMCC South Pole program continued operation for the 1979 season in the new Clean Air Facility (CAF) (diagrams in GMCC Summary Report 1978). No major modifications were made to the internal layout.

The two transformers in the CAF that caused power problems in the previous season were replaced with one transformer large enough to handle all CAF power requirements without overheating.

This year only three sampling stacks were used by the University of Maryland for the atmospheric chemistry program. Since the stacks create a shadow on the solar radiation equipment, the unused ones were taken down this December.

This year the drifting downwind of the building is becoming very noticeable and may soon become a problem (see figs. 1 and 2). The path leading from the station to the stairs is exactly downwind of the stairs and is raised above the surrounding snow several feet, mainly because foot traffic packs snow too tightly to drift away. During the year the path has gained at least 6 ft in places.

No problems were encountered with the building itself, and it continues to be an excellent location for the program.

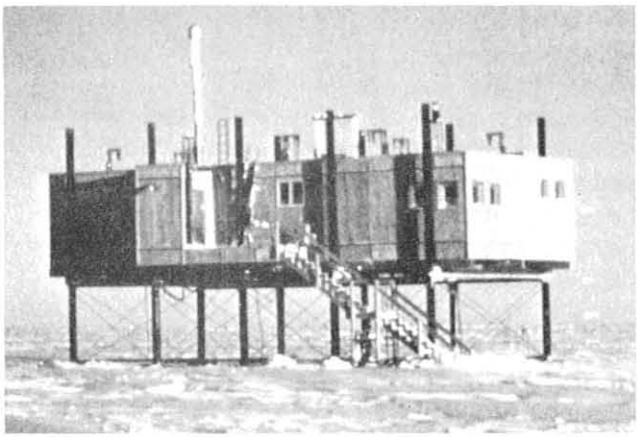

Figure 1.--Clean Air Facility at SPO. Photo was taken in January 1977.

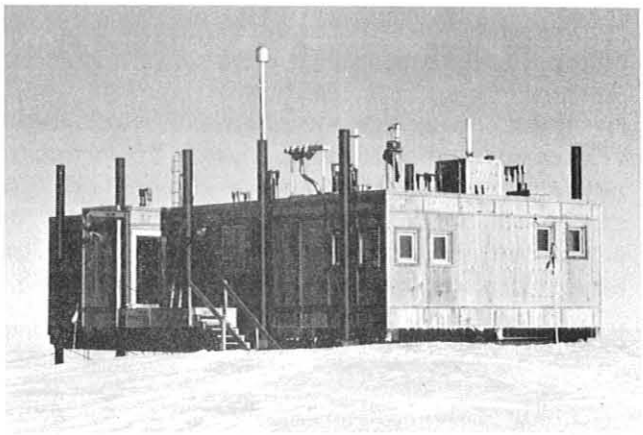

Figure 2.--Clean Air Facility at SPO. Photo was taken in January 1981.

2.4.2 Programs

SPO programs for 1979 are listed in table 4 and briefly described below.

ICDAS

The NOVA 1220 and all other ICDAS associated equipment ran continuously all year without failure. In January a new Wangco tape drive replaced the old one, which was stored in the CAF for the year as backup. A new Chronolog clock was shipped to SPO, but it had an improper ground connection. This was not discovered at the South Pole, and it was returned to Boulder. The old clock ran well all year so this created no problem. The only equipment malfunction was a loose attachment between the platen and paper roll on teleprinter, which was repaired with Permabond glue.

Because of cracked batteries the uniterruptable power source was not used. Since the year had very minimal power downtime, this created no problem.

Carbon Dioxide

The URAS-2T was secured for the year in mid-November 1978. The program consisted of exposing pairs of 0.5-ℓ glass flasks by hand, aspirating them on the roof of the CAF. Samples were taken at the rate of one pair per week until March, then two pairs per week until November when the URAS was restarted.

Table 4.--Summary of sampling programs at South Pole in 1979

Monitoring program	Instrument	Sampling frequency	Data record
Gases			
Carbon dioxide	0.5-ℓ evacuated glass flasks, hand aspirated	1 pair wk^{-1}	Dec 78-Mar 79
		2 pair wk^{-1}	Mar 79-Nov 79
Surface ozone	Electrochemical concentration cell	Continuous	Dec 71-Jan 79
	Dasibi ozone meter	Continuous	Jan 76-present
Total ozone	Dobson spectrophotometer	Discrete	Dec 63-present
Fluorocarbons	300-ml stainless steel sampling cylinders	1 pair wk^{-1}	Jan 77-Dec 78
Aerosols			
Condensation nuclei	G.E. CN counter	Continuous	Jan 74-present
	Pollak CN counter	Discrete, 2-4 day^{-1}	Jan 74-present
	Long tubed Gardner CN counter	Discrete, 1 day^{-1}	Jan 74-present
Optical properties	4-wavelength nephelometer	Continuous	Jan 79-present
Solar radiation			
Global spectral irradiance	4 Eppley pyranometers with quartz, G6-22, OG-1, and RG-8 filters	Continuous during austral summer	Feb 74-present
	Ultraviolet radiometer	Continuous during austral summer	Feb 74-present
Direct spectral irradiance	NIP on meridional tracker	Continuous during austral summer	Oct 75-present
	Filter wheel normal incidence pyrheliometer with quartz, OG-1, RG-2, RG-8 filters	Discrete during austral summer	Jan 77-present
Meteorology			
Air temperature	Thermistor (naturally ventilated shield)	Continuous	Mar 77-present
Snow temperature	Thermistor	Continuous	Jul 77-present
Pressure	Transducer	Continuous	Dec 75-present
Wind (speed and direction)	Bendix-Friez aerovane and recording system	Continuous	Dec 75-present
Atmosphere moisture content	Dupont 303 moisture monitor	Continuous	Mar 77-present
Miscellaneous			
Room temperature	Thermistor	Continuous	Jul 78-present
Cooperative programs			
Carbon dioxide (SIO)	5-ℓ evacuated glass flasks	2 mo^{-1} (3 flasks per sample)	1957-present
Total surface particulates (atmosphere trace metals) (DOE/ERDA/HASL)	Motor driven rotary lobe blower (high volume air sampling through filters)	Continuous (filters changed 4 times mo^{-1})	May 70-present
Turbidity (NOAA/ARL)	Dual wavelength sunphotometer	Discrete during austral summer	Jan 74-present
Carbon-14 sampling (NOAA/ARL)	Pressurized steel spheres	500 P.S.I. ambient air day^{-1}, for 6 days	Jan 74-present
Ionospheric opacity (Univ. of Calif., San Diego; NOAA/EDIS)	30- and 50-MHz riometers	Continuous	1974-Jan 80
Aerosol chemistry (CSRIO)	Grid impactor	Continuous	Jan 79-Jan 80
Atmospheric chemistry (Univ. of Maryland and URI)	High volume filters	Continuous	Jan 79-present
Aerosol concentration (Laboratoire du Glaciology, Fr.)	Coulter counter	8 h day^{-1}	Feb 79-Dec 79
Atmospheric tritium (Univ. of Miami, Fla.)	Tritium traps	48 h (6 days)$^{-1}$	Jan 79-Dec 79
Individual particle analysis (NOAA/APCL)	Nuclepore filters	1 mo^{-1}	Jan 79-Dec 79

Surface Ozone

The ECC and Dasibi 1326 were run until mid-January 1979. At that time a new modified Dasibi (1316) was sent to SPO. After numerous intercomparisons the old Dasibi and the ECC were retrograded to Boulder. The new instrument gave a very quiet signal and ran well until May. A problem in the display board caused a 7 to appear in the display just left of the decimal point; this did not affect the output. The solenoid began jamming, and the valve diaphragm was found to be very badly worn. The air pump bearings became worn and were shimmed but finally seized in July. A pump from another project was patched into the system. Lamp cracking was a problem as in previous years, and after a power down in October the last good lamp cracked. The output was so unstable that no amount of adjustment could give a signal. The new Dasibi was difficult to repair because it was a modified version, and most available spare parts fit only the older version. Even the spare solenoid, a frequent source of breakdown, could not be used.

Total Ozone

The Dobson no. 80 was operated all year without malfunction. Observations were made at approximately 2200, 0000, and 0200 CUT during the austral summer. Moon observations were made when the disc was three-quarters full or fuller. Any blowing snow or thick ice haze made the signal too weak and noisy to get a usable trace from the moon.

Aerosols

Aerosol observations were taken twice daily at approximately 1030 and 2230 to coordinate with the radiosonde balloon launches. Only routine maintenance was required for the Gardner and Pollak counters. In early August after routine cleaning and regreasing the GECNC background was offscale. A thorough overhaul only increased the background. Finally it was discovered that the positions of both the lamp and PM tube are extremely critical for a low background and an output in the proper range. Eventually all adjustments were made to minimize background. It was also noted that a very small change in vacuum causes large changes in output, which was useful in getting the signal into the proper range.

The nephelometer was run for the first year at SPO. It ran well with only minor breakdowns. Very strange variations in output and occasional drops to zero output were seen throughout the year. The cause has not yet been determined.

Meteorology

Only minor problems were encountered in the electronics of the meteorology program. Loose connections and dirty contacts accounted for most of these. The pressure measured by the GMCC instrument was consistantly 2.8 mb lower than the station readout. Whenever winds were calm, the ICDAS output for windspeed was 1.19 m s^{-1}. This may have been a MUX offset but was consistant all year.

Solar Radiation

Heavy icing of the pyranometers was still a problem, especially in the coldest part of summer shortly after sunrise. The only breakdown all year was a burnt out bodine motor in the equatorial tracker, which was replaced with a spare.

Halocarbons

In the past the winter samples, which were stored over long periods, were found to give poor data. The schedule was modified this year so that only summer samples were taken, at the rate of one pair per week. The equipment ran perfectly all year.

2.4.3 Cooperative Programs

Several cooperative programs were added this year (see table 4), which created no strain on the GMCC program or personnel.

3. CONTINUING GMCC PROGRAMS

3.1 Carbon Dioxide

3.1.1 Analyzer CO_2 Measurements

CO_2 measurements made with continuously operating nondispersive infrared gas analyzers were continued during 1979 at BRW, MLO, and SMO. At SPO, where similar observations were discontinued in November 1978, the CO_2 measurement program was reinstated in December 1979.

Data acquisition and processing procedures remained identical in 1979 to those employed previously (see GMCC Summary Reports 1977 and 1978). Mean monthly CO_2 mole fractions were computed from edited hourly CO_2 values for BRW and MLO and added to the existing data for these stations as shown in tables 5 and 6. Results in these tables are expressed in the 1974 WMO CO_2-in-air mole fraction scale with tentative pressure broadening corrections applied. Plots of the data are shown in fig. 3.

The data presented are preliminary since results from BRW have yet to be updated by using improved working reference gas concentration values; also, pressure broadening corrections applied to both the BRW and MLO data are tentative. Relative errors in the plotted data are estimated to be $\leq$1 ppm for BRW and $\leq$ 0.5 ppm for MLO. Systematic errors for both data sets are believed to be less than ±1 ppm when referred to an absolute CO_2 mole fraction calibration scale.

CO_2 analyzer data for SMO are not presented in this report since an air intake line problem affecting data quality is being investigated. Final data processing has been postponed until recent test data are evaluated and pressure broadening corrections are determined for the URAS-2T (no. 016) CO_2 analyzer in use at SMO.

3.1.2 Flask Sample CO_2 Measurements

The NOAA Environmental Research Laboratories CO_2 flask sampling program dates from 1968 when the Atmospheric Physics and Chemistry Laboratory began to measure CO_2 at Niwot Ridge near Boulder, Colo., and at Ocean Station Charlie in the North Atlantic. When Air Resources Laboratories GMCC program was formed in 1971, CO_2 flask sampling was gradually expanded to include air sample collections at the

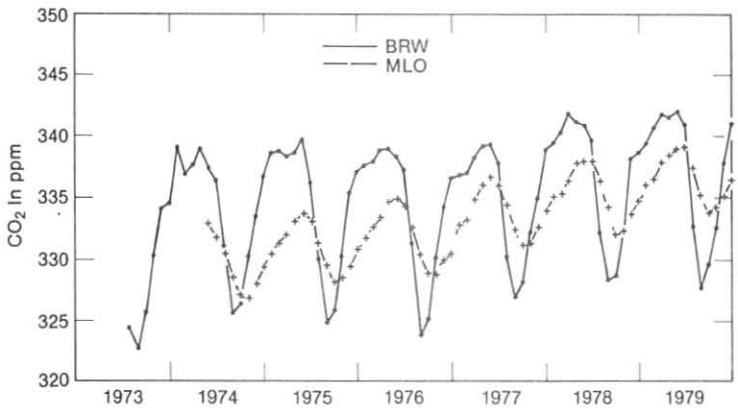

Figure 3.--Mean monthly CO_2 mole fractions for Barrow (solid line) and Mauna Loa (dashed line) plotted in the 1974 WMO mole fraction CO_2-in-air scale.

Table 5.--Barrow Observatory monthly mean CO_2 mole fractions*

Month	1973	1974	1975	1976	1977	1978	1979
Jan		339.11	338.50	337.56	336.68	339.38	339.35
Feb		336.82	338.73	337.80	336.90	340.24	340.59
Mar		337.57	338.22	338.77	338.19	341.73	341.65
Apr		338.87	338.53	338.90	339.09	341.06	341.43
May		337.35	339.62	338.24	339.25	340.83	341.90
Jun		336.40	336.07	337.12	337.78	339.57	340.94
Jul	324.44	331.00	329.94	331.26	330.14	332.02	332.61
Aug	322.69	325.52	324.74	323.78	326.79	328.29	327.60
Sep	325.68	326.38	325.78	325.09	328.04	328.62	329.55
Oct	330.29	330.06	330.20	330.06	332.17	332.20	332.54
Nov	334.07	333.27	335.32	334.17	334.92	338.12	337.71
Dec	334.48	336.65	337.01	336.46	338.78	338.60	340.98

*Values expressed in ppm 1974 WMO CO_2-in-air mole fraction scale.

GMCC stations at BRW, SMO, SPO, MLO, and two other sites, Key Biscayne, Fla., and Cape Kumakahi, Hawaii.

Because of the importance of the CO_2 problem to U.S. energy policy requirements, a program was started in 1978 in the Office of the Assistant Secretary for Environment, DOE, with the goal of developing the ability to predict future environmental, agricultural, and social consequences of increasing atmospheric CO_2 concentrations. This multifaceted national research and assessment effort includes developing and validating a global carbon cycle model for use in forecasting future CO_2 growth. Among required inputs to the model are CO_2 measurement data from an expanded network of stations that can provide information on globally averaged CO_2 trends, global CO_2 gradients, global as well as temporal CO_2 annual-cycle amplitude variations, and CO_2 sources and sinks.

Table 6.--Mauna Loa Observatory monthly mean CO_2 mole fractions*

Month	1974	1975	1976	1977	1978	1979
Jan		330.45	331.58	332.73	335.06	336.03
Feb		331.21	332.54	333.13	335.28	336.45
Mar		331.86	333.27	334.70	336.36	337.85
Apr		330.00	334.59	335.93	337.75	338.46
May	332.89	333.60	334.82	336.60	337.91	338.98
Jun	331.79	333.04	334.24	336.00	337.87	339.11
Jul	330.51	331.29	332.52	334.35	336.72	337.37
Aug	328.48	329.43	330.31	332.30	334.18	335.16
Sep	326.92	328.09	328.84	331.08	331.99	333.79
Oct	326.77	328.43	328.63	331.24	332.36	334.26
Nov	327.97	329.37	329.92	332.56	333.65	335.05
Dec	329.31	330.69	330.40	333.86	334.77	336.41

*Values expressed in ppm 1974 WMO CO_2-in-air mole fraction scale.

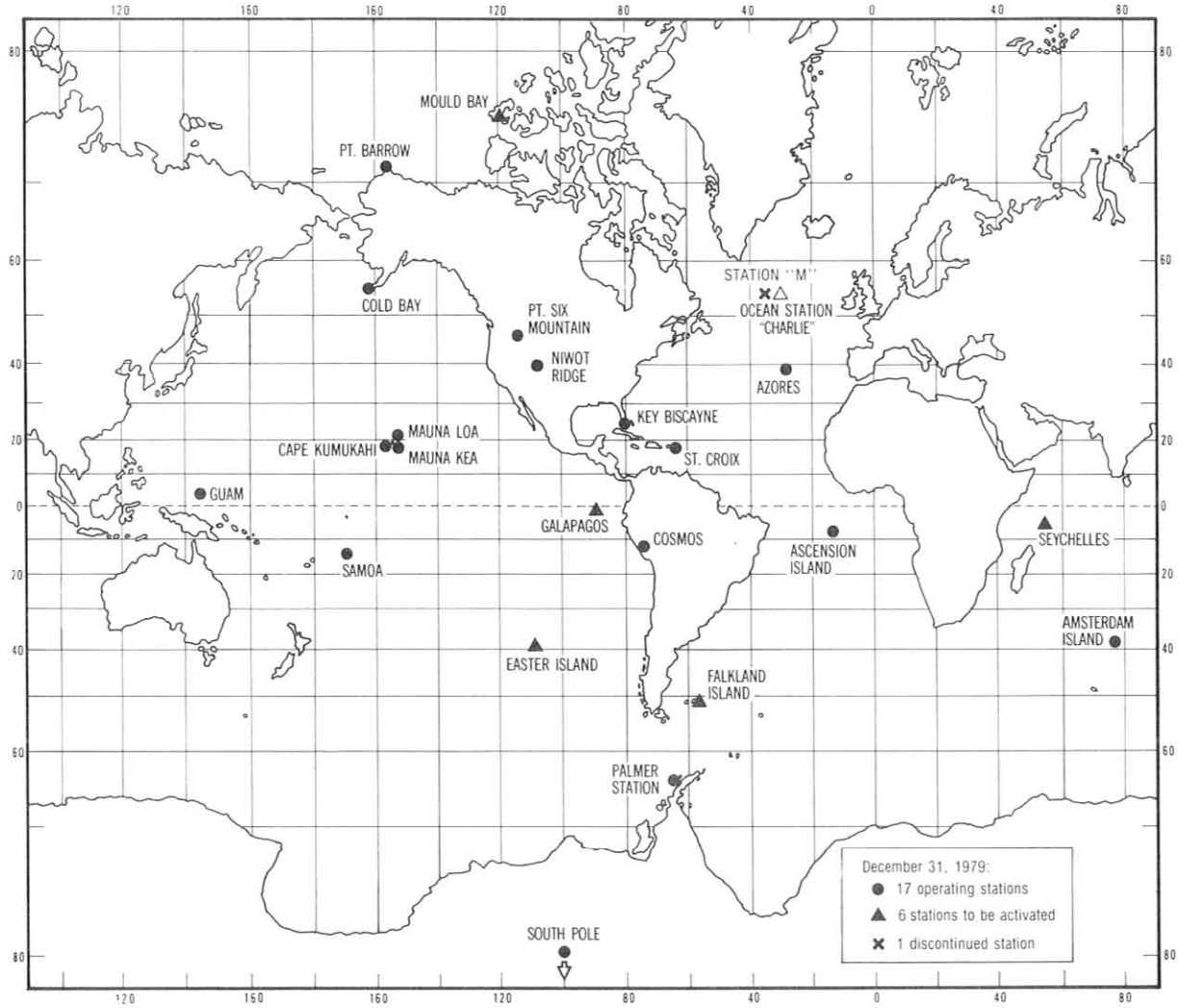

Figure 4.--Map showing the global distribution of existing, planned, and defunct NOAA and cooperative CO_2 sampling stations on 31 December 1979.

To obtain the needed data, the GMCC program with financial support from DOE began expanding in 1978 its eight-station CO_2 network to 23 stations (fig. 4 and table 7). CO_2 samples are periodically collected at the sites and forwarded to the GMCC laboratory in Boulder for analysis. One aim of the program is to identify stations where high quality global background data are obtainable, with a view of upgrading the CO_2 monitoring at these sites with continuously operating CO_2 analyzers.

Air is collected at the stations in paired 0.5-ℓ glass flasks. All sample analyses have been performed at GMCC Boulder using Mines Safety Appliance Company (MSA) infrared CO_2 analyzers (type 200, S/N 1809 before 5 April 1975, and type 202, S/N 20719), except that an H. Haihak Company UNOR-2 (S/N 631521) instrument was used to analyze air samples collected during 1979 at Amsterdam Island, Indian Ocean, and Palmer Station, Antarctica. Air samples from the flasks were transferred into the MSA analyzers by using a mercury displacement pump (Bischof, 1975). Samples were analyzed with the UNOR-2 instrument on a newly developed semi-automatic apparatus (Komhyr et al., 1979) that has a displacement pump made

Table 7.--CO_2 flask sampling station summary

Station	Country	Lat./long.	Elevation (m)	Cooperating agency	Period of record	Site type
SMO	U.S. territory	14°15'S, 170°34'W	30	(GMCC station)	Jan 1972 to present	Island rocky promontory
Amsterdam Is., Indian Ocean	France	37°52'S, 77°32'E	150?	Centre des Faibles Radioactivities	Jan 1979 to present	Island seashore
SPO	Antarctica	89°59'S, 24°48'W	2,810	(GMCC station)	Jan 1975 to present	Ice & snow covered plateau
Ascension Is., South Atlantic	U.K.	7°55'S, 14°25'W	54	USAF/Pan American World Airways	Aug 1979 to present	Island seashore
Azores (Terceira Is.), N. Atlantic	Portugal	38°45'N, 27°05'W	30?	U.S. Dept. Air Force 7th Weather Wing	Dec 1979 to present	Island seashore
Cape Kumakahi, Hawaii	U.S.	19°31'N, 154°49'W	3	(GMCC site)	Mar 1976 to present	Island seashore
Cold Bay, Alaska	U.S.	55°12'N, 162°43'W	25	NOAA, NWS	Oct 1978 to present	Treeless peninsula
Cosmos	Peru	12°07'S, 75°20'W	4,600	Instituto Geofisico de Peru	Sep 1979 to present	Alpine mountain
Easter Is., South Pacific	Chile	27°06'S, 109°15'W	200	Ministro de Defensa Nacional Direccion Meteorologica de Chile	(Program to begin in 1981)	Island seashore bluff
Falkland Is.	U.K.	51°42'S, 57°52'W	51	British Meteorological Service	(Program to begin in 1980)	Island seashore
Galapagos (Chatham Is.), South Pacific	Equador	00°54'S, 89°37'W	6	Instituto National de Meteorologia e Hidrologia	(Program to begin in 1981)	Island seashore
Guam (Marianas Is.), N. Pacific	U.S. territory	13°26'N, 144°47'E	2	University of Guam	Mar 1979 to present	Island seashore
Key Biscayne, Fla.	U.S.	25°40'N, 80°10'W	3	NOAA, Sea-Air Interaction Laboratory	Dec 1972 to Mar 1974 Mar 1976 to present	Coastal island seashore
Mauna Loa, Hawaii	U.S.	19°32'N, 155°35'W	3,397	(GMCC station)	Jun 1976 to present	Barren, volcanic mountain slope
Mauna Kea, Hawaii	U.S.	19°50'N, 155°28'W	4,220	Institute for Astronomy, Univ. of Hawaii	Jan 1979 to present	Alpine mountain peak
Mould Bay, N.W.T.	Canada	76°14'N, 119°20'W	15	Dept. of Environment, Atmospheric Environment Service	(Program to begin in 1980)	Island tundra
Niwot Ridge, Colo.	U.S.	40°03'N, 105°38'W	3,749	INSTAAR, Univ. of Colorado	Feb 1968 to Jan 1974 Jan 1976 to present	Alpine mountain
Ocean Station Charlie (U.S.)	N. Atlantic	54°00'N, 35°00'W	6	NOAA, NWS	Nov 1968 to May 1973	Open ocean
Ocean Station M	N. Atlantic	54°00'N, 35°00'W	6	Norwegian Meteorological Institute	(Program to begin in 1981	Open ocean
Palmer Station (Anvers Is.)	Antarctica	64°55'S, 64°00'W	10?	Desert Research Lab., Univ. of Nevada	Feb 1978 to present	Barren island seashore
Point Barrow, Alaska	U.S.	71°19'N, 156°36'W	11	(GMCC station)	Apr 1971 to present	Arctic coastal seashore
Point Six Mountain, Mont.	U.S.	47°02'N, 113°59'W	2,462	U.S. NWS	May 1978 to present	Wooded mountain top
Seychelles (Mahe Is.), Indian Ocean	Seychelles	5°20'S, 55°10'E	3?	Physical Science Lab., New Mexico State Univ.	(Program to begin in 1980)	Island seashore
St. Croix, Virgin Islands	U.S. Territory	17°45'N, 64°45'W	3	Fairleigh Dickinson Univ.	Mar 1979 to present	Island seashore

up of a glass cylinder with a free-floating piston fabricated from Teflon reinforced with glass fibers. Additional details concerning sample collection and analysis procedures are given in Komhyr and Harris (1976).

Before 31 December 1978 all samples were analyzed using CO_2-in-N_2 reference gases calibrated by the Scripps Institution of Oceanography (SIO). Beginning with air samples collected in 1979 and including samples collected at Palmer and South Pole stations during 1978, analyses were performed using CO_2-in-air reference gases, also calibrated by SIO. The carrier gas was changed from N_2 to air to eliminate the need to apply data corrections arising from differences in 4.3-μm infrared radiation absorption characteristics of CO_2-in-N_2 as opposed to CO_2-in-air.

The CO_2-in-air reference gases used in analyzing most 1979 air samples were obtained during April and May 1977 by pumping air to a pressure of 150 atm into large, chrome-molybdenum steel tanks fitted with noncontaminating bellows valves.

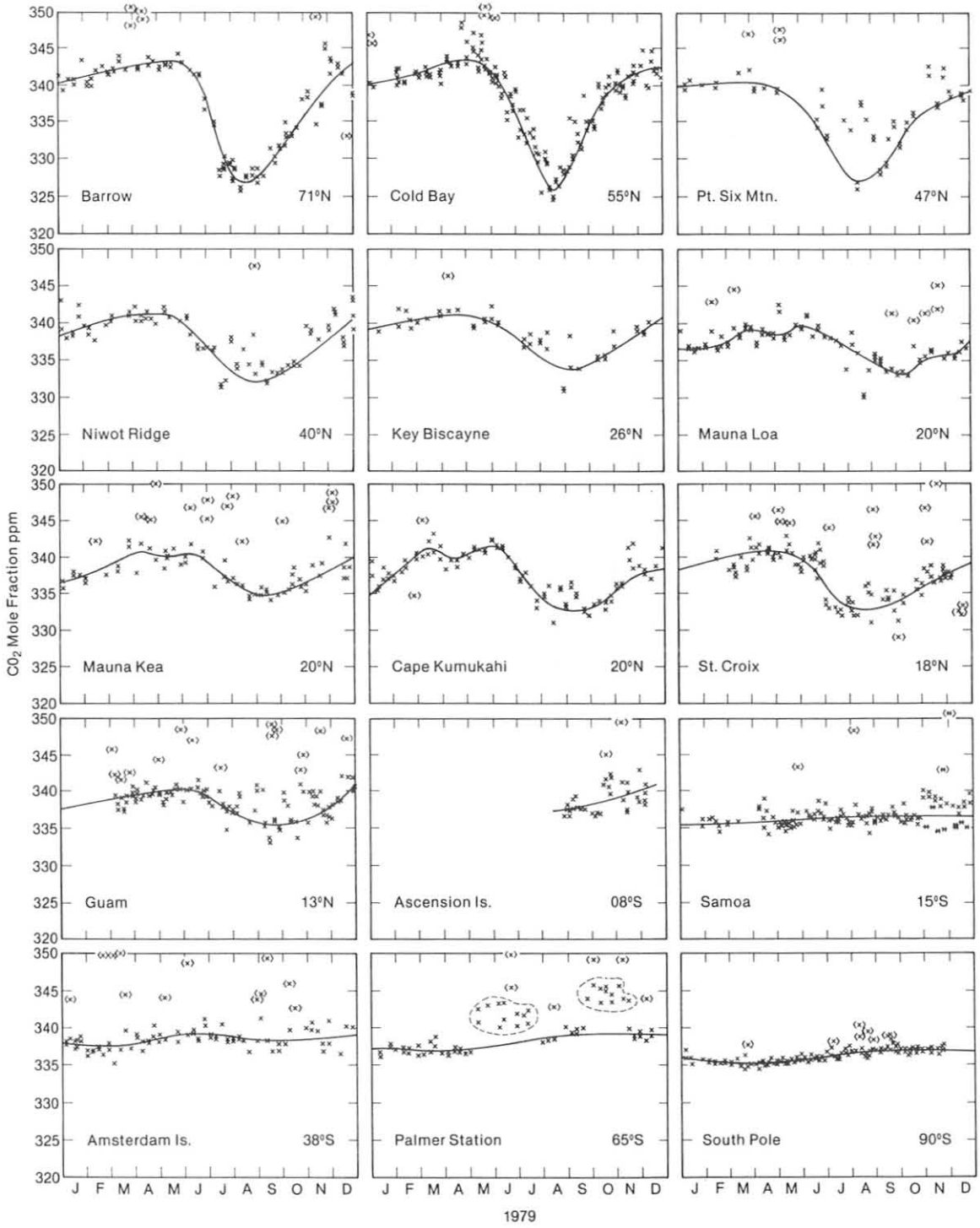

Figure 5.--CO_2 data obtained during 1979 at 15 stations from discrete sampling. Hand drawn curves are fitted to the data.

Air was collected at the University of Colorado Alpine Research Station C1 site, in the mountains west of Boulder at 3-m elevation. Pumping was performed only during clean air, downslope wind conditions at times when Aitken nuclei counts were less than 6,000 cm^{-3} and occasionally below 1,000 cm^{-3}. The air compressor used was a noncontaminating, three-stage, RIX Industries model 153B-3 piston cylinder pump fitted with reinforced TFE Teflon piston rings that enable the unit to operate without lubrication. Type 3A molecular sieve material was used with the pump to dry the compressed air to a dew point temperature of about -70°C. Tank CO_2 concentrations were adjusted by either partial removal of CO_2 from the pumped air with a type 13X molecular sieve material, or by adding small quantities of 99.99% purity CO_2 to the pumped air.

CO_2-in-air reference gases used with the semi-automatic analysis apparatus were procured from Liquid Carbonic Corporation, Los Angeles, Calif. They are comprised of CO_2 in dry (dew point less than -73°C) synthetic air containing natural proportions of nitrogen, oxygen, and argon. High purity nitrogen and argon are used to prepare the carrier gas together with oxygen derived from electrolysis of water. Intercalibration of these synthetically produced gases with natural air reference gases indicated that both types are equally suitable for calibrating nondispersive infrared CO_2 analyzers.

Individual CO_2 flask sample analysis data, for samples collected during 1979 at 15 stations, are plotted in fig. 5. Results are expressed in SIO 1974 provisional CO_2-in-air mole fraction scale. Smooth hand drawn curves fitted to the data plots are provisionally assumed to be representative of background CO_2 data at the stations.

In a preliminary attempt to improve data quality through data selection, visible outliers in fig. 5 have been identified as representing unreliable data. Such data are shown enclosed in brackets. Two groups of Palmer Station data (circled in fig. 5) are also taken to be unreliable, even though they may be representative of some local source of CO_2. Measurements made at that site in 1980 may shed light on this apparent data anomaly.

Mean monthly, seasonal, and annual CO_2 mole fractions for 14 of 15 CO_2 flask sampling stations are listed in table 8. The values have been derived by averaging sample data plotted in fig. 5, excluding bracketed data. In a few instances where measurements were not made, or the measurement data were deemed unreliable, the monthly means were inferred from the hand drawn curves in fig. 5. Such values are shown enclosed in parentheses in table 8.

Seasonal and annual CO_2 mole fractions plotted vs. latitude are shown in fig. 6. (Data for Amsterdam Island and Palmer Station are not included in the plots since an adjustment to the data from these stations may be necessary.) The seasonal uptake of CO_2 by vegetation in the Northern Hemisphere is clearly evident in the plots. In fig. 7, peak-to-peak CO_2 annual cycle amplitudes are plotted as a function of latitude. A maximum CO_2 amplitude of 17.4 pmm peak to peak is observed at Cold Bay, Alaska, whereas a minimum value of 1.4 ppm peak to peak occurred at Samoa. Corresponding data for other stations are provided in table 9.

The results discussed above are tentative. A more definitive study of these data is in progress.

Table 8.--Mean CO_2 mole fractions in ppm*

Month	Station													
	BRW	CBA	PSM	NWR	KEY	MLO	MKO	KUM	AVI	GMI	SMO	AMS	PSA	SPO
Jan	340.8	340.4	340.0	338.7	340.0	336.7	336.8	336.1	(338.7)	(337.8)	335.1	338.0	337.0	335.8
Feb	341.5	341.2	340.3	339.9	340.7	336.9	337.9	339.3	339.7	(338.3)	335.2	337.2	336.9	335.5
Mar	342.0	342.1	340.5	340.6	341.2	339.1	339.5	341.2	340.3	339.0	335.5	337.3	337.2	335.3
Apr	342.8	343.0	340.3	341.0	341.4	338.9	340.5	339.8	340.8	339.5	335.6	338.3	336.7	335.3
May	343.0	342.9	338.9	341.0	341.0	339.0	339.9	341.3	340.5	340.1	335.8	338.7	(337.3)	335.5
Jun	341.7	339.2	335.5	338.4	339.7	339.3	340.4	340.1	338.5	340.0	336.0	339.5	(337.8)	336.0
Jul	332.5	332.3	330.0	335.0	336.9	337.7	338.0	336.0	334.4	338.1	336.0	339.0	(338.2)	336.3
Aug	326.9	325.8	327.2	332.5	334.5	335.8	335.7	333.2	333.0	336.4	336.1	338.1	339.0	336.9
Sep	329.0	330.5	329.9	332.2	334.0	333.9	334.8	332.7	333.5	335.5	336.2	338.2	(339.0)	336.9
Oct	333.3	337.2	335.0	334.0	335.6	333.9	335.7	334.0	335.0	335.6	336.2	340.0	(339.1)	337.1
Nov	337.5	340.6	337.5	336.2	337.8	335.7	337.3	336.8	336.9	336.8	336.2	339.0	(339.0)	337.0
Dec	341.2	342.0	339.2	339.0	340.0	336.8	339.1	338.1	338.5	339.1	336.3	338.7	338.9	(337.0)
J-F-M	341.4	341.2	340.3	339.7	340.6	337.6	337.8	338.9	(339.6)	(338.4)	335.3	337.5	337.0	335.5
A-M-J	342.5	341.7	338.2	340.1	340.7	339.1	340.3	340.4	339.9	339.9	335.8	338.9	(337.3)	335.6
J-A-S	329.5	329.5	329.0	333.2	335.1	335.8	336.2	334.0	333.6	336.7	336.1	338.4	(338.7)	336.7
O-N-D	337.3	339.9	337.2	336.4	337.8	335.5	337.4	336.3	336.8	337.2	336.2	339.3	(339.0)	337.0
Annual	337.7	338.0	336.2	337.4	338.6	337.0	337.9	337.4	(337.5)	(338.0)	335.8	338.5	(338.0)	(336.2)

*Values derived from plots in fig. 5.

Table 9.--Peak-to-peak amplitudes of CO_2 annual cycles *

Station	ppm/max.	ppm/min.	ampl. (ppm)
BRW	343.3	326.9	16.4
CBA	343.3	325.9	17.4
PSM	340.6	327.5	13.1
NWR	341.2	332.0	9.2
KEY	341.3	340.0	7.2
MKO	340.7	334.7	6.0
MLO	339.8	333.5	6.3
KUM	341.7	332.8	8.9
AVI	340.7	333.0	7.7
GMI	340.2	335.4	4.8
SMO	336.7	335.4	1.4
AMS	339.2	337.5	1.7
PSA	339.0	337.0	2.0
SPO	337.2	335.3	1.9

*Data extracted from plots of fig. 5.

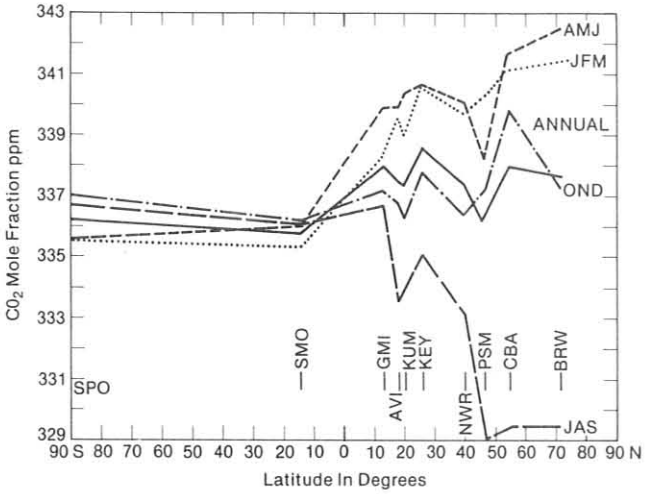

Figure 6.--1979 seasonal and annual meridional distributions of CO_2.

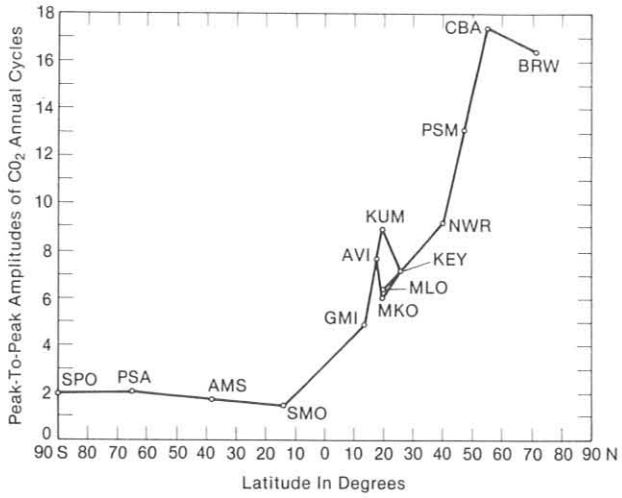

Figure 7.--Meridional distribution of peak-to-peak CO_2 annual cycle amplitudes.

3.2 Total Ozone

3.2.1 Observations of Total Ozone

Total ozone observations were continued throughout 1979 at 11 of 12 stations listed in table 10. In May 1979, the Department of Meteorology at Florida State University, Tallahassee, notified NOAA that it would no longer fund the total ozone program, and that observations would be terminated at the end of May 1979. Plans are under way to re-establish the program either in Tallahassee at the NWS site or at some other location in southeastern United States.

During June, July, and August 1979, world standard Dobson ozone spectrophotometer no. 83 was operated at MLO to check its calibration. The data obtained, together with similar data from past years, will be analyzed to determine whether solar constant variations at the Dobson instrument wavelengths occur during the course of a solar (sunspot) cycle.

3.2.2 Modernization and Calibration of Dobson Spectrophotometers

Under auspices of the WMO Global Ozone Research and Monitoring Project, three foreign Dobson spectrophotometers were modernized, optically aligned, and calibrated: no. 74, Hradec Králové, Czechoslovakia; no. 110, Budapest, Hungary; and no. 121, Bucuresti, Romania.

New U.S. designed electronic systems that use solid state circuitry and electro-mechanical phase sensitive signal rectifiers were installed into the instruments. The instruments were then calibrated by comparison with European regional standard Dobson spectrophotometer no. 64, maintained by the German Democratic Republic (GDR). Calibration of instrument no. 64 is traceable to U.S. standard Dobson instrument no. 83.

The instrument calibrations were performed in Potsdam, GDR, in July 1979, at international comparisons sponsored by WMO; participants are listed in table 11.

3.2.3 Data Analyses and Related Research

The quality of total ozone data obtained by NOAA (and it predecessors ESSA and the National Weather Bureau) from the early 1960's continued to be assessed. Research into the overall accuracy of Dobson spectrophotometer ozone measurements indicated that a systematic error of about 5% may be associated with Dobson instrument readings (Komhyr, 1980). The error is postulated to stem from use of an erroneous Dobson instrument short A wavelength absorption coefficient. This research has received considerable interest, and several investigators are examining the problem.

A related investigation concerning the accuracy of Dobson spectrophotometer ozone observations revealed that SO_2 and NO_2 can potentially interfere with ozone measurements since they possess absorption spectra at the Dobson instrument wavelengths (Komhyr and Evans, 1980). In cases of extreme pollution, total ozone measurement errors are estimated to approach 25% because of SO_2 interference and 5% because of NO_2 interference. A number of other constituents of polluted air (i.e., N_2O_5, H_2O_2, HNO_3, acetaldehyde, acetone, and acrolein) have been identified as having absorption spectra at the Dobson instrument wavelengths. Because the absorption coefficients of these trace gas pollutants are small, however, their total contribution to errors in ozone data is negligible.

3.2.4 The Data

Daily 1979 total ozone amounts (applicable to local apparent noon at each station) for all stations in the U.S. network have been submitted for publication on behalf of WMO and are available in Ozone Data for the World, published by the World Ozone Data Center. Mean monthly total ozone values for NOAA observatories and cooperative stations are presented in table 12.

Table 10.--1979 U.S. Dobson ozone spectrophotometer station network

Station	Period of record	Instrument no.	Agency
Bismarck, N. Dak.	010163 - present	33	NOAA
Caribou, Maine	010163 - present	34	NOAA
Tutuila Is., Samoa	121975 - present	42	NOAA
Tallahassee, Fla.	060273 - 053179	58	NOAA/Fla. State Univ.
Mauna Loa, Hawaii	010264 - present	63	NOAA
Wallops Is., Va.	070167 - present	72 & 38	NOAA/NASA
Barrow, Alaska	080273 - present	76	NOAA
Nashville, Tenn.	010163 - present	79	NOAA
Boulder, Colo.	090166 - present	82, 83, & 38	NOAA
White Sands, N. Mex.	010572 - present	86	NOAA/Dept. of Army
Huancayo, Peru	021464 - present	87	NOAA/Huancayo Obs.
Amundsen-Scott, Antarctica	120563 - present	80	NOAA

Table 11.--Participants in the Potsdam international Dobson spectrophotometer comparisons

Country	Inst. No.	Participants
German Democratic Republic	64	A. Bohme, K. Grasnick, P. Plessing, and U. Feister
Czechoslovakia	74	J. Picha, Cenok
Hungary	110	F. Miskolci, A. Sebestyen
Romania	121	M. Frimescu
Poland	84	A. Losiowa, M. Degorska, and B. Rajewska-Wiech
German Federal Republic	44	H. Neuhoff, G. Pereira Brose
France	11	A. Louisa, G. Armand
Canada	-	A. Asbridge
United States	-	R. D. Grass
United Kingdom	-	C. D. Walshaw

Table 12.--1979 provisional mean monthly total ozone amounts (milli-atm-cm)

Location	Jan	Feb	Mar	Apr	May	Jun	Jul	Aug	Sep	Oct	Nov	Dec
Bismarck, N. Dak.	380	396	396	398	385	342	329	309	297	303	330	310
Caribou, Maine	381	430	415	435	375	363	353	335	314	311	347	364
Tutuila Is., Samoa	256	254	251	256	262	261	259	261	267	270	260	265
Tallahassee, Fla.	298	308	330	331	344							
Mauna Loa, Hawaii	262	262	282	299	296	285	277	274	269	258	258	244
Barrow, Alaska			448	450	415	376	334	306	327			
Wallops Is., Va.	350	355	372	380	355	341	329	317	292	297	282	307
Nashville, Tenn.	343	344	383	383	375	348			317	315	298	311
Boulder, Colo.	352	368	375	382	361	323	320	307	295	286	312	293
White Sands, N. Mex.	320	330	336	357	349	318	309	309	297	289	290	288
Huancayo, Peru	259	258	259	261	262	264	268	269	275	267	271	267
Amundsen-Scott, Antarctica	304	284								289	348	351

3.3 Ozone Vertical Distribution

3.3.1 Operations

Since February 1978, regular measurements of atmospheric ozone vertical distribution have been made at Boulder, Colo., using the Umkehr technique (see figs. 8 and 9). Observations are made with a Dobson spectrophotometer, which measures, at large solar zenith angles, the ratio of intensities of scattered light from the zenith sky at two wavelengths in the Huggins ozone absorption bands. The manner in which this light intensity ratio varies with zenith angle depends on the ozone vertical distribution, which can therefore be deduced (see Craig, 1965). Mateer et al. (1980) recently described and tested a short Umkehr technique that utilizes Sun angle and wavelength variations, considerably shortening the observation time.

Observations of the Umkehr effect at Boulder, Colo., have been made using three standard Dobson spectrophotometer wavelength pairs: A, C, and D. Although the ozone vertical profile data presented here were obtained by using the standard evaluation technique (Mateer and Dütsch, 1964) in use at the World Ozone Data Center, Toronto, Canada, the observations on three different wavelength pairs will allow recomputation using the short Umkehr evaluation technique. Umkehr observations and ozone vertical profiles derived from the observations are published by the World Ozone Data Center, Toronto.

In addition to regular Umkehr observations, a series of simultaneous ozonesonde and Umkehr measurements was made. The primary purpose of this simultaneous set of measurements was to help provide a data base for use in developing the short Umkehr method. The balloon-borne ozonesondes provided in situ verification of results obtained by the remote Umkehr technique.

3.3.2 Data Analysis

Figure 8 gives mean monthly ozone amounts deduced in Boulder from Umkehr observations in each of nine atmospheric layers, beginning in February 1978. Pressure ranges for each layer are indicated in the plots. Except for the first few months of the program when observations were relatively sparse, the monthly means have been derived from three to eight observations per month.

An example of a comparison of ozone profiles obtained by the standard Umkehr evaluation technique and a simultaneous balloon-borne electrochemical concentration cell (ECC) ozonesonde measurement is shown in fig. 9.

3.4 Surface Ozone

3.4.1 Operations

Surface ozone measurements were made using the Dasibi ozone photometer at the four GMCC baseline observatories. In addition, the ECC meter was used to make concurrent measurements with the photometer at Mauna Loa and Samoa and, through June, at Barrow. Because of problems with the Dasibi ozone photometer at Samoa during much of the year, most data obtained there came from the ECC meter.

3.4.2 Data Analysis

GMCC Summary Report 1978 (Mendonca, 1979) describes several important variations in surface ozone found at the GMCC baseline observatories. At Mauna Loa,

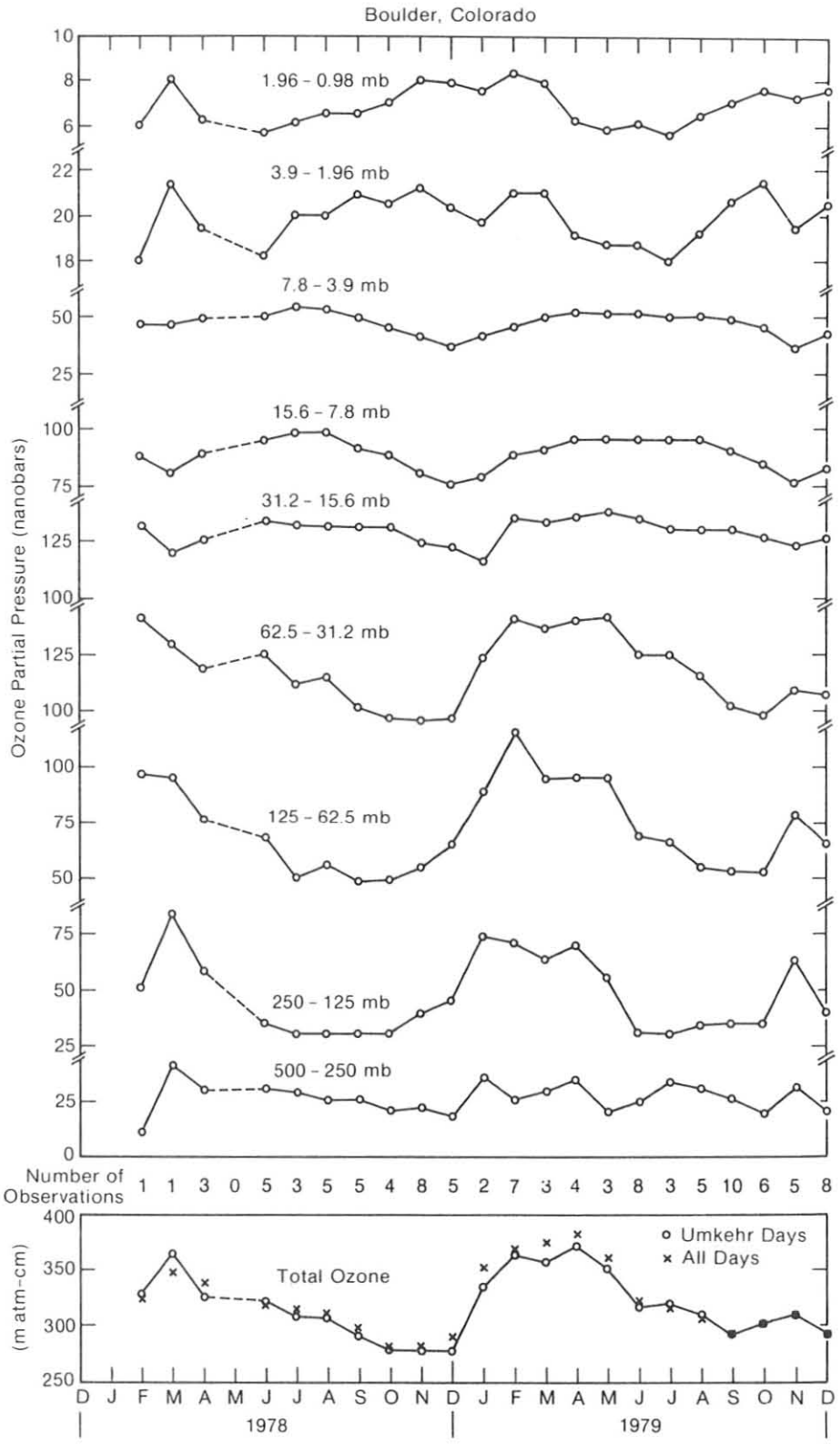

Figure 8.--Umkehr observation mean monthly ozone partial pressures as a function of altitude at Boulder, Colo.

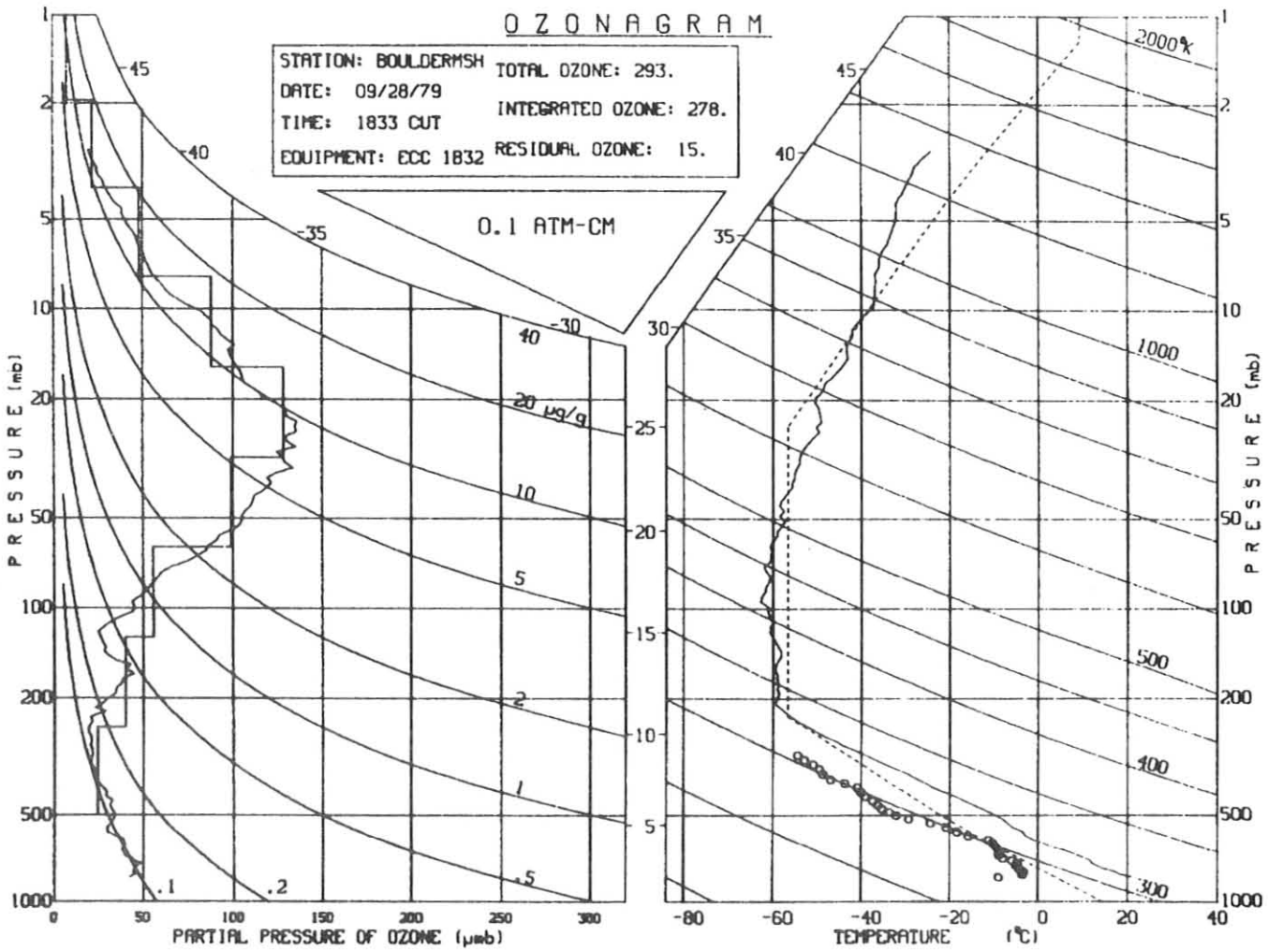

Figure 9.--Example of simultaneous ozonesonde and Umkehr observations made at Boulder, Colo.

for example, there is a strong diurnal variation in surface ozone associated with the mountain wind circulation. The downslope wind regime, beginning in the evening and continuing into the following morning, brings air from the region of the troposphere above the observatory. This air should generally be representative of the ozone content of the free troposphere. During the day, air reaches the observatory from below after passing over vegetated areas at lower altitudes. On the average, the range of this variation is about 15% to 20% of the mean concentration, with the larger values occurring during the downslope wind regime. To check whether the upslope and downslope wind regimes represent different large scale processes in determining the ozone distribution, the annual variation was studied for the two regimes separately. The downslope regime was represented by daily ozone maximum values, whereas upslope flow was represented by daily ozone minimum values. As seen in fig. 10, the behaviors of the seasonal variation for these two regimes are similar on the average. This indicates that the large scale influences on tropospheric ozone are similar throughout the troposphere at Mauna Loa.

The importance of determining the representativeness of surface ozone for understanding tropospheric ozone behavior can be seen by comparing surface data

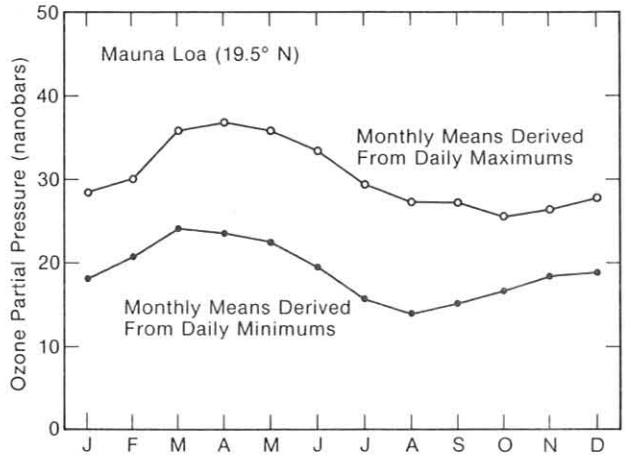

Figure 10.--Monthly mean maximum and minimum surface ozone partial pressure at MLO derived from observations of daily ozone maximum and minimum values.

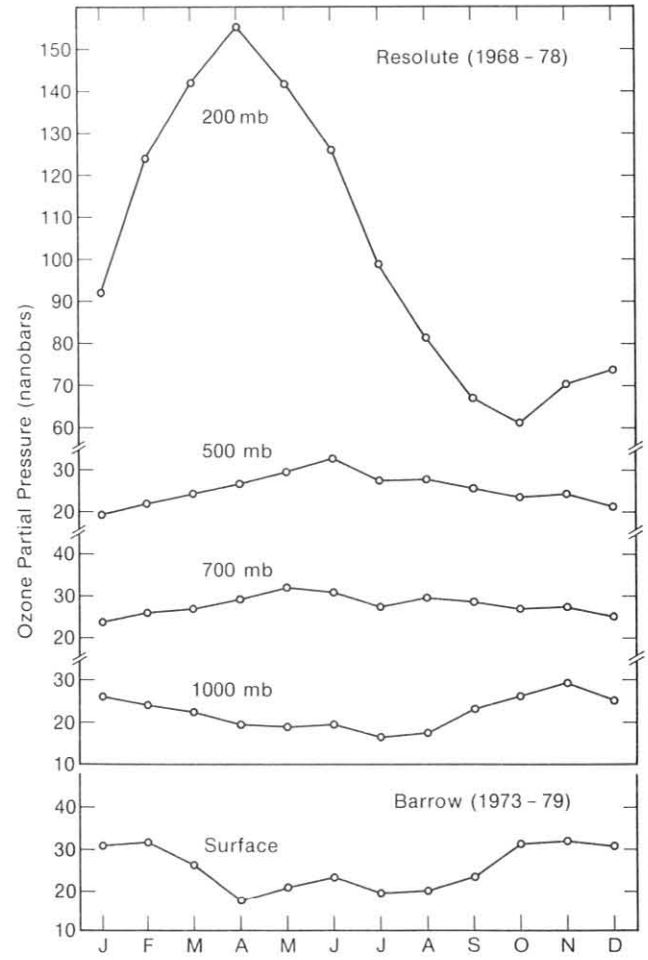

Figure 11.--Monthly ozone partial pressures at various levels in the troposphere at Resolute, NWT, compared with surface ozone at BRW.

from Barrow with data from ozonesondes at Resolute, Northwest Territory. The average monthly ozone behavior at Resolute as a function of altitude for the period 1966 to 1978 is shown in fig. 11. The average Barrow monthly surface ozone variation for 1973 to 1979 (see fig. 11) closely parallels that at 1,000 mb at Resolute. But at higher levels in the troposphere at Resolute the annual cycle is quite different from that at 1,000 mb, indicating that near surface air is not closely coupled with the free troposphere above. The Barrow surface ozone data are useful primarily in studying processes occurring in the lowest layer of the atmosphere, but the data are not highly representative of the free troposphere.

Figure 12 shows updated monthly mean surface ozone values for each of the four GMCC baseline observatories through 1979. Except at Samoa, the 1979 data were obtained with the Dasibi ozone photometer. At Samoa, the more complete ECC data were used. As were data from previous years, daily mean, minimum, and maximum values are archived at the World Ozone Data Center in Toronto, Canada.

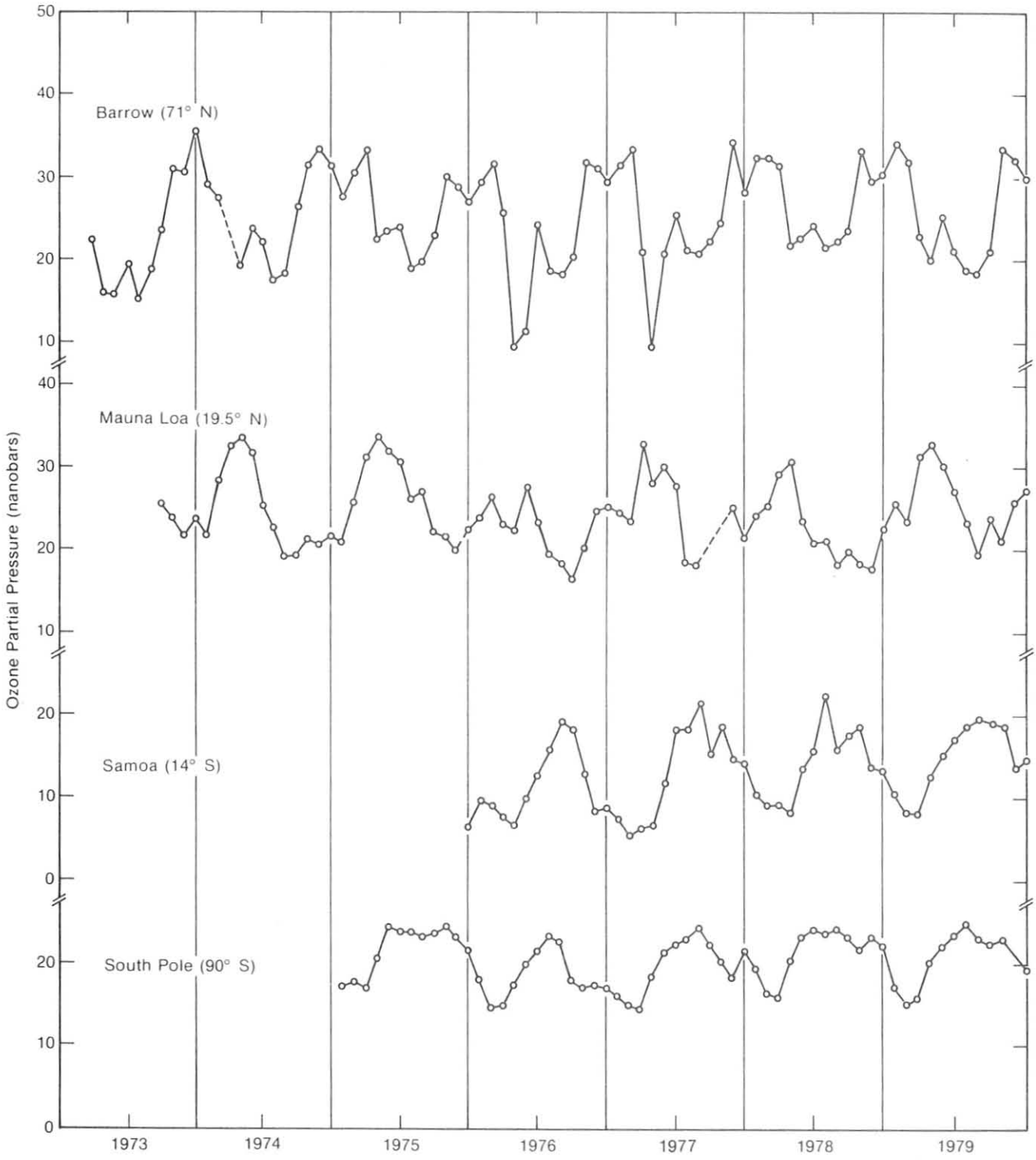

Figure 12.--Monthly mean surface ozone partial pressures measured at GMCC stations.

3.5 Stratospheric Water Vapor

Establishing a program for routine stratospheric water vapor profile measurements was much slower than anticipated. Problems developed in two crucial areas: the balloon system used to carry the frost point instrument in the stratosphere, and the production of the frost point instrument by the manufacturer.

For many years a 7,000-gm neoprene balloon was used to carry the instrument aloft. This specially produced balloon was no longer satisfactory because a number of balloons burst before reaching the desired altitude. It thus became necessary to develop a new balloon system. Working with J. Mastenbrook of the Naval Research Laboratory, we designed and tested a 700-m^3 plastic balloon with a controlled rip patch. This balloon, which ascends at a rate of about 275 m min^{-1} and descends at a rate of about 450 m min^{-1}, has proved moderately reliable but is more cumbersome to launch than the neoprene balloon. Further work is being carried out to make the balloon system more reliable and simpler to launch.

The other major problem experienced during the year was delay in transferring the technology for producing the frost point hygrometer to a commercial manufacturer. Several design changes were made by J. Mastenbrook to simplify the manufacture and improve performance. In earlier versions of the frost point instrument (see GMCC Summary Report 1978) the mirror temperature was kept at the frost point temperature by maintaining the size of the condensate on the mirror essentially constant. A recent improvement to the instrument maintains uniform density (thickness) of the condensate deposit and uses a more sensitive optical detection system to maintain the mirror temperature at the frost point temperature.

3.6 Halocarbons and N_2O

3.6.1 Operations

Collection of air samples for CCl_3F (Freon-11), CCl_2F_2 (Freon-12), and N_2O (nitrous oxide) analyses was continued during 1979 at the four GMCC stations and Niwot Ridge, Colo. Sampling and chromatographic analysis procedures remained virtually identical to those established in mid-1977 (Komhyr et al., 1980). During 1979 sampling frequency was increased at SPO. Beginning with the 1979-1980 austral summer, the sampling rate at SPO one pair sample per week during summer and two pair samples per month during winter. At Niwot Ridge the evacuated flask sampling was replaced with pressurized air sampling, the method of sample collection used at all other GMCC stations. During an overlap period, 7 December 1979 to 30 April 1980, air samples at Niwot Ridge were collected by both methods.

Several problem areas were studied during the year. The scatter in the SPO data for all three constituents was relatively high compared with the data scatter at other stations. In most cases, questionable trace gas concentrations were probably too high because of contamination, but some unreasonably low concentrations were also noted. It is unlikely that such low values are representative of the Antarctic atmosphere. They probably result from adsorption of the trace gases onto walls of the sample cylinders because of prolonged sample storage. An attempt is being made to reduce the magnitude of this problem by selecting and using sample cylinders that have given reliable data in the past. The difficulties experienced point to the desirability of having an on-site gas chromotograph at SPO for halocarbons and N_2O measurements.

We determine halocarbon and N_2O concentrations relative to moist air and use theoretically deduced conversion factors, including relative humidity data, to express results in terms of dry air. Experiments were conducted during 1979 to assess the validity of the theoretical conversion factors in use.

Investigations were also conducted into the stability of trace gas concentrations stored in sample cylinders. It was possible to show that halocarbon and N_2O concentrations did not change by more than 1% in air samples stored for 2 to 3 weeks. This is a normal cylinder residence time for air samples collected at all GMCC stations except SPO.

An important aspect of halocarbon and N_2O monitoring is the procurement and maintenance of stable calibration gases. Uncertainties among various laboratories that prepare calibration gases range from ±5% for F-11 to ±10% for F-12 and N_2O. Instead of preparing calibration gases, we used a high pressure tank of air as a standard. The stability of the halocarbon and N_2O concentrations in this primary standard tank (no. 3072) is being monitored by comparison with similar trace gas concentrations in several other tanks, as well as by interlaboratory comparisons. To date, we have no evidence of any change in F-11 and N_2O in this primary standard. F-12, however, has been drifting at a rate of about 1% per year. F-11, F-12, and N_2O concentrations within our primary standard tank no. 3072 have been calibrated by several laboratories. Results are summarized in table 13.

In table 14 results of four multilaboratory F-11, F-12, and N_2O intercomparisons are listed. GMCC concentrations for specific air samples are compared with

Table 13.--Concentration in GMCC F-11, F-12, N_2O primary reference standard tank no. 3072 as determined by various laboratories

Date	Calibrating laboratory	Type of calibration	Concentration N_2O(ppbr)	F-12(pptv)	F-11(pptv)
Dec 1977	OGC	D*	331.4	353.4	149.1
Oct 1978	OGC	D	331.3	355.3	147.3
Nov 1978	OGC	D	331.5	357.2	149.4
Apr 1979	NCAR	D	317.7	253.7	140.3
Apr 1979	AL/NOAA	D	-	-	139.0
Aug 1979	OGC	I+	328.0	243.2	148.9
Oct 1978	NCAR	I	325.3	255.6	139.0
Oct 1978	AL/NOAA	I	325.3	244	141
Oct 1979	AL/NOAA	I	360.6	251	151

*Direct; +Indirect.

Table 14.--Interlaboratory trace gas concentration comparisons

Comparison organizer	GMCC value (Rasmussen calibration)		No. participating labs	Consensus value	σ
Rasmussen 1976	F-11	145	15	140.2	16
NBS 1976	F-11	194	15	171	23
Fraser 1978	F-11	143.6	7	146.7	3.0
		156.0	8	156.0	5.5
	F-12	250.4	5	255.8	12.3
		258	5	254	7.3
	N_2O	335.4	5	325.6	16
		332.0	5	323	14
Rasmussen 1979	F-11	71	19	62	8
		174		162	23
	F-12	123	19	110	13
		294		279	16
	N_2O	233	19	207	25
		337		321	13

average concentrations for the samples obtained by several other laboratories. Rasmussen (OGC) calibration values were used for GMCC standards in these comparisons. Although most laboratories report a measurement precision of ±1%, the absolute calibrations vary by as much as ±10%, as shown by the standard deviations of the concensus values in table 14. Preliminary tests conducted in the Boulder laboratory indicate that the GMCC N_2O data, reported in the OGC calibration scale, should be adjusted by the factor 0.898.

3.6.2 The Data

F-11, F-12, and N_2O sample data for 1979 are plotted in figs. 13 to 15. All collected data are included in the plots except several (<10) values that fell off scale. The gap in the South Pole record resulted from concentrating sampling there during the austral summer months. More sampling cylinders have since been procured, which will allow enhanced sampling frequency during summer months and sampling during winter.

The gas chromatograph used for sample analyses was inoperative during much of August 1979, resulting in a 1 week or more data loss at all stations, followed by a several week period of questionable results. A small gap in the data record, followed by a number of scattered values, is evident in the August data plots.

The data in figs. 13 to 15 have not been screened for background atmospheric conditions. One unexplained event indicated in fig. 14 is the significant increase

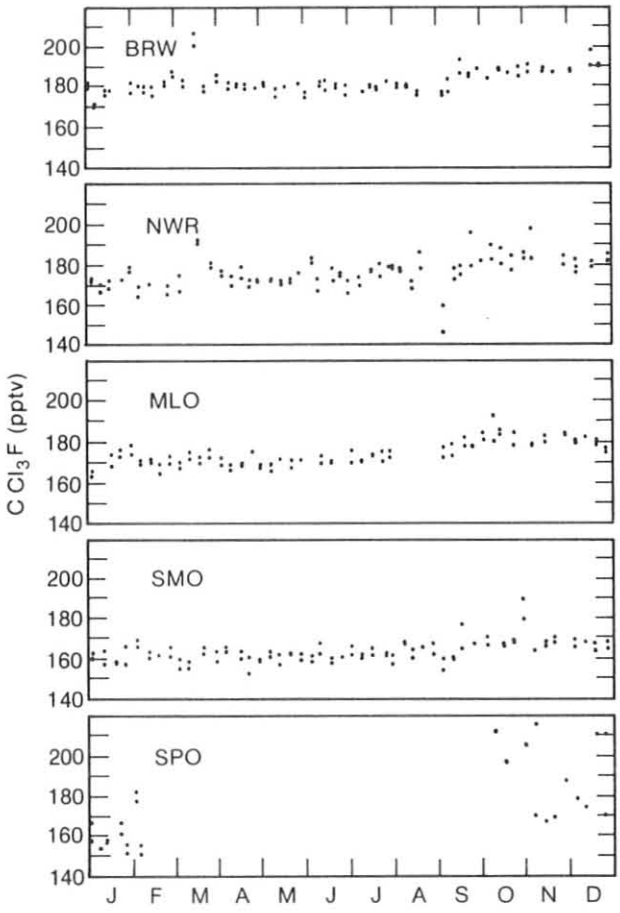

Figure 13.--CCl_3F sample data obtained during 1979 at BRW, Niwot Ridge, MLO, SMO, and SPO.

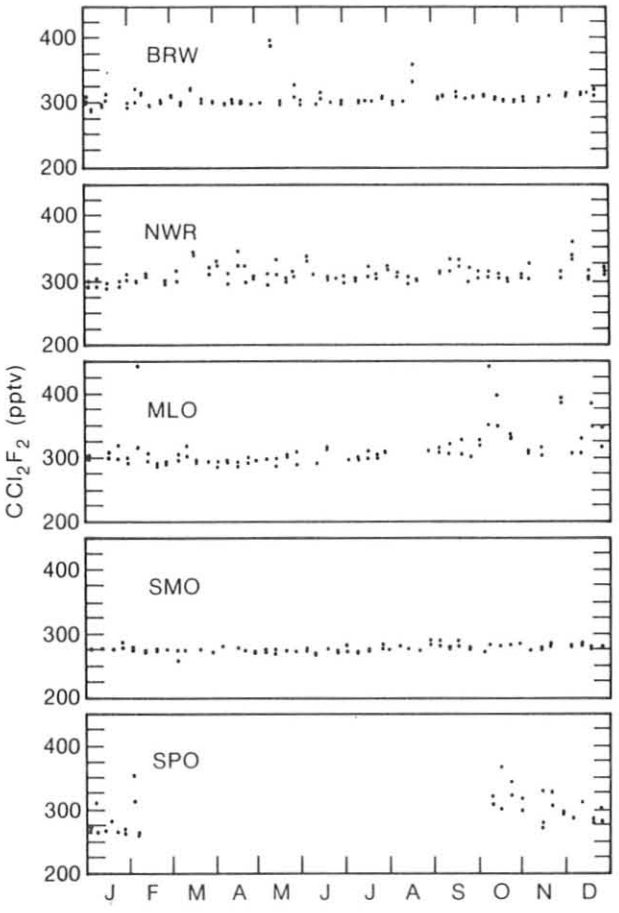

Figure 14.--CCl_2F_2 sample data obtained during 1979 at BRW, Niwot Ridge, MLO, SMO, and SPO.

in scatter of the Mauna Loa F-12 data toward the end of the year. Another perplexing feature is the relatively high N_2O growth rate (~1% yr^{-1}) observed at SMO compared to that measured at all other stations. Whether this growth rate is real or an artifact of sample collection and analyses is not known.

3.6.3 Data Analysis

The 1979 data support the conclusions concerning F-11, F-12, and N_2O global abundances, latitudinal distributions, global growth rates, interhemispheric exchange rates, and atmospheric lifetimes reported in the GMCC Summary Report 1978. A decrease in the rate of increase of F-11 and F-12 in the global background atmosphere is indicated, however, reflecting the decrease in production and release of these chemicals into the atmosphere. The global growth rate of N_2O is still not well established by the data that nevertheless suggest a small interhemispheric gradient with larger values in the north.

Geophysical Monitoring for Climatic Change No. 9

Summary Report 1980

John J. DeLuisi, Editor
Air Resources Laboratories
Boulder, Colorado

December 1981

U.S. DEPARTMENT OF COMMERCE
Malcolm Baldrige, Secretary

National Oceanic and Atmospheric Administration
John V. Byrne, Administrator

Environmental Research Laboratories
George H. Ludwig, Director

NOTICE

Mention of a commercial company or product does not constitute an endorsement by NOAA Environmental Research Laboratories. Use for publicity or advertising purposes of information from this publication concerning proprietary products or the tests of such products is not authorized.

CONTENTS

ACRONYMS AND ABBREVIATIONS

ARL	Air Resources Laboratories, Washington, D.C. (NOAA)
BRW	Barrow Observatory, Barrow, Alaska (GMCC)
CAF	Clean Air Facility, South Pole Observatory, Antarctica (GMCC)
CIT	California Institute of Technology, Pasadena, Calif.
CNC	Condensation nucleus counter
DOE	U.S. Department of Energy, Washington, D.C.
ECC	Electrochemical concentration cell
EML	Environmental Measurements Laboratory, U.S. Department of Energy, New York, N.Y.
EPA	Environmental Protection Agency
G.E.	General Electric
HAMEC	Hawaii Mesoscale Energy and Climate project
HVO	Hawaii Volcano Observatory
IAEA	International Atomic Energy Agency, Vienna, Austria
IAMAP	International Association of Meteorology and Atmospheric Physics
ICDAS	Instrumentation control and data acquisition system
ISWS	Illinois State Water Survey
LBL	Lawrence Berkeley Laboratory, Berkeley, Calif.
MLO	Mauna Loa Observatory, Mauna Loa, Hawaii (GMCC)
MPI	Max Planck Institute, Mainz, Germany
NADP	National Atmospheric Deposition Program
NARL	Naval Arctic Research Laboratory, Barrow, Alaska
NBS	National Bureau of Standards, Gaithersburg, Md.
NCAR	National Center for Atmospheric Research, Boulder, Colo.
NCC	National Climatic Center, Asheville, N.C.
NIP	Normal incidence pyrheliometer
NOAA	National Oceanic and Atmospheric Administration, U.S. Dept. of Commerce
NRL	Naval Research Laboratory
NSF	National Science Foundation, Washington, D.C.
NWS	National Weather Service, Washington, D.C. (NOAA)
OGC	Oregon Graduate Center, Beaverton, Ore.
PIXE	Particle (or proton) induced X-ray emission
SEAREX	Sea-Air Exchange program
SIO	Scripps Institution of Oceanography, La Jolla, Calif.
SMO	Samoa Observatory, American Samoa (GMCC)
SPO	South Pole Observatory, Antarctica (GMCC)
SRL	Smithsonian Institution Radiation Biology Laboratory
SUNYA	State University of New York at Albany
URI	University of Rhode Island, Kingston, R.I.
USGS	United States Geological Survey
WMO	World Meteorological Organization, Geneva, Switzerland
WDC-A	World Data Center-A, Asheville, N.C.

However we may define climate, and I know of no satisfactory formal way, we do know that it changes. We know this from the 200 or 300 years of local instrumental records, from the 100 years of global instrumental coverage, and, more certainly and significantly, from what Wilmot Hess, in the foreword to the first of these Summary Reports, called "ingenious studies of glaciers, pollen, tree rings, sea sediments, and vintners' records." The changes appear on all the time and space scales we have been able to study, and, where it has been possible to quantify the changes statistically, the statistics are neither stationary nor homogeneous and, furthermore, do not lend themselves easily even to quantitative extrapolation in time.

What then can be the purpose of an organization devoted to "Geophysical Monitoring for Climatic Change"? Clearly not to establish the fact that climate changes, nor, in view of the very large quantity of standardized meteorological observations and of the growing potential of satellite systems, to document climate change on the global or any regional scale. The traditional role of monitoring is to provide a timely indication of situations which are about to become manifest, and the traditional monitor is a very sensitive detector of some parameter which is itself a very sensitive indicator that the situation is in being. (A simple analogy to this is a smoke detector alarm.) I do not believe that such an indicator of climate change has yet been unambiguously identified, but there are some very likely candidates, and GMCC is observing them, systematically and with the greatest precision possible, in locations where interference by strictly local activity is absent or can be contained. Such locations are remote, preferably barren, and usually uncomfortable, and operation there is expensive.

Economic conditions change as well as statistics of weather, and, as I write, I am only too well aware of a potentially significant reduction in the resources available for study of the atmosphere. Therefore, the general atmospheric research community is being faced with the problem of curtailing certain programs. Serious thought must be given to retaining the continuity of measurement programs that offer a reasonable chance for unraveling the factors and combinations thereof that cause climate change. Consider, for example, the record of CO_2 concentration in the atmosphere. If much of the thinking on this problem is not in error, the effects of CO_2 concentration increases on global climate should begin to show in the global statistics (perhaps of temperatures in the higher stratosphere) within the next 10 years. If effects do not show, we will have a scientific problem, and, in considering the problem, detail in the record of CO_2 concentration will be important. If the effects do show, we will have an economic problem with enormous implications, and detail in the record of CO_2 concentration will be important in studying its impact. At the present time GMCC carries a major responsibility for the continuity and precision of the CO_2 record. The same reasoning can be applied to the other trace gases and aerosols measured by GMCC. It is a responsibility to the world community.

For a 10-yr period some time ago, I was the Superintendent of Kew Observatory. This institution, for a total of 120 years, has maintained a commendably continuous record of certain weather elements measured in precisely defined conditions. This record has been used for assessments of past climate conditions. (For example, it clearly showed the cold spell of 1880-1890.) When the record was begun, I believe it was unique. After very careful consideration of the Kew record in relation to other records from nearby sources,

and for reasons of economy, the Observatory was recently closed and the record ended. It was ascertained that continuity would not be lost because of the overlapping measurements made by the other nearby observation facilities. The physical surroundings of Kew had unavoidably changed over the years, and the effects could be seen in the record. Therefore, although I have sentimental regrets, I cannot think of any possible adverse effect of the closure on atmospheric science.

I view GMCC as representing a new generation of observatories which are designed partially on the basis of experiences of the older observatories, but which are now internationally connected and judiciously located for detecting changes that are more likely to be global in nature. Modern equipment has greatly improved capabilities for measuring an extended variety of atmospheric variables, including aerosols and chemistry, and it is expected that the remotely located sites will ensure minimum influence from changes in surroundings for many years. A valuable and more complete record for climate research is now being accumulated by these newer observatories, and I believe it will be a considerable number of years before these observatories will have found their mission fulfilled.

G. D. Robinson
Past President and Honorary Member
Royal Meteorological Society

PREFACE

This document presents a summary of the research operations and accomplishments by the Geophysical Monitoring for Climatic Change (GMCC) program and by outside investigators working cooperatively with GMCC in 1980. It includes descriptions of management and operations at GMCC's four baseline sites, scientific data from the measurement projects, conclusions from analyses of data, and recent basic research achievements.

The GMCC program, established in 1971, is one of five research programs within the Air Resources Laboratories under the directorship of Lester Machta. Its four observatories are located at Barrow, Alaska (in service since 1973); Mauna Loa, Hawaii (in service since 1956); American Samoa (in service since 1973); and South Pole (in service since 1957). Background measurements of aerosols, gases, and solar radiation that are important to the climate of the Earth are made at the observatories. The primary groups within GMCC are Monitoring Trace Gases, Aerosols and Radiation Monitoring, Acquisition and Data Management, and Analysis and Interpretation. Specific names of individuals in GMCC are not given in the main text of the report; however, the membership of each GMCC group is given in sec. 9. Publications and presentations by GMCC staff are given in sec. 7.

GEOPHYSICAL MONITORING FOR CLIMATIC CHANGE

NO. 9

Summary Report 1980

1. SUMMARY

At Mauna Loa, an LSI-11 computer system was ordered for the Hilo office to be used for local research projects. An investigation of CO_2 vertical gradients started. Complete refurbishing of the lidar system laser greatly improved operations in 1980. The Meteorological Museum was in operation for its first full year. At Barrow, the Naval Arctic Research Laboratory went to caretaker status, thus terminating its science support activities. GMCC personnel moved to housing provided by NWS in the town of Barrow.

At Samoa, five temporary facility additions were made in preparation for hosting the SEAREX experiment. A comprehensive tracer study of the airflow around Matatula Point was performed by SEAREX and GMCC personnel to determine possible contamination effects from local vegetation and terrain. At South Pole, no additions to facilities were made and all programs operated normally.

The main ongoing GMCC measurement programs at the Observatories continued; these include carbon dioxide, surface and total column ozone, fluorocarbons-11 and -12, nitrous oxide, aerosol scattering coefficient, Aitkin nuclei, solar radiation components, chemistry of precipitation, and associated meteorology. In addition, balloon measurements of stratospheric water vapor and ozone profiles were made at Boulder along with frequent Umkehr ozone profiles. Lidar measurements continued at Mauna Loa. Total ozone was regularly measured at eight additional sites by Dobson spectrophotometers. The CO_2 flask sampling program was expanded by three, to 18 locations (including the Observatories). Many of these data are being archived at the World Data Center-A, Asheville, N.C., and at the World Ozone Data Center, Downsview, Ontario.

Upgrading of foreign Dobson spectrophotometers, under the auspices of the WMO Global Ozone Research and Monitoring Project, continued. To date, 40 instruments have been directly calibrated and 40 others indirectly calibrated relative to the World Primary Standard Dobson no. 83, maintained at GMCC in Boulder. Work continued on automation of a Dobson for routine Umkehr measurements using the short technique. This will allow an increased number of ozone profiles at reduced staff costs.

Climatology analyses for the four GMCC Observatories, using the stations' meteorology data, were performed and reported. Precipitation chemistry protocol at the baseline and regional stations was changed significantly in 1980; all GMCC sites adopted common protocol and procedures of the National Atmospheric Deposition Program.

New hardware was acquired to upgrade the Boulder data reduction facility. This included a NOVA 4/X minicomputer and a Winchester-type disk. Also, stand-alone microprocessor-based data loggers were being developed.

GMCC personnel conducted numerous research projects and data analyses from ongoing programs. Among the topics included were analyses of secular trends of North American total ozone, fluorocarbon-11 and -12, N_2O, Aitkin nuclei, and aerosol light scatter. In recent years, total ozone showed a slight decrease, whereas fluorocarbons continued their marked increase. Aitkin nucleus values at the South Pole (for example) have shown little year-to-year change.

A climatology of airflow arriving at Samoa indicates that during late summer Northern Hemisphere air occasionally, but infrequently, reaches the Observatory. CO_2 anomalies have been detected during such times.

Mauna Loa normal incidence pyrheliometer data were used to develop a technique for obtaining thin-cloud climatology. A persistent trend in thin-cloud transmittance would indicate regional changes in cloud optical thickness.

GMCC CO_2 data were used for several studies. Intermittent flask samplings at selected sites around the globe are expected to contain fluctuations due to small-scale events not of interest for global-scale concerns. The effect of station distribution and frequency of sampling was studied to develop a strategy for providing a truly global annual CO_2 increase. In another study, an eigenvalue analysis of GMCC flask samples yielded large-scale characteristic patterns.

The GMCC CO_2 measurement record from Barrow, 1973-79, was analyzed in some detail. An annual cycle of about 15 ppm was identified. These other investigations of atmospheric CO_2 characteristics are summarized in this report: relationships between Pacific Ocean temperatures and concentrations of atmospheric CO_2 concentrations at Barrow and Mauna Loa; a possible drought-induced signal in the global atmospheric CO_2 record; the variability of CO_2 concentration at Barrow related to synoptic meteorology; and a comparison of midtropospheric airborne samples with measurements at MLO as part of the HAMEC project.

Further work was accomplished on the short Umkehr method. A computer program to invert short Umkehr measurements was completed and tested on 46 short Umkehr observations, and the results were compared with concurrent ozonesonde measurements. Generally good agreement was obtained.

Measurements of the atmospheric radiative effects of the Mt. St. Helens volcanic cloud that appeared over Boulder on May 19 and June 3 were made and subsequently analyzed for the optical properties of the cloud. About 5% of the solar attenuation occurred as absorption. Stratospheric lidar measurements were also made of the cloud at various times between May and August. Distinct aerosol layers were detected at altitudes between 10 and 20 km.

Solar radiation measurements made at Barrow were analyzed for optical properties of the Arctic haze during specific episodes when haze was evident. The technique used to analyze radiation measurements for aerosol properties indicates that a preponderance of small particles exist in the haze. The direct solar beam was depleted by as much as 29%.

In 1980, GMCC supported a substantial number of cooperative research projects. (At Mauna Loa alone, there were about 20 cooperative programs.)

Thirteen summary reports from the projects were contributed to this volume. Several aerosol chemistry investigations were conducted, leading to valuable quantitative interpretation of the characteristics of aerosols sampled at the Observatories. Measurements at Barrow further confirmed that Arctic haze is probably anthropogenic. Moreover, the radiative properties of the Barrow winter aerosol appear to be strongly absorbing in the solar visible band. The solar spectral irradiance and transmission by the atmosphere at Mauna Loa were critically investigated. Sampling of atmospheric gases, crucial to the photochemistry of ozone production, continued, further extending the record built from the previous sampling projects. Methane measurements at Barrow and Samoa were used to document a global secular increase. A major atmospheric chemistry field program, SEAREX, with multi-institution participation, began at Samoa.

2. OBSERVATORY REPORTS

2.1 Mauna Loa

2.1.1 Equipment and Facilities

No major changes to the basic facilities at Mauna Loa (MLO) were effected during the year. Perhaps the most important action was identifying a new computer system for quality control of MLO data and for computations related to special research projects of MLO staff members. The specified system is based on the LSI-11 microprocessor, with peripherals including a disk system, video terminal, and line printer. In addition, an automatic plotter was obtained as government excess equipment.

Aside from the computer system order, the following problems with, or modifications to, the MLO facilities occurred during 1980.

(1) A severe storm accompanied by winds gusting to 85 mi h^{-1} buffeted Hawaii during the period January 8-12 and caused some damage to the buildings at the observatory. The most serious damage was sustained by the storage building, which lost part of its roof. Minor damage at other locations was caused by flooding from the 5-in rainfall accompanying the strong wind. Cleanup and repairs of the damage were completed by the end of January.

(2) Operation of the instrumentation control and data acquisition system (ICDAS) was interrupted 25 times during the year, most frequently because of instantaneous dropouts of line power, but, closely second, because of static discharges in the vicinity of the computer. The reason for one 5-day outage was inadvertent shorting of a destructive voltage through a special circuit that had been installed for monitoring the magnetic tape unit. Problems in reading the operating system tape were experienced on occasion. In general, however, ICDAS operations were as satisfactory as can be expected for a complicated system in a remote location.

(3) A damaged sun photometer was replaced by a new one in March.

(4) A major improvement of the lidar system was completed, with an increase of laser power by about an order of magnitude. The previously used 3/8-in ruby rod was replaced by a 5/8-in rod, and previously damaged windows and mirrors were replaced by new ones. Fortunately, this was all accomplished before the eruption of the Mt. St. Helens volcano.

(5) A detailed map of the MLO site, the first such map ever developed for MLO, was completed in June. Not only are the building locations defined precisely for the first time, but a very useful diagram of the electric power distribution system of the observatory was developed. As a result, two completely useless loops in the electric cables were discovered and eliminated.

(6) A URAS-1 carbon dioxide analyzer was received from Boulder in July and was set up with a multilevel air intake system for investigating vertical gradients of CO_2 concentration under different meteorological conditions.

(7) In a continuing effort to protect the observatory from possible lava flows resulting from eruptions of the volcano, a very detailed and precise topographic map of the upper regions of Mauna Loa was completed in December by

the U.S. Geological Survey (USGS), Flagstaff, Arizona, from special aerial photos. Arrangements for both the aerial survey and construction of the map were made by J. P. Lockwood of the Hawaii Volcano Observatory (HVO), who is also developing plans for the construction of lava barriers above the observatory for deflecting any lava flows that may originate on the higher slopes of the volcano.

(8) One of the automobiles (a Plymouth Fury) assigned to MLO was replaced by a newer model (a Ford Fairmont station wagon) in 1980. This vehicle is much more suitable for hauling the many boxes of flasks and instruments used at the observatory.

2.1.2 Programs at MLO during 1980.

The principal programs carried out at MLO during 1980 are listed in table 1. Brief comments on the programs follow.

Carbon Dioxide

The URAS-2 infrared analyzer continued to operate without major problems during the year, the output being recorded on both the ICDAS magnetic tape and a strip chart recorder. In addition, pairs of 500-mℓ glass flasks were exposed weekly at MLO and Cape Kumukahi and sent to Boulder for analysis. A number of special high density, flask sampling periods occurred throughout the year in connection with programs such as the HAMEC (Hawaii Mesoscale Energy and Climate) project and tests of new methods of flask sample analysis in Boulder.

A special project for investigating vertical gradients of CO_2 concentration was started near the end of the year. Samples are taken at five different levels up to a maximum height of 88 ft above the surface. No definite results were obtained before the end of the year.

Outgassing from the volcanic caldera at the summit of Mauna Loa continued to be recorded in the CO_2 continuous-monitoring measurements, mainly during a downslope windflow regime. Table 2 shows the monthly frequency of occurrence of the outgassing for 1980. The total frequency of outgassing from the caldera for 1980 corresponded well with frequencies in 1978 and 1979, as shown by table 3, but was lower than the years immediately following the July 1975 summit eruption of Mauna Loa. Seismic and other measurements of HVO indicate that the volcano will remain in a generally stable condition, with a slow expansion of the summit area.

Atmospheric Ozone

Total ozone in the atmospheric column was measured on each of approximately 250 days during 1980 by Dobson spectrophotometer no. 63. In addition, the standard reference spectrophotometer no. 83 was shipped from Boulder to make a special series of measurements over approximately 2 months.

Surface ozone concentration was monitored continuously throughout the year by Dasibi and ECC (electrochemical concentration cell) instruments.

Table 1.--Summary of monitoring programs at Mauna Loa in 1980

Monitoring Program	Instrument	Sampling frequency	Remarks
Gases			
Carbon dioxide	URAS-2 infrared gas analyzer	Continuous	
	Evacuated glass flasks	Weekly	Mountain and seacoast
Surface ozone	Electrochemical concentration cell	Continuous	
	Dasibi ozone meter	Continuous	
Total ozone	Dobson spectrophotometer (#63)	Discrete	3 meas., weekdays; 0, weekends
	Dobson spectrophotometer (#83)	Discrete	Special obs. during summer
Fluorocarbons	Pressurized flasks	Weekly	
Aerosols			
Stratospheric aerosols	Lidar	Weekly	694.3 nm, 1 J
Condensation nuclei	Pollak CN counter	Discrete	4 meas., weekdays; 0, weekends
	G.E. CN counter	Continuous	
Optical properties	Four-wavelength nephelometer	Continuous	Wavelengths 450, 550, 700, 850 nm
Skylight polarization	Polarizing radiometer	Discrete	8 wavelengths
Solar radiation			
Global irradiance	Four Eppley pyranometers	Continuous	Cutoff filters at 280, 390, 530, 695 nm
Ultraviolet irradiance	Eppley ultraviolet pyranometer	Continuous	Wavelength range 295 to 385 nm
Direct beam irradiance	Eppley pyrheliometer	Continuous	Wavelength range 280 to 3,000 nm
	Eppley pyrheliometer with filters	Discrete	Cutoff filters at 280, 530, 630, 695 nm
	Eppley 13-channel pyrheliometer	Continuous	13 spectral regions
Meteorology			
Maximum temperature	Maximum thermometer	Daily	
Minimum temperature	Minimum thermometer	Daily	
Ambient temperature	Thermistor	Continuous	
	Hygrothermograph	Continuous	At MLO and Kulani Mauka
Dewpoint temperature	Dewpoint hygrometer	Continuous	
Relative humidity	Hygrothermograph	Continuous	At MLO and Kulani Mauka
Total precipitable water	Foskett infrared hygrometer	Continuous	
Pressure	Electronic pressure transducer	Continuous	
	Microbarograph	Continuous	
Precipitation	Rain gage, 8-in	Daily	At MLO
	Rain gage, 8-in	Twice weekly	At Kulani Mauka
	Rain gage, tipping bucket	Continuous	
Windspeed	Anemometer	Continuous	
Wind direction	Wind vane	Continuous	
Precipitation chemistry			
Acidity of rainwater	pH meter	Discrete	Rainwater collections at 6 sites
Conductivity of water	Conductivity bridge	Discrete	
Chemical components	Ion chromatograph	Discrete	
Cooperative programs			
Carbon dioxide (SIO)	Infrared analyzer (Applied Physics)	Continuous	
	Evacuated flasks	8 mo^{-1}	Mountain and seacoast
Carbon monoxide (MPI)	Special system	Continuous	Chemical reaction with HgO
Surface SO_2 (EPA)	Chemical bubbler system	Every 12 days	
Total surface particulates (DOE)	High-volume filter	Continuous	Dependent on wind direction
Total surface particulates (EPA)	High-volume filter	Every 12 days	
Atmospheric electricity (Univ. of Minnesota)	Field mill, air conductivity meter, surface antenna	Continuous	
Ultraviolet radiation (Temple Univ.)	Ultraviolet radiometer	Continuous	Radiation responsible for sunburning of skin
Precipitation collection (DOE)	Wet-dry collector (Health and Safety Lab.)	Continuous	
Precipitation collection (EPA)	Misco model 93	Continuous	
Precipitation collection (Univ. of Paris)	Likens funnel collector	Twice weekly	
Precipitation collection (IAEA)	Likens funnel collector	Twice weekly	
Wet-dry deposition (Univ. of Illinois)	Exposed collection pails	Continuous	Natl. Atmos. Deposition Program
Atmospheric aerosols (Florida State Univ.)	Special filters	Continuous	
Atmospheric aerosols (Univ. of Maryland)	Nuclepore filters	Continuous	Day-night discrimination
Atmospheric aerosols (Univ. of California)	Nuclepore filters and impactors	Night only	
Atmospheric aerosols (Univ. of Arizona)	Quartz filters	Continuous	Day-night discrimination

Table 2.--Monthly occurrences of outgassing from the volcanic caldera on Mauna Loa

	Jan	Feb	Mar	Apr	May	Jun	Jul	Aug	Sep	Oct	Nov	Dec
No. of days	3	0	9	8	7	16	19	21	11	10	9	8
Percent of days	10	0	29	27	23	53	61	68	37	32	30	26

Atmospheric Aerosols

The aerosol-monitoring program, including the volume scattering coefficient and concentration of condensation nuclei (CN) in the air, continued without major interruptions during the year.

Lidar Observations

As mentioned above, complete refurbishing of the laser, a process which involved purchasing new optical components and repolishing some existing components, resulted in lidar operations in 1980 that were much improved over previous years. Although the optics were all in order by the end of March, electronic problems continued to prevent regular observations for another month. Beginning in May, however, lidar observations were made routinely throughout summer and fall. Twice-weekly observations were made for several weeks following the Mt. St. Helens eruption, but this schedule caused an undue burden on the available staff, so a weekly schedule was set up. The Mt. St. Helens volcanic cloud was first detected over Mauna Loa in early July, some 6 weeks after the May 18 eruption. Intense public interest in the cloud was evidenced by numerous telephone calls received in Hilo following a press release on the event issued by NOAA in Boulder. The lidar continued to operate well, and evidence of the volcanic cloud persisted, until failure of the laser on December 24 terminated lidar measurements for the year.

Solar Radiation

Solar radiation observations continued without serious problems during 1980. Perhaps the most significant difficulty was that improper alignment of

Table 3.--Annual frequency of occurrence of outgassing from the caldera on Mauna Loa during the period immediately before and since the last summit eruption, July 1975

	1975		1976	1977	1978	1979	1980
	Jan-Jul	Aug-Dec					
Percent of occurrences	28	49	42	43	32	32	33

the shading disk for diffuse solar radiation measurements degraded the measurements on occasion during the first 8 months of the year. A careful realignment on September 11 eliminated the difficulty, however, and completely reliable diffuse data were obtained during the remainder of the year. Lightning discharge near the observatory burned out the preamplifier for diffuse radiation measurements on May 12 and again on May 20. Installation of lightning protectors on May 25 apparently corrected the problem. The quartz window pyranometer and two normal incidence pyrheliometers were compared with the Boulder traveling standards, from January 29 to February 1.

Meteorological Parameters

Satisfactory monitoring of the basic meteorological parameters continued during 1980, with only the normal number of equipment problems. An intermittent problem was encountered in automatic recording of ambient temperature, an erroneous thermometer calibration constant in the data acquisition system was discovered and corrected in August, and a spare temperature card and sensor were installed in late September. The aerovane directional servomotor malfunctioned and caused erroneous wind direction data from July 17 to 23. The triple register for wind and precipitation was inoperable April through May, but was put back online on June 6 and operated satisfactorily for the remainder of the year.

Precipitation Chemistry

Measurements of the acidity, conductivity, and ion content of rainwater samples from six sites in Hawaii, as well as of samples from the other GMCC observatories, were continued on a regular basis, and rainwater samples were sent regularly to the International Atomic Energy Agency (IAEA) and the University of Paris. A special effort in collecting and analyzing numerous rainwater samples was made during the HAMEC project, the official period of which was June 11 to 24. Aid was also given to the Illinois State Water Survey (ISWS) in its sequential rain-sampling program.

Fluorocarbons (Halocarbons)

Dual flask samples were taken on a weekly basis and mailed to Boulder for analysis.

Skylight Polarization and Intensity

Measurements of the polarization and intensity of skylight, mainly during periods of morning twilight, were coordinated with lidar measurements of stratospheric aerosols.

Cooperative Programs

A significant component of MLO is the cooperative projects that are carried out by observatory personnel for various universities and government agencies. Most of the cooperative programs listed in table 1 were continued through 1980 without major difficulties. The following items are worthy of special note.

(1) A. Dittenhoefer, an associate in the National Research Council Associateship Program, spent the entire year at MLO conducting a study of

the sulfate content of atmospheric aerosols. The results are scheduled for publication during 1981.

(2) Special solar radiation measurements, which covered the period of January 22 to the end of the year, were conducted by G. Shaw of the University of Alaska. The measurements were made by a 10-filter solar tracking radiometer operated by G. Ferrel, a University of Alaska technician who was stationed at MLO throughout the period.

(3) New instrumentation for carbon monoxide measurements was installed during March by scientists from the Max Planck Institut (MPI), Mainz, Germany. This equipment is much more sensitive than the previous instrument, and, except for a short period during early May, it operated satisfactorily the remainder of the year.

(4) Special solar radiation measurements were made by R. Angione, R. Roosen, and F. Beale of San Diego State University for several days during late March. A malfunction of the microprocessor caused a premature termination of the measurements, however, and the equipment was returned to San Diego in time for investigating the radiative effects of the Mt. St. Helens volcanic cloud as it passed over San Diego.

(5) At the request of R. Fraser of the Goddard Space Flight Center, special measurements of solar radiation in eight different spectral bands were made during late June and early July to obtain an approximate calibration of Fraser's radiometer using Langley plots of the radiation data.

(6) During March, V. Neitzert of MPI took fifty 3-h samples for atmospheric formaldehyde analysis. Liquid nitrogen was used to freeze from the samples many of the atmospheric gases, formaldehyde among them, and the resulting material was fixed in a liquid reagent and taken back to Germany for analysis.

(7) Also during March, M. Darzi of Florida State University used Cascade impactors at several locations on the island for special aerosol collections that were later analyzed in Darzi's laboratory by the particle induced X-ray emission technique (PIXE).

(8) A major revision of the aerosol collection experiment of the University of Maryland was made during the latter part of April. The previous three pumps were replaced by much more powerful ones, thereby increasing the airflow rate by a factor of 4 to 5. Operation of the new pumps is controlled by a sophisticated system of circuitry triggered by four environmental parameters at the observatory: windspeed, wind direction, atmospheric scattering coefficient, and concentration of condensation nuclei. The system operated well during the remainder of the year.

(9) A new procedure for handling wet-dry atmospheric deposition samples was instituted on June 19, at the time of the HAMEC project. Following that date, weekly samples of wet fallout and bimonthly samples of dry fallout have been submitted to ISWS for chemical analysis. The samples are taken as a part of the National Atmospheric Deposition Program (NADP).

(10) Word was received during July that management of the atmospheric electricity program was being transferred from W. Boeck, Niagara University,

to D. Olson, University of Minnesota. One month later, a new and improved field mill and a new antenna for measuring air-Earth current were installed at the observatory. It had been anticipated that data from all the atmospheric electricity instruments would be recorded on magnetic tape by an electronic data acquisition system to be delivered with the new instruments. Unfortunately, the theft of the data logger from an automobile parked overnight in Hilo forced the use of two antiquated strip chart recorders on an interim basis until a new electronic system can be obtained. The strip chart recorders were still in use at the end of 1980.

(11) Two scientists, A. Ashbridge and J. Bellfleur of the Environmental Service of Canada, brought the Canadian Dobson spectrophotometer and a Brewer ozone meter to MLO in late July for comparison of their instruments with the standard Dobson no. 83. They returned to Canada on August 8, having experienced exceptionally good sky conditions at MLO during the comparison period.

(12) A. Hogan, State University of New York at Albany (SUNYA), made some special aerosol collections at MLO during the period June 10 to 18 to measure the size-frequency distribution of the particles.

(13) The laborious task of reading values from the meteorological data charts and transcribing them by hand into tabular format for use by the Scripps Institution of Oceanography (SIO) carbon dioxide program was terminated on July 1. After that date, the meteorological data were transcribed in Boulder from the MLO magnetic data tape. Hand reduction of the CO_2 data from recorder strip charts continues as it has since the start of the measurements in 1958.

2.1.3 Mauna Loa Meteorological Museum

1980 was the first full year of the existence of the Meteorological Museum at MLO. The collections were increased during the year by the following items:

(1) A 4- by 8-ft airbrush painting of Mauna Loa and its environs.

(2) Eight meteorological instruments of various types.

(3) Several dozen books, charts, pamphlets, and other published material on meteorological and related topics.

(4) Original hand-written letters and manuscripts, mainly by the late C. G. Abbot.

(5) Magnetic tape cassettes of conversations with C. P. Butler, former observer at the Smithsonian Solar Observatory, Mt. Montezuma, Chile.

2.2 Barrow

2.2.1 Facilities

The only modification of Barrow (BRW) station facilities in 1980 was the installation of a thermostat-controlled ventilation system in May. Heating and cooling were previously regulated by adjusting individual heaters or cranking windows open, which had little effect during long summer days.

The Naval Arctic Research Laboratory (NARL) started closedown procedures in 1980, culminating in the termination of science support activities and the

departure of University of Alaska staff in October. Operations and maintenance personnel were also reduced as closedown operations progressed, although the final phase has not yet been implemented. GMCC staff moved to housing provided by the National Weather Service (NWS) in the town of Barrow in July and found alternate sources for all supplies and services formerly provided by NARL, with the exception of station electricity, which is still being supplied by NARL.

2.2.2 Programs

Programs carried out at BRW are listed in table 4. Comments on some of the programs follow.

Carbon Dioxide

The continuous analyzer was switched from CO_2-in-N_2 reference gases to CO_2-in-air gases in 1980, with three intercomparisons of CO_2/N_2 and CO_2/air standards being done onsite. Unfortunately, the CO_2/N_2 standards were drained while in transit to Scripps for final calibration, necessitating another series of runs to infer a final value for the lost tanks. Now our procedure for shipping valuable reference tanks is to send the tanks and valve handles separately.

The Cincinnati subzero freezer for freezing water vapor out of samples failed in April, causing suspension of the continuous CO_2 program until a new Cryo-Cool freezer arrived in May.

A second CO_2 sampling line was installed in May. This line, which alternately serves as a quality check on the sampling stack and a ground-level sampling line for periods of high CO_2 activity in the tundra, runs on a time-share basis with the stack.

A 5-ℓ glass flask sampling program began in 1980. Pairs of 5-ℓ flask samples are taken twice-monthly to augment the other CO_2 flask programs.

ICDAS

Severe difficulties with the Xerox multiplexor and Wang tape drive caused much downtime late in the year. New components and a visit to Barrow by some of the Boulder electronics staff solved most of the problems.

Lidar

The lidar hut was repositioned in July to get it out of the winter snowdrift pattern caused by neighboring buildings. System components began arriving in August, but the final parts did not arrive until December. Consequently, there were no lidar operations in 1980.

Total and Surface Ozone

Barrow's Dobson spectrophotometer no. 76 was in Boulder from January to May 1980 for calibration and refitting.

A modernized Dasibi ozone meter was installed in September.

Table 4.--Summary of sampling programs at Barrow in 1980

Monitoring program	Instrument	Sampling frequency
Gases		
Carbon dioxide	URAS-2T infrared analyzer	Continuous
	Glass flask pairs	1 pair wk^{-1}
	5-ℓ glass flask pairs	2 pair mo^{-1}
Surface ozone	Dasibi ozone meter	Continuous
Halocarbons	Flask samples	1 pair wk^{-1}
Total ozone	Dobson spectrophotometer #76	3 day^{-1}
Aerosols		
Condensation nuclei	G.E. CN counter	Continuous
	Pollack counter	Discrete
Optical properties	Four-wavelength nephelometer	Continuous
Vertical distribution	Lidar	Discrete
Solar radiation		
Global spectral irradiance	Four Eppley pyranometers with Q1, GG22, OG1 and RG8 filters	Continuous
Direct spectral irradiance	Eppley normal incidence pyrheliometer with filter wheel	Discrete
Turbidity	Eppley sun photometer	Discrete
Meteorology		
Air temperature	Thermistor	Continuous
	Hygrothermograph	Continuous
Relative humidity	Dewpoint hygrometer	Continuous
	Sling psychrometer	Discrete
Air pressure	Transducer	Continuous
	Microbarograph	Continuous
	Mercurial barometer	Discrete
Wind (speed and direction)	Bendix aerovane	Continuous
Ground temperature	Thermistor	Continuous
Precipitation chemistry		
pH and conductivity	Wide-mouth polyethylene collector (samples analyzed at MLO)	Discrete
	Collection of snow on tundra (samples analyzed at MLO)	2 mo^{-1}
Cooperative programs		
Total surface particulates (DOE/EML)	High-volume sampler	Continuous
Arctic haze particulates (URI)	High-volume samplers	Continuous
	Radon monitors	Discrete
Global radiation (SRL)	Eppley pyranometers	Continuous
	Temple U. sunburning meter	Continuous
CO_2 sampling (SIO)	Flask samples	2 sets mo^{-1}
Precipitation gage (Soil Conservation Service)	Wyoming shielded precipitation gage	2 readings mo^{-1}
Carbonaceous particles (LBL)	High-volume sampler	Continuous
	Surface snow samples	2 mo^{-1}
Halocarbons (OGC)	Flask samples	3 flasks wk^{-1}
Incident and reflected radiation (U. of Alaska)	Up-down pyranometers	Continuous

2.2.3 Cooperative Programs

A halocarbon flask sampling program began with the Oregon Graduate Center (OGC) in May. Three flask samples are taken per week.

The University of Rhode Island (URI) radon experiment was terminated in August.

OGC, Brookhaven National Laboratories, and the National Bureau of Standards ran filters on one of URI's samplers during winter, 1980-81.

A four-radiometer system, composed of two upward-looking and two downward-looking instruments, was installed by the University of Alaska Geophysical Institute in September.

The Barrow staff began making occasional trips to the neighboring village of Atkasuk, 60 mi SSW of Barrow, to read and record measurements by a Wyoming shielded precipitation gage located near there, for the U.S. Soil Conservation Service.

A temporary filter project, to sample for HNO_3, NH_3, and SO_2, was run for the National Center for Atmospheric Research (NCAR) from April through June.

2.3 Samoa

2.3.1 Facilities

There were no permanent additions or modifications to the Samoa Observatory (SMO) facilities during 1980. However, temporary facility additions were made for SEAREX (Sea-Air Exchange program), a planned 1981 project sponsored by the National Science Foundation (NSF). The additions consisted of a number of small prefab buildings located on Matatula Point, where the SEAREX air-sampling experiments will be performed. Five buildings were added: four on the point and one on the ridge adjacent to the GMCC remote sampling tower. Three of the five buildings will be used for laboratory work and two for storage and personnel shelter. Disposition of the buildings after completion of the experiments will be decided later.

The primary SEAREX facility at Matatula Point consists of two walkup towers (Upright Scaffold brand) of 60- and 42-ft heights, used for air and precipitation samplings, respectively. All materials for the buildings and towers were furnished by SEAREX. In anticipation of the increased electrical load from air-sampling pumps, an additional power line was also installed to Matatula Point, with its own meter. The SEAREX project will thus be able to purchase its own electrical power and not overload the GMCC system and backup generator.

2.3.2 Programs

All 1980 programs at SMO are summarized in table 5. Additional comments follow.

Table 5.--Summary of sampling programs at Samoa in 1980

Monitoring program	Instrument	Sampling frequency
Gases		
Carbon dioxide	URAS-2T NDIR analyzer	Continuous
	Evacuated glass flasks	Discrete
Surface ozone	Electrochemical concentration cell	Continuous
	Dasibi ozone meter	Continuous
Total ozone	Dobson spectrophotometer #42	Discrete
Fluorocarbons	Flask sampling	1 wk^{-1}
Aerosols		
Condensation nuclei	G.E. CN counter	Continuous
	Pollak CN counter	Discrete
Scattering properties (surface air)	Four-wavelength nephelometer	Offline all year
Atmospheric turbidity	Volz sun photometer	Discrete
Solar Radiation		
Global spectral irradiance	Four Eppley pyranometers with quartz, GG22, OG1, and RG8 filters	Continuous
Direct spectral irradiance	Eppley NIP with filter wheel (OG1, RG2, RG8)	Discrete
	Eppley NIP/equatorial mount combination	Continuous
Meteorology		
Temperature (air)	Thermistor	Continuous
	Thermograph	Continuous
	Psychrometer	Discrete
	Max.-min. thermometers	Discrete
Temperature (soil)	Thermistor	Continuous
Temperature (dew-point)	thermistor with LiCl dew cell	Continuous
Relative humidity	Hygrothermograph	Continuous
Wind (speed and direction)	Bendix aerovane	Continuous
Pressure	Transducer (capacitance type)	Continuous
	Microbarograph	Continuous
	Mercurial barometer	Discrete
Precipitation chemistry		
pH and conductivity	Orion pH meter	Discrete
	Beckman conductivity bridge	
	Samples sent to MLO for further analysis on ion chromatograph	
Cooperative programs		
ALE project--F-11, F-12, N_2O, $CHCl_3$, CCl_4 (OGC)	HP 5840A gas chromatograph	1 h^{-1}
CH_4, CO, CO_2 (OGC)	Carle gas chromatograph	3 h^{-1}
Flask program--CH_3I, CH_3Cl, CH_4, CO (OGC)	SS flasks, analyzed at OGC--3 flasks per set	1 wk^{-1}
Wet-dry deposition--since may 1980 (NADP)	HASL wet-dry collector	1 wk^{-1}
Wet-dry deposition (DOE/EML)	HASL wet-dry collector	1 mo^{-1}
Wet deposition	Misco collector	1 mo^{-1}

The GMCC group of trace gas and aerosol sensors remained unchanged at the Samoa station during 1980. Absent, however, for the entire year, was the four-wavelength nephelometer. It had been returned to the United States for installation of a new PM tube detector that requires no cooling. It is hoped that this modification will eliminate the moisture problems experienced with the older model detector that required cooling.

A comprehensive CO_2 flask sampling program was also maintained throughout the year as a check for the GMCC/SMO continuous-analyzer air sample line and also as a means of examining possible effects of excessive water vapor, characteristic of Samoan ambient air, on flask samples sent to Boulder.

2.3.3 Cooperative Programs

In May 1980, Samoa GMCC became an NADP collection site, and a weekly rain sample plus a bimonthly dry-deposition sample has been sent regularly to the Central Analytical Laboratory of ISWS. The EPA Misco collector as well as the DOE/EML wet-dry collector will eventually be phased out.

The OGC gas chromatograph installation was operational all year and is the only other major cooperative program. In addition, an OGC weekly flask sampling program was begun to measure methyl iodide concentrations.

2.3.4 Special Projects

A comprehensive tracer study of Matatula Point was performed during April. F. Shais, professor of chemical engineering at California Institute of Technology (CIT), was the principal investigator. D. Reible (CIT), R. Cayer (URI/SEAREX), and Samoa GMCC personnel assisted in 18 experiments using SF_6, smoke flares, and balloons. The purpose of the investigation was to examine the possible contamination effects that local vegetation and terrain might have on planned SEAREX operations in 1981. Results of the tracer study confirmed Cape Matatula as a very good sampling platform. Discussions have begun that may possibly result in publication of the tracer experiment results as a NOAA Technical Memorandum.

2.4 South Pole

2.4.1 Facilities

A structural defect in the Clean Air Facility (CAF) at the South Pole Observatory (SPO) was discovered in late 1979. Cross-member I-beams were found to be deflected more than the design allowed. Reinforcements were made in the 1980-81 summer season.

Electrical power to the CAF was adequate. The room housing GMCC equipment, however, was not adequately wired for the load. Additional equipment placed on certain outlets caused circuit breakers to trip because the room was wired more as living quarters than as a scientific laboratory.

The CAF was adequately built and insulated so that the provided heaters maintained an average room temperature of 21°C. Since all the heaters were

manually set, outside fluctuations in windspeed and temperature caused room temperature fluctuations. There appeared to be a direct correlation between room temperature change and CO_2 analyzer drift. Thermostatically controlled heat would reduce these fluctuations.

The sampling stacks used by GMCC, the University of Maryland, and the Department of Energy (DOE), all required cleaning during the winter because of snow and frost accumulations. At one time, high winds blowing from grid 310° over the inlet of the GMCC gas-sampling stack caused sufficient vacuum force to draw room air up into the stack.

A humidifier was used throughout the year to suppress static discharge. At no time was static buildup noticed.

2.4.2 Programs

SPO programs for 1980 are listed in table 6 and briefly described below.

ICDAS

The NOVA 1220 and associated equipment ran well during the year with only minor outages. (The NOVA power supply failed in December 1979.) The Wang tape drive failed on October 19, 1980, with a burned-out fixed-reel file arm sense lamp.

Modifications to ICDAS included a new NOVA front panel, new Chronolog clock, and a revised edition of the basic operating software (BOSS 79001). The revised software was implemented in November 1979.

The Deltec uninterruptible power supply was shipped to American Samoa in December 1979.

Carbon Dioxide

Continuous measurements of carbon dioxide began on November 18, 1979. The program was restarted after being shut down in November 1978. The same reference gases used before this shutdown were used in the restart. During the first few months the program was characterized by a high zero drift rate and a need for frequent alignments. After station closing, the analyzer settled down and the program proceeded smoothly. A CO_2-in-air reference tank was installed on March 16, 1980, as a surveillance gas. Discrete sampling by flasks continued but at a rate of one pair per week. Samples were alternately taken on the CAF roof and through the analyzer system.

Solar Radiation

The heater blower system worked fairly well in preventing ice buildup on the pyranometer domes. Heavy insulation of the system prevented heat loss and allowed more warm air to the domes.

Calibrations were made once per month on the solar radiation preamplifiers.

Data were collected to study the effect of thermal gradients on the pyranometers' casings and filters caused by heating from the deicing blowers.

Table 6.--Summary of sampling programs at South Pole in 1980

Monitoring program	Instrument	Sampling frequency	Data record
Gases			
Carbon dioxide	0.5-ℓ evacuated glass flasks, hand aspirated/through analyzer	1 pair wk^{-1}	Nov 79-present
Surface ozone	Dasibi ozone meter	Continuous	Jan 76-present
Total ozone	Dobson spectrophotometer #80	Discrete	Dec 63-present
Fluorocarbons	300-mℓ stainless steel sampling cylinders	1 pair wk^{-1}	Jan 77-Dec 79
		1 pair wk^{-1} austral summer	Jan 80-present
		2 pair mo^{-1} austral winter	Jan 80-present
Aerosols			
Condensation nuclei	G.E. CN counter	Continuous	Jan 74-present
	Pollak CN counter	Discrete, 2-4 day^{-1}	Jan 74-present
	Long-tubed Gardner CN counter	Discrete, 1 day^{-1}	Jan 74-Aug 80
Optical properties	Four-wavelength nephelometer	Continuous	Jan 79-Jan 80
Solar radiation			
Global spectral irradiance	Four Eppley pyranometers with quartz, G622, OG1, and RG8 filters	Continuous during austral summer	Feb 74-present
	Ultraviolet radiometer	Continuous during austral summer	Feb 74-present
Direct spectral irradiance	NIP on equatorial tracker	Continuous during austral summer	Oct 75-present
	Filter wheel normal incidence pyrheliometer with quartz, OG1, RG2, and RG8 filers	Discrete during austral summer	Jan 77-present
Meteorology			
Air temperature	Thermistor (naturally ventilated shield)	Continuous	Mar 77-present
Snow temperature	Thermistor	Continuous	Jul 77-present
Pressure	Transducer	Continous	Dec 75-present
	Microbarograph	Continuous	Feb 80-present
	Mercury column	3 day^{-1}	Jan 80-present
Wind (speed and direction)	Bendix-Friez aerovane and recording system	Continuous	Dec 75-present
Atmosphere moisture content	Du Pont 303 moisture monitor	Continuous	Mar 77-present
Miscellaneous			
Room temperature	Thermistor	Continuous	Jul 78-present
Cooperative programs			
Carbon dioxide (SIO)	5-ℓ evacuated glass flasks	2 mo^{-1} (3 flasks per sample)	1957-present
Total surface particulates (atmosphere trace metals) (DOE/ERDA/HASL)	Motor-driven rotary lobe blower (high-volume air sampling through filters)	Continuous (filters changed 4 times mo^{-1})	May 70-present
Turbidity (NOAA/ARL)	Dual-wavelength sun photometer	Discrete during austral summer	Jan 74-present
Carbon-14 sampling (NOAA/ARL)	Pressurized steel spheres	500 lb in^{-2} ambient air day^{-1}, for 6 days	Jan 74-present
Atmospheric chemistry (U. of Maryland and URI)	High-volume filters	Continuous	Jan 79-present
Fluorocarbons (OGC)	5-ℓ evacuated stainless steel cyclinders	3 times during austral summer (3 flasks per sample)	1980

Aerosols

The four-wavelength nephelometer was shipped to Boulder in January 1980 for upgrading. Observations with the long-tubed Gardner CN counter stopped in November 1980 because of poor performance. Continuous aerosol measurements with the G.E. CN counter were made all year and were checked daily with the Pollak CN counter.

Surface Ozone

Surface ozone was measured using a Dasibi ozone meter. Measurements with the ECC meter were discontinued the previous year. No major problems occurred. The MEC-1000 ozone generator failed on two occasions.

The Dasibi manual recommends inspection of the absorption tubes once every 2 months, and cleaning if necessary. Regular cleaning of the tubes, regardless of the inspection, reduced meter noise significantly.

Halocarbons

Sampling frequency was once per week during the austral summer as in previous years. Sampling in the winter was changed from once per month to twice per month. Flasks for use in the winter were pressurized with outside air and stored.

Meteorology

The GMCC wind sensor was realigned to a north-south line surveyed by USGS. The system was overhauled at the same time.

A microbarograph and a mercury column were received in early 1980. These provided a backup and check on the pressure transducer.

The Du Pont 303 moisture monitor malfunctioned between February 14 and November 9, 1980. At that time, the data were found to be several orders of magnitude low. The problem was corrected by replacing the sensor cell.

2.4.3 Special Project

A special project involving processing of GMCC data tapes was carried out at SPO. Fortran programs were written to enable SPO, for the first time, to examine the tapes written by ICDAS. These programs print and plot data in various ICDAS channels for data quality checks. Visual checks of the data by means of graphs help ensure that the instruments and ICDAS are performing properly. These programs are rudimentary, but can be expanded for more sophisticated use.

The computer system at SPO is composed of two 32K and one 16K Hewlett-Packard minicomputers. Peripherals include five tape drives, three terminals, two line printers, and one x-y plotter. The programing languages available on the system are Basic and Fortran IV.

During the winter-over period, six separate Fortran programs were written to read and print compositely either the six solar radiation channels, the six meteorological channels, the resultant windspeed and wind direction, or the separate channels of carbon dioxide, surface ozone, and aerosols. Plots of data in the various channels are made through a different program. For convenience, a program was written to pack hourly averages from the GMCC data tape onto a separate tape. One tape holds nearly 1 year of hourly averaged data. All programs that read directly from the GMCC data tape make use of a routine, written by W. Smythe of UCLA, which converts Data General floating point numbers to HP floating point numbers.

In the future, the SPO system could be used to provide many additional services: for example, to perform statistical calculations, to provide tape-copying facilities to ensure against data loss, and to maintain detailed records of instrument performance.

3. CONTINUING GMCC PROGRAMS

3.1 Carbon Dioxide

3.1.1 Analyzer CO_2 Measurements

CO_2 measurements made with continuously operating nondispersive infrared gas analyzers were continued during 1980 at the four GMCC stations. Data acquisition and processing procedures remained identical to those used in the past. The complete record (including 1980 data) of provisional mean monthly CO_2 mole fractions for BRW, MLO, SMO, and SPO is given in table 7. Plots of the data are shown in fig. 1.

The data are presented in the WMO 1974 CO_2-in-air mole fraction scale, i.e., with tentative pressure-broadening corrections applied. Final corrections to the data are yet to be made and will be based on reprocessing of the data, using improved working-reference-gas concentration values and applications of more precise pressure-broadening corrections. Additional corrections to the SMO data will be needed to account for air line sampling problems that were experienced at the station in the past, caused by the high moisture content of the Samoa atmosphere.

Table 7.--Provisional mean monthly CO_2 mole fractions in ppm for Barrow, Mauna Loa, Samoa, and South Pole

Year	Jan	Feb	Mar	Apr	May	Jun	Jul	Aug	Sep	Oct	Nov	Dec
Barrow												
1973	--	--	--	--	--	--	324.4	322.7	325.7	330.3	334.1	334.5
1974	339.1	336.8	337.6	338.9	337.4	336.4	331.0	325.5	326.4	330.1	333.3	336.7
1975	338.5	338.7	338.2	338.5	339.6	336.1	329.9	324.7	325.8	330.2	335.3	337.0
1976	337.6	337.8	338.8	338.9	338.2	337.1	331.3	323.8	325.1	330.1	334.2	336.5
1977	336.7	336.9	338.2	339.1	339.3	337.8	330.1	326.8	328.0	332.2	334.9	338.8
1978	339.4	340.2	341.7	341.1	340.8	339.6	332.0	328.3	328.6	332.2	338.1	338.6
1979	339.4	340.6	341.7	341.4	341.9	340.9	332.4	327.4	329.4	332.3	337.6	340.7
1980	341.1	341.9	342.9	343.5	343.1	342.7	336.5	331.7	331.3	338.1	340.4	342.9
Mauna Loa												
1974	--	--	--	--	332.9	331.8	330.5	328.5	326.9	326.8	328.0	329.3
1975	330.5	331.2	331.9	333.0	333.6	333.0	331.3	329.4	328.1	328.4	329.4	330.7
1976	331.6	332.5	333.3	334.6	334.8	334.2	332.5	330.3	328.8	328.6	329.9	330.4
1977	332.7	333.1	334.7	335.9	336.6	336.0	334.4	332.3	331.1	331.2	332.6	333.9
1978	335.1	335.3	336.4	337.8	337.9	337.9	336.3	334.2	332.0	332.4	333.7	334.8
1979	336.0	336.5	337.9	338.5	339.0	339.1	337.4	335.2	333.8	334.3	335.1	336.4
1980	337.6	337.9	339.6	340.4	341.1	340.8	338.7	336.8	335.1	335.2	336.4	337.5
Samoa												
1976	333.4	333.0	332.5	332.4	331.7	332.2	332.1	332.2	332.4	332.5	333.1	333.3
1977	333.0	332.5	333.3	333.3	333.6	334.6	334.2	334.1	333.8	335.0	335.2	--
1978	--	335.6	335.4	335.8	335.4	335.7	335.2	335.7	--	--	--	--
1979	--	--	335.7	336.6	336.0	336.4	336.7	336.7	336.6	336.9	337.0	337.3
1980	338.1	338.1	338.1	337.8	338.3	338.0	338.0	337.4	337.3	337.4	337.8	338.6
South Pole												
1975	329.1	329.2	329.3	328.9	328.6	329.1	329.8	330.5	331.0	331.3	330.5	329.4
1976	329.2	328.8	328.7	328.6	328.7	328.9	329.3	329.8	330.4	330.5	330.6	330.5
1977	330.0	330.9	330.7	330.8	330.9	331.1	331.3	331.7	332.1	332.4	332.4	332.1
1978	331.8	331.9	332.6	333.1	333.1	333.5	333.9	334.8	335.4	335.4	335.2	0.0
1979	--	--	--	--	--	--	--	--	--	--	--	--
1980	335.2	335.1	335.1	334.9	335.1	335.4	335.9	336.2	336.5	337.1	337.0	336.7

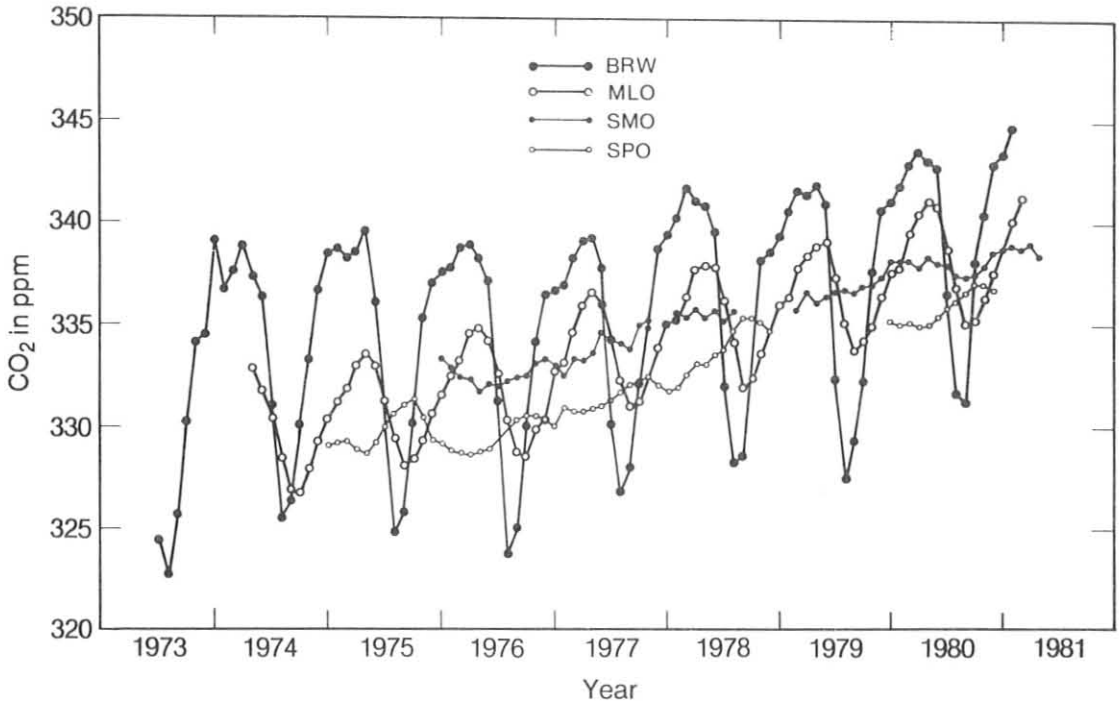

Figure 1.--Provisional mean monthly CO_2 mole fractions for GMCC observatories.

Relative errors in the data are estimated to be less than 1 ppm, except for the first 3 years of the Barrow data and sporadic intervals of the South Pole data where pressure-broadening corrections have been estimated only roughly. Systematic errors are believed to be generally less than ±1 ppm when referred to an absolute CO_2 mole fraction calibration scale.

3.1.2 Flask Sample CO_2 Measurements

The GMCC CO_2 flask sampling program was expanded in 1980 to include three new stations, viz., Azores (Terceira Island, North Atlantic), Mould Bay (N.W.T.), and Seychelles (Mahé Island, Indian Ocean). A list of stations operating in 1980 is given below. Detailed information about these stations, e.g., location, siting, and cooperative agencies, is provided on page 19 of the GMCC No. 8 Summary Report for 1979 (Herbert, 1980).

1980 CO_2 flask sampling station network

American Samoa, S. Pac.
Amsterdam Is., Ind. Oc.
Ascension Is., S. Atl.
Azores (Terceira Is.), N. Atl.
Cape Kumukahi, Hawaii
Cold Bay, Alaska
Cosmos, Peru
Guam (Marianas Is.), N. Pac.
Key Biscayne, Fla.
Mauna Loa, Hawaii
Mould Bay, N.W.T.
Niwot Ridge, Colo.
Ocean Station M, N. Atl.
Palmer Station (Anvers Is.), Ant.
Pt. Barrow, Alaska
Pt. Six Mountain, Mont.
Seychelles (Mahé Is.), Ind. Oc.
South Pole, Ant.

Plots of 1979 and 1980 provisional CO_2 mole fractions, expressed in the 1974 WMO CO_2-in-air mole fraction scale, are shown in fig. 2. Here, pair sample CO_2 values agreeing to within 1 ppm have been averaged; for pair samples differing by more than 1 ppm, the lower value has been plotted. Some available data have been excluded from the plots following subjective analysis because of sampling problems experienced particularly in 1980.

These problems resulted primarily from contamination of the glass flasks with silicone grease residue following annealing of the flasks for cleaning. Additional problems were experienced when contamination occurred at times during flask evacuation and when CO_2-rich air leaked occasionally into evacuated flasks through improperly greased stopcocks. To avoid these sampling problems, the collection of ambient pressure samples in evacuated flasks is currently being phased out. Instead, a method of collecting pressurized air samples in reference-gas-filled flasks is being introduced. Flushing and filling of the flasks during sample collection is accomplished with a portable, mechanized pump apparatus. The flask stopcocks are, furthermore, now greased with Apiezon-N grease.

A prominent feature of the data plots of fig. 2 is the decrease in the amplitude of the CO_2 annual cycle in the Northern Hemisphere, with far-northern peak-to-peak values of approximately 15 ppm decreasing to essentially 0 ppm at the Equator. In the Southern Hemisphere, peak-to-peak annual cycle amplitudes of about 1 ppm are discernible.

Provisional 1979 annual mean, winter (January through March), and summer (July through September) CO_2 latitudinal gradients have been derived from the 1979 and 1980 flask sample data (see fig. 3). Note the large drawdown of CO_2 by growing plants in the Northern Hemisphere summer. The annual mean gradient plot of fig. 3 exhibits several interesting features. The pole-to-pole CO_2 difference is slightly greater than 3 ppm. Also, several maxima appear in the distribution. One occurs in the Northern Hemisphere north of approximately 40°N, which is where most fossil fuel CO_2 is released into the atmosphere. A second occurs at the Equator. A third maximum, possibly representing a Southern Hemisphere CO_2 source, is evident at about 65°S latitude. The existence of this maximum has been inferred from highly tenuous CO_2 observations made at Palmer Station, Antarctica. Additional analyses of the data as well as CO_2 measurements in middle-to-high latitudes of the Southern Hemisphere are needed to verify that this maximum is real.

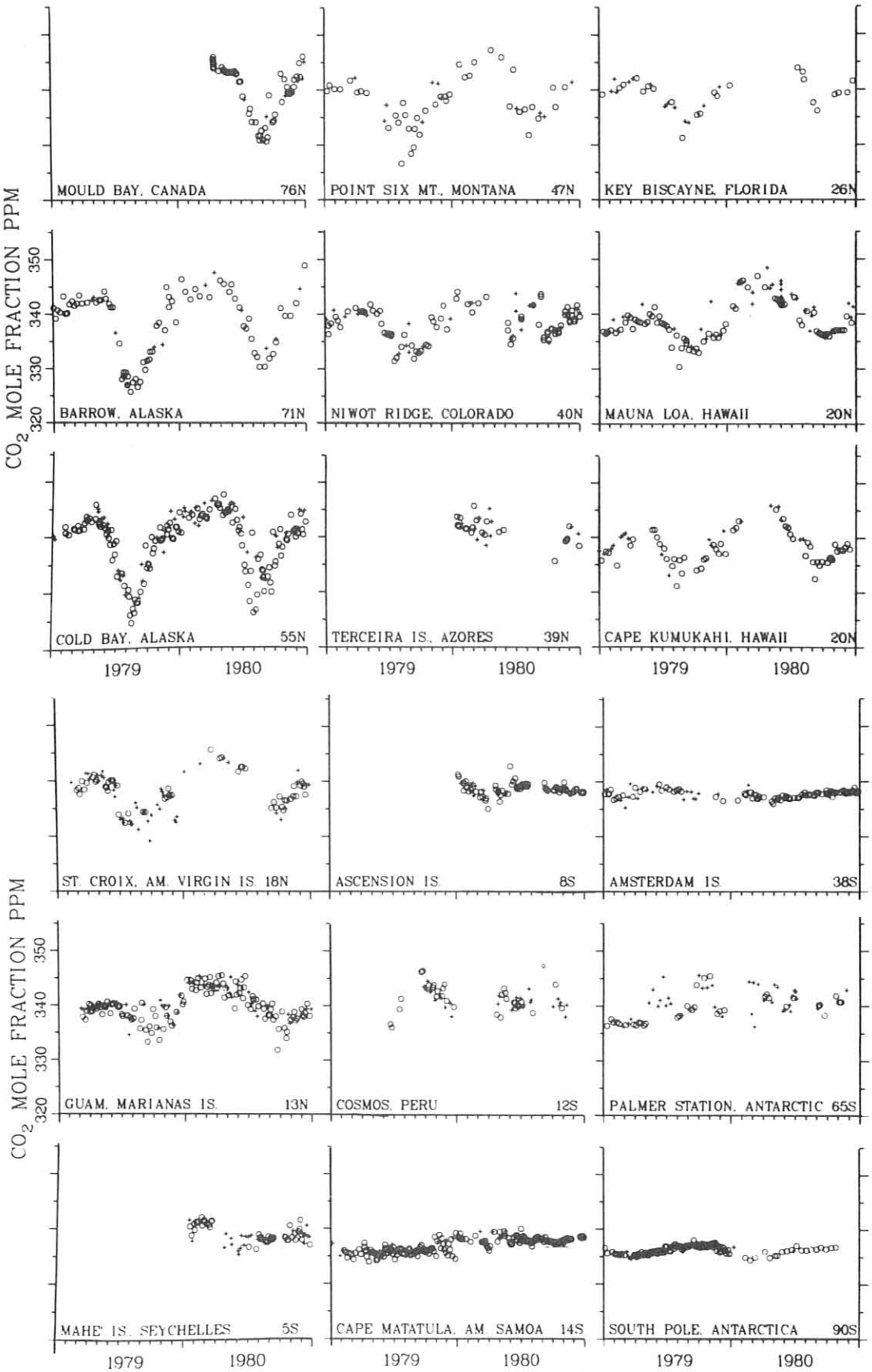

Figure 2.--Flask sample CO_2 mole fractions for stations in the GMCC CO_2 station network.

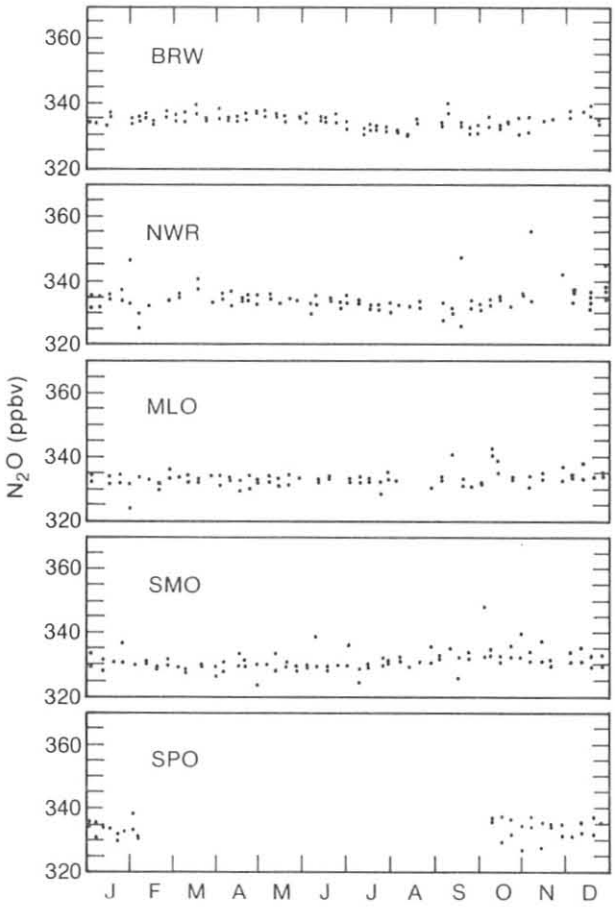

Figure 15.--N_2O sample data obtained during 1979 at BRW, Niwot Ridge, MLO, SMO, and SPO.

3.7 Surface Aerosols

The routine GMCC surface aerosol program for 1979 included the measurement of condensation nuclei concentration and volumetric light scattering at BRW, MLO, SMO, and SPO. Condensation nuclei concentration is measured continuously with a modified version of the G.E. condensation nuclei counter at all four sites. A Pollak (manually operated) condensation nuclei counter is located at each site to serve as a secondary standard and provide calibration points for the automatic nuclei counter. A four-wavelength nephelometer was operating at each site during 1979. This report will present the first light scattering data acquired at SPO.

The calibration of the automatic nuclei counter is checked daily by comparison with the Pollak nuclei counter. If necessary, the automatic nuclei counter is forced to agree with the Pollak counter. The complete calibration procedure and scaling of the data are described by Bodhaine and Murphy (1980). The four-wavelength nephelometers are calibrated by filling them with carbon dioxide gas at 2-mo intervals. The output of the instrument can then be adjusted to give the known volumetric scattering coefficients of carbon dioxide. Bodhaine (1979) gives details of the theory and practice of nephelometer calibration and the latest recommended values of the scattering coefficients of air, argon, carbon dioxide, and Freon-12.

3.7.1 Barrow

Pollak counter SN16 was operated routinely throughout 1979 at BRW. The automatic nuclei counter had several brief periods of downtime on DOY 1-3, 14-15, 123-126, 164-165, 176, 178, and 196-200, with acceptable data for 94% of the hours of the year. The principal cause of downtime was a problem with the high voltage power supply. All data were recorded on magnetic tape and a backup chart recorder. The Barrow nephelometer SN105 operated properly during 1979 except for DOY 84-89, with acceptable data for 96% of the hours of the year. The principal cause of downtime was the weekly relative calibration; however, the instrument was inadvertently left in the test mode, causing the DOY 84-89 downtime.

3.7.2 Mauna Loa

The MLO Pollak counter SN13, the GMCC reference instrument, was operated daily throughout 1979 to provide a record of Pollak counter observations and routine calibration for the automatic nuclei counter. The automatic nuclei counter produced acceptable data during 93% of the year. Most of the downtime (DOY 80-94) resulted from electronic problems caused by a lightning strike at the station.

The MLO nephelometer produced acceptable data for 95% of the year. The lightning strike caused downtime during DOY 80-87; however, channel one of the nephelometer experienced an intermittent problem throughout the year (caused by an AD540J operational amplifier) and produced good data for only 77% of the year. All data were recorded on magnetic tape and a backup chart recorder.

3.7.3 Samoa

Pollak counter SN20 operated routinely at SMO during 1979. The automatic nuclei counter also operated properly throughout the year but because of numerous power outages produced data for only 95% of the year.

The SMO four-wavelength nephelometer, after being in Boulder for repair, was again installed at SMO on DOY 87. However, the instrument developed an intermittent electronic problem and was shipped to the University of Washington for modification and repair on DOY 270. Data were acceptable for approximately 26% of the year. All data were recorded on magnetic tape and a backup chart recorder.

3.7.4 South Pole

SPO Pollak counter SN15 was operated twice daily with no problems during 1979. At the time of each observation, meteorological variables are recorded on the observation form. These observations are subsequently keypunched and are available along with condensation nuclei concentration in the Pollak counter data file. The automatic nuclei counter operated routinely for the entire year producing acceptable data for an astounding 99% of the year.

A four-wavelength nephelometer (SN107) was installed at SPO on DOY 13 and operated satisfactorily until DOY 317 when electronic problems interrupted the data record. Because of long recovery times following power interruptions and relative calibrations, only 68% of the data were acceptable for the year. The instrument was shipped back to Boulder in December 1979. All data were recorded on magnetic tape and a backup chart recorder.

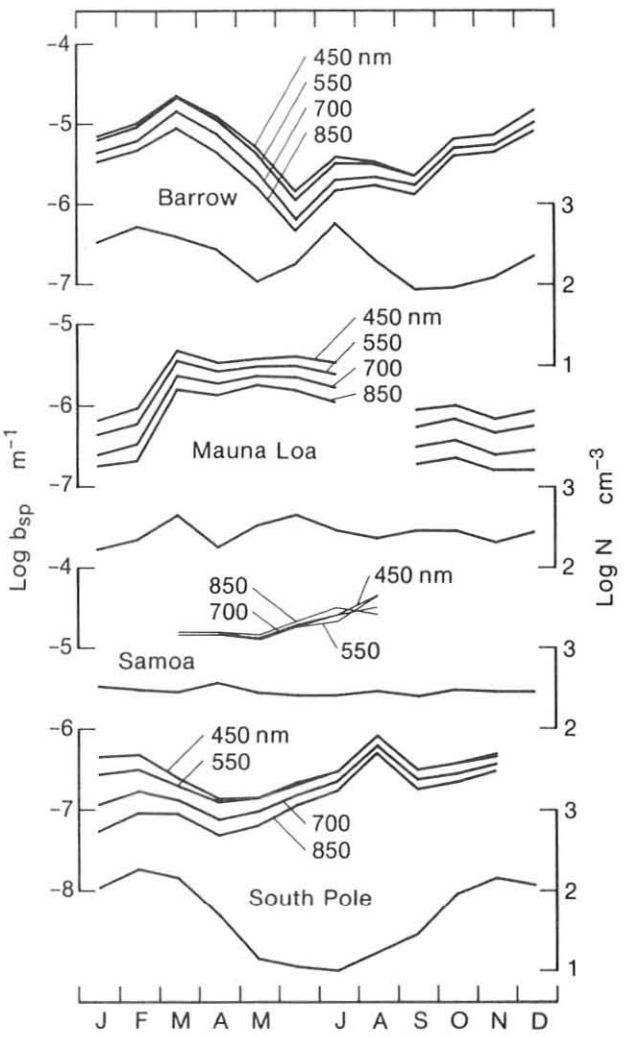

Figure 16.--Light scattering (bsp) and condensation nuclei (N) data for all GMCC stations for 1979. Monthly geometric means were calculated using all data for BRW, SMO, and SPO, and 0000-0800 LST data for MLO.

3.7.5 Data Analysis

Routine aerosol data analysis continues as described in previous GMCC Summary Reports. Observer notes and chart records are perused when received to verify instrument performance and data quality. Monthly tapes constructed by the Data Acquisition and Management Group are accessed and stripped of aerosol data to produce a file of hourly means and a graphic display of 10-min means. At this time the chart record, 10-min mean graphics, and the observer notes are consulted so that a decision can be made as to when the instruments were operating properly and missing computer data may be filled in from the chart recorder data. Finally, data quality is evaluated, data are scaled, and a file of all acceptable data is constructed. All data are available from GMCC in computer printout, microfiche, magnetic tape, or graphics in groups of 10 days per page, 3 months per page, or 1 year per page. The graphics can be presented using hourly means or daily means.

3.7.6 Discussion of Selected Data

Light scattering and condensation nuclei data for 1979 for all stations are presented in fig. 16. All available data were used to calculate monthly geometric

means except for MLO for which only data from 0000-0800 LST were used, to avoid possible contamination from the upslope winds.

The Barrow light scattering data exhibit the same seasonal trend as in the past, with the Arctic haze event in March exceeding 10^{-5} m^{-1} and a minimum in June approximately an order of magnitude smaller. These curves closely follow the seasonal sulfate trend given by Rahn and McCaffrey (1980b), including the small peak in December preceeding the larger peak in March. Condensation nuclei data also show a strong spring peak exceeding 500 cm^{-3} and a second peak in July, caused primarily by small particles since only a small peak in light scattering is seen in July. This summer peak occurs more often in August but is nevertheless seen every year in the Barrow aerosol data.

To identify local sources of contamination in the vicinity of Barrow, Bodhaine et al. (1981) examined the distribution of condensation nuclei (CN) concentration as a function of surface wind direction. Figure 17 gives the mean CN concentration (solid line) calculated from hourly data on a 36-point windrose for the years 1977 and 1978 at Barrow. The pooled standard deviations calculated from 1-min data are also given (dashed line). Winds from the west clearly bring conditions of high nuclei concentration and high variability. Possible local pollution sources at Barrow, as determined by T. DeFoor (Barrow station chief in 1978-79) are shown in fig. 18. The sources to the west of the station coincide with the major peaks of CN concentration shown in fig. 17. Further, the gas well located to the southeast of the station appears to be a fairly constant source in fig. 17. For comparison, a map of the Barrow area may be found in GMCC Summary Report 1973, p. 8.

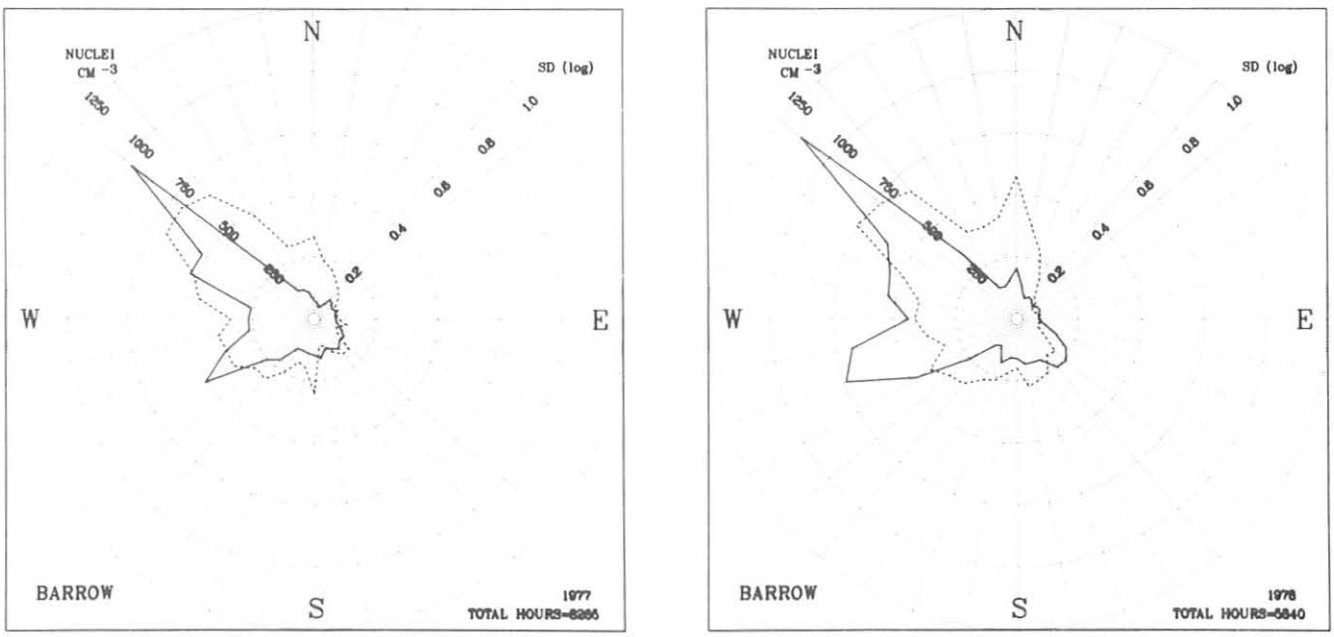

Figure 17.--Geometric mean condensation nuclei concentration (solid lines) as a function of wind direction plotted on a 36-point windrose for BRW during 1977 (left) and 1978 (right). The dashed lines give pooled standard deviations calculated from 1-min data to give a measure of nuclei variability as a function of wind direction.

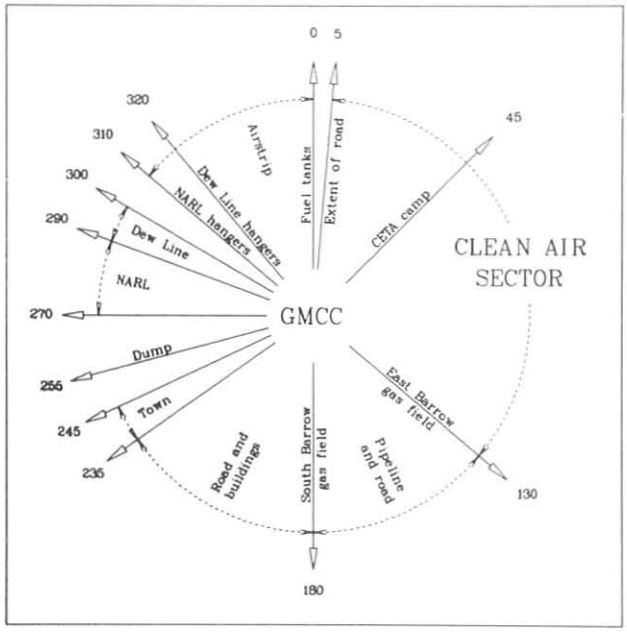

Figure 18.--Locations of possible local pollution sources relative to BRW GMCC site.

Figure 19 presents a 36-point windrose for aerosol light scattering (550 nm) for 1978 and for March 1978 at BRW. Local pollution episodes apparently do not affect light scattering measurements significantly because the instrument responds primarily to particles in the 0.1 μm<r<1.0 μm size range and local pollution episodes consist primarily of smaller particles. The bars at the center of each graph in fig. 19 give the wind frequency for each direction interval. Winds obviously have an easterly component most of the time.

MLO light scattering data shown in fig. 16 exhibit the same annual cycle seen in previous years. The spring maximum is nearly an order of magnitude higher than the clear winter values. The CN data for Mauna Loa again do not show an obvious annual cycle although they appear to follow the light scattering data in a qualitative sense.

Samoa light scattering and condensation nuclei data continue at about the same levels with no obvious seasonal or long term trends.

The first light scattering data for SPO were obtained during the austral winter 1979. These data, presented at the bottom of fig. 16, were surprising because the minimum appears in late April and early May unlike the condensation nuclei minimum that appears in June and July. This difference results because the nephelometer responds primarily to particles in the size range 0.1 μm<r<1.0 μm whereas the nuclei counter also responds to the smaller particles. The winter months apparently are dominated by episodes when sea salt aerosols are transported inland by storms whereas the summer months are dominated by crustal aerosols (see Zoller's summary, p. 93, in Mendonca, 1979). Since the sea salt particles lie in a larger size range, smaller numbers can dominate the light scattering in the winter, with the transition in April and May.

The large peak in light scattering in August tends to dominate the trace for the whole year. This event can be seen more clearly in fig. 20, which gives daily geometric means of both light scattering and CN concentration for the entire year 1979. The event began on 31 July and lasted for about 5 days, reaching a maximum

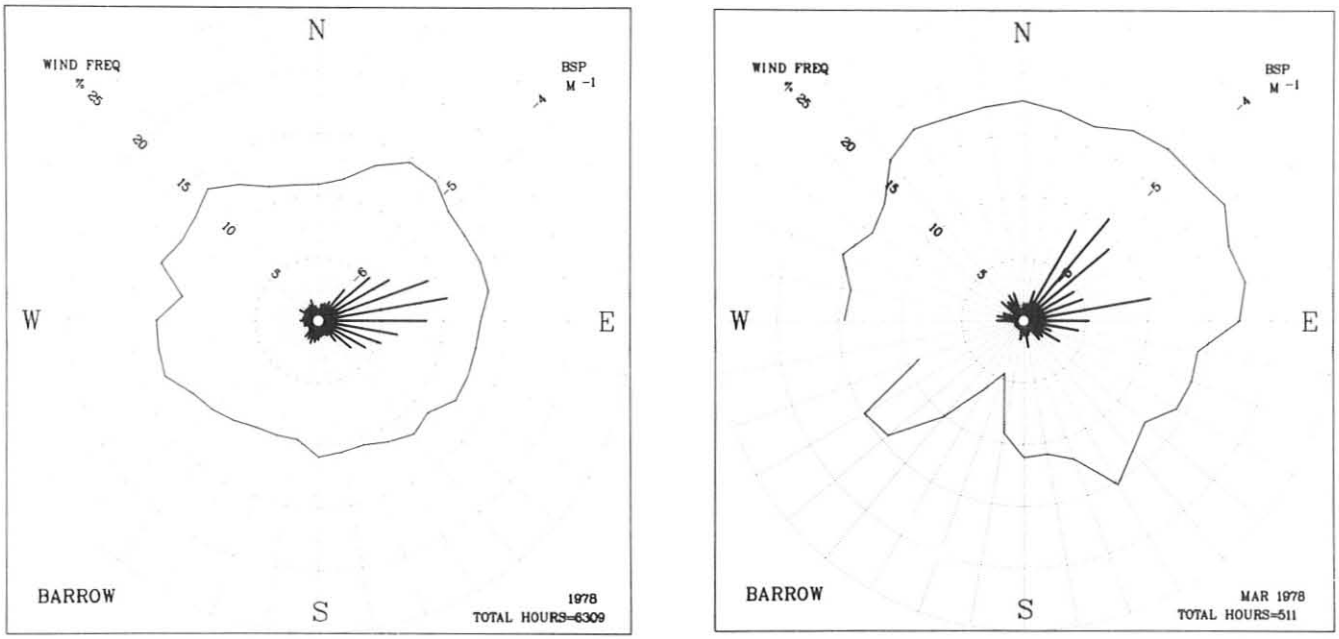

Figure 19.--Windroses showing the geometric mean aerosol light scattering (solid) and wind frequency (center bars) as a function of wind direction for 1978 (left) and March 1978 (right) at BRW.

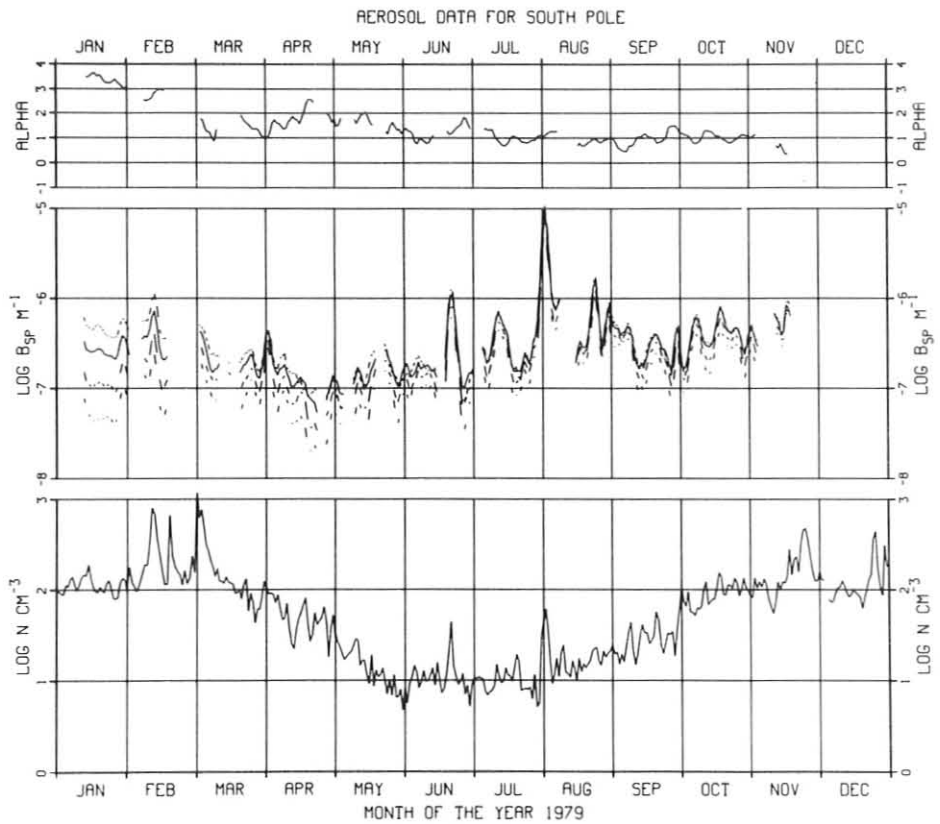

Figure 20.--Daily geometric mean condensation nuclei concentration (bottom), four-wavelength aerosol light scattering (middle), and Angstrom exponent (top) for 1979 at South Pole. The order of the four data channels is shown in fig. 16. The Angstrom exponent was calculated from the 550-nm and 700-nm light scattering data.

of about 10^{-5} m^{-1} for the 550-nm channel. If the relation suggested by Waggoner and Weiss (1980) is used, this corresponds to a mass loading of about 3.2 $\mu g\ m^{-3}$ at the peak of the event. A Nuclepore filter sample of the aerosol in this event was obtained by J. Bortniak, chief of the program that year. Subsequent analysis of the sample by Parungo et al. (1981), using scanning electron microscopy and X-ray dispersive analysis, showed that the aerosol was mostly sea salt with larger sizes than other aerosol samples taken during the year. Bodhaine and Bortniak (1981) have discussed this event in more detail.

The SPO condensation nuclei record continues as in previous years. Murphy and Bodhaine (1980) have presented a detailed description of all CN measurements at SPO.

3.8 Solar Radiation Measurements

Solar irradiance measuring continued at all four baseline stations during 1979, as an integral part of GMCC's long term benchmark parameter monitoring. Discrete normal incidence measurements, plus global irradiance and normal incidence continuous measurements, constitute the program. The measuring instruments that have composed the basic station set since 1975-76 are four Eppley global pyranometers with quartz, GG-22, OG-1, and RG-8 Schott glass hemispheric filter domes, an Eppley UV pyranometer (excluding SMO) with diffusing disk, an Eppley normal incidence pyheliometer (NIP) mounted on a solar tracker (excluding BRW), and a second Eppley NIP with quartz, OG-1, RG-2, and RG-8 Schott glass filter windows on a rotating wheel. Data from the pyranometers and tracking NIP constitute the continuous program, and discrete measuring is done with the filter wheel NIP. The various filters on both the pyranometers and the NIP divide the solar spectrum into narrow bandpass regions. Table 15 gives the wavelengths of the mean windows of transmittance.

3.8.1 Data Acquisition and Verification

NOVA minicomputers at the four baseline stations acquire the solar radiation data, with analog strip chart recorders providing secondary acquisition capabilities. The continuously measuring instruments send milivolt data signals every second into calibrated amplifiers, before digitization and preliminary online

Table 15.--Windows of measurements for quartz and Schott glass cutoff filters*

Filter	Wavelength window (μm)
Quartz	0.28-3.0
GG-22	0.39-3.0
OG-1	0.53-3.0
RG-2	0.63-3.0
RG-8	0.695-3.0
UV	0.295-0.385

*Transmittances can vary slightly with ambient temperature changes and different filter production characteristics.

processing. Monthly calibration checks verify amplifier accuracy. Only amplified voltages are recorded on chart. Magnetic tape records both 1-min voltage sums and hourly irradiance values (miliwatts/square centimeter). Data reformating, editing, and final offline processing occur in Boulder. The processing procedures take into account small scale amplifier performance changes, documented conditions such as dome obstructions or distinctive atmospheric phenomena, and instrument or data acquisition system malfunctions. The final archived continuous pyranometer data are 2-min integrals expressed in kilojoules per square meter, on the absolute radiation scale, as determined by the Davos, Switzerland, pyheliometric intercomparisons of October 1975. Table 16 lists global radiation data archived with the National Climatic Center, Asheville, North Carolina, during 1979 and early 1980. Hourly integral tables and 2-min average global radiation microfilm plots are currently maintained in Boulder.

The GMCC Acquisition and Data Management Group maintains the unedited continuous NIP voltage and irradiance data on the monthly station tapes they create, because no formalized processing routine has been developed. Punch card files of discrete NIP filter wheel measurements along with the corresponding optical air mass values are also maintained in Boulder.

Table 16.--Global solar irradiance data archived during 1979

Station	Tape no.	Time period
MLO	A79208	Jan-Jun 1978
SMO	A79222	Jan-Jun 1978
BRW	A80036	Jan-Jun 1978
SPO	A80075	Jan-Dec 1978

3.8.2 Instrument Calibration History

All field solar radiation instruments are calibrated by intercomparison with Boulder working standard instruments. At approximately 1-yr intervals the instruments are field located so the intercomparisons can be performed. Field instrument instability or degrading bandpass filters, which are age or exposure dependent, as seen in annual standard to station instrument output ratio changes, can be seen in a calibration result time series.

The standard and field global pyranometer intercomparison methodology involves putting the standard instrument online with a calibrated amplifier, simultaneous to the online station set. The instruments are left online together for a given time period, so that they encounter all the station's regional synoptic conditions. Mean ratios (standard quartz/station quartz and station filter domed/standard quartz) are then computed using tabulated hourly instrument irradiance values. Repeating this procedure annually reveals filter dome transmission or station instrument characteristic changes. We assume that the standard instrument, because it is used infrequently, shows no year-to-year sensing changes. Table 17 is a compilation of field pyranometer calibration data over a 4-yr period. SMO intercomparison data reveal noticeable filter dome degrading and transmission reducing, probably because of the corrosive marine environment. The SMO station quartz pyranometer shows a 2.55% degrading output over 3 years. This is not

Table 17.--1977-1980 field pyranometer calibration tests

Station	Date	Std. ins. serial no.	Cal. con. (mV mW^{-1} cm^{-2})	Test ins. serial no.	Cal con. (mV mW^{-1} cm^{-2})	Response std./test	Diff. (%)	Response test/std.
MLO	1/26-1/31/77	10155	0.0725	12616	0.0794	0.9651	3.49	
		10155	0.0725	10151	0.0695			0.9903(GG-22)
		10155	0.0725	10152	0.0735			0.7846(OG-1)
		10155	0.0725	10153	0.0767			0.5832(RG-8)
MLO	6/19-7/11/78	12617	0.0810	12616	0.0794	1.0041	-0.41	
		12617	0.0810	12560	0.0970	0.9864	1.36	
		12617	0.0810	10151	0.0695			0.9422(GG-22)
		12617	0.0810	10152	0.0735			0.7309(OG-1)
		12617	0.0810	10153	0.0767			0.5308(RG-8)
MLO	5/16-5/31/79	12617	0.0810	12616	0.0794	1.0091	-0.91	
		12617	0.0810	12502	0.0952	0.9785	2.15	
		12617	0.0810	10151	0.0695			0.9539(GG-22)
		12617	0.0810	10152	0.0735			0.7450(OG-1)
MLO	1/30-2/1/80	12617	0.0810	12616	0.0794	1.0018	-0.18	
		12617	0.0810	10151	0.0695			0.9631(GG-22)
		12617	0.0810	10152	0.0735			0.7375(OG-1)
		12617	0.0810	10153	0.0767			0.5334(RG-8)
BRW	5/2-5/6/77	10155	0.0725	12263	0.0956	0.9969	0.81	
		10155	0.0725	12265	0.0983			0.9025(GG-22)
		10155	0.0725	12264	0.1051			0.6811(OG-1)
		10155	0.0725	12267	0.0965			0.4697(RG-8)
BRW	4/29-5/9/79	12617	0.0810	12263	0.0956	1.0145	-1.45	
		12617	0.0810	12265	0.0983			0.9043(GG-22)
		12617	0.0810	12264	0.1051			0.6930(OG-1)
SMO	7/19-8/6/78	12617	0.0810	12273	0.0927	1.0100	-1.00	
		12617	0.0810	12274	0.0963			0.9284(GG-22)
		12617	0.0810	15347	0.1048			0.7335(OG-1)
		12617	0.0810	15348	0.1047			0.4984(RG-8)
SMO	6/12-7/2/79	12617	0.0810	12273	0.0927	1.0216	-2.16	
		12617	0.0810	12274	0.0963			0.9270(GG-22)
		12617	0.0810	15347	0.1048			0.7285(OG-1)
		12617	0.0810	15348	0.1047			0.4998(RG-8)
SPO	1/21-1/23/80	12617	0.0810	12273	0.0927	1.0343	-3.43	
		12617	0.0810	12274	0.0963			0.9121(GG-22)
		12617	0.0810	15347	0.1048			0.7034(OG-1)
		12617	0.0810	15348	0.1047			0.4658(RG-8)
SMO	1/7-1/9/77	12617	0.0810	12271	0.1072	0.9905	0.95	
		12617	0.0810	12268	0.1028			0.9144(GG-22)
		12617	0.0810	12269	0.1036			0.7080(OG-1)
		12617	0.0810	12270	0.0978			0.5256(RG-8)
SPO	1/1-1/10/78	12617	0.0810	12271	0.1072	0.9961	0.39	
		12617	0.0810	12268	0.1028			0.9368(GG-22)
		12617	0.0810	12269	0.1036			0.7394(OG-1)
		12617	0.0810	12270	0.0978			0.5310(RG-8)
SPO	1/11-1/13/80	12617	0.0810	12271	0.1072	0.9870	1.30	
		12617	0.0810	12268	0.1028			0.9208(GG-22)
		12617	0.0810	12269	0.1036			0.7080(OG-1)
		12617	0.0810	12270	0.0978			0.4990(RG-8)

considered excessive. All other station data show good stability over the listed time periods.

Pyrheliometer calibration is essentially a simultaneous standard and station instrument measurement, using their respective quartz windows, under the same atmospheric conditions, assuming the same stable standard instrument as with the pyranometer calibration procedure. Intercomparisons are taken only under clear observing conditions. The two instruments are aligned side by side, with their plugs connected to a toggle switch, which is itself connected to a voltmeter. After milivolt instrument outputs are taken, irradiance values are computed and a mean ratio (standard quartz/station quartz) calculated. Table 18 is a compilation of pyrheliometer calibration data for 4 years, using the quartz window. All station instruments are maintaining good stable outputs.

Table 18.--1977-1980 field pyrheliometer calibration tests

Station	Date	Std. ins. serial no.	Cal. con. (mV mW^{-1} cm^{-2})	Test ins. serial no.	Cal con. (mV mW^{-1} cm^{-2})	Response std./test	Diff. (%)
MLO	11/22-11/28/77	13909	0.0774	13910	0.0825	1.0071	-0.71
		13909	0.0774	2119	0.0295	0.9998	0.02
MLO	6/30-7/11/78	13909	0.0774	13910	0.0825	1.0097	-0.97
		13909	0.0774	2119	0.0295	1.0079	-0.21
MLO	5/16-6/1/79	13909	0.0774	13910	0.0825	1.0056	-0.56
MLO	1/29-1/31/80	13909	0.0774	13910	0.0825	1.0016	-0.16
BRW	2/2-2/4/77	13911	0.0856	13913	0.0826	0.9845	1.55
BRW	5/2-5/5/77	13909	0.0774	13913	0.0826	1.0039	-0.39
BRW	4/26-5/9/79	13909	0.0774	13913	0.0826	1.0038	-0.38
SMO	1/6-1/8/77	13909	0.0774	13914	0.0829	1.0110	-1.10
SMO	1/5-1/6/78	13909	0.0774	13914	0.0829	1.0123	-1.23
SMO	7/19-8/9/78	13909	0.0774	13914	0.0829	1.0075	-0.75
SMO	6/21-7/2/79	13909	0.0774	13914	0.0829	1.0124	-1.24
SMO	1/21-1/22/80	13909	0.0774	13914	0.0829	1.0083	-0.83
SPO	12/19-12/30/78	13911	0.0856	13912	0.0815	0.9978	0.22
SPO	12/19-12/30/78	13911	0.0856	2968	0.0259	1.0706	-7.06
SPO	1/12-1/13/80	13909	0.0774	13912	0.0815	.9959	0.41

Calibrating the Schott filters involves the standard instrument with both standard and station filter wheels. The standard pyrheliometer holds the two filter wheels in alignment. Measurements are taken with each filter through one wheel, then two, then reversing the filter wheel order and repeating the procedure. Mean output ratios (one filter/two filters) are computed. This develops a correcting factor that is station filter transmission dependent. Table 19 is a compilation of station filter factor data over the same 4-yr period as table 18. Some shifting transmission characteristics are seen, the greatest being an approximately 3% MLO RG-8 filter transmission increase between 1979 and 1980. However, no continuous filter transmission degrading, with any filter, is seen at any station.

Table 19.--1977-1980 field pyrheliometer filter factor compilation

Station	Date	Std. ins. serial no.	Cal. con. (mV mW^{-1} cm^{-2})	OG-1	RG-2	RG-8
MLO	11/22-11/28/77	13909	0.0774	1.095	1.093	1.103
MLO	6/30-7/11/78	13909	0.0774	1.108	1.096	1.107
MLO	5/16-6/1/79	13909	0.0774	1.091	1.086	1.109
MLO	1/29-1/31/80	13909	0.0774	1.092	1.080	1.076
BRW	2/2-2/4/77	13911	0.0856	1.105	1.110	1.111
BRW	4/26-5/9/79	13909	0.0774	1.089	1.088	1.103
SMO	1/6-1/8/77	13909	0.0774	1.095	1.105	1.100
SMO	1/5-1/6/78	13909	0.0774	1.098	1.103	1.100
SMO	7/19-8/9/78	13909	0.0774	1.095	1.100	1.104
SMO	6/21-7/2/79	13909	0.0774	1.091	1.098	1.099
SMO	1/21-1/22/80	13909	0.0774	1.101	1.112	1.099
SPO	12/19-12/30/78	13911	0.0856	1.094	1.098	1.122
SPO	1/12-1/13/80	13909	0.0774	1.094	1.098	1.122

3.8.3 Field Site Activities Summary

Mauna Loa

Station instruments, trackers, cables, etc., received routine preventive maintenance throughout the year. Regular voltage checks at amplifier board test points verified their performance. When the amplifiers remained undamaged, monthly calibration records revealed steady offset and gain. During January, UV radiometer SN10232 was replaced with UV radiometer SN12350. OG-1 and RG-8 pyranometer amplifiers, plus diffuse pyranometer and 13-channel radiometer amplifiers, because of a February lightning strike, were replaced and recalibrated. Diffuse pyranometer SN12560 was replaced with diffuse pyranometer SN12502 during April.

Samoa

During 1979, as specified in the station daily documentation sheets, solar radiation instruments received regular maintenance at SMO. Amplifier calibration records here show steady offset and gain during the year. A new OG-1 pyranometer amplifier was installed during April. SMO global pyranometers continue exhibiting slow but steady degrading of filter domes, which necessitates more frequent dome replacing than the other stations.

Barrow

BRW station staff carried out routine program maintenance throughout 1979. New OG-1 (SN12264) and RG-8 (SN12267) pyranometer levels and OG-1 mounting holes were installed and cut during July. Instrument orientation was not changed. The filter dome ice crystal buildup problem continues at BRW. Both instrument ring blowers and larger blowers flanking the instruments, which ventilate the filter dome exteriors with warmed air, are used. An intercomparison between the two, involving alternating them online and checking nighttime offset voltage differences which was begun to determine the different blower effects on solar radiation data output, proved inconclusive. Both blowers remain online.

South Pole

During 1979 SPO winterover personnel carried out routine instrument inspecting and scheduled maintenance, as listed in the daily station documentation sheets. The filter dome ice crystal buildup problem occurs at SPO too, although it is less intense and dome buildup is not as severe. Light brushing with a horsehair artist brush will usually clear the domes, although alcohol cleaning is sometimes necessary. The very cold, dry polar plateau air inhibits ice crystal adherance. The instrument ring blower system also does a reasonably effective clearing job. However, its effect on data output is undetermined.

3.8.4 Data

Figures 21 through 28 present 2-min average irradiance plots (kilojoules/square meter) over the true solar day, at the four baseline stations, under the respective area's various representative synoptic conditions. Top to bottom, the curves are flat surface extraterrestrial irradiance, quartz, GG-22, OG-1, and RG-8 pyranometer and UV radiometer (excluding SMO) irradiance data. Contaminated data and instrument or ICDAS malfunctions must be segregated from synoptic induced radiation intensity variations at the Earth's surface. Knowing each station's general regional synoptics and examining the plots allow the segregating. The curve shape is a qualitative identifier of daily synoptic conditions.

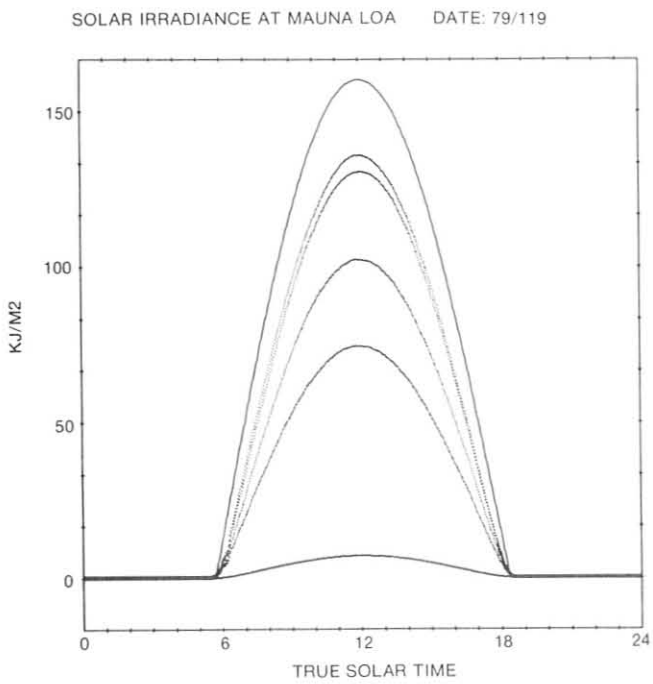

Figure 21.--Solar irradiance at MLO, 29 April 1979. Clear sky conditions under both upslope and downslope air flow regimes, for entire day.

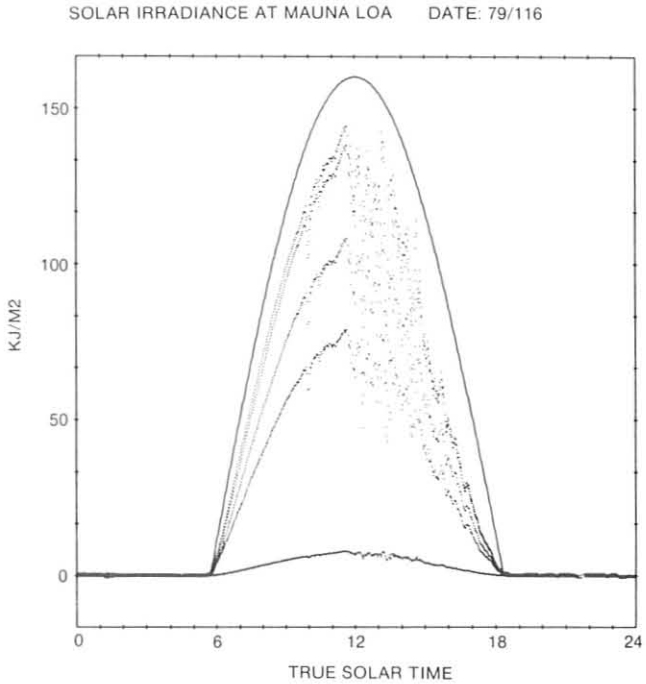

Figure 22.--Solar irradiance at MLO, 26 April 1979. Clear morning sky conditions, sporadic orographic cloud buildup in afternoon (cumulus and stratocumulus).

Figures 21 and 22 show MLO data during diverse conditions. Under the downslope airflow influence during the early morning, upper tropospheric air dominates, and clear sky conditions prevail both days. On 29 April (see fig. 21), the upslope airflow regime, beginning during midmorning, is relatively dry, and the trade wind temperature inversion has remained strong. This effectively inhibits orographic cloud buildup above MLO. During 26 April (fig. 22), the inversion is weak, and the midmorning to afternoon upslope flow is more moist; hence orographic cloud buildup takes place over the station, and the chaotic irradiance patterns are observed.

Figures 23 and 24 present SPO data under differing wind regimes. On December 10 the surface winds were from 060° at 5 m s^{-1}. This indicates cold downslope flow off the polar plateau. Under this regime, clear, very dry conditions occur, with little or no precipitating ice crystals (see smooth irradiance curves in fig. 23). The SPO station complex's solar overpass is between 0700 and 1000 TST. The minute data scatter seen at this time could be related to the station's warm air plume causing sporadic global radiation refraction or attenuation. However, it is more likely that the station power plant exhaust plume causes the scatter, because the plume rises until it reaches the inversion level, under surface wind control, there trailing off in the inversion level wind direction and mixing with ambient air. This could cause small scale clear day curve perturbations. Six weeks earlier on October 23, as depicted in fig. 24, surface winds were off the Weddell Sea, from 340° to 360° at 6 to 10 m s^{-1}. This speed causes moderate to heavy blowing snow that reaches well above the surface. Further, there is greater relative moisture and more ice crystal precipitation. Veiled cirrostratus cloud cover predominates. The pyranometer data point scatter and the irregularity of the curve reflect all these conditions. Filter dome ice crystal precipitation

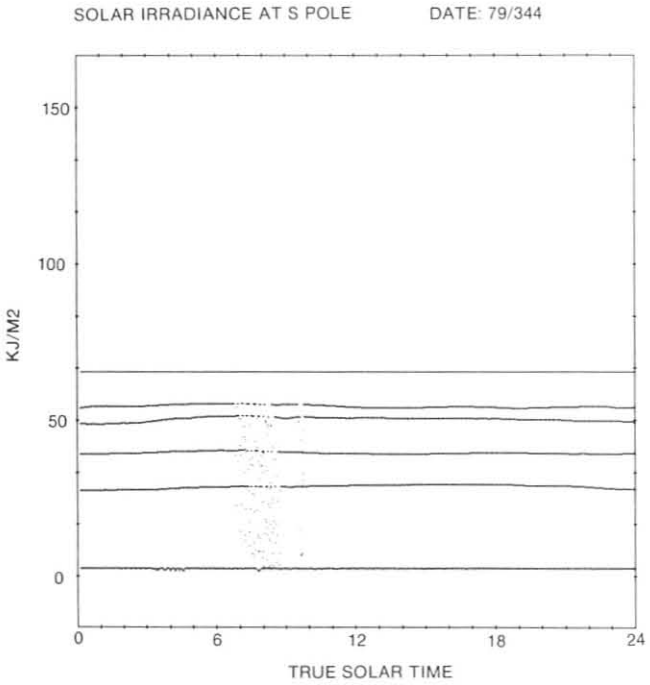

Figure 23.--Solar irradiance at SPO, 10 December 1979. Clear sky conditions for entire day. Isolated sporadic nature of available global radiation in midmorning possibly results from warm air plume or power plant exhaust plume.

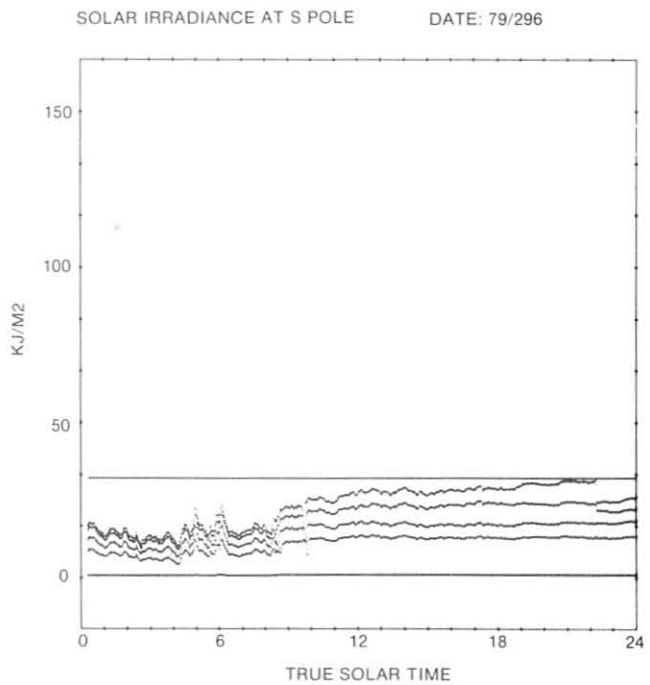

Figure 24.--Solar irradiance at SPO, 23 October 1979. 10/10 thin veil of cirrostratus plus heavy blowing snow and ice crystals in the early morning. 4/10 veil and lightly blowing ice crystals in afternoon. Note quartz and GG-22 filter dome IC buildup (1000-2200 TST) and cleaning (2200 TST).

buildup caused erroneous quartz and GG-22 data between 1000 and 2200 TST. The final data set has these data edited out before archiving.

Figures 25 and 26 shows SMO data plots during different synoptic conditions. The plot for 11 January shows very little available global irradiance reaching the surface. Easterly tropical trade wind induced rain and rainshowers with 10/10 cumulus and stratus cloud cover, both caused by orographic moist trade winds air lifting against the island's central mountains, dominate the synoptic pattern for the day. Data point variability and curve shape in fig. 25 show these conditions. Figure 26, the 30 January irradiance data plot, accurately represents the weather pattern for the day. Broken orographically induced cumulus, which average 4/10 cover over the day, cause the quantitative variance between small and large data point scatter throughout the day.

Figures 27 and 28 present BRW pyranometer data under varying cloud covers. During 20 April, a thin veil of cirrostratus with 6/10 average sky cover and moderate blowing snow were observed throughout the day. Scatter about clear day curves in fig. 27 depict these conditions. Further, April is the month when the Arctic haze phenomenon occurs and various European industrial region pollutants are transported toward BRW over the polar region. These phenomena could cause additional data point variability. Note that the variability is comparable to that in fig. 24, which presents SPO data under similar conditions. Figure 28,

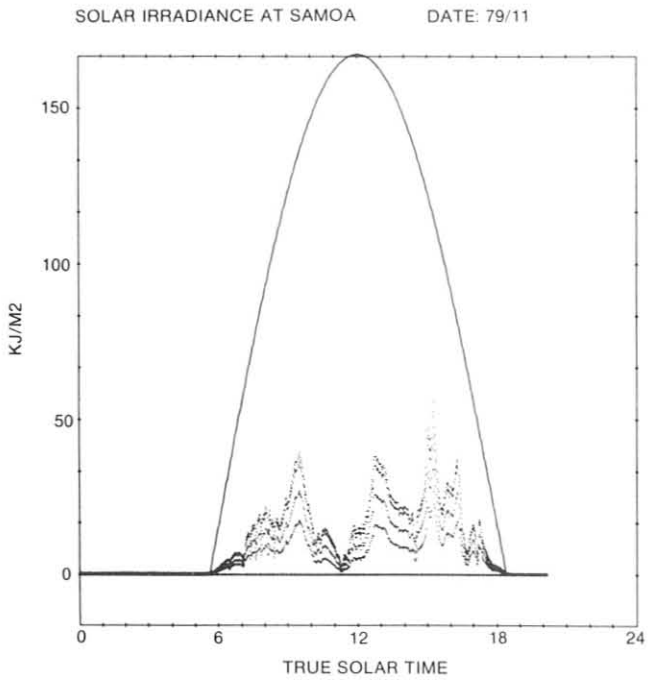

Figure 25.--Solar irradiance at SMO, 11 January 1979. 10/10 cumulus and stratus cloud cover for the day with rain and rainshowers.

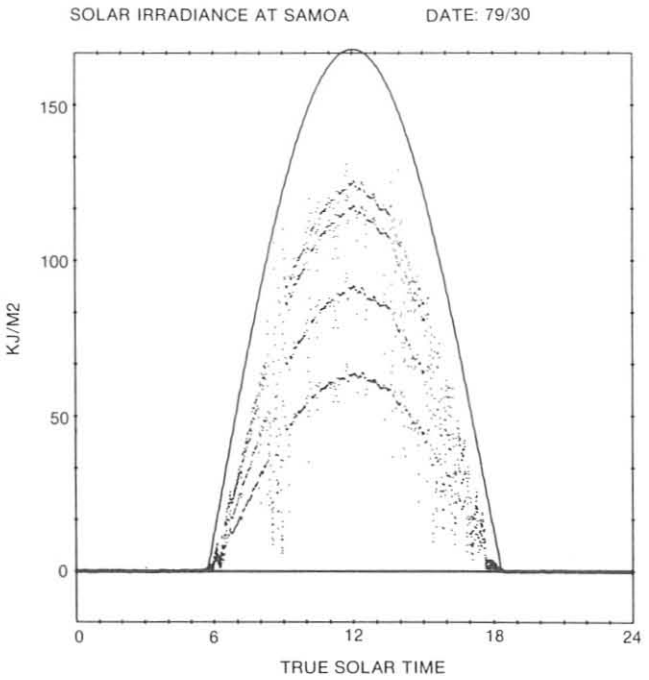

Figure 26.--Solar irradiance at SMO, 30 January 1979. Broken cumulus cloud cover averaging 4/10 for the day.

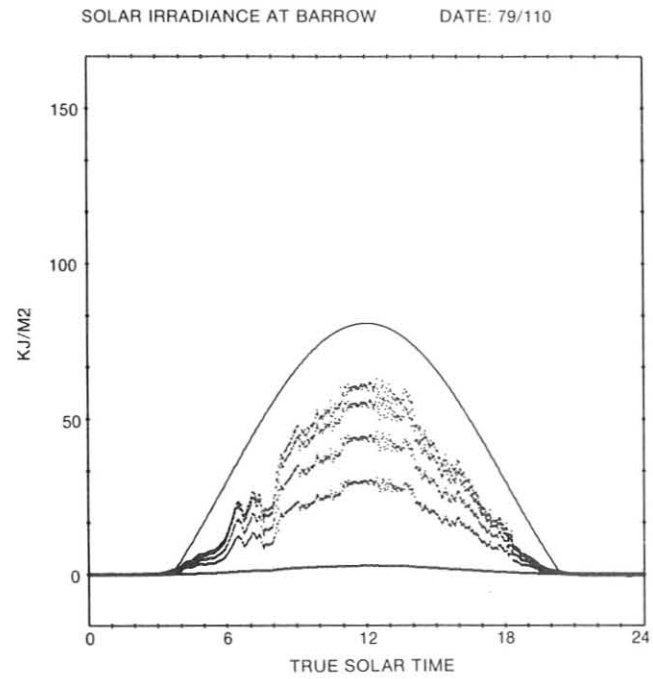

Figure 27.--Solar irradiance at BRW, 20 April 1979. 6/10 thin veil of cirrostratus and moderate blowing snow throughout observing day.

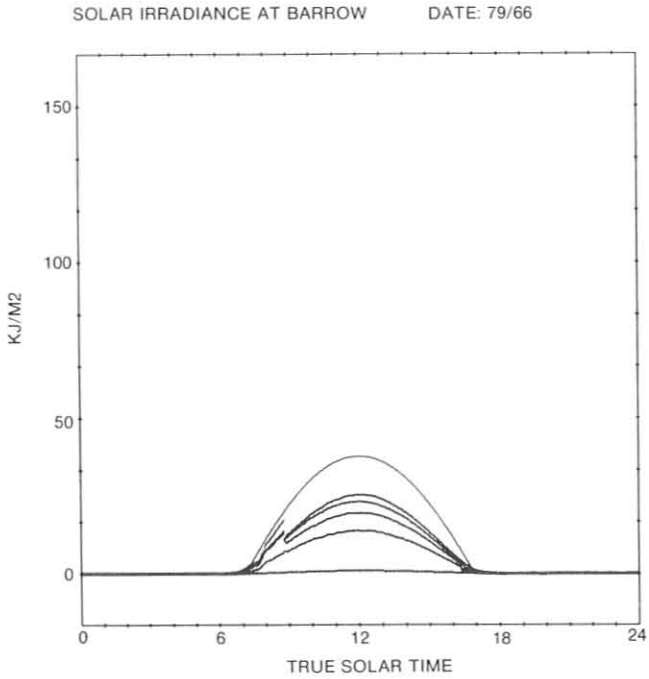

Figure 28.--Solar irradiance at BRW, 7 March 1979. Clear sky conditions for entire day. Note quartz, GG-22, and OG-1 filter dome IC buildup (0800-0900 TST) and cleaning (0900 TST).

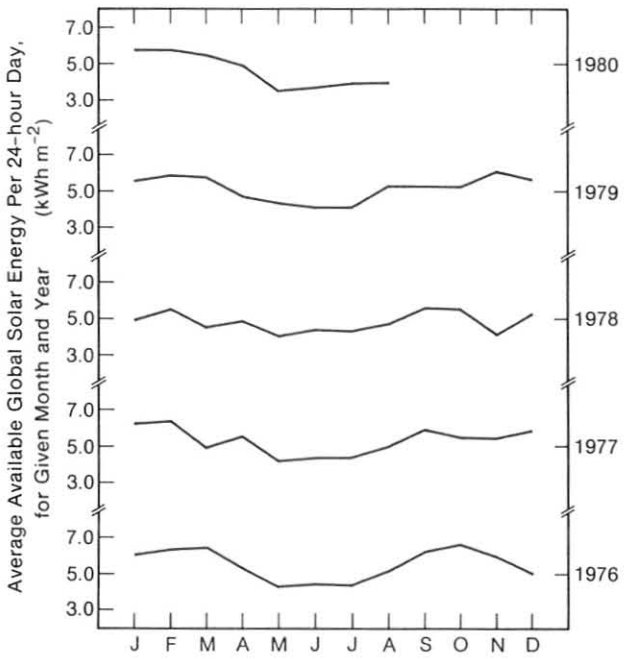

Figure 29.--Available solar energy at SMO in 1976-80.

representing 7 March, shows BRW data under clear sky conditions all day. As in fig. 24, erroneous pyranometer data are seen between 0800 and 0900 TST because of precipitation obscured quartz, GG-22, and OG-1 filter domes. Edit routines before archiving eliminate these.

As a part of GMCC's Acquisition and Data Management Group's project to convert SMO station power to a solar and wind system, a daily and monthly dependent available global solar energy study was undertaken. Daily total available, monthly total available, and average daily available global solar energy data (kilowatt-hour/square meter) over a 4½-yr period were prepared for analysis. Figure 29 presents measurements of average daily available energy, during any given month and year, from January 1976 to August 1980. The expected midyear decrease is evident, because austral winter solar elevation is lower. The year-to-year average daily available energy changes during the austral winter months are less than the summer month changes, which implies more synoptic variability during these warmer, wetter months (September to March). Figure 30, which presents a daily total available global solar energy during 1978, shows the day-to-day synoptic variation reflected in available energy changes. Examining the overall curve reveals the austral winter decrease previously mentioned and a pattern equivalent to the 1979 curve in fig. 30. However, the wide ranging day-to-day variability is caused primarily by the changing weather patterns, specifically cloud cover and precipitation.

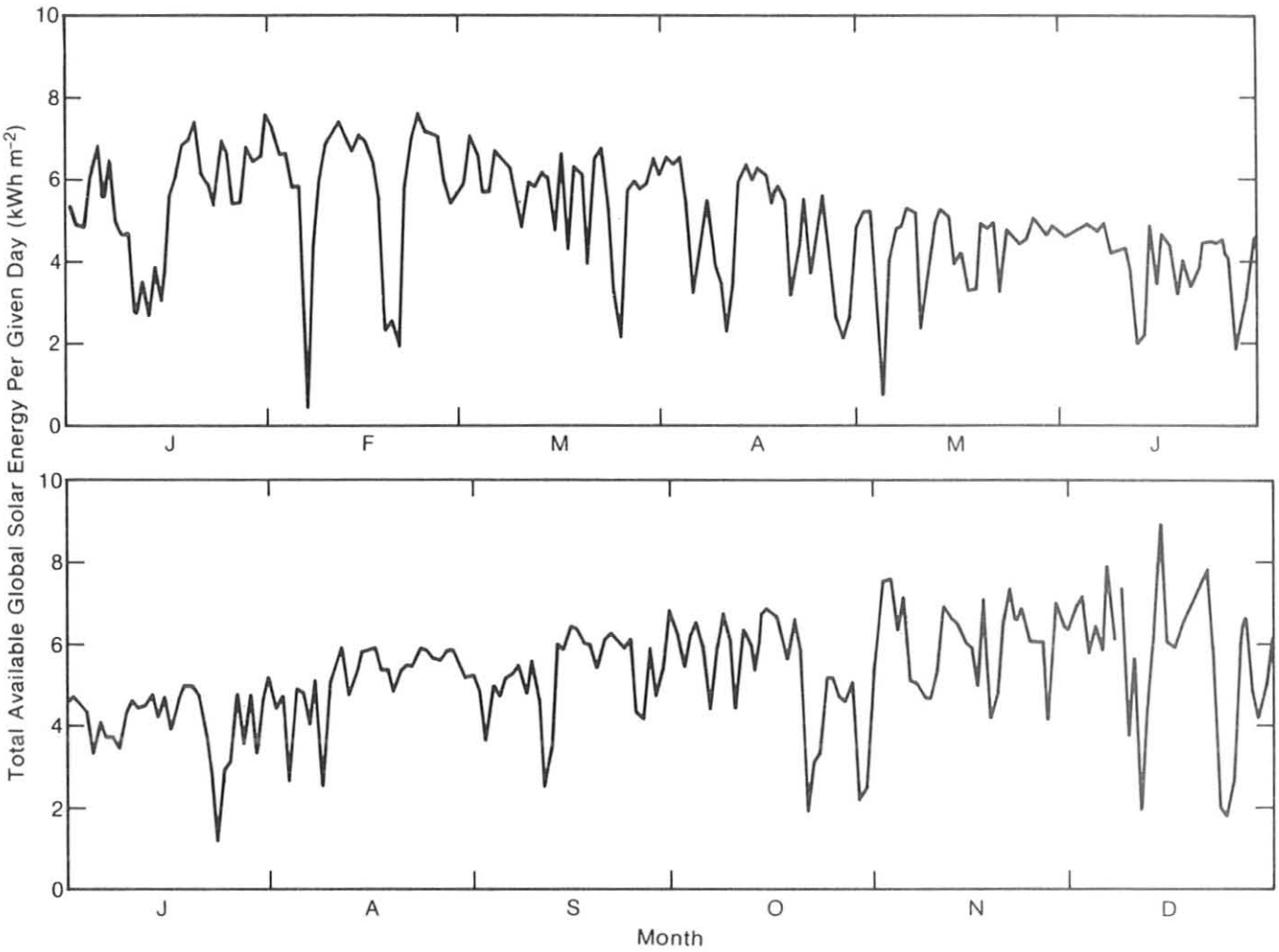

Figure 30.--Daily variation in available solar energy at SMO in 1979.

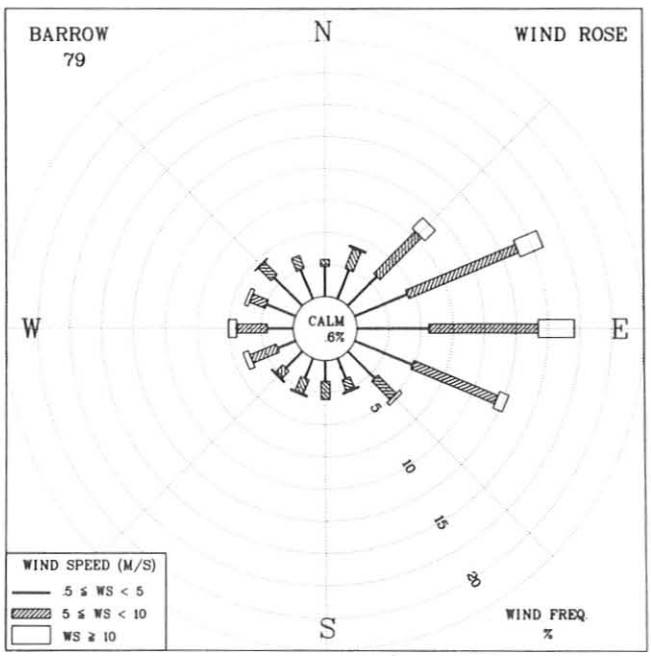

Figure 31.--Windrose for the GMCC Barrow observatory for 1979. The distribution of wind direction and windspeed are in units of percent occurrence for the year. Windspeed is shown as a function of direction in three speed ranges: less than 5 m s^{-1}, 5 to less than 10 m s^{-1}, and 10 m s^{-1} or greater.

3.9 Meteorological Measurements

3.9.1 Barrow Climatology

The Barrow GMCC Observatory is located about 9 km southwest of Point Barrow on a small rise in the tundra between two saltwater lagoons. A uniform snow cover hides these topographic features during 8 months of the year. No other topographic barriers exist within a 300-km radius of the observatory; thus the surface winds are mostly determined by large scale pressure systems. Between stormy periods, when most westerly winds occur, the surface winds are easterly, resulting from the outflow from the polar anticyclone. The radiation climate at BRW is strongly influenced by the stratus cloud layer that forms in the late spring and persists throughout the summer. The stratus layer denotes the top of the boundary layer cooled from below by the Arctic Ocean and warmed on top by subsiding air aloft. Onset of the stratus in the spring is closely tied to the appearance of leads (ice-free regions) along the coast.

The distribution of hourly average resultant windspeed as a function of the resultant wind direction is presented in fig. 31. As in 1978 and previous years, easterly winds are dominant, occurring about 64% of the time. The largest percentage of stronger winds also occurs in this sector; 81% of the winds greater or equal to 10 m s^{-1} are in this sector. At the other extreme, calm winds (less than 0.5 m s^{-1}) occur 0.6% of the time. Table 20 lists a breakdown of the meteorological measurements by month. Northeasterly through easterly winds are predominant in all months except December when winds from a westerly direction are most common.

Table 20.--1979 Barrow Observatory monthly climate summary

	Jan	Feb	Mar	Apr	May	Jun	Jul	Aug	Sep	Oct	Nov	Dec
Prevailing wind directions	ENE	ESE	ENE	ENE	ENE	E	ESE	E	E	NE	NE	W
Average wind speed (m s^{-1})	5.8	4.3	6.0	6.9	5.3	4.9	4.3	5.5	4.9	7.9	7.0	5.6
Maximum wind speed* (m s^{-1})	14	11	12	18	13	12	9	12	11	16	18	19
Direction of max. wind* (deg.)	201	257	94	250	113	250	258	264	119	82	89	269
Average station pressure (mb)	1012.4	1027.5	1024.9	1018.4	1014.2	1012.0	1009.8	1007.5	1010.4	1009.4	1001.3	1010.2
Maximum pressure* (mb)	1035	1044	1036	1040	1023	1021	1017	1018	1028	1022	1027	1041
Minimum pressure* (mb)	977	1004	1009	989	1002	994	996	995	990	992	977	973
Average air temperature (°C)	-18.7	-29.4	-27.6	-18.3	-6.4	0.1	4.8	6.0	1.1	-8.2	-13.1	-25.7
Maximum temperature* (°C)	-6	-14	-8	1	5	12	15	18	8	0	0	-5
Minimum temperature* (°C)	-36	-43	-40	-34	-18	-5	-2	0	-6	-19	-26	-38

*Maximum and minimum values are hourly averages.

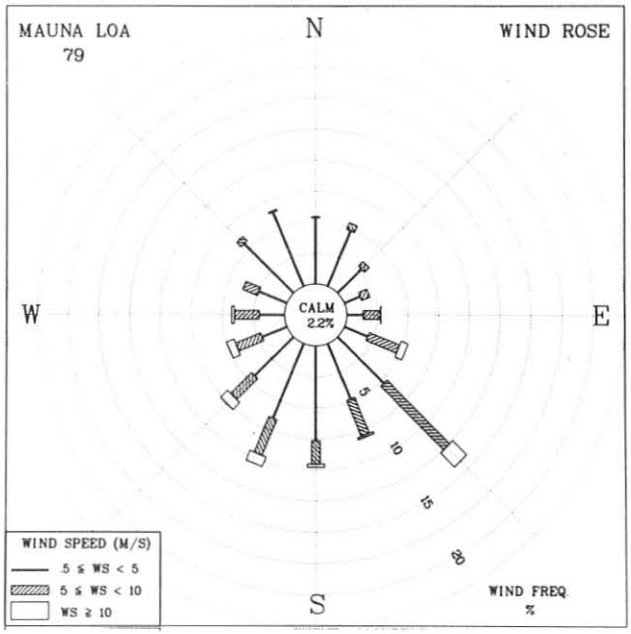

Figure 32.--Windrose for the Mauna Loa Observatory for 1979. See legend for fig. 31.

Table 21.--1979 Mauna Loa Observatory monthly climate summary

	Jan	Feb	Mar	Apr	May	Jun	Jul	Aug	Sep	Oct	Nov	Dec
Prevailing wind directions	WSW	WSW	SSW	SSW	NW	SSE	SE	SE	SE	SE	SE	SW
Average wind speed ($m\ s^{-1}$)	5.2	4.9	4.7	5.9	3.9	3.5	4.3	4.3	3.5	4.0	4.6	4.4
Maximum wind speed* ($m\ s^{-1}$)	12	14	15	14	10	10	13	15	9	14	14	13
Direction of max. wind* (deg.)	257	188	191	207	138	146	139	116	86	138	138	141
Average station pressure (mb)	679.0	678.7	679.5	679.2	681.4	681.8	682.5	682.2	681.9	682.2	680.5	681.0
Maximum pressure* (mb)	683	682	682	684	685	685	686	685	684	685	684	685
Minimum pressure* (mb)	675	673	673	674	677	679	678	679	679	679	676	674
Average air temperature (°C)	2.4	2.6	4.8	6.1	8.0	8.2	8.6	8.6	8.4	7.1	6.3	6.8
Maximum temperature* (°C)	13	11	17	14	16	15	15	18	16	15	16	16
Minimum temperature* (°C)	-4	-3	-2	0	0	1	2	2	2	2	0	0

*Maximum and minimum values are hourly averages.

The month-to-month changes in temperature and wind indicate the extent of the winter at Barrow. Winds are stronger during winter, and the temperatures follow an orderly progression except during January. In 1979 the minimum hourly average temperature was 43°C. The average temperature for the year was -11.3°C. NWS in Barrow village reported an average value of -10.6°C. The average pressure for the year was 1013.5 mb, 2.7 mb below the value reported by NWS. The average windspeed was 5.7 m s^{-1}; NWS reported 5.3 m s^{-1}.

3.9.2 Mauna Loa Climatology

Throughout most of the year the meteorological situation at MLO is controlled by the diurnal heating and cooling of the surface of the mountain. At the level of the observatory (3.4 km) the nocturnal downslope condition lasts about 12 to 13 hours a day, and the upslope flow lasts about 8 hours each day. In the intervening transition periods the winds are light and variable. The windrose (fig. 32) shows the general prevalence of downslope conditions with winds from the south-southeast and southwest. Higher windspeeds ($\geq$10 m s^{-1}) occur most commonly (80% of the time) with stormy periods and come from these southerly directions. The upslope or northerly winds are predominately less than 10 m s^{-1}. Calm conditions (windspeeds <0.5 m s^{-1}) occurred less than 2.2% of the time in 1979. The maximum average resultant windspeed reported for the year was 15 m s^{-1}.

Month-to-month variations in the important meteorological parameters are listed in table 21. Westerly winds are the most prevalent throughout the winter and spring months (December through April). Southeasterly winds are most prevalent between June and November. The average monthly station pressure changes very little, less than 3.5 mb. The average for the year was 680.8 mb. The average monthly temperatures vary over a range of 4.2°C with the annual average at 6.5°C.

3.9.3 South Pole Climatology

The persistent surface wind from a grid northeasterly direction is the overriding climatological feature at SPO. It is an inversion wind from approximately 50° to the right of the Antarctic Dome. SPO is located on the Amendsen-Scott plateau (elev. 2.85 km), which has little topographic relief within a 100-km radius of the station. The plateau is a slight depression near the western edge of the main ridge of eastern Antarctica. The highest point (elev. 4 km) on the plateau is about 900 km east-northeast of the Pole.

In fig. 33 the distribution of windspeed is presented in polar coordinates as a function of wind direction. The most prevalent wind direction is from the east-northeast, which is at variance with the preceeding 3 years when north-northeasterly winds dominated. During 85% of the hours in the year, the wind blows from the northeasterly quadrant. The winds associated with storms are from the north, but windspeeds equal to or greater than 10 m s^{-1} occur during only 1% of the hours. The maximum hourly-average windspeed observed during the year was only 12 m s^{-1}. Calm conditions were reported for only 3 hours in 1979. The GMCC anemometer is mounted at a height of about 10 m and positioned about 30 m grid north of the CAF.

Table 22 lists monthly average temperatures, which show the extent of austral winter on the Antarctic plateau. The average temperature remains below -50°C for 8 months of the year. The annual average temperature for 1979 was -48.9°C, only 0.5°C colder than 1978. The maximum hourly average temperature was -18°C, and the minimum was -77°C.

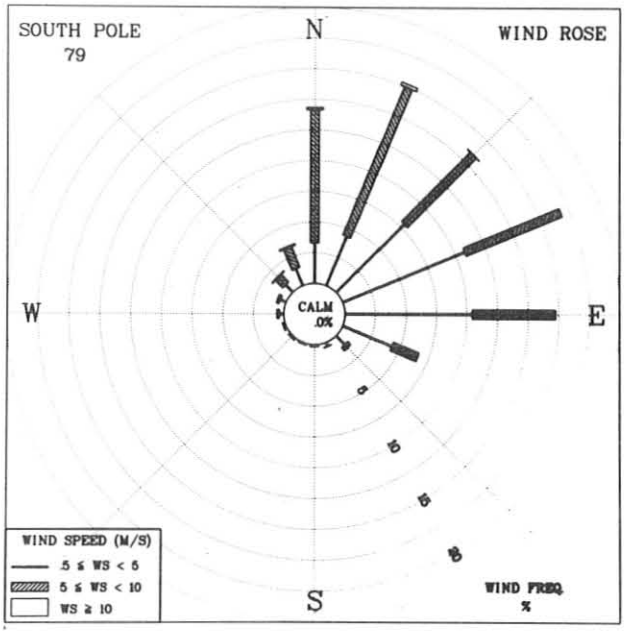

Figure 33.--Windrose for the South Pole Observatory for 1979. See legend for fig. 31.

Table 22.--1979 South Pole Observatory monthly climate summary

	Jan	Feb	Mar	Apr	May	Jun	Jul	Aug	Sep	Oct	Nov	Dec
Prevailing wind directions	ENE	E	NE	NE	ENE	E	ENE	NNE	N	NE	N	NNE
Average wind speed ($m\ s^{-1}$)	4.5	4.7	5.5	5.9	4.9	5.2	4.9	6.1	6.4	5.6	5.4	4.2
Maximum wind speed* ($m\ s^{-1}$)	9	10	11	10	8	11	9	10	12	9	11	9
Direction of max. wind* (deg.)	340	110	360	010	040	360	100	020	320	020	020	020
Average station pressure (mb)	685.8	681.1	676.1	681.1	670.4	676.1	662.1	671.4	674.7	672.2	682.4	687.0
Maximum pressure* (mb)	693	692	688	696	683	684	672	691	693	691	696	700
Minimum pressure* (mb)	676	670	666	666	659	666	647	659	657	662	668	676
Average air temperature (°C)	-25.7	-41.4	-51.2	-53.5	-62.0	-57.2	-63.9	-61.6	-56.0	-52.2	-36.4	-26.1
Maximum temperature* (°C)	-18	-29	-35	-38	-43	-46	-45	-47	-38	-36	-27	-18
Minimum temperature* (°C)	-35	-52	-65	-66	-73	-69	-77	-72	-69	-64	-48	-32

*Maximum and minimum values are hourly averages.

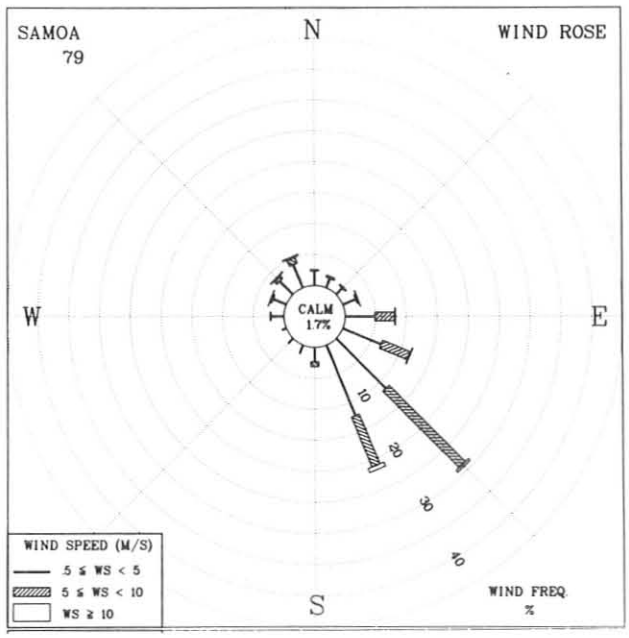

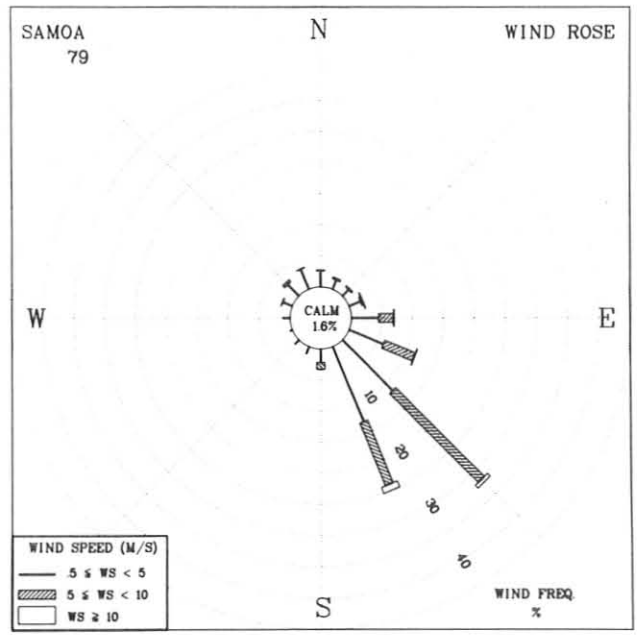

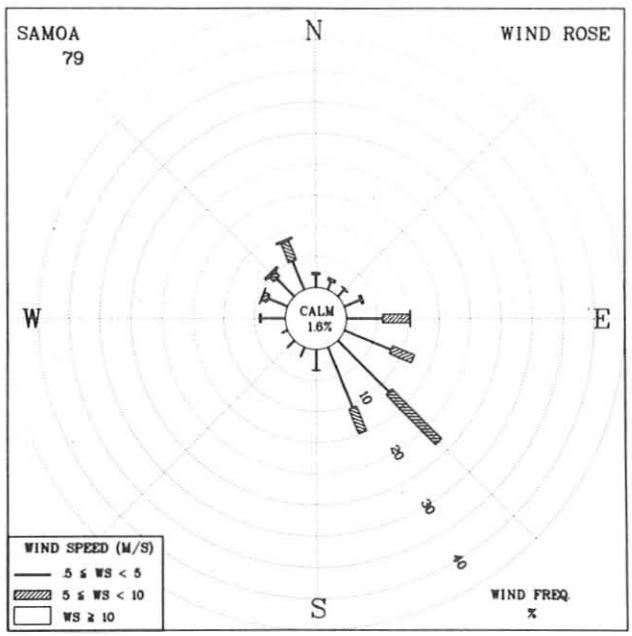

Figure 34.--Windrose for the Samoa Observatory for 1979. See legend for fig. 31.

3.9.4 Samoa Climatology

The SMO anemometer and thermometer were located on the sampling tower atop Lauagae Ridge during 1979. The anemometer was 14 m above ground near the sampling stack intake, and the thermometers were at 4-m height. Figure 34 shows the distribution of the resultant windspeed, in three classes, as a function of the resultant wind direction, in 16 classes. The trade winds at Cape Matatula are depicted, with the occurrence of directions in the southeastern quadrant occurring 71% of the time. During the year, winds from the northwesterly direction occur 14% of the time, with the northeasterly and southwesterly quadrants contributing the remaining 15%. When the summer months (December-March) are considered separately, a significant change in the distribution occurs.

Table 23.--1979 Samoa Observatory monthly climate summary

	Jan	Feb	Mar	Apr	May	Jun	Jul	Aug	Sep	Oct	Nov	Dec
Prevailing wind directions	SSE	SE	SE	SSE	SE	SE	SSE	SE	SE	SE	SE	SSE
Average wind speed ($m\ s^{-1}$)	3.7	5.1	3.7	2.5	4.4	5.8	5.2	4.2	5.7	5.3	4.3	3.7
Maximum wind speed* ($m\ s^{-1}$)	10	10	8	7	9	13	12	8	10	11	9	13
Direction of max. wind* (deg.)	290	141	149	139	140	110	151	110	152	117	165	320
Average station pressure (mb)	997.1	1000.2	999.9	1000.6	1000.9	1001.5	1002.5	1002.2	1001.8	1000.7	999.9	998.4
Maximum pressure* (mb)	1002	1004	1003	1004	1007	1005	1007	1005	1007	1005	1004	1004
Minimum pressure* (mb)	991	995	996	996	996	996	995	996	995	995	993	992
Average air temperature (°C)	28.6	28.3	28.7	28.6	28.4	28.2	27.3	27.1	27.3	27.5	27.8	27.9
Maximum temperature* (°C)	34	31	32	32	31	32	31	32	30	30	31	32
Minimum temperature* (°C)	24	22	23	24	24	24	24	21	23	23	23	23

*Maximum and minimum values are hourly averages.

Figure 34 shows the windroses for 1979 with December, January, February, and March winds. Clearly the percentage of wind directions in the northeasterly quadrant are affected most. Seventy-four percent of all winds greater than 5 $m\ s^{-1}$ from the northwesterly directions (N, NNW, NW, WNW) occur during the summer. During the remainder of the year, windflow is strongly dominated (72% of the time) by the southeasterly trade winds. Stronger winds occur during a larger percentage of the time in those directions as well.

As shown in table 23, seasonal variations of all other parameters are small. There is only a small indication of stronger winds and cooler temperatures in winter than summer. The average temperature for 1979 was 28°C, compared with a 27°C measurement at the airport in Tafuna. The average windspeed was 4.5 $m\ s^{-1}$ compared with 5.2 $m\ s^{-1}$ at Tafuna, and the average station pressures was 1,000.5 mb, compared with 1,010.6 mb measured by NWS. The height difference between the GMCC observatory and the airport station is about 78 m, which accounts for 8.9 mb of the 10.1 mb difference.

3.10 Precipitation Chemistry

The precipitation chemistry program continued with little change during 1979. Precipitation samples were collected at the 4 baseline observatories, 10 regional sites, and 6 Washington, D.C., locations. Monthly samples were sent from the regional and baseline sites to EPA laboratories for chemical analysis. Special studies were continued at MLO, using the ion chromatograph.

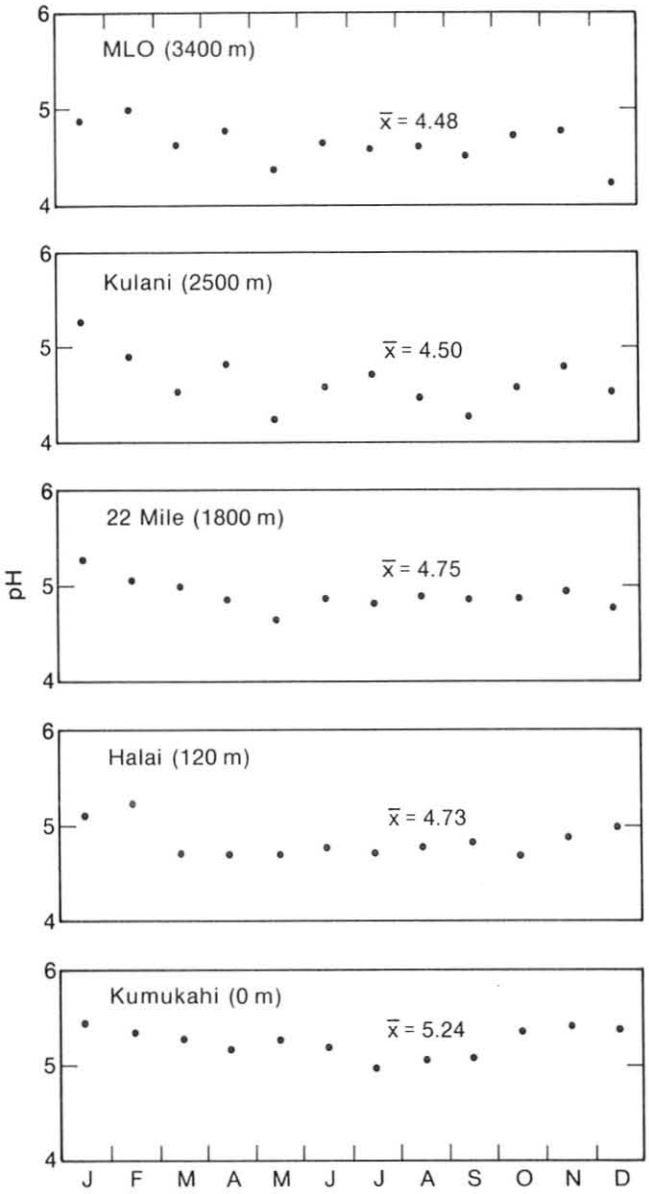

Figure 35.--Monthly precipitation weighted means for five sites on the Island of Hawaii during 1979.

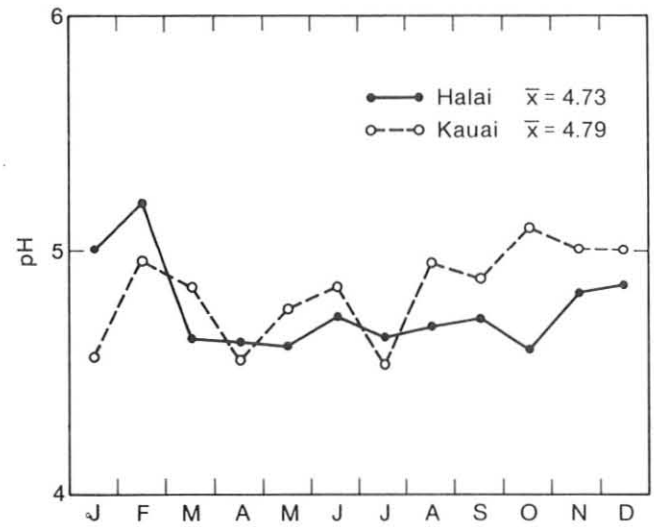

Figure 36.--Comparison of monthly precipitation weighted pH values for Hawaii and Kauai during 1979.

3.10.1 Baseline Measurements

The five-site special network on the Island of Hawaii continued on a daily-biweekly schedule; for details on locations, see previous GMCC Summary Reports. The monthly weighted pH values are plotted in fig. 35. The steady increase in acidity with elevation is still evident in the 1979 data as it was in previous years. Concern about the volcano as a source of the acidity prompted establishment of a site on the island of Kauai. Figure 36 shows the weighted average monthly values of pH with those of Hilo. The two sites are the most comparable in relation to elevation and orientation into the trade winds and show no significant difference in acidity levels.

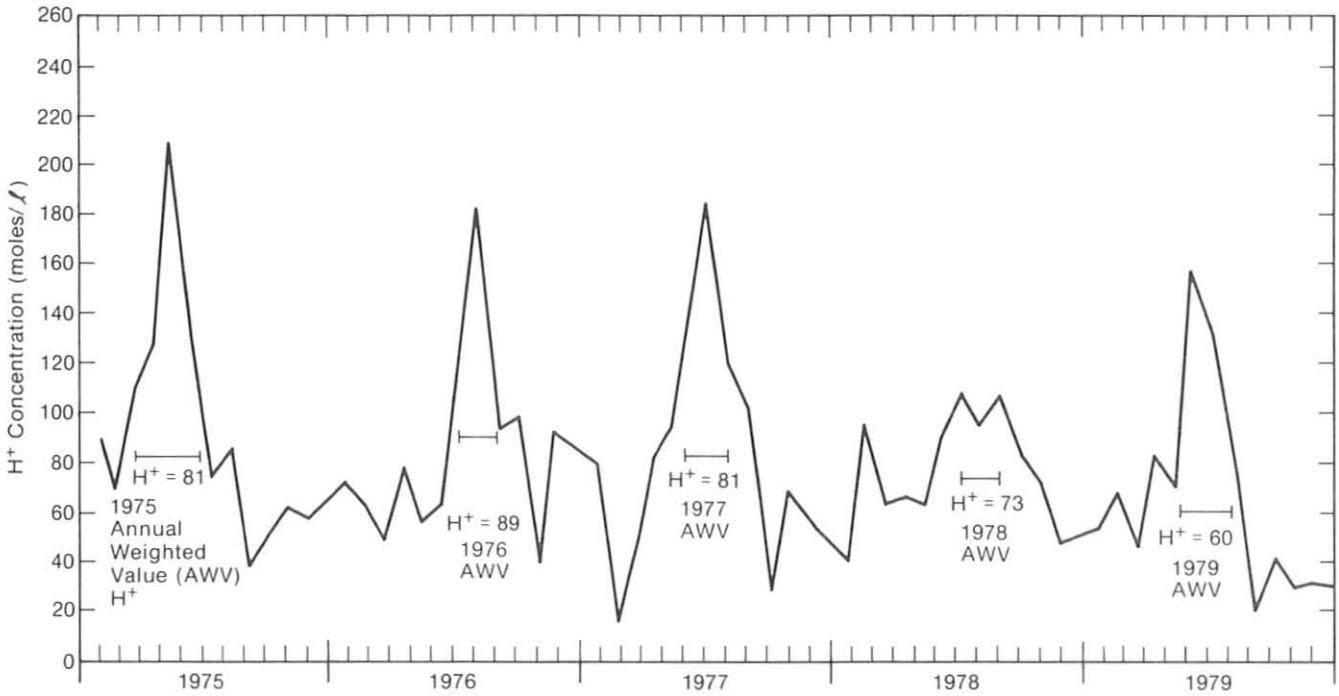

Figure 37.--Monthly precipitation weighted hydrogen ion concentration for the Washington, D.C., area.

3.10.2 Regional Measurements

The 10 WMO regional sites continued to be reevaluated during 1979 in expectation that they would become part of the National Atmospheric Deposition Program in 1980. At that time, precipitation would be sampled weekly instead of monthly.

3.10.3 Washington, D.C., Network

The data for the Washington network are shown in fig. 37.

3.11 Meteorological Trajectories

GMCC personnel use such meteorological data as back air trajectories calculated from the Heffter/ARL model to interpret data at baseline sites. At BRW, 5-day back trajectories (300 to 2,000 m) have been drawn from February 1975 to January 1980. At MLO, 10-day back trajectories (300 to 5,000 m) have been calculated for the same period. These series of back trajectories for both stations are available from GMCC on microfilm.

Figure 38 shows back trajectories to MLO for a given day. A, B, C, and D refer to 0000, 0600, 1200, and 1800 CUT, the times when these trajectories passed over MLO. To summarize the 5-yr data period by using trajectories, a climatology was constructed using a classification system shown in fig. 39. Trajectory directions were divided into six classifications. Four types, NE, SE, SW, and NW, are trajectories whose paths are in the four quadrants, 0°-90°, 90°-180°, 180°-270°, 270°-360°, respectively. A special case (NW/E) was created because a large number of trajectories crossed the 0° line, influenced first by the westerlies and then by the easterlies. Figure 40 summarizes all trajectory classifications for the 5-yr period. The seasonal nature of the flow to MLO is shown by the peaks of easterly flow in summer and westerly flow in winter.

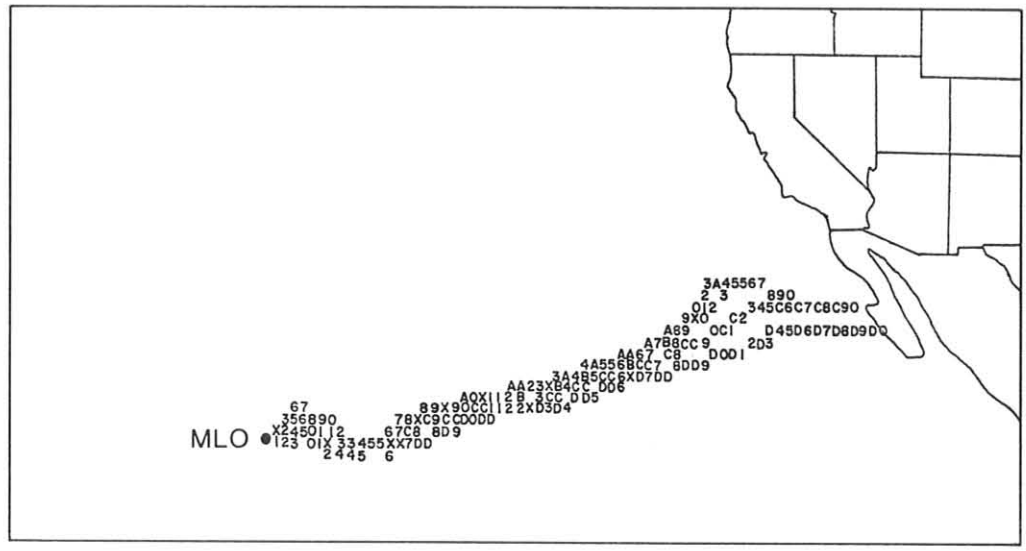

Figure 38.--Example of a 10-day back trajectory to MLO.

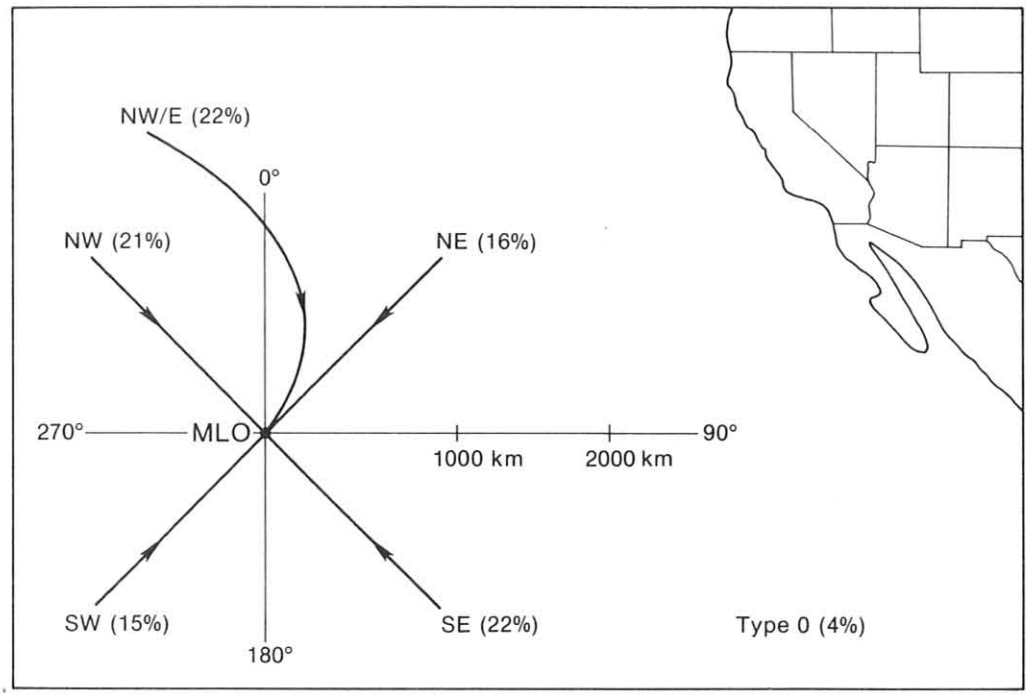

Figure 39.--Trajectory types used in classifying trajectories from February 1975 to January 1980 to MLO. Percentage over the total period is given in parentheses.

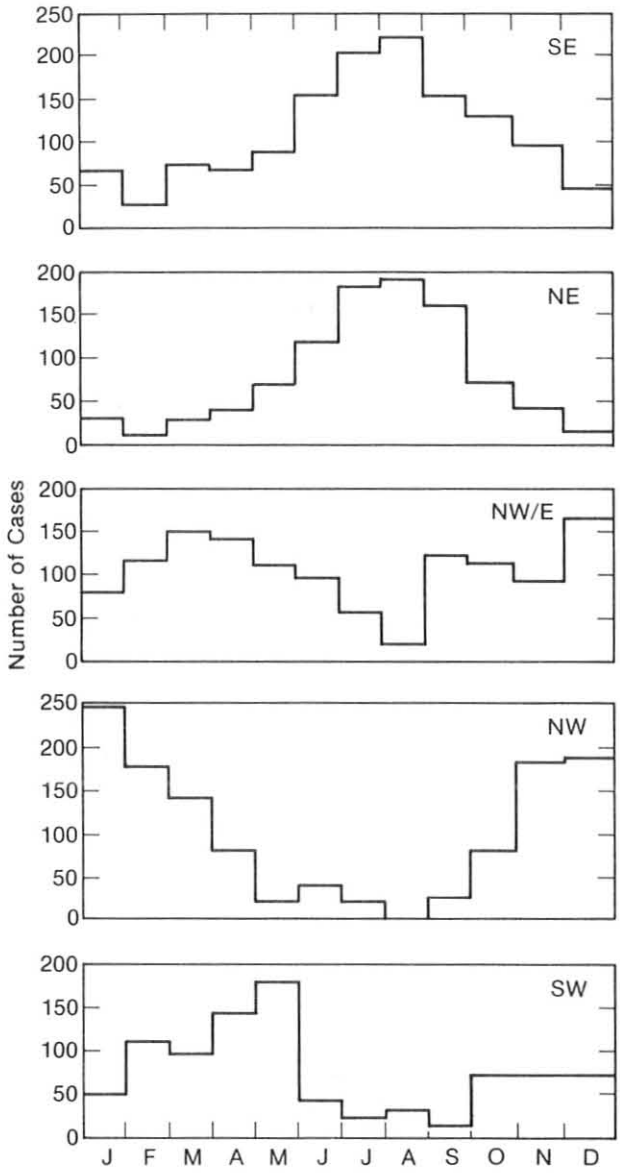

Figure 40.--Summary of the number of cases of a given trajectory for the 5-yr period on a monthly basis.

3.12 Data Management

3.12.1 Data Acquisition

Hardware

The Acquisition and Data Management Group oversees the Instrumentation Control and Data Acquisition System (ICDAS). During the past 3 years the overall performance of the system has improved to only 5% nonoperational in 1979 (see fig. 41). For all stations combined the ICDAS was down an average of only 18 days.

The BRW system functioned well for 94% of the time in 1979; this record is consistent with that for previous years. Most downtime at BRW resulted from a multiplexor-digitizer problem and tape drive alignment difficulties. The ICDAS at MLO operated for 89% of the time in 1978, which matched its 1978 performance. Most downtime at MLO occurred during the second half of the year when the station's

system had power problems, a misadjusted memory voltage, and tape drive problems. The performance of the SMO ICDAS improved over that for 1978 to only 3% downtime in 1979, mainly caused by power problems, although the tape drive caused some data loss. The SPO ICDAS had a remarkable year with less than 24 hours of downtime.

In 1979 more data were lost because of tape drive problems than for any other reason. Sometimes these problems resulted because the tape drives were misaligned. Toward the end of the year the drives at BRW, SMO, and MLO were all experiencing an occasional mysterious rewind or backspace to the beginning of tape. During 1980 we will clarify and standardize the maintenance procedures for the tape drive to minimize data lost from tape drive problems.

Hardware modification to the ICDAS, designed to reduce system noise, proceeded during the year. The NOVA minicomputer's switching power supply, which could generate RF noise as well as an audible high frequency, was replaced with a quieter, linear power supply. Another modification was replacement of the NOVA's front panel incandescent light bulbs with light-emitting diodes. The LED's require less power and have the added benefit of hardly ever burning out.

These modifications were made to the MLO and BRW computers in April. SMO's upgrading occurred in December after a delay for further testing. Although the front panel on the SPO's NOVA has been modified, the power supply will not be changed until the station opens in November 1980. In addition to the station computers, the spare NOVA and the NOVA in the reduction lab have been upgraded.

Another hardware project completed in 1979 was the design, building, and checkout of controllers for CO_2 tank and flask analysis. This work was done in cooperation with the GMCC Monitoring Trace Gases Group. The "brains" of each controller is a Z-80 microprocessor that we programmed to accept information from an operator, switch solenoids, collect data, and perform other functions of tank and flask analysis. The results are sent to an HP desktop computer for final processing and output. The tank controller was installed in March and the flask

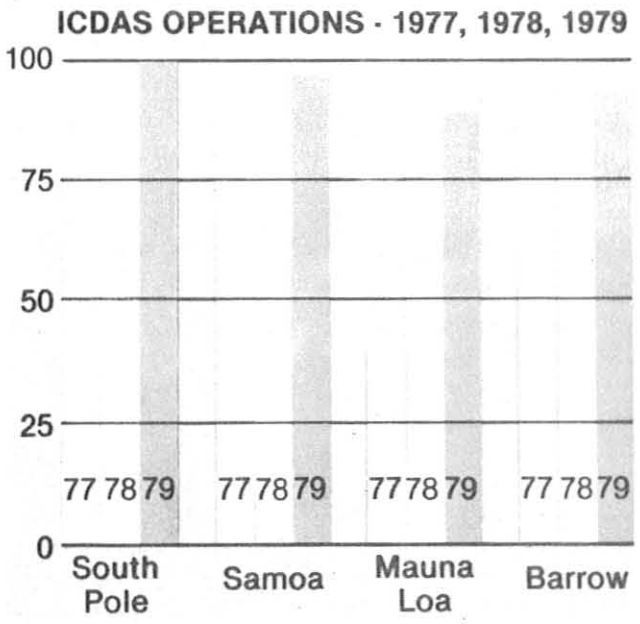

Figure 41.--ICDAS operations for 1977, 1978, and 1979. For each year the percentage of operation time is shown.

Table 24.--Inventory of GMCC data tapes at World Data Center-A

No.	Tape name	Date of issue	Parameter	Stations	Period of data
1	MLONF1	12/9/77	Volumetric light scattering	MLO	1974-1976
2	GPOLO1	1/16/78	Condensation nuclei	BRW	1975, 1976
	GPOLØ1		concentration	MLO	1975, 1976
				SPO	1975, 1976
3	A78Ø76	3/17/78	Solar irradiance	MLO	1977
4	A78083	3/24/78	Solar irradiance	SMO	1977
5	A78100	4/10/78	Solar irradiance	BRW	1977
6	A78104	4/14/78	Solar irradiance	MLO	1976
7	A78132	5/12/78	NIP radiation	BRW, MLO SMO, SPO	1977
8	A78139	5/19/78	Wind, pressure, temp., humidity	BRW, MLO SMO, SPO	1977
9	A78146	5/26/78	Solar irradiance	SMO	1976
10	A78160	6/9/78	Solar irradiance	SPO	1976, 1977
11	A78230	8/18/78	Solar irradiance	BRW	1976
12	A78272	9/29/78	Solar irradiance	BRW, MLO	First half 1978
13	A78279	10/6/78	Solar irradiance	SMO	First half 1978
14	A79127	5/7/79	Solar irradiance (research-cooperator format)	SMO	1976
15	A79128	5/7/79	Solar irradiance (research-cooperator format)	SMO	1977
16	A79208	7/27/79	Solar irradiance	MLO	Second half 1978
17	A79222	8/10/79	Solar irradiance	SMO	Second half 1978
18	A80010	1/25/80	Carbon dioxide	MLO	1974-1978
19	A80011	1/25/80	Carbon dioxide	SPO	1976
20	A80012	1/25/80	Carbon dioxide	BRW	1973-1978

controller in August. The Acquisition and Data Management Group's part in the project was documented in a paper presented at the WMO technical conference in Boulder this August (Harris et al., 1980).

A prototype controller for CO_2 field operations has been built, and work is being done on the software to support it. We are also evaluating a Deck Tape II cartridge system, which if viable, will allow the controllers to become stand alone, data logging systems.

3.12.2 Archiving

Table 24 lists the GMCC data archived at the World Data Center-A in Asheville, North Carolina. Each file on the archive tapes is preceded by a description of the data in alphanumeric form. Copies of these tapes can be obtained from the Computer Products Branch, National Climatic Center, Asheville, NC 28801, FTS 672-0203 or (704) 258-2850 ext. 203. GMCC archived data tapes are located in tape deck no. 9708.

3.12.3 Processing

A new data set combines important GMCC measurements with information about variability, instrument performance, and evidence of local pollution. The form of the data set, consistent with guidelines set down in WMO 299, has a line for each hour of the station year. The data on each line are described in table 25.

Figure 42 shows sample output from a program written this year to utilize this new data set. The plot labeled windrose shows the wind distribution according to 16 22.5° wind direction intervals and 3 windspeed intervals. Carbon dioxide and condensation nuclei measurements were also averaged within the 16 wind direction intervals and plotted on the graph labeled climatology. The table below the graphs presents the same data in tabular form with the addition of CO_2 and CN standard deviations based on minute data.

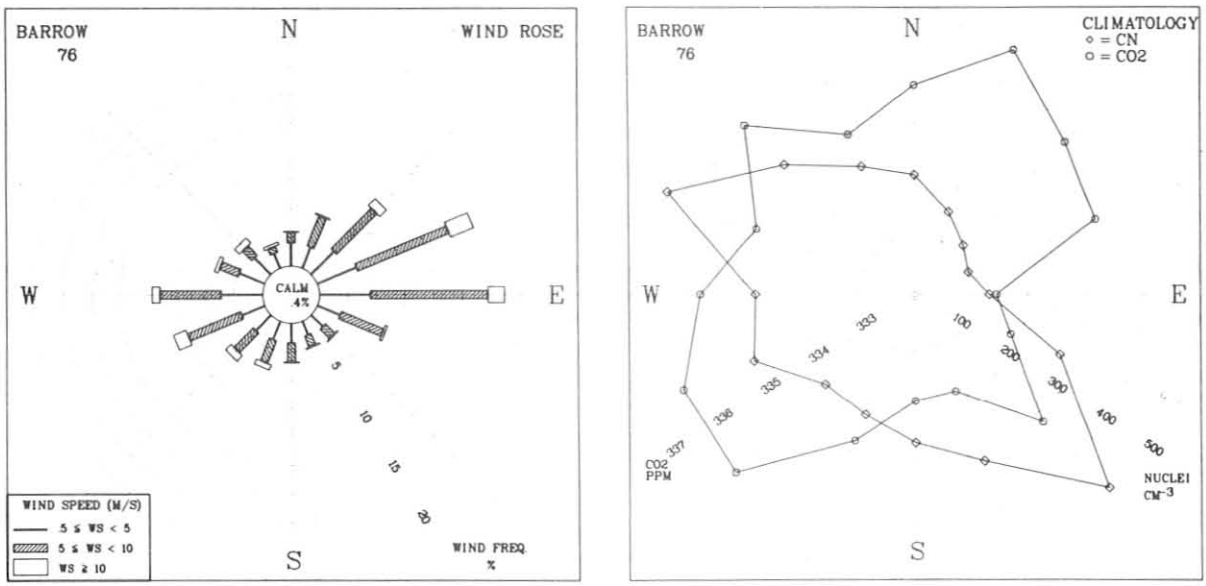

CLIMATOLOGICAL SUMMARY

DATA FOR BARROW YEAR 1976

DIR	CO2 (PPM)	CO2SD (PPM)	CO2 (TALLY)	CN (CM-3)	CN SD	CN (TALLY)	WIND SPEED (METERS PER SECOND) CALM (TALLY)	.5<=WS<5 (TALLY)	5<=WS<10 (TALLY)	WS>=10 (TALLY)	SUM (TALLY)	DIST (PCT)
N	335.7	1.231*	195	209	.253*	91	3	177	83	2	262	3.0
NNE	336.6	.454*	316	156	.238*	135	0	172	251	5	428	4.9
NE	335.8	.200*	451	121	.115	238	1	247	439	71	757	8.7
ENE	335.4	.924*	822	102	.188	483	1	323	752	188	1263	14.5
E	333.4	1.244*	1052	131	.190*	524	3	390	891	125	1406	16.1
ESE	333.8	.445*	417	276	.250*	273	0	186	350	20	556	6.4
SE	335.2	.913*	182	480	.406*	121	0	122	107	2	231	2.6
SSE	333.8	.193*	159	317	.280*	110	3	111	94	1	206	2.4
S	333.9	.188*	232	261	.285	163	2	148	146	6	300	3.4
SSW	334.8	.341*	310	229	.187	237	2	148	188	41	377	4.3
SW	336.4	.170*	351	223	.222	270	3	165	211	59	435	5.0
WSW	336.4	.542*	599	304	.146	520	2	189	443	102	734	8.4
W	335.7	.983*	621	278	.328	426	2	316	472	57	845	9.7
WNW	335.0	1.338*	293	467	.333	219	3	211	154	29	394	4.5
NW	336.2	.555*	243	320	.424	127	2	179	102	52	333	3.8
NNW	335.0	.197*	131	242	.305	58	5	120	50	22	192	2.2
AVG/TOT	335.1	.701*	6374	214	.246	3995	32	3204	4733	782	8719	100.0

EACH DIRECTION BIN CONTAINS +-11.25 DEGREES FROM INDICATED DIRECTION.
VALUES REPORTED FOR CN ARE GEOMETRIC MEAN AND LOGARITHMIC STANDARD DEVIATION.
FIELDS WHICH ARE FILLED WITH NINES DENOTE MISSING DATA.

STANDARD DEVIATIONS ARE DERIVED FROM ONE MINUTE AVERAGE VALUES.
A STAR (*) INDICATES THAT ONE-MINUTE DATA WERE AVAILABLE
FOR LESS THAN 75% OF THE HOURS WITHIN THIS BIN.

Figure 42.--Sample output from program using new data set from GMCC Barrow station for 1976. Left: windrose. Right: distribution of aerosol and carbon dioxide concentrations as a function of wind direction. Bottom: climatological summary.

Table 25.--Descriptions of data for each line of new data set

Field no.	Parameter	Format	Comment
1	ISTA	1X, I3	BRW = 199, MLO = 31, SMO = 191, SPO = 111
2	IDATE	1X, I5	YYDDD, GMT, Julian date
3	IHR	1X, I2	Hour beginning (0-23), GMT
4	CO2	1X, F6.1	CO_2 average in 1959 SIO index
5	CO2SD	1X, F6.3	Hourly standard of CO_2 based on minute data
6	ITAL	1X, I3	Tally of minutes in hour for CO_2
7	IGE	1X, I5	Geometric mean condensation nuclei concentration (cm^{-3})
8	GESD	1X, F6.3	Logarithmic standard deviation for the hour based on minute data (cm^{-3})
9	JTAL	1X, I3	Tally of minutes in hour for CN
10	NEPH1	1X, I7	Geometric mean of volumetric light scattering ($m^{-1} * 10^{-9}$)*, 450 nm
11	NEPH2	I7	Same as above, 550 nm
12	NEPH3	I7	Same as above, 700 nm
13	NEPH4	I7	Same as above, 850 nm
14	IRWD	2X, I3	Resultant wind direction in degrees
15	RWS	2X, F4.1	Resultant wind speed ($m\ s^{-1}$)
16	PRESS	1X, F7.1	Atmospheric pressure (mb)
17	AIRT	1X, F6.1	Air temperature (°C)
18	DEW	1X, F6.1	Dew point temperature (°C)
19	IFLG	2X, A2	Waterman CO_2 flags:
			Codes identifying data suspected as not being representative of background conditions: AC Airline contaminated GA Ground air - intake unintentionally near ground level LC Local contamination (e.g., automobile traffic at observatory) RV Stripchart recorder trouble causing variability SI Suspect instrument - data are not markedly different from surrounding hours, specific instrumental problem has been identified ST Suspect time (possibility data are logged at wrong hours of day) SW Suspect high winds (causing pressure reversal in air intake) V Stripchart trace variable VA Variability caused by wind flow from Aunuu Island (SMO) (Wind direction approx. 150 to 180 degs.) VO Variability caused by volcanic activity (MLO) VV Variability probably caused by vegetation (SMO) VW Variability caused by wind direction (MET data indicate contamination coming from known source of pollution)
			Codes giving the reason for missing data: AL Air pump leak C Weekly calibration I Instrument (and instrument related problems) MA Moving analyzer to new location PF Power failure (unintentional) PO Power outage (intentional) R Stripchart recorder trouble (no computer logged record) T Water vapor trap-related problems TF Water vapor trap frozen U Unknown (unable to assign specific cause for missing data)
			Other codes - data probably OK, but some supporting information missing: NC No stripchart record available (computer logged data OK) NT Water vapor trap not in use RC Reference gas conserved (calibration frequency reduced)
20	IPLFLG	1X, A1	P: Evidence of local pollution from CN record and observer comments
21	ICDFLG	2X, A2	NI: No ICDAS data available
22	ICO2FL	2X, A2	CF: CO_2 fill data used (don't compute SD from ICDAS)
23	IGEFL	2X, A2, 2X	GF: CN fill data used (don't compute SD from ICDAS)

*Original Bsp have been multiplied by 10^9.

4. SPECIAL PROJECTS

4.1 Comprehensive Theoretical Examination of the Optical Effects of Aerosols on the Umkehr Measurement

The present investigation is concerned with error on the Umkehr measurement resulting from a variety of aerosol size distributions, refractive indices, and vertical profiles of aerosol concentrations including augmentation in the stratosphere originating from volcanic and possibly anthropogenic sources. All orders of scattering are included in the theoretical calculations. Several different ozone profiles are used to simulate low, middle, and high latitude conditions. Some preliminary results of this investigation are given here.

The technique used to calculate the haze errors on the Umkehr measurement is a modified version of the one used by Dave (1978) for calculating the aerosol errors on total ozone estimated from satellite ultraviolet measurements of the backscattered radiance. The aerosol error on the Umkehr measurement is found by taking the difference between simulated Umkehr measurements calculated for modeled atmospheres with and without aerosols.

The method used to deduce ozone profiles from Umkehr measurements is essentially the one developed by Mateer and Dutsch (1964), which is now the standard evaluation system used by the World Ozone Data Center, Toronto. The haze error on the deduced ozone profile is found by taking the difference between ozone profiles, which were deduced from simulated Umkehr measurements calculated with and without aerosol effects, respectively.

4.1.1 Haze Error On the Umkehr Ozone Profile

Umkehr measurements simulated for atmospheres with and without aerosols and for a variety of ozone profiles were evaluated by the standard Umkehr evaluation system (Mateer and Dütsch, 1964). A difference $Xi^{(H)}$ is defined by the equation

$$\Delta X_i^{(H)} = X_i^{(H)} - X_i,$$

where $X_i^{(H)}$ and X_i are the ozone amounts in the i-th layer deduced from simulated measurements for models with and without aerosol, respectively.

In fig. 43 we show plots of Umkehr layer number vs. percent haze error E to the ozone profiles where

$$E(\%) = 100\ \Delta X_i^{(H)}/X_i\ .$$

Layer 1 has midlayer atmospheric pressure of 500 mb whereas layers 2 to 9 have midlayer pressures of 117, 88, 44, 22, 11, 5.5, 2.8, and 1.4 mb, respectively.

In figs. 43-45, T stands for tropospheric aerosols, S for stratospheric aerosols, and ST for both combined. Haze models are taken from Dave (1978) and ozone and aerosol profiles are taken from Dave (1979). Figure 44 shows the effect of changing tropospheric ozone profiles, and fig. 45 shows the effect of changing aerosol profiles.

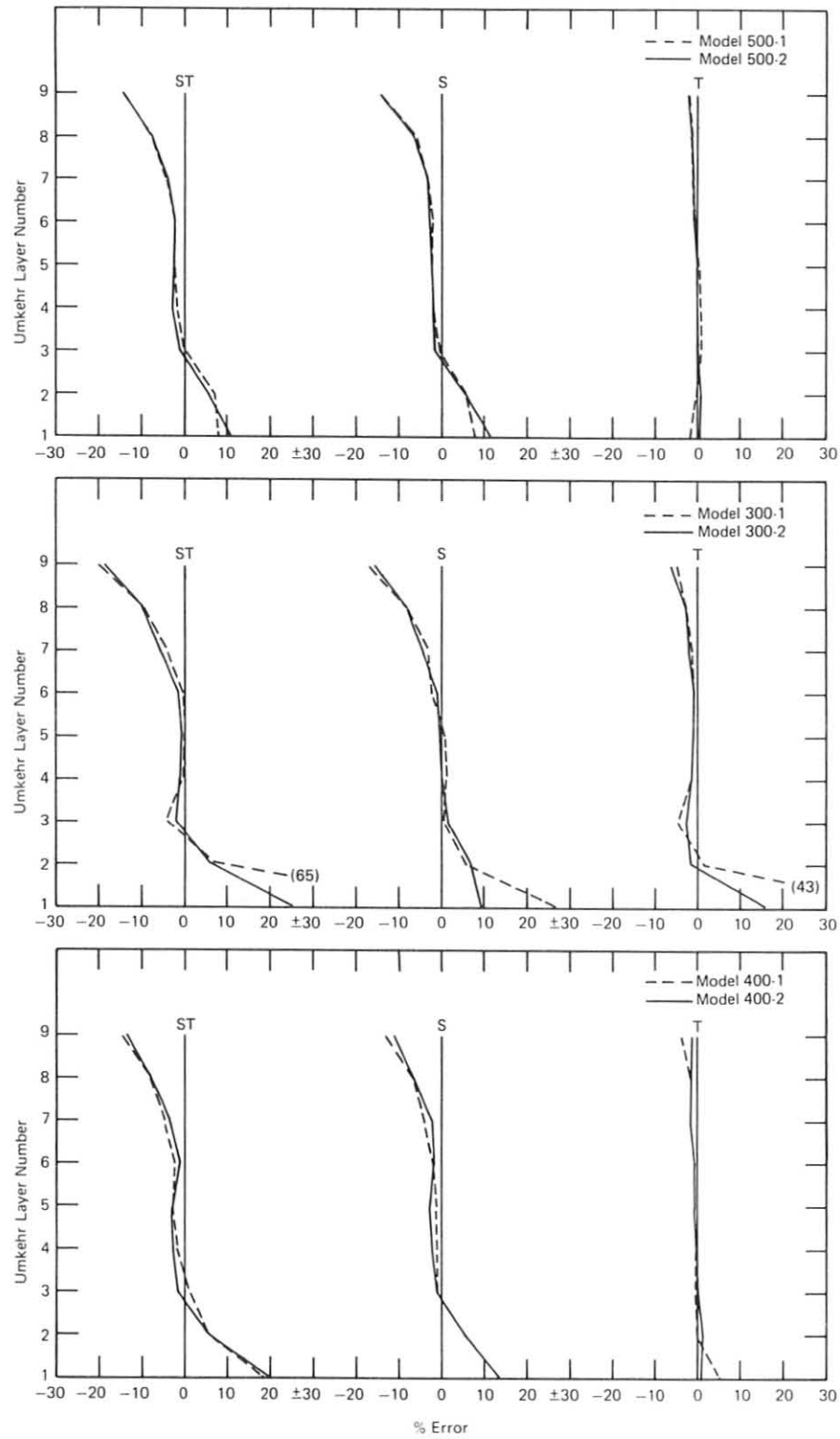

Figure 43.--Haze error caused by ozone profiles. Aerosol profile and optical properties are held fixed: Haze H, stratosphere; Haze L, troposphere; aerosol refractive index is 1.5 to 0.0i. Aerosol profiles 1 and 3 are used. Models 500-1 and 500-2 are two different ozone profiles having a total ozone of 500 m-atm-cm.

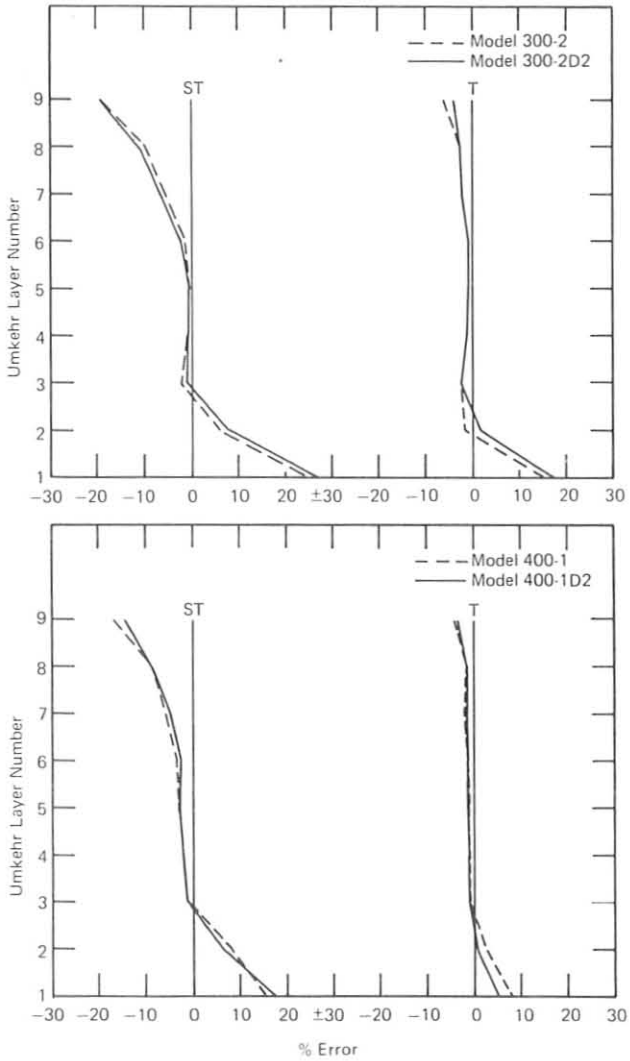

Figure 44.--Effect of changing tropospheric aerosol profile. Aerosol optical properties are defined as Haze H, stratosphere; Haze L, troposphere; refractive index is 1.5. to 0.01i. D2 is modified profile 2, etc.

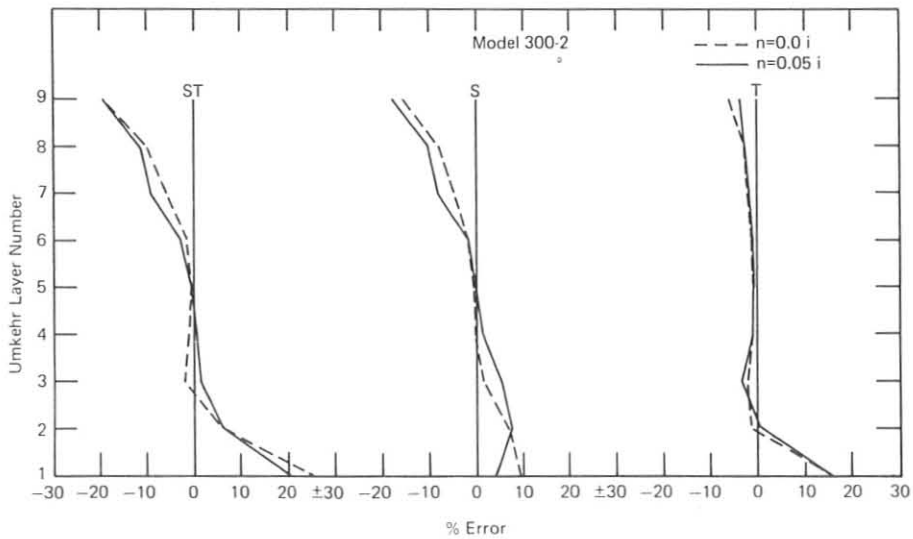

Figure 45.--Effect of changing aerosol absorption refractive index. Haze H, stratosphere; Haze L, troposphere; imaginary terms for aerosol refractive index n are given on figure. Aerosol profiles are fixed.

4.1.2 Summary

Even though we have included a wide variety of aerosol characteristics in our treatment of their error effects on Umkehr ozone profiles, we note that there is a commonality in the features of the errors in the deduced ozone profiles. Both stratospheric and tropospheric aerosols tend to (1) induce a significant negative ozone error in the uppermost layers 7-9; (2) induce a small, usually negative ozone error in layers 3 to 6, and (3) induce a significant positive ozone error in layers 1 and 2. Compared to tropospheric aerosols, stratospheric aerosols are much more effective in producing errors on the deduced ozone profiles. Tropospheric aerosols induce a small negative ozone error on the order of 2% to 5% in layer 9 (the region of importance in ozone production), whereas stratospheric aerosols induce errors of 10% to 20% in the same layer.

In all cases studied, multiple scattering tended to reduce the magnitude of primary scattering estimates of the haze effect. This encouraging result means that we need not be as concerned with tropospheric aerosols as previously thought; however, this does not preclude the utility of deriving some correctional schemes for tropospheric aerosols to improve the accuracy of the Umkehr method. Stratospheric aerosols, on the other hand, must be considered as serious to the Umkehr measurement when optical depths are abnormally high, which is normally a consequence of significant volcanic activity. Again, correctional schemes for stratospheric aerosols may improve the accuracy of the Umkehr measurement, but the extent of the improvement will rely heavily on the accuracy of the measurement of stratospheric aerosols themselves. Aerosol optical depth is the most important variable.

Finally, a few calculations that were performed to examine the aerosol error on the new shortened multiwavelength version of the Umkehr measurement (now in the process of development) indicate that the ozone profile errors for this method possess the same characteristics as those for the standard Umkehr method. The magnitudes of these errors seem to be slightly smaller, but it is too soon to be certain that this would be true for all conditions.

4.2 Disparities in Ozone Measurement

Figure 46 shows a plot of DeLuisi's (1975) ozone data in terms of departures from a mean of 0.294 (atm-cm vs. λ for every 0.2 nm, beginning at 298.1 nm and ending at 319.5 nm. The mean total ozone was calculated from all data not exceeding 313.0 nm, because total ozone determinations became intolerably noisy beyond this wavelength; that is, ozone optical depth becomes comparable to the Rayleigh and aerosol optical depths. It was also necessary to eliminate a few data points at wavelengths above 313.0 nm because they displayed high standard deviations related to occasional spurious signals in the measurement system. Finally, a three-point unweighted smoother was applied to the entire set of data. The smoother had little effect on reducing the magnitude of the maxima and minima at wavelengths less than 310.0 nm.

The variations in the total ozone at different wavelengths seem to display occasional positive correlation with the variations in the UV spectra at the same or nearly corresponding wavelengths. If there is some definite relationship, it is puzzling because the Langley method for obtaining optical depth is thought to be independent of the wavelength structure of the incident solar UV radiation source. The deeper and wider Fraunhofer line structure (where deduced ozone seems

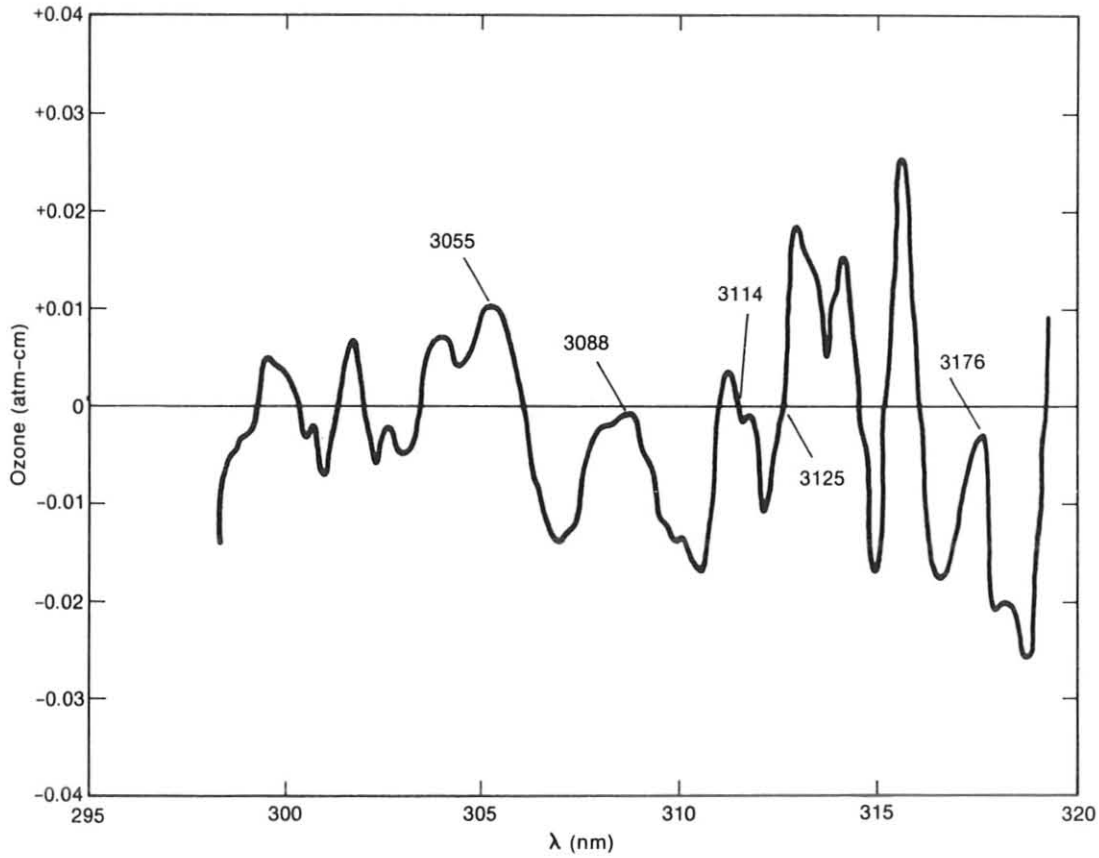

Figure 46.--Plot of DeLuisi's (1975) ozone data, in terms of departures from a mean of 0.294 atm-cm vs. λ at 0.2-nm intervals beginning at 298.1 nm and ending at 319.5 nm. Spectrometer bandpass is 1.0 nm. The mean total ozone was derived from all ozone values for wavelengths $\leq$3.13.0 nm.

to be most affected) may be responsible in some way for producing an apparent ambiguity; e.g., a significant Ring effect (Brinkman, 1968) might reduce the magnitude of the slope of a Langley plot, thereby resulting in a lower value of total ozone deduced from the slope. This could produce a positive correlation between total ozone and the extraterrestrial spectrum.

4.3 Selection of CO_2 Values from Whole Air Samples

An algorithm for selecting CO_2 concentration values from whole air samples was based on two assumptions:

(1) Independence of flask values obtained with at least 2-day separation. We assume the statistical independence of the residuals of means of flask pairs about a least squares polynomial fit of degree one through five.

(2) Normality of the same residuals.

These assumptions are shown to be valid for CO_2 concentrations at MLO and BRW. At these stations minute mean values from continuous analyzer records were used from

about the same time interval as for flask samples. In addition, the residual sum of squares for the fitted polynomials was calculated from the continuous data and used as an estimate of the "pure error" sum of squares.

A schematic diagram of the CO_2 selection scheme is shown in fig. 47. Because of serial correlation, paired CO_2 values are averaged unless they exceed 3 ppm, a value unlikely to result from real CO_2 concentration fluctuations. If the pair values differed by more than 3 ppm, they are probably independent because of experimental error. The values are fitted to a polynomial of degree one. Residuals are tested for normality by comparing their skewness with that of the Biometrika tables for 1% point (Pearson and Hartley, 1966). If the skewness of the residuals exceeds the Biometrika value for the same number of sample points, the largest absolute residual is removed and the fit is redone. When this procedure yields an acceptable value for skewness, the residual sum of squares is tested against the "pure error" sum of squares explained above. If the F test fails (i.e., the fitted sum of squares is significantly larger than the sum of squares found to be appropriate for a good fit), then all data points are restored and the fitted polynomial degree is increased by one. The procedure is continued until the residuals are acceptably normal and the unexplained variance is at an acceptable level.

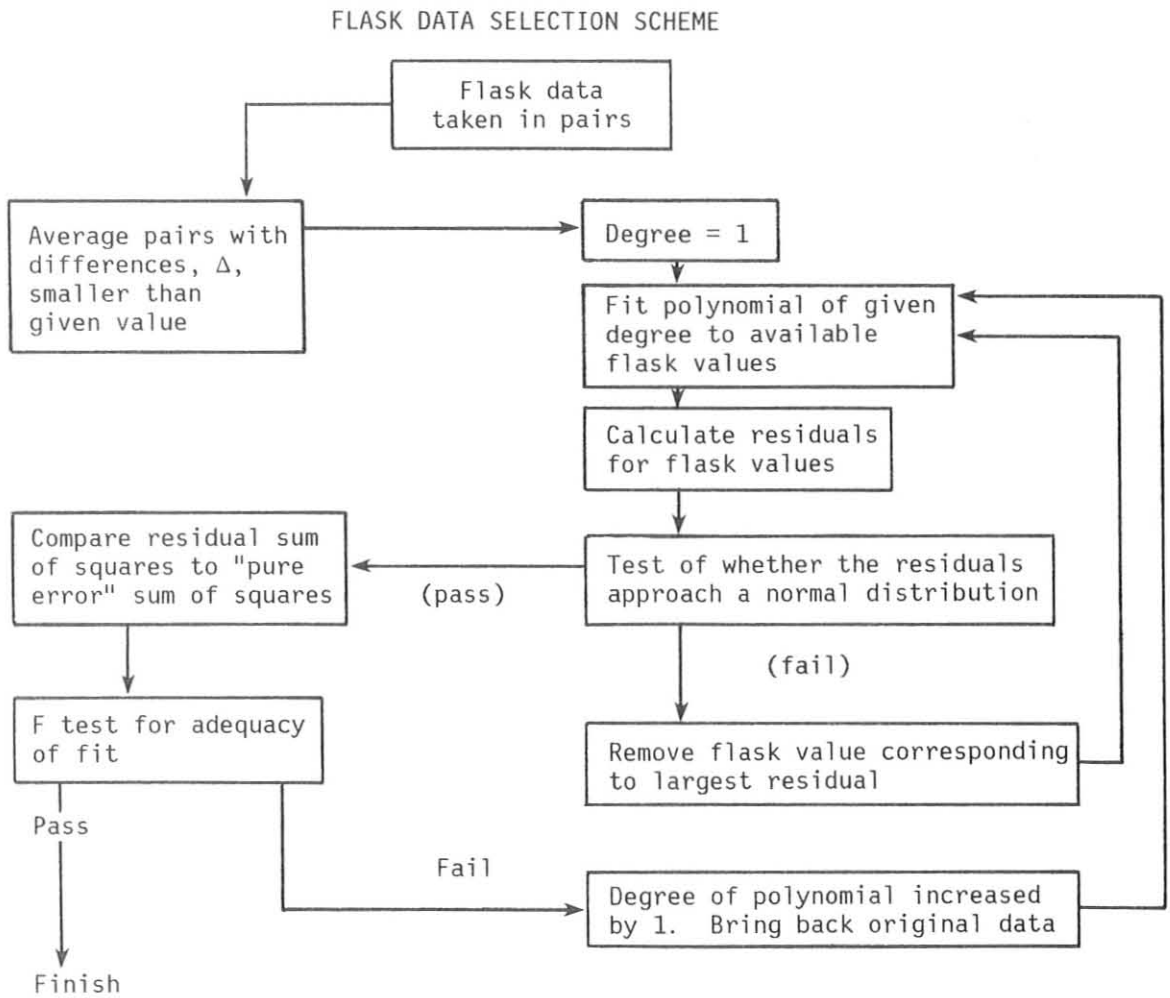

Figure 47.--Algorithm for selecting CO_2 values obtained from flask samples of air.

4.3.1 Number of Flasks Sampled at One Time

The data selection scheme, used with artificial data, was

$$CO_2 = 330 + 3 \sin \frac{2\pi T}{365} + RV$$

where T is time in days and RV is a random variable having two components. The first component is a random variable having mean 0 and standard deviation 0.3; the probability of this component occurring is 0.87. The second component is a random variable having the mean 1 and standard deviation 1 in case 1 and mean 2 and standard deviation 1 in case 2. The sampling was simulated by a monte-carlo technique using a total of 208 original points for pair sampling and 207 original points for triple sampling.

Since the individual samples were composed of independent variables, the selection scheme did not average individual samples as above. The mean sum of squares from the function

$$330 + 3 \sin \frac{2\pi T}{365}$$

was calculated for each trial. Since the total number of samplings was about the same, the triple sampling was done two-thirds as many times as pair sampling. Table 26 shows the results for cases 1 and 2. About 50 trials were used for each

Table 26.--Flash selection of CO_2 data*†

	Pair sampling (208 original points)	Triple sampling (207 original points)
Case 1: $RV^1 = N(1,1)$		
No. of flasks	196 ± 4	194 ± 4
% of original	94.2	93.7
Mean sum of sq.	0.15 ± 0.03	0.26 ± 0.13
Trials	49	46
Case 2: $RV^1 = N(2,2)$		
No. of flasks	189 ± 6	184 ± 6
% of original	90.9	88.9
Mean sum of sq.	0.19 ± 0.11	0.46 ± 0.34
Trials	51	52

*$CO_2 = 330 + 3 \sin \frac{2\pi T}{365} + RV$

$RV = N(0,0.3)$ $p = 0.83$

$RV = RV^1$ $p = 0.17$

†95% confidence intervals are given.

case for both triple and pair sampling, and the results show that approximately the same number of samples are chosen regardless of pair or triple sampling. This approximate equality is caused by the effort of the selection scheme to save individual CO_2 value paired differences that exceed a preassigned value.

4.3.2 Data Comparison between Flask Selected and Continuous Analyzer Data

A continuous data set different from those examined above and corresponding to 1 year of flask data was examined. The flask data from MLO were selected as described above and presented in fig. 48. Since the collections were made at about the same time each sampling day, hourly mean values from the continuous CO_2 analyzer record from the same sampling time for every day of the year were used for comparison. Those hourly mean values are shown in fig. 49. The comparison technique was the extra sum of squares principle described by Draper and Smith (1966).

The null hypothesis used was that there is no difference in the structure of the data series. The null hypothesis could not be rejected at the 95% confidence level, and the approximate equivalence of the flask data to the hourly mean data led us to confirm the value of the data selection scheme.

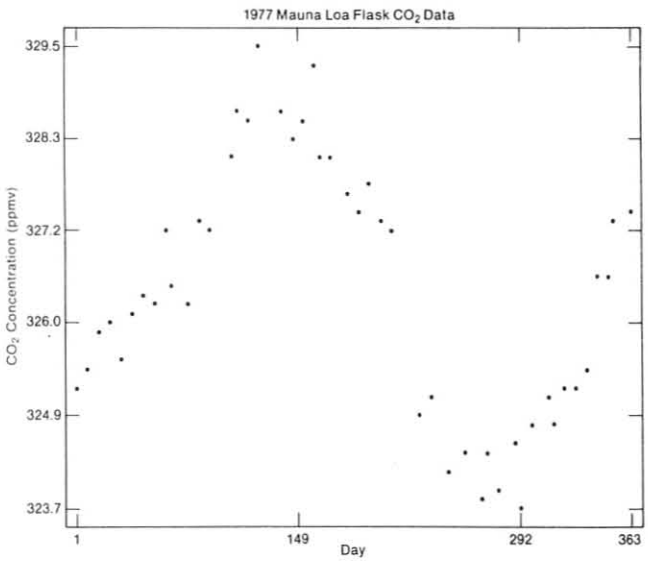

Figure 48.--Mean concentrations of CO_2 for pairs of flask air samples taken at MLO in 1977.

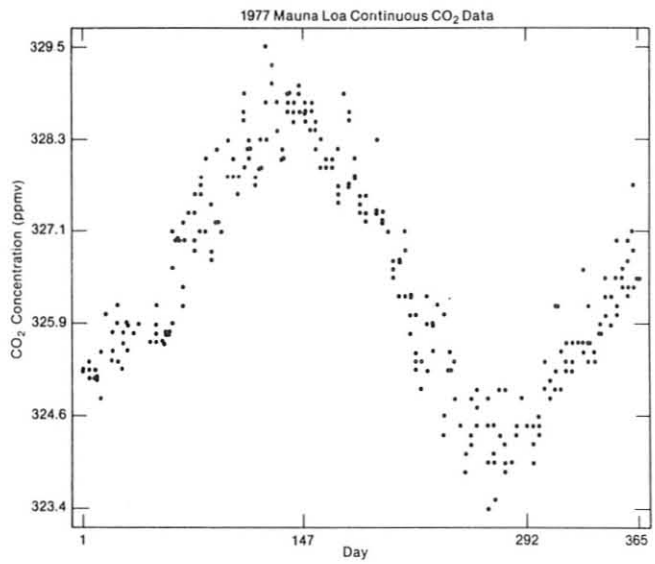

Figure 49.--Hourly mean values for the time of flask sampling at MLO in 1977.

4.4 Analysis of North Carolina Turbidity Data

In 1960, R. A. McCormick established a national turbidity network, with support from the U.S. Environmental Protection Agency (EPA) and NOAA, to provide data on the geographical, seasonal, and long term variations of atmospheric aerosols (Flowers et al., 1969). Turbidity, or aerosol optical thickness, is indirectly obtained from measurements of direct solar beam intensity and has been customarily computed on the decadic base. While standardizing and calibrating network instruments, some 8,500 turbidity observations were obtained at Raleigh, N.C., from July 1969 through July 1975. This comprehensive 6-yr data set of turbidity values was analyzed for within-day, day-to-day, and year-to-year variations and for dependnece on meteorological parameters. A full report of the analyses is in press (Peterson et al., 1981).

Table 27 summarized the 1969-1976 Raleigh turbidity measurements. A very wide range of values was detected in both instantaneous measurements and monthly averages. The annual average of 0.147 is near the highest nonurban turdidity value in the United States.

A distinct diurnal turbidity cycle was most pronounced in winter and least in summer. The daily maximum occurred in early afternoon. The early morning minimum was slightly less than the late afternoon minimum. Although we could not identify the specific cause of this cycle from available data, we believe that the cycle is a real atmospheric feature rather than an instrumental artifact.

Table 27.--Summary of atmospheric turbidity (B) and vertical transmission (T) at 500-nm wavelength for Raleigh, N.C., 1969-1976

B	T	Remarks
0	0.855	Rayleigh scattering (τ_r) and ozone absorption (τ_z) only ($\tau_r = 0.063$, $\tau_z = 0.005$)
0.010	0.836	Minimum observed value (approx.)
0.042	0.776	Smallest monthly average (Dec 1972)
0.054	0.755	Dec average
0.127	0.638	Smallest annual average (1971)
0.147	0.610	Average annual average
0.164	0.586	Largest annual average (1973)
0.318	0.411	Jul average
0.433	0.316	Largest monthly average (Aug 1974)
1.000	0.086	Maximum observed value (approx.)

The very extensive data base allowed us to describe the annual turbidity cycle in some detail. Monthly statistics showed the well known general features of high turbidity and day-to-day variation during summer and low values and variation during winter. A cubic spline best fit to daily averages, which gave a continuous estimate of turbidity during the year, revealed an asymmetric annual cycle, with a flat 1-mo-long minimum centered on 1 January rising to a peaked maximum centered on 1 August.

The dependence of turbidity on meteorological conditions was investigated by comparing individual observations with local meteorological parameters and through classification of air mass trajectories. Turbidity showed a slight dependence on surface wind measurements with higher values with lowest windspeeds. Aside from winter, highest average turbidities occurred with southeast winds and lowest turbidities with either northeast or northwest winds. A fair correlation was obtained between turbidity and relative humidity; when relative humidity was less than 40%, turbidity averaged significantly less than when it was greater than 40%. The best correlations were during winter. A better moisture parameter for turbidity correlations was dew point. For all seasons, turbidity markedly increased as dew point increased, with the most significant correlations during winter and spring. Correlations between turbidity and local visibility showed a pronounced increase for visibilities less than 7 mi, but an ambiguous visibility-turbidity dependence for visibilities greater than 7 mi.

The dependence of turbidity on synoptic air mass was investigated by using air mass trajectories arriving at Raleigh. Independent of season, air masses with a southern origin had greater turbidities than air masses arriving from either north or west. Turbidity of an air mass significantly increased as its residence time over the continental United States increased. Finally, turbidity changed more rapidly with residence time during summer than during other seasons.

Year-to-year turbidity changes were studied by combining the Raleigh (1969-present), Greensboro, N.C. (1965-1976), and Raleigh-Durham airport (1972-1975 and 1979) records. Figure 50 illustrates the monthly average turbidities from these locations. There was a distinct summer increase through 1976. Summer turbidities subsequently decreased, but a reduced measurement frequency partly obscured the significance of that decrease. Turbidity during winter has been largely unchanged. A linear regression analysis of annual averages for the complete record gave an 18% per decade turbidity increase.

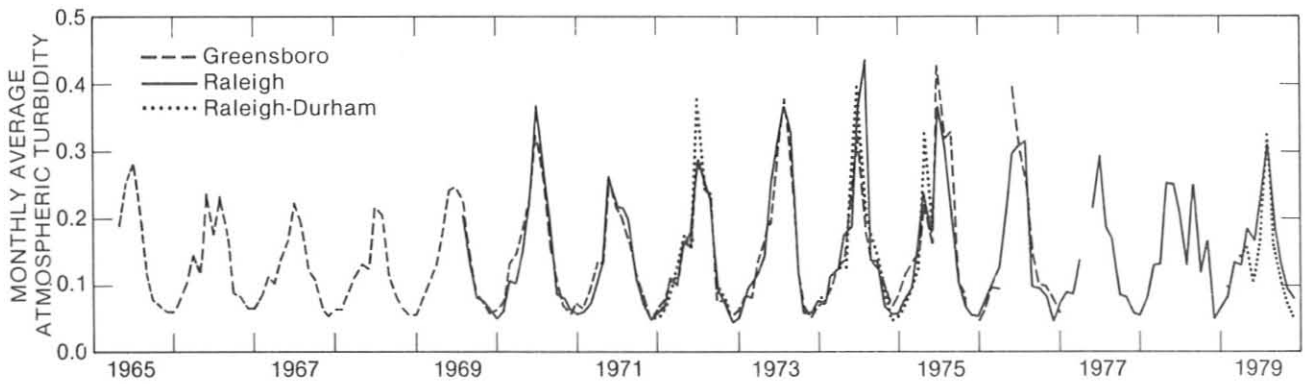

Figure 50.--Monthly average atmospheric turbidity (500-nm wavelength) at Greensboro, Raleigh, and Raleigh-Durham airport, N.C.

4.5 Barrow CO_2, Aerosol, and Ozone Dependence on Air Trajectories

One aspect of the GMCC measurement programs involves research into understanding the variability of those measurements. A method we have used for Barrow data is to link measured concentrations to air trajectories (Peterson et al., 1980). This section summarizes the research described in that report.

Daily average CO_2 concentrations at Barrow for January through April 1977 and 1978 are characterized by quasi-cyclical variations with amplitudes of 1 to 3 ppm. Ten CO_2 events were identified during these periods when concentrations significantly departed from the short term average. To investigate a meteorological cause for these variations we obtained trajectories of air flow arriving at Barrow using the method described by Hefter et al. (1975). The trajectory calculations are based on rawinsonde windspeed and direction measurements over the height interval 300 to 2,000 m above ground. Specific trajectories from 1 day of each of the 10 events are presented in fig. 51. Trajectory paths during the events were usually persistent with small day-to-day variation. Days with above and below average CO_2 concentrations are represented by dashed and solid trajectory paths, respectively. The open circles indicate 1-day travel time. The 5-day origin of four trajectories from the south was off the map.

The trajectories (fig. 51) are distinctly separated between those associated with high and those with low CO_2 concentrations. All five cases with high CO_2 had associated trajectories with air flowing from the Arctic Basin. All air trajectories associated with low CO_2 concentrations came from the south; four of these came out of the Gulf of Alaska. Synoptic meteorological charts for these periods showed that the southerly air flow usually occurred in association with a well developed low pressure system (from the surface to 500 mb or higher) in the Bering Sea-Aleutian region.

Average daily condensation nuclei concentrations, aerosol light scattering coefficients at 0.55-μm wavelength, and ozone concentrations for the 10 days

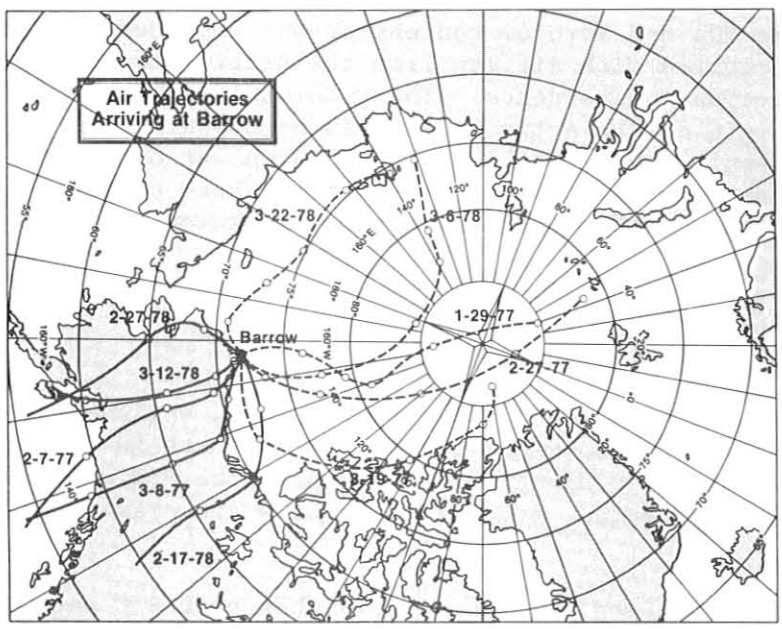

Figure 51.--Five-day trajectories of airflow arriving at Barrow, Alaska, on the indicated dates. Open circles indicate 1-day travel time. Dashed lines correspond to days with high CO_2 at Barrow and solid lines to days with low CO_2.

identified by fig. 51 trajectories were also computed. Every light scattering value associated with southerly trajectories is less than every value associated with northerly air flow. The same distribution is true for condensation nuclei concentrations, except for one occurrence. In contrast, the ozone measurements have no dependence on the north-south trajectories. The largest positive and negative departures from monthly means, for example, both occur with northerly trajectories.

The higher concentrations in air originating to the north imply a northern source of CO_2. We suggest two possibilities for such a source. The first is the Arctic Ocean itself. Gosink and Kelley (personal communication) found that during winter CO_2 is transferred to the atmosphere through the annual sea ice, which can be quite porous because of brine channels. Thus, the wintertime Arctic should not be considered as an ice-sealed passive surface with regard to exchange of gaseous carbon dioxide.

A second possible source of CO_2 "north" of Barrow is advection to the Arctic from midlatitude anthropogenic sources, primarily the northeastern United States and western Europe. Rahn and McCaffrey (1980a) suggested such sources and pathways for aerosols, based on their measurements at Barrow and other Arctic locations. They believed that the elevated aerosol mass over the Arctic from December through April probably is caused by advection from midlatitude anthropogenic sources, especially European sources, to the Arctic. Our reported dependence of aerosol measurements on north-south wind flow supports Rahn and McCaffrey's hypothesis. Although the Arctic Ocean annual ice could be a natural pathway for CO_2 to the atmosphere, we do not know of any significant natural aerosol sources from the Arctic during winter.

Our ozone measurements showed little dependence on trajectory origin, suggesting either nonexistent or spatially uniform sources or sinks in the Alaskan-Arctic region at this time of year. Thus, the fact that we see no trajectory direction dependence of ozone lends significance to an argument for spatial non-uniformity of aerosol and CO_2 sources and sinks.

In summary, we analyzed measurements of CO_2, aerosol, and ozone from the baseline observatory at Barrow, Alaska, in conjunction with low level trajectories of airflow arriving at Barrow. The CO_2 and aerosol concentrations depended on trajectory origin; higher values occurred with airflow from the Arctic Basin than from the south. Ozone had no directional dependence. These aerosol findings support the hypothesis that the origin of the Artic haze is anthropogenic. The CO_2 findings suggest two possible sources for the higher CO_2 concentrations: transfer from the ocean through annual sea ice to the Arctic atmosphere or advection to the Arctic from midlatitude anthropogenic sources by a mechanism similar to that of the Arctic haze.

4.6 Intercomparison of GMCC and SIO CO_2 Measurements at Mauna Loa

The Scripps Institution of Oceanography (SIO) has operated a CO_2 analyzer at Mauna Loa Observatory since 1958. GMCC has operated its own analyzer there since May 1974. During 1978 we began a program to directly intercompare the SIO and GMCC measurements through an exchange of data. Some first results are presented here.

Average CO_2 concentrations were compiled for those hours when both SIO and GMCC determined that their records were free of local contamination. Then we

computed the GMCC minus SIO differences by hour. Monthly summaries for 1976 are presented in table 28. The mean hourly difference, the standard deviation about that mean (SD), and the number of hours of computed differences (N) are included for each month. A histogram of the January data is shown in fig. 52.

The agreement between the two systems during 1976 was very good. Although the data from both systems were in the 1959 SIO Adjusted Index Scale (no pressure broadening correction applied), they agree well in absolute value because the pressure broadening corrections for the SIO (Applied Physics) and GMCC (URAS) instruments are similar (Pearman, 1977). Although the hourly differences averaged by month are very small, they did exhibit some small systematic variations related to the typical diurnal meteorological cycle at Mauna Loa. For example, the average nighttime differences were about 0.1 ppm greater than those during afternoon, and the differences with very dry air averaged about 0.15 ppm greater than those associated with highest dew points. Research is continuing into the cause of these small systematic differences since they indicate that the two systems do not respond similarly to some environmental factor.

The long term difference between the systems is also under investigation. Although they agreed very well during 1976, there are indications of disagreement of about 1/2 ppm in subsequent years. This cooperative investigation with SIO is being continued to determine possible causes for periods of disagreement and improve the overall data quality of both records.

Table 28.--Comparison of 1976 Mauna Loa hourly average CO_2 measurements (GMCC minus Scripps, ppm)

Month	Mean	SD	N
Jan	-0.03	0.22	362
Feb	0.00	0.21	379
Mar	-0.05	0.27	203
Apr	0.21	0.22	264
May	0.05	0.28	407
Jun	-0.08	0.18	345
Jul	0.00	0.23	229
Aug	0.01	0.23	251
Sep	0.00	0.21	163
Oct	0.03	0.27	229
Nov	0.04	0.23	427
Dec	0.13	0.21	348
Ave. (less Apr)	0.01		3,343

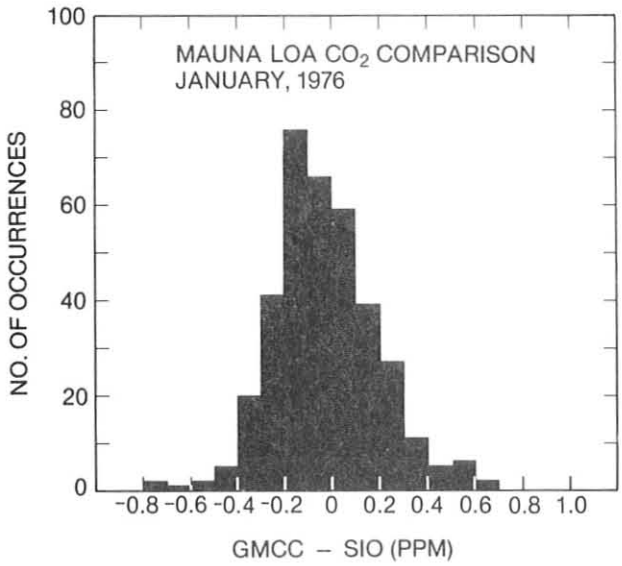

Figure 52.--Histogram of the number of occurrences at Mauna Loa GMCC minus SIO hourly CO_2 measurements. Three hundred sixty-two hourly differences from January 1976 are presented.

4.7 Signatures in Atmospheric Transmission Variations at Mauna Loa Observatory, Hawaii, and Other Parts of the World

Computation of clear sky atmospheric transmission from normal incident pyrheliometer measurements made at MLO from 1958 have been reported by Ellis and Pueschel (1971) and Mendonca et al. (1978). In both studies secular trends in clear sky transmission and a well defined annual periodicity were observed (fig. 53). The secular trends were as much as two times larger than the annual variation and attributed to explosive volcanic ejections of ash and gases into the stratosphere.

The annual variation in transmission (late spring-early summer minimum in transmission) was observed for the duration of the observation record regardless of whether volcanic explosions perturbed the atmospheric transmission at irregular intervals. When the Mauna Loa record is examined for long term secular trends in transmission, an obvious signature is not evident. If the volcanic perturbations are overlooked, a very gradual long term decrease ($\approx$0.2%) can be discerned from 1958 to 1976. But in 1977 the transmission values are as high or higher than those measured in 1958 to 1960.

In fig. 54 the annual amplitude of the atmospheric transmission for Mauna Loa is plotted with time, after the perturbations in transmission from volcanic events have been subtracted from the record. A general upward trend in amplitude is observed. Although the magnitude of the increase in annual amplitude is small ($\approx$1.0%), the percentage increase ($\approx$50%) is significant.

To investigate whether similar trends exist elsewhere, data were examined from the United States and the Orient, which are the nearest continental land masses to Mauna Loa.

Figure 55 shows a plot of atmospheric turbidity for winter and summer and the difference between the two (annual amplitude) for several stations in the continental United States. An upward trend in the annual amplitude of turbidity is evident, and an increase in summer values is the primary cause for the increase in annual amplitude with time.

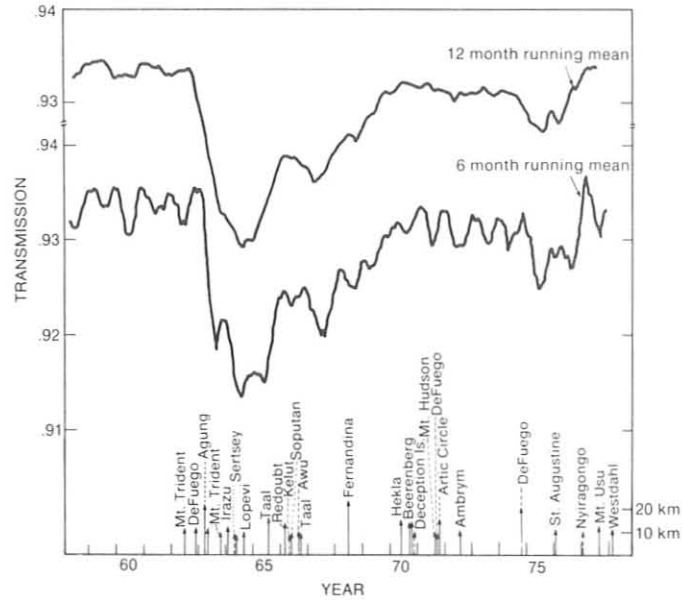

Figure 53.--Six-mo and 12-mo smoothing of Mauna Loa transmission values for 20-yr record. Episodic explosive volcanic eruptions are listed on bottom for the record period. Heights of the arrows designate the atmospheric height that the visible volcanic cloud reached. The 12-mo running mean plot shows the secular perturbations in transmission. The 6-mo running mean plot shows the annual variation as well as the secular trends. Several sharp decreases are seen in the trace after Agung, Awu, and DeFuego. From the pre-Agung period to 1976 the upper envelope of the trace suggests a gradual decrease in transmission, but in 1977 the transmissions recover and are as high or higher than during the pre-Agung period.

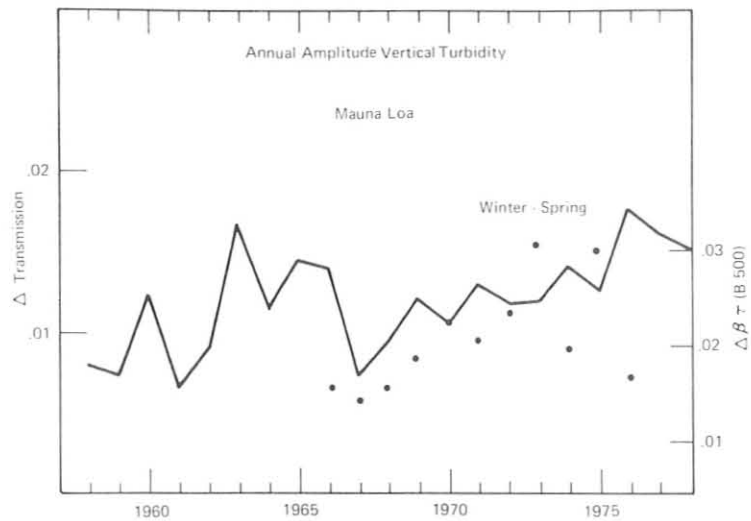

Figure 54.--The annual variation in atmospheric transmission and turbidity is plotted with time. The annual variations (ΔT and $\Delta\beta$) are obtained by taking the difference between winter and spring values. The line trace was obtained by using the transmission values from Mendonca et al. (1978); the dots are obtained from Volz turbidity measurements at MLO. The wide scatter in the turbidity data in the later years may be partially caused by instruments. The upward trend in the amplitude of transmission is detectable especially in the later years.

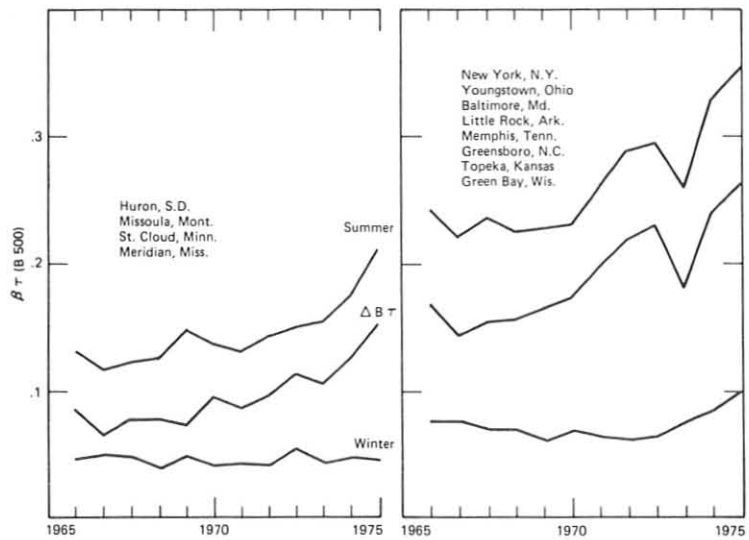

Figure 55.--Plots of Volz turbidity measurements for two groups of U.S. stations, showing trend in turbidity with time. Top and bottom curves are for summer and winter, respectively. The difference of the two ($\Delta\beta$) is the annual amplitude.

When the annual variation of vertical atmospheric turbidity is examined for Mauna Loa and the two sections of the continental United States, different signatures are evident (fig. 56). Stations in the eastern United States have the highest turbidity, standard deviations, and annual amplitude, as would be expected for measurements near a source region. As the measurements progress westward to middle America the annual amplitude decreases and the maximum shifts toward spring, with smaller standard deviations. This appears to be a feature of cleaner sites.

In fig. 57 a comparison between the annual variation of atmospheric transmission between Asia and Mauna Loa is shown. In contrast to the comparison between Mauna Loa and the continental United States, the annual transmission variations in fig. 57 are in phase. The transparency of the atmosphere has been determined by several methods with the same results.

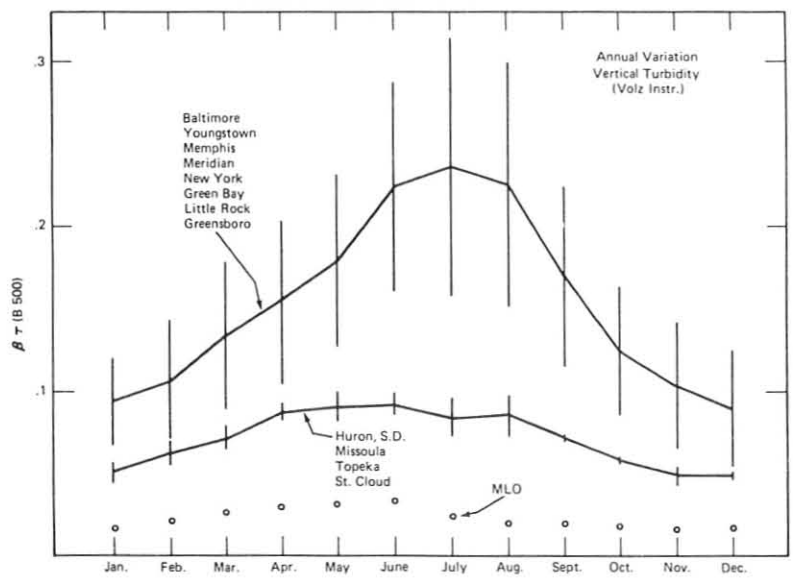

Figure 56.--Average monthly turbidities and standard deviation for three groups of stations.

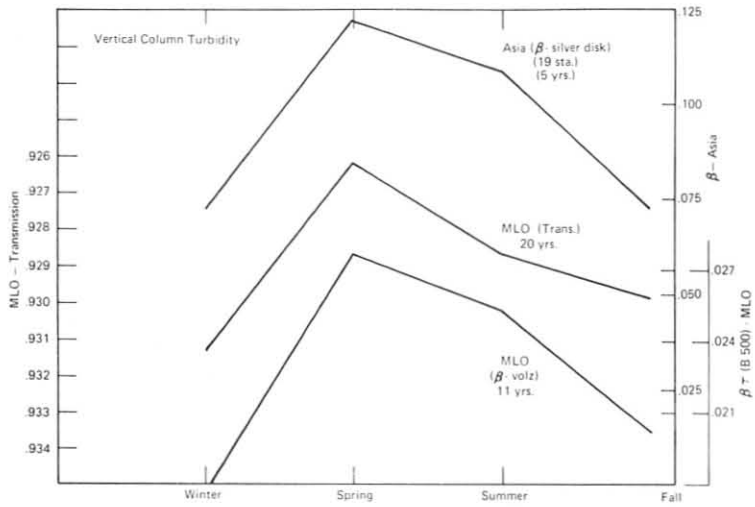

Figure 57.--Average seasonal variations in turbidity for Mauna Loa and Asia. The Mauna Loa transmission values and Volz turbidity measurements are compared with atmospheric turbidity values determined from silver disc pyrheliometer measurements made in Japan, Korea, and China (Yamamoto et al., 1968).

The annual amplitude of vertical turbidity for several stations in Japan is presented in fig. 58. Although the scatter is large, an increasing trend in annual amplitude is also discerned from the record. The increase in annual amplitude for Japan is more pronounced from the 1950's to the present than for the earlier years. Yamamoto et al. (1968) suggest that the decrease in industrial activity in Japan immediately after World War II explains the decrease in turbidity in that period.

From all data examined the annual amplitude in atmospheric transparency shows an increasing trend with time from the 1950's in the eastern and central United States, Mauna Loa, and east Asia. The increase in annual amplitude results mainly from an increase in turbidity in summer or spring, when turbidity is at the annual maximum. Whether this long term increase in summer and spring results from increases in industrial activity coupled with the greater atmospheric vertical mixing and consequential longer aerosol residence time (spring-summer) must still be examined. If industrial activity contributes to the increasing turbidities in summer and spring, then gas-to-particle conversions with increased sunlight and vertical moisture convection at these times could also add to the long term turbidity increases in summer and spring.

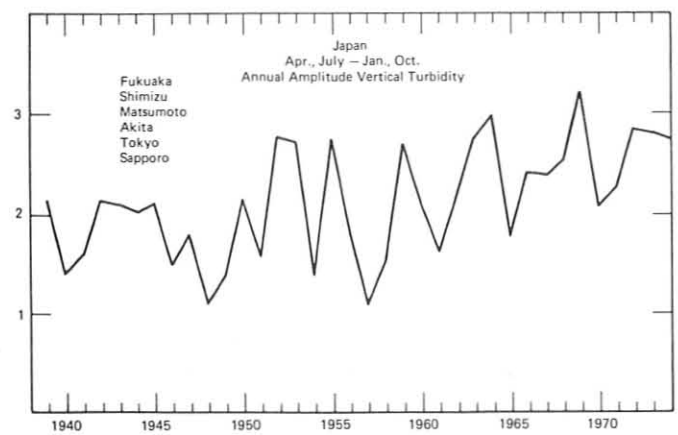

Figure 58.--The annual amplitude in atmospheric turbidity over Japan is plotted with time. The ordinate scale is a relative measurement of the annual amplitude.

5. COOPERATIVE PROGRAMS

5.1 Air Chemistry Studies at Barrow During 1979

Kenneth A. Rahn
University of Rhode Island
Kingston, RI 02881

During 1979 the University of Rhode Island continued to study air chemistry at Barrow. Routine 4-day high volume samples of the near surface aerosol were taken throughout the year. In September, the fourth consecutive year of such sampling began.

In July and August, an improved, expanded relay box for the sample control system was installed by R. J. McCaffrey, designed to accept multiple high and low volume samplers simultaneously, and operate them in nearly any combination of clean sector, dirty sector, and continuous sampling. At the same time, a second high volume aerosol sampler, identical to the first, was installed, to allow us to take samples for other researchers, or to take different types of samples simultaneously. A problem in the sector control box was discovered in August and rectified at URI during fall. The entire control system was put into operation in December. We now have a mini sampling center at BRW that H. Rosen of LBL has used for his low volume sampling of carbonaceous aerosol.

In Summary Report 1978 we presented data from our 1976-77 samples; this year, we show data (fig. 59) for $SO_4^=$, V, and ^{210}Pb for individual samples of 1977-78 (Rahn and McCaffrey, 1980a). $SO_4^=$ and V, which we believe are derived from distant pollution sources, show similar patterns to those of 1976-77, with a spring maximum superimposed on a broader winter plateau. $SO_4^=$ decreases some weeks later in spring than does the V. Both show pronounced quasi-monthly cycles of concentration.

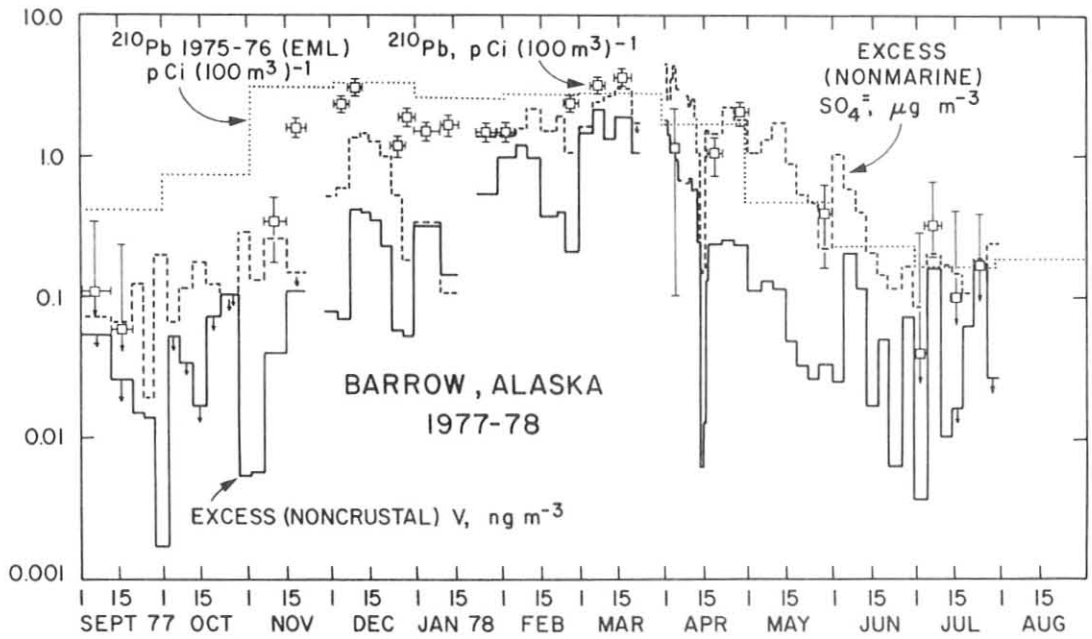

Figure 59.--Concentrations of noncrustal V, nonmarine sulfate, and ^{210}Pb in individual filter samples at Barrow, Alaska, during 1977-78. Monthly mean concentrations of ^{210}Pb at Barrow during 1975-76 (EML) are given for comparison. (After Rahn and McCaffrey, 1980a).

Both our ^{210}Pb data for individual samples and earlier ^{210}Pb data from Environmental Measurements Laboratory (monthly means) agree in magnitude and point to a nearly level winter plateau beginning in November. This rapid early rise is probably related to the early peak of the precursor ^{222}Rn.

Several special experiments were conducted at BRW during 1979 by our group and in cooperation with other groups. In March and August-September, aerosol samples were taken on glass fiber filters for J. Daisey of NYU for organic analysis. Her results have shown that organic matter is probably the second most abundant constituent of the Arctic winter submicron aerosol, and that its sources are different from winter to summer. Portions of her extracts have been analyzed by C. Weschler of Bell Laboratories; among the most interesting of his results is the presence of high concentrations of silicones.

From 31 March through 14 April, aerosol was sampled simultaneously at BRW and Narwahl Island, a remote location 30 km north of Prudhoe Bay, to check the regional representativity of the clean sector of the Barrow atmosphere. T. J. Conway of URI undertook this experiment in response to suggestions that the high concentrations of aerosol at Barrow, even in its clean sector, were from Barrow itself and not representative of the North American Arctic in general. The Narwahl Island site was upwind of all human activity when the winds came from the north, and hence was considered the baseline. The results showed conclusively that Barrow clean sector air truly represents the Alaskan Arctic air. Concentrations of the pollutants $SO_4^=$ and V were nearly the same at BRW and Narwahl. Filters from both locations were equally gray (from sooty carbon) and could not be told apart by eye. These results give confidence to comparisons between data from Barrow and those from other Arctic locations. One example of such a comparison is the map of typical winter concentrations of $SO_4^=$ shown in fig. 60 (Rahn and McCaffrey, 1980a), which shows sulfate on both sides of the Arctic.

From 27 July to 7 August, R. D. Borys of Colorado State University took a series of aerosol samples at Barrow, as part of a six site study of cloud active aerosol (cloud condensation nuclei and ice nuclei) in and around the Arctic. This work will form the bulk of his Ph.D. thesis.

Beginning in August, we obtained a series of measurements of fluxes of ^{222}Rn from the tundra and ambient concentrations of ^{222}Rn, through a cooperative experiment between R. J. McCaffrey and EML in New York. Fluxes were measured by absorbing the ^{222}Rn in activated charcoal cannisters mounted on pipes driven into the tundra. The results, which are still uncertain because of slow mail service between Barrow and New York, show very low fluxes of roughly 1 to 7 atto Ci $cm^{-2}s^{-1}$. Comparable values in New Jersey are 40 to 100 atto Ci $cm^{-2}s^{-1}$, decreasing to roughly 5 atto Ci $cm^{-2}s^{-1}$ when the ground is frozen. By contrast, the atmospheric concentrations of ^{222}Rn were 20 to 70 pCi m^{-3} (2-wk averages), the highest yet measured for coastal regions of Alaska. Figure 61 shows that Barrow has the same fall maximum reported earlier for Kodiak and Wales, Alaska, but higher concentrations. These data are consistent with an Alaskan source to the south or a distant source to the north; more detailed experiments will be required to reveal which explanation is correct.

In December we began a program to sample daily the Barrow aerosol with the second high volume sampler. This project had several purposes: to better correlate our results with GMCC data and the NOAA trajectories to Barrow, to compare concentrations with locations of air masses and synoptic systems near Barrow, and to investigate the relative amplitudes of the various temporal cycles of the aerosol at Barrow. The experiment will be repeated during winter 1980-81.

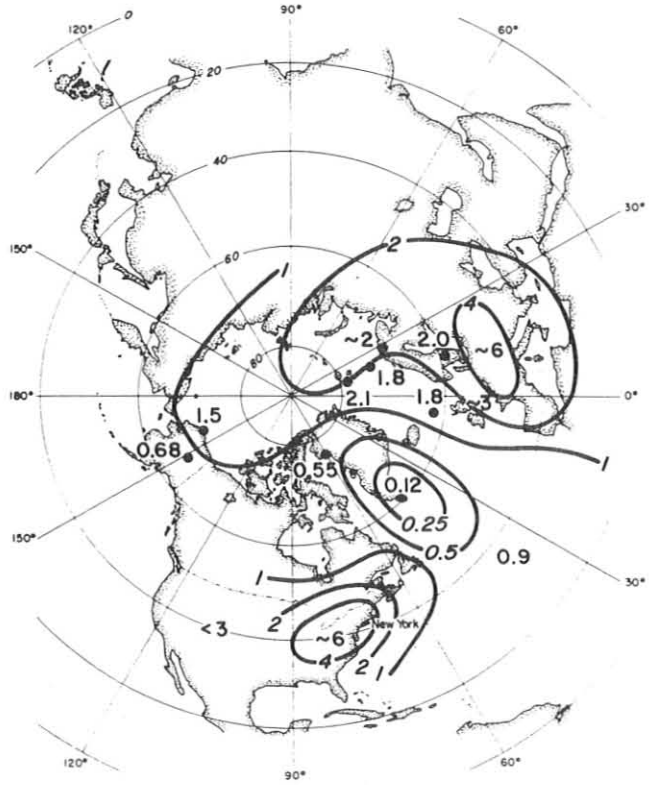

Figure 60.--Winter concentrations of nonmarine sulfate, μg m^{-3}. (After Rahn and McCaffrey, 1980a).

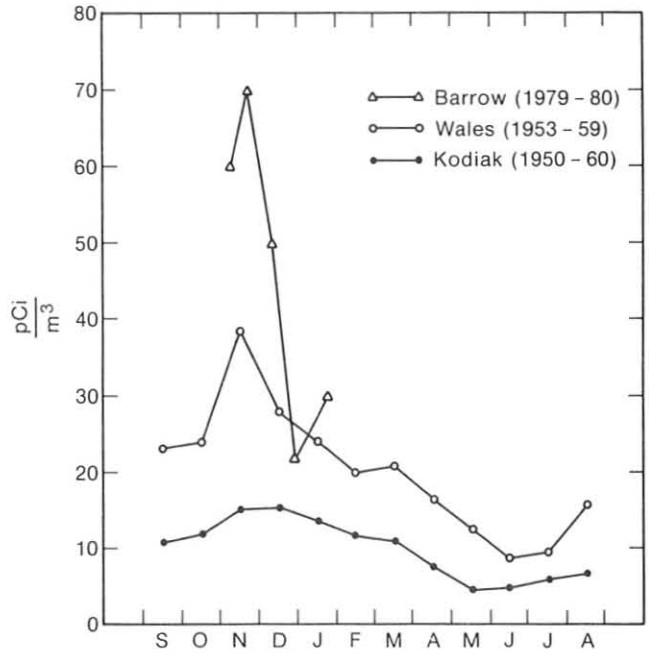

Figure 61.--Monthly mean concentrations of the continental gas ^{222}Rn at Barrow and two other Alaskan sites. Wales and Kodiak data are from Lockhart (1962).

5.2 Soot in the Arctic

H. Rosen and T. Novakov
University of California
Berkeley, CA 94720

A sampling program for characterizing the carbonaceous aerosol was started in August 1979 in Barrow, Alaska. The preliminary results of this study show the following important features:

(1) The concentrations of the aerosol particles dramatically increase from fall to early spring with the levels of carbonaceous particles approaching 2 μg m^{-3}, which is only about a factor of 4 less than the loadings typically found in urban environments.

(2) The Arctic haze contains a large graphitic component, which in the spring can account for approximately 40% of the carbonaceous mass. This component can only be produced by combustion processes, and therefore, if forest fires ignored, it must have an anthropogenic origin.

(3) Graphitic carbon has a large optical absorptivity, evidenced by the grey or black appearance of the filter deposits. The magnitude of the absorption coefficient b_{ab} during the spring is approximately 5 x 10^{-6} m^{-1}, which could be climatically significant if the absorbing species extends over several kilometers

in height. Visual observation (Mitchell, 1956) from airplane flights indicates that the Arctic haze extends up to 10 km. A simple model calculation using the two stream approximation of Chylek and Coakley and assuming a 10-km pathlength and a snow albedo of 0.8 yields a change in the planetary albedo of 10%, which is quite large and may significantly affect the heat balance over the Arctic region (Shaw and Stamnes, 1980).

(4) The ratio of total carbon to sulfate content of the aerosol at Barrow is similar to that found for Brosset's (1979) black episodes in Sweden, which have been postulated as resulting from long range transport. The Arctic haze may be due to a continuation of this transport process, as suggested by Rahn and McCaffrey (1980b).

(5) Results obtained with samples collected with and without a wind controller suggest that there is no significant contamination from local sources. Further, aerosol samples collected at other sites across the Arctic (Mould Bay, Spitzbergen) seem to show the same general features as those collected at Barrow (Barrie et al., 1980; Ottar et al., 1980).

These preliminary observations suggest that antropogenically generated aerosol concentrations comparable to those found at urban locations can develop even in remote environments.

An aerosol sampler was designed and constructed at Lawrence Berkeley Laboratory to collect parallel filter samples on 47-mm quartz fiber and millipore substrates at a flowrate of approximately 1.5 cfm. The sampler was put into operation on 18 October 1979 and coupled to a wind controller on 7 January 1980, to minimize local contamination by collecting samples only when the wind was blowing from the clean air sector. Approximately 50 filter pairs have been collected at sampling time intervals ranging between 2 days and 1 week. All these filters have been analyzed to determine the total carbon content of the aerosol, the absorption coefficient of the aerosol, and the concentration of elements with $Z > 11$ by the X-ray fluorescence technique. Only selected filters have been analyzed by Raman spectroscopy and opticothermal analysis.

Raman spectroscopy was applied to the analysis of several samples collected at Barrow. The results are shown in fig. 62, where the spectrum of an Arctic haze sample is compared to that of urban particulates, various source emissions, and carbon black. All these spectra show the presence of two intense Raman modes located at 1,350 and 1,600 cm^{-1}, which have been identified as resulting from phonons propagating with graphitic planes. This result shows that graphitic structures similar to carbon black and caused by combustion processes are present in the Arctic aerosol. Further, the large intensity in these modes indicates that the graphitic structures represent a major component of the aerosol.

The filters collected at Barrow from fall through late spring have a grey or black appearance similar to that found for urban particulates. For the urban samples, this optically absorbing component has been identified as the graphitic species determined by Raman spectroscopy (Rosen et al., 1978). For the Arctic samples, a similar identification is presumably valid but needs to be tested. Preliminary measurement on a limited number of samples shows that the optically absorbing species has a $1/\lambda$ wavelength dependence, is insoluble in a wide range of solvents, and has a high temperature stability with an oxidation threshold of approximately 500°C. These results are consistent with the properties of graphitic carbon and strongly suggest that the optically absorbing species at Barrow is graphitic.

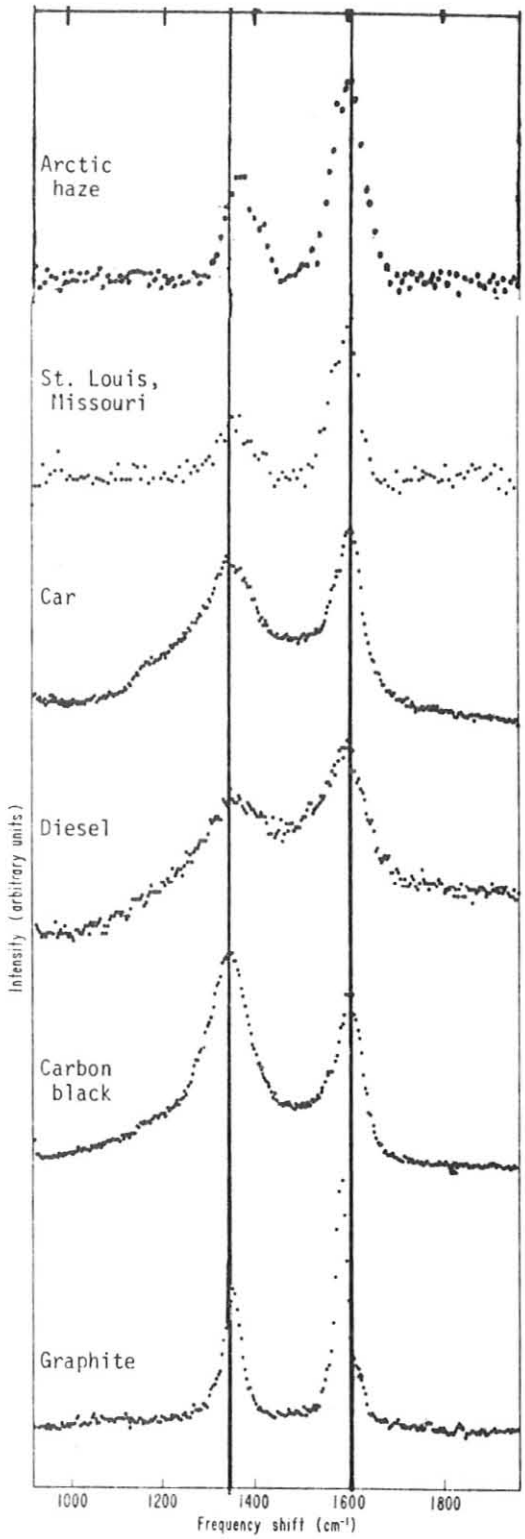

Figure 62.--Raman spectra between 920 and 1,950 cm^{-1} of Arctic haze, urban, and various source particulate samples.

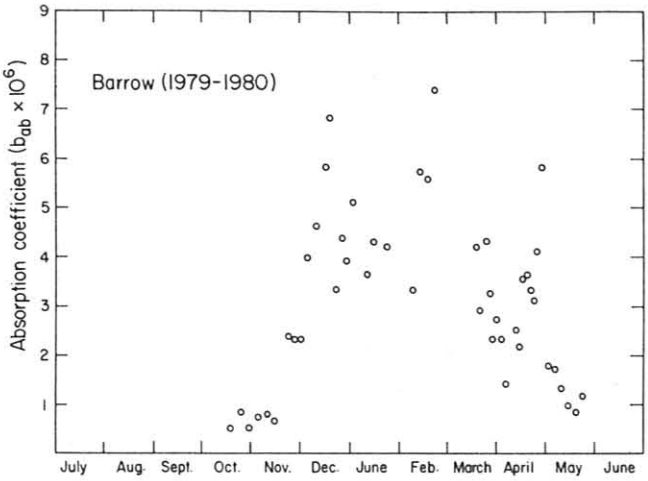

Figure 63.--Biweekly averages of absorption coefficient at Barrow from October 1979 through May 1980.

The variation of the optical absorptivity (or graphitic carbon concentration) of the Barrow aerosol is rather dramatic (fig. 63). The absorption coefficient changes by about an order of magnitude from early November to early January and remains at a relatively high level throughout most of February, March, and April. It decreases substantially in May. The magnitude of the absorption coefficient during winter and spring is comparable to that found in urban environments (i.e., about a factor of 5 less than Berkeley and Denver and a factor of 10 less than New York) and appears to be an areawide phenomenon with similar annual variations occurring at widely spaced sites across the Arctic (Mould Bay, Spitzbergen) (Barrie et al., 1980; Ottar et al., 1980); see fig. 64.

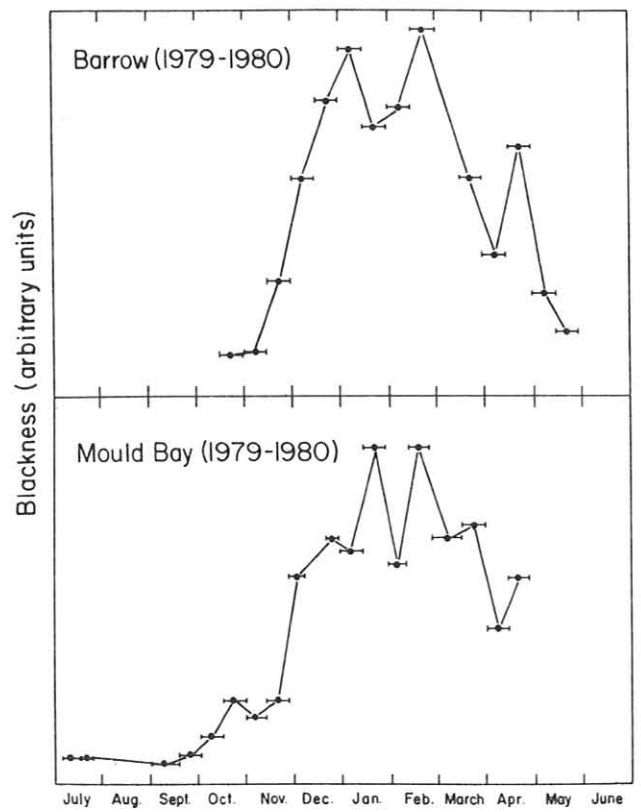

Figure 64.--Comparison between seasonal variation in blackness of filter deposits collected at Barrow, Alaska, and Mould Bay, Canada, in 1979 and 1980. Mould Bay samples were provided by L. A. Barrie and R. M. Hoff of the Canadian Atmospheric Environment Science.

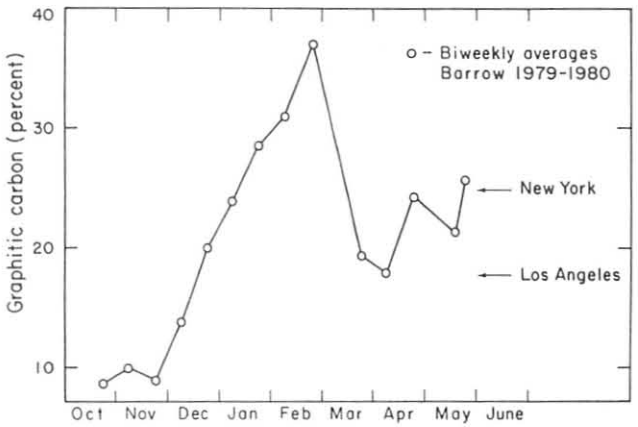

Figure 65.--Biweekly averages of the graphitic content as a percentage of the total carbon content of the Barrow aerosol from October 1979 through May 1980.

Using the optical constants of graphitic carbon determined from our urban studies, we can estimate the graphitic carbon concentration at Barrow. (Measurements are under way to test these determinations by an independent methodology.) These results are shown in fig. 65, where we plot the graphitic carbon concentration as a fraction of the total carbon content of the aerosol for various periods of time during the year. The results show a strong enrichment of the graphitic fraction of the carbonaceous aerosol from early to late winter. The concentration of graphitic carbon in late February is almost 40% of the carbonaceous mass. The percentage is higher than that found in urban centers like New York City and Los Angeles. After its peak in February, the fraction of graphitic carbon seems to level off to a value more typical of that in urban environments.

5.3 Chemical Composition of Atmospheric Aerosols

William H. Zoller, William C. Cunningham, and Namik K. Aras
University of Maryland
College Park, MD 20742

Our project was designed to measure the chemical composition of atmospheric particulate material in remote areas. Since different sources of airborne particulate material have different chemical compositions, the important sources can be identified for a given location. Through these measurements we hope to observe changes in the chemical composition of remote aerosols that result from changes in the sources (seasonal variations or anthropogenic emissions) or in the mode of transport to remote areas. Measurements began in 1970 at the South Pole, and the record of aerosol chemical composition is nearly continuous from 1975. Measurements began in February 1979 at Mauna Loa Observatory.

At present aerosols are collected on filters at each location using high volume vacuum pumps and all plastic sampling systems. Nuclepore, Fluropore, and Whatman 541 filters are currently used at the sampling sites along with Battelle-type cascade impactors for particle sizing experiments. At SPO, sampling is controlled by a wind directional controller that allows sampling only when the wind is from the Clean Air Quadrant and windspeed exceeds 1.3 m s^{-1}. The Clean Air Quadrant is defined as a 140°-wide area to the northeast of the station. The wind comes from this area almost 90% of the time, and the quadrant is off limits to all vehicles and people to minimize contamination.

At MLO, we collected downslope samples between 2100 and 0500 and upslope between 0800 and 1800. During the day sunlight heats up the island's lava, which in turn heats up the air, making it rise up the slope of the volcano, and sea breezes transport sea salt up onto the higher areas. At night the island cools rapidly, and air flows down the mountain allowing clean air from above the boundary layer to flow over the station. Sample collection periods at SPO are 10 days and at MLO 7 days. Samples for shorter periods are occasionally collected, but because of the low concentration in clean, remote areas, only a few (10 to 15) elements can be determined above the filter blanks. All samples are analyzed by nondestructive neutron activation analysis for the trace elements, and soluble sulfate is determined by flash volatilization using flame photometric detection.

5.3.1 South Pole Station

Measurements have been taken at the South Pole almost continuously since the 1974-75 austral summer season (Maenhaut et al., 1979; Cunningham, 1979; Zoller et al., 1979). The results of these measurements show that a relatively consistent pattern of atmospheric aerosol composition reflects changes in the transport mechanisms of aerosols into the interior of the Antarctic continent. The observed chemical composition variations can be compared with the known composition patterns of sources to identify some major aerosol contributors in the Antarctic: crustal dust, sea salt, meteorite burnup in the atmosphere, and tropospheric plus stratospheric sulfate. The source of the anomously enriched elements (Se, As, Sb, Zn, In, Pb, Cd, Au, Ag and Br) is unknown, or in doubt. These elements only account for a few percent of the total mass but are greatly enriched over that expected for known sources of airborne particulates. A portion of these elements is believed to come from volcanic emissions and the ocean (Br).

In fig. 66, the time variations for four austral summer seasons and two over-winter periods are shown. The variations are compared with those for ^{7}Be, a radionuclide produced in the stratosphere that shows regular seasonal patterns related to the transport of stratospheric material into the troposphere and then into the interior of Antarctica. The results show that sulfate, crustal dust, and meteorite debris are correlated to ^{7}Be in that they have higher concentrations in austral summer and significantly lower concentrations during winter. Sea salt, on the other hand, shows a significant increase during winter. Se does not show any significant variations during these periods, making it difficult to assess its sources or transport to Antarctica. For sulfate, the over-winter mass observed is corrected for the contribution of marine salts and in many cases is only an upper limit, since the levels were below the detection limit of the analytical procedures. The results in fig. 66 are calculated as follows for each component.

Crustal dust: The mass of dust is calculated on the basis of the elements Al, V, and Sc, using the crustal composition pattern of Taylor. At first we also used Mn and Fe, but significant variations of these elements were observed on some samples which we found to be correlated with enhanced cobalt believed to be of meteoritic origin.

Meteorite: Excess Co is used as the tracer of this component, but excess Fe, Mn, and occasionally Mg are also used to calculate the mass of this component, using the composition of average chondritic meteorites for comparison (B. Mason, personal communication, 1979). Of these elements, the ones with the greatest influence are Co and Fe.

Sea salt: Sodium, the major element that indicates sea salt, is used to calculate the mass of this component after correction for its crustal contribution.

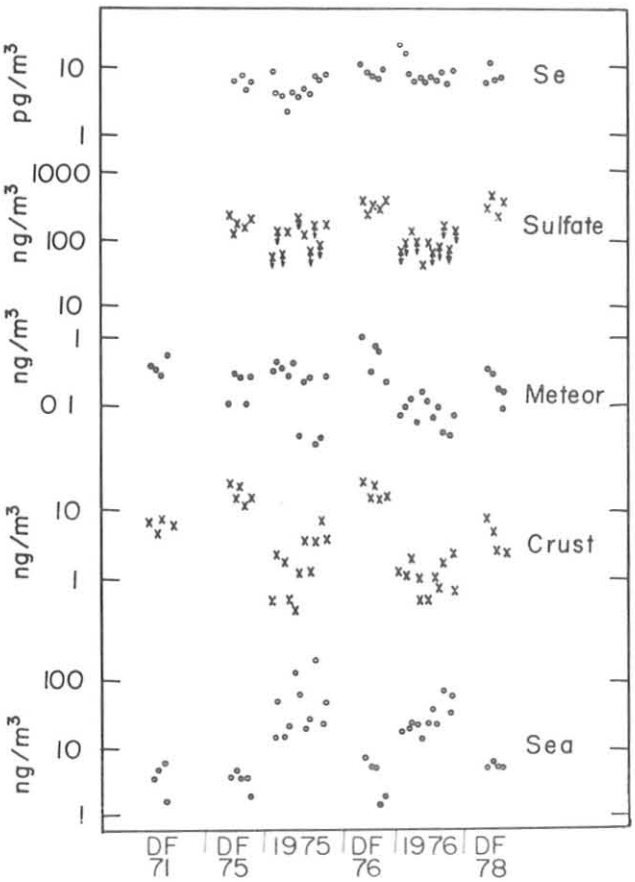

Figure 66.--Temporal variation of components in the Antarctic atmosphere.

Other elements (K, Ca, and Mg) are used as checks, but uncertainties with respect to their possible fractionation at the sea surface and analytical uncertainties make their use questionable.

Sulfate: Sulfur is measured and the sulfate mass is calculated by assuming that all sulfur is present as So_4^{2-}. Correction is made for marine source sulfate, so that the mass given is for excess sulfate, which is believed to come from the stratosphere as well as troposphere. During winter, a majority of levels were below the sensitivity of neutron activation analysis and so only upper limits could be determined. In more recent studies, more sensitive analytical techniques have been employed.

From the observed time variations of each component and the meteorology of the region, a model of transport has been developed that shows a strong seasonal variation of the sources and the mode of transport to the interior of Antarctica. During the austral summer, transport is enhanced between the stratosphere and troposphere, causing the higher levels of ^{7}Be, sulfate, and meteorite debris observed then. The mixing probably occurs near the margins of the Antarctic continent, and the air moves over the continent where it gradually mixes and diffuses toward the surface. During summer the entire area around and over Antarctica is relatively calm, with minimal storm activity, so that the sea salt has little chance of mixing to an altitude high enough to be carried into the interior of Antarctica. The small amount of sea salt and the crustal dust that reaches the interior of Antarctica is believed to be transported through the upper troposphere from areas distant from the Antarctic.

The transport during the winter season is exactly the reverse, with exchange between the troposphere and stratosphere substantially reduced, while intense storm activity off the coast of Antarctica mixes sea salt into the upper troposphere. Since passing weather systems tend to circle the Antarctic continent and not move toward the interior, they act as a barrier to air masses moving to the south from the continental areas of Australia, Africa, and South America. This effect results in the washout or rainout of crustal dust being transported toward Antarctica. Some sea salt aerosols are transported to the upper areas of the troposphere, where water vapor evaporates leaving sea salt particles that are then transported into the interior of the Antarctic continent by persistant air flows in the mid to upper troposphere. Some of this sea salt then finds its way to the surface in the interior and, in some cases, can be identified with large storm activity off the coast as observed during fall 1979.

5.3.2 Mauna Loa Observatory

The results of the sample analyses from MLO are handled similarly to those for South Pole samples. We have compared the cleanest conditions at MLO with summer conditions at SPO. Table 29 shows a comparison of the concentrations of some elements associated with crustal dust or sea salt and a few anomously enriched elements for each site. We have also included the winter and summer data for the South Pole and have calculated the ratios of some values. The downslope sulfur levels are comparable with the South Pole summer results but are higher than the

Table 29.--Mean atmospheric chemical concentrations of atmospheric aerosol

Element	South Pole (all data)		Mauna Loa (clean)			DS/summer
	Summer*	Winter†	Downslope	Upslope	US/DS	
S (ng m^{-3})	76±24	29±10	74±12	230±90	3.1	0.97
Na (n m^{-3})	5.1±1.7	40±31	3.3±2.5	88±56	27	0.65
Al (ng m^{-3})	0.83±0.41	0.30±0.04	5.0±3.2	14±8	2.8	6.0
Mn (pg m^{-3})	14±6	6.7±4.5	85±65	190±110	2.2	6.1
V (pg m^{-3})	1.6±0.6	~0.9	11±9	27±13	2.4	6.9
As (pg m^{-3})**	24±7	-	17±3	23±20	1.4	0.71
As (pg m^{-3})††	8.4±1.1	17±9	-	-	-	-
Se (pg m^{-3})	6.3±0.6	6.9±2.7	35±24	25±8	0.7	5.6
Sb (pg m^{-3})**	2.0±1.6	-	6.6±2.9	5.8±3.3	0.9	3.3
Sb (pg m^{-3})††	0.45±0.16	2.1±1.5	-	-	-	-

*Average of four summers.

†Average of two winters.

**Nuclepore filters.

††Whatman 541 filters.

winter results. The upslope sulfur concentrations are higher by a factor of three than the downslope values because of the increase in sea salt sulfate. The downslope sodium values are also approximately the same as observed in Antarctica, whereas the upslope values are nearly 30 times higher. All crustal elements (Al, Mn, and V) show downslope levels six times higher than during the average Antarctic summer season. These crustal elements also show an increase in the upslope samples presumably indicating soil derived particles from the Island of Hawaii itself.

The volatile elements show some very startling differences. The concentrations observed in the upslope and downslope samples are essentially the same, showing no change with wind direction or meteorological conditions. The levels of As are very similar for SPO and MLO, whereas Se and Sb levels are higher in Hawaii. The differences observed for the Whatman and Nuclepore filters are believed to be caused by the efficiency differences for these filters for small aerosols (Maenhaut et al., 1979). Since the winter Whatman samples have concentrations similar to the summer Nuclepore samples, it is tempting to suggest that the observed differences in the Whatman concentration during the summer and winter are caused by different scavenging mechanisms that occur during the colder seasons. The large increases in Se and Sb in Hawaii are very interesting. Although the number of observations during 'clean' conditions in Hawaii is small, one is tempted to suggest that the higher levels are caused by antropogenic production. A majority of anthropogenic emissions are in the Northern Hemisphere and these two elements (Se and Sb) are enriched in anthropogenic sources (Gladney et al., 1976; Greenberg et al., 1978, and Kowalczyk et al., 1978).

Another important aspect of the measurements in Hawaii has been the identification of the source of the aerosols that cause hazy conditions each spring. These conditions are typified by a drastic increase in the light scattering ($b_{scat} = 10^{-7} \rightarrow 10^{-5}$ m $^{-1}$) without a comparable rise in the number of condensation nuclei. During 1979, we collected samples that showed that the large increase in the mass of the atmospheric aerosol at Hawaii results from an increase in the amount of crustal component usually observed. This relation is evidenced by the large increase in the crustal elements such as Al, Mn, Fe, V, Sc, etc. Figure 67 shows the aerosol mass for crustal dust and salt during upslope samples collected in spring 1979. A similar plot for the downslope samples is shown in fig. 68. The downslope results show a similar increase in crustal mass with the highest concentration occurring in early May. The mass of the marine aerosol in the downslope samples is much lower than that in the upslope ones. The large increase in the downslope samples in early June appears to be caused by contamination of the site by winds during evening. This is confirmed by the chemistry of the aerosols, which is similar to that of the weathered island lava. There is some slight indication, because of excessive levels as As, that venting of Mauna Loa volcano may be partially responsible, but no substantial increase in Se or Sb was detected. To be more certain of the potential of the volcano to impact these samples, samples of gaseous and particulate emissions from Mauna Loa volcano should be collected and characterized for the minor and trace elements that are uniquely enriched by each volcano.

The chemical composition of the dust during the April-May episode is significantly different from the chemistry of Hawaiian basalt and compares more favorably with that observed for desert dust. A more detailed comparison is currently under way using the concentrations of more than 35 trace elements in the Hawaiian aerosol samples and desert dust samples from different areas of the world. It appears that the desert dust samples and the anomolous Hawaiian aerosol samples are both enriched in the rare earth elements and some of the heavy metals so that it appears possible to develop a unique chemical fingerprint for this dust and

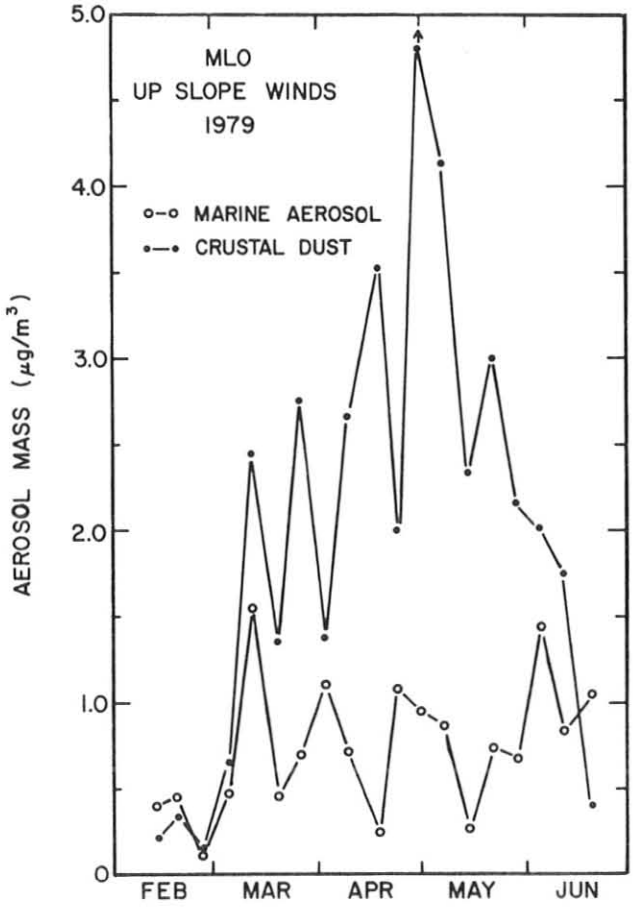

Figure 67.--Temporal variation of crustal dust and sea salt during up-slope wind conditions at MLO when Asian dust impacts the area.

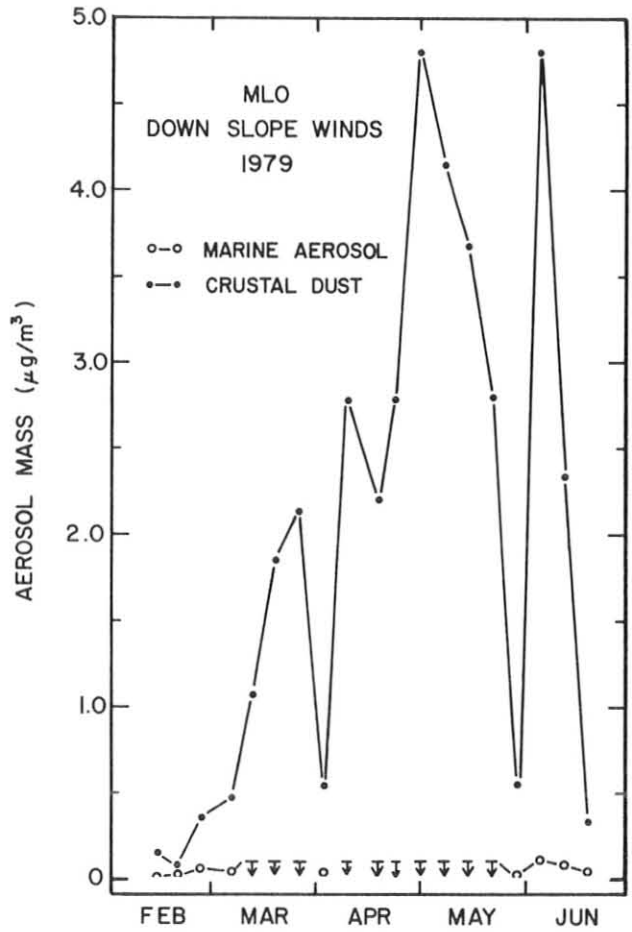

Figure 68.--Temporal variations of crustal dust and sea salt during down-slope wind conditions at MLO when Asian dust impacts the area.

identify its source by the chemical composition when samples of the source dust are analyzed.

J. Miller of NOAA, who has calculated air mass trajectories during the time period, has shown that the air masses carrying the dust came from the west. The trajectories all point toward the northwest Pacific ocean and would indicate that the dust observed comes from the Asian mainland. These results agree very well with the characteristics observed by Duce et al. (1980) at Eniwetok, where they observed an increase in aluminum (dust) during the same period, and their air mass trajectories also point back toward the Asian mainland. The dust has been previously observed in Japan where it is generally yellowish or light brown (Kadowski, 1979). It would appear that during each spring season Asian desert dust is blown throughout a majority of the north Pacific basin. Further studies of the composition of dust samples from the Asian mainland and Hawaiian aerosols will provide more conclusive evidence for this long range transport.

5.4 Nuclear Fallout and High Volume Aerosol Collections

Herbert W. Feely
Environmental Measurements Laboratory
U.S. Department of Energy, New York, NY 10014

Precipitation samples, analyzed for ^{90}Sr fallout from atmospheric tests of nuclear weapons, are collected monthly in plastic buckets at MLO and SMO. They are combined into quarterly composites and analyzed with samples from about 70 other stations (see Feely et al., 1978).

High volume filter samplers, which sample air at about 1 m^3 min^{-1}, are operated for EML at all four GMCC observatories. These are part of a network of about 20 samplers operated for EML, mainly in the Western Hemisphere. Monthly composites of the filter samples are analyzed routinely by gamma spectrometry for ^{7}Be, ^{95}Zr, ^{137}Cs, and ^{144}Ce. Until mid-1976 they were also routinely analyzed radiochemically for ^{210}Pb, ^{90}Sr, and $^{239,240}Pu$. Results are reported quarterly.

Table 30.--Quarterly mean concentrations of radionuclides in surface air filter samples collected at GMCC observatories, 1978 to 1979

	1978				1979			
	1	2	3	4	1	2	3	4
^{7}BE (fCi m^{-3})								
BRW	66	50	26	48	84	50	21	54
MLO	194	197	149	175	144	220	181	161
SMO	-	83	92	61	69	49	75	65
SPO	118	141	114	192	232	89	116	140
^{95}Zr (fCi m^{-3})								
BRW	1.7	1.7	<0.5	<0.5	<0.5	<0.5	<0.5	<0.5
MLO	1.7	1.4	<0.5	<0.5	<0.5	<0.5	<0.5	<0.5
SMO	-	<0.5	<0.5	<0.5	<0.5	<0.5	<0.5	<0.5
SPO	<0.5	<0.5	<0.5	<0.5	<0.5	<0.5	<0.5	<0.5
^{137}Cs (fCi m^{-3})								
BRW	1.7	2.1	0.5	0.4	0.7	0.5	<0.1	0.2
MLO	3.9	4.7	1.2	0.5	1.1	1.7	0.5	0.2
SMO	-	<0.1	0.1	0.1	<0.1	<0.1	<0.1	0.1
SPO	0.1	0.2	0.1	0.2	0.3	0.2	0.1	0.1
^{144}Ce (fCi m^{-3})								
BRW	13.6	13.7	3.8	1.7	2.2	1.6	0.3	<0.4
MLO	32.4	34.0	7.2	2.7	3.7	4.6	2.2	<0.5
SMO	-	<0.5	0.5	<0.5	0.4	<0.3	<0.2	<0.3
SPO	<0.5	<0.5	<0.5	<0.5	<0.3	<0.3	<0.3	<0.3

Table 30 summarizes quarterly mean concentrations of the various radionuclides measured in surface air filters for 1978 and 1979. The cosmic ray product, ^{7}Be, is usually high in concentration at MLO throughout the year. This station appears to represent adequately the air of the upper troposphere. Samples from BRW and other Arctic sites show a summer minimum and winter maximum in ^{7}Be concentration. ^{7}Be is produced predominantly in the upper troposphere and lower stratosphere, and reaches the surface layer of air preferentially at midlatitudes. Evidently it is transported into the Arctic from midlatitudes most rapidly during winter, at the time of formation of the Arctic haze layer.

The artificial radionuclides from nuclear weapons tests currently measured in the filters are the fission products ^{95}Zr, ^{137}Cs, and ^{144}Ce. At MLO high concentration of ^{95}Zr were found throughout 1977, and significant concentrations of ^{137}Cs and ^{144}Ce persisted through the first half of 1978 as a result of fallout from the 17 November 1976 Chinese nuclear test, which had a yield of 4 megatons. Lower concentrations of these radionuclides were found at BRW during this period, and negligible amounts of the radioactive debris from this Chinese test reached the stations in the Southern Hemisphere. Only low concentrations of fission products were found at any of the GMCC sites by the end of 1979.

5.5 Attenuation of Solar Radiation by Atmospheric Particles at MLO, 1958-1978

G. D. Robinson
The Center for the Environment & Man, Inc.
Hartford, CT 06120

The MLO pyrheliometric record (discussed in Mendonca et al., 1978) was examined in terms of the total atmospheric attenuation of the direct solar beam to isolate the effect of suspended particles from other attenuations, specifically Rayleigh scattering, O_2 and O_3 absorption, and H_2O absorption. First the attenuation was computed by known sources and subtracted from the observed attenuation. The record consists of monthly means of measurements on meteorologically quiet days, so that variation of surface pressure (the only unknown in the Rayleigh and O_2 terms) is very small. Trial computation showed that in these conditions at MLO the variance of the attenuation of the monthly mean averaged direct solar radiation by O_3 could be neglected in comparison with the variance of that connected with particles and H_2O. The investigation then became a search for a method of separating the effects of these two major variable attenuators, based on the different relations between attenuation and solar zenith angle for the highly selective H_2O absorption and the relatively grey attenuation by particles.

The analysis was carried out on a set of tabulations prepared by the GMCC staff. The MLO pyrheliometric measurements were multiplied by the square of the radius vector and combined into six parameters, monthly means of which were tabulated. These parameters are

$$T_{ij} \text{ and } S^{o}_{ij},\ i = 2 \text{ to } 4,\ j = i + 1,$$

where

$$T_{ij} = I_j / I_i,$$

$$S^{o}_{ij} = (I_i + I_j)/2T_{ij}, \text{ and}$$

I_i = measured solar intensity at zenith angle s^{-1} i corrected to mean solar distance.

The datum examined by Mendonca et al. (1978) is $\sum_i T_{ij}/3$, a conventionally specified transmissivity combining the effect of molecular and particle scattering and gaseous and particle absorption. The principle of this method of reduction, from Ellis and Pueschel (1971), is

$$\alpha\beta M_i = \beta I_i = I_o T_i,$$

where

M is an instrument reading,

α is the applied instrument calibration factor,

β is the ratio of the true (but unknown) instrument calibration factor to α,

I_o is the true (but unknown) value of the solar constant,

so that $T_{ij} = I_j/I_i = M_j/M_i$ is independent of the unknowns β and I_o as long as they remain constant during a measuring period, but $S^o_{ij} = (I_o/2\beta), (T_i + T_j)/T_{ij}$ depends on both I_o and β.

The original Ellis-Pueschel method further assumes that the transmissions may be approximated by Beer's law

$$T_i \simeq \exp(-\kappa i),$$

where κ is the zenith optical path from all attenuators,

so that $T_{ij} \simeq T \simeq \exp(-\kappa)$, $T_i \simeq (T)^i$, and

$$S^o_{ij} = (I_o/2\beta)\ (T)^{i-1}(1+T).$$

A third set of parameters was examined, defined by

$$B^o_{ij} \equiv [T_{ij}^{(i-1)} + (T_{ij})^i]S^o_{ij}$$

$$= [(T_{ij})^i + (T_{ij})^j]/[T_i + T_j].$$

If the attenuation by particles alone follows Beer's law (a much less restrictive assumption than that of Ellis and Pueschel), the B^o_{ij} depend only on β and the H_2O path, and are independent of τ, the optical depth of the particles.

A catalogue of the transmissions (I^c_i) of a set of standard atmospheres of specified O_3 and H_2O content and specified optical depth caused by particles (τ) was computed for the set of zenith angles $s^{-1}i$. From these computed intensities the sets of parameters

$$T^c_{ij} = I^c_j / I^c_i,$$

$$S^c_{ij} = (I^c_i + I^c_j)/T^c_{ij}\ I_o,$$

and

$$B^c_{ij} \equiv [(T^c_{ij})^{i-1} + (T^c_{ij})^i]/S^c_{ij}$$

$$= [(T^c_{ij})^i + (T^c_{ij})^j]/[T^c_i + T^c_j] = (T^c_j)^i/(T^c_i)^j$$

were formed.

Details of the comparison process of the observed parameters with the computed catalogue and of interpolation procedures will be reported in a month-to-month tabulation over the record period (see figs. 69 and 70).

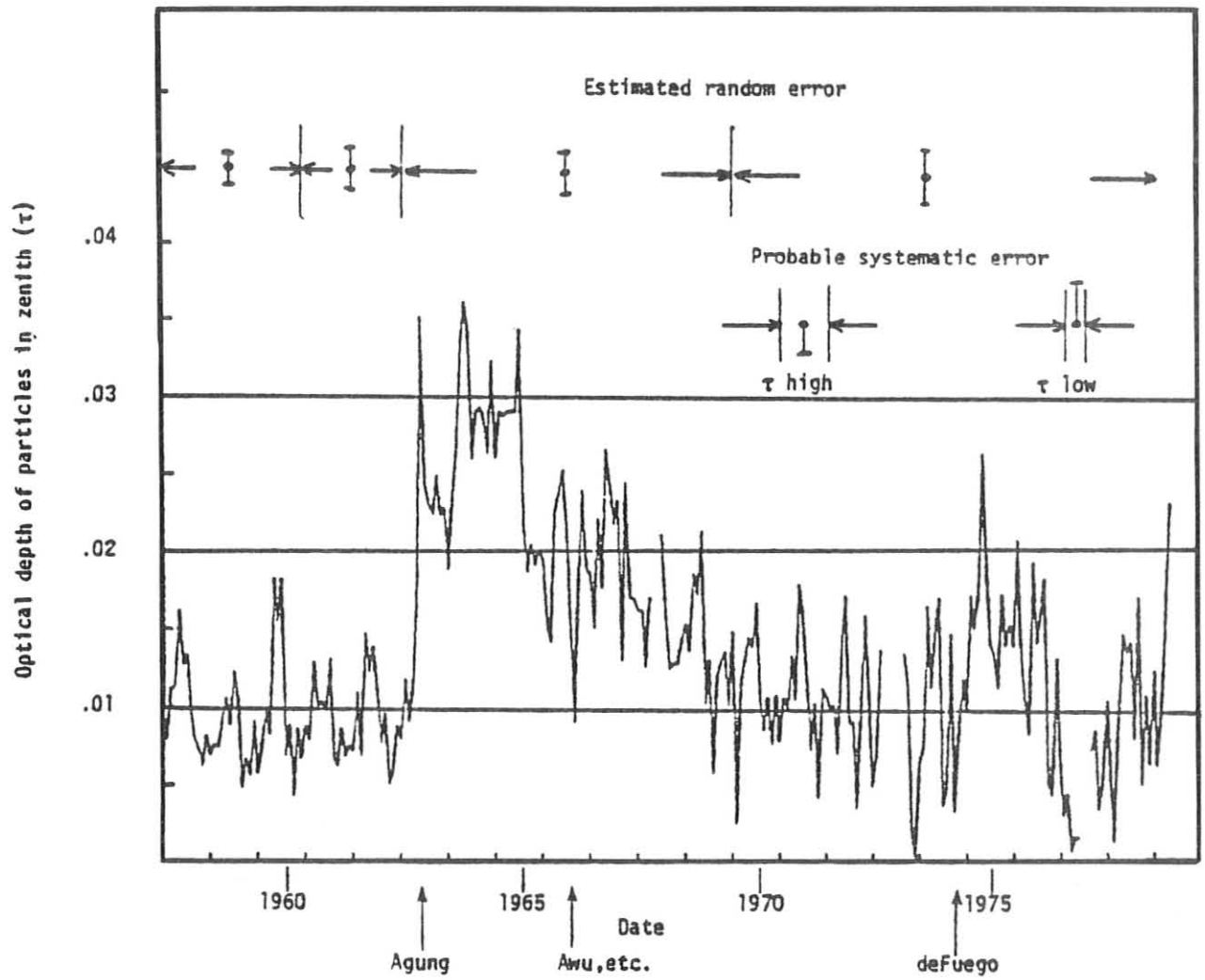

Figure 69.--Monthly mean zenith optical path of particles at MLO.

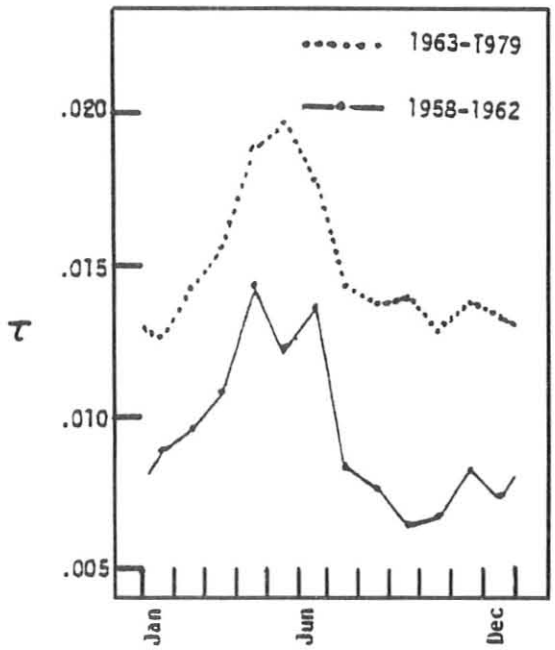

Figure 70.--Annual variation of particle optical depth.

5.6 Mauna Loa Solar Spectral Irradiance Program

Glen E. Shaw
Geophysical Institute, University of Alaska
Fairbanks, AL 99701

The University of Alaska has establihed a program at MLO to search for tiny fluctuations in the Sun's radiation near the time of maximum solar activity. The research is supported by the NSF's Office of Climate Dynamics, and its goal is determining solar spectral irradiance in 12 narrow (10-nm) wavelength passbands in the near ultraviolet and visible regions of the electromagnetic spectrum. On each clear day the extraterrestrial spectral solar irradiance is monitored to a precision of ~0.1%, and the day-averaged measurements are transferred to an absolute electrical scale of units to an accuracy of 1% for later comparison with measurements carried out around the time of minimum solar activity. It has been suspected that although the solar constant (the total solar radiation at all wavelengths) is apparently constant to a fraction of 1%, the spectral irradiance, especially at blue and near ultraviolet wavelengths, may be fluctuating in response to periodic changes in dynamical activity taking place beneath the Sun's photosphere. The changes in total solar radiation caused by fluctuating spectral irradiance at short wavelengths may be compensated by simultaneous slight increases or decreases in the radiation at the longer wavelength by a greenhouse effect mechanism. That is, the total area under the curve of solar spectral irradiance (the solar constant) tends to be stationary in time, although the shape of the spectral distribution of sunlight undergoes variations. Identifying spectral irradiance variations could improve understanding of Sun-Earth climatic coupling mechanisms. For example, the equilibrium vertical distribution and concentration of trace constituents in the Earth's upper atmosphere (OH, O_3, etc.) may be modulated and force alterations in climate parameters through interactive feedback loops.

The solar spectral irradiance program began operation at MLO in February 1980. Data will be taken continually for at least 1 year. A by-product of the program will be a set of determinations of the spectral atmospheric optical transmissivity above Mauna Loa that will represent benchmark data for comparison with similar measurements in the future, to see if global aerosol loading is slowly increasing.

5.7 Ultraviolet Erythema Global Measuring Network 1979

Daniel Berger
Temple University
Philadelphia, PA 19140

The sunburn ultraviolet meter network has operated since September 1973. Data represent energy in the UV-B and can be related to sunburn, DNA damage, and other effects of ultraviolet light on biologic systems. At present 30 stations are in operation (see table 31). NOAA is now preparing a 5-yr summary of network data. Collected data are disseminated on request by NOAA, 8060 13th Street, Silver Spring, MD 20910.

5.8 Ozone and Solar Radiometry

Ronald J. Angione and Robert Roosen
San Diego State University
San Diego, CA 92182

Three instruments were brought to MLO in March 1979 for intercomparison. The main instrument was a microprocessor controlled filter wheel radiometer employing a temperature controlled (±0.1°C) photodiode detector and 11 narrow band (100 Å FWHM) filters. The filters were selected to determine the amount of atmospheric dust, total ozone from the Chappuis band, and total precipitable water vapor from the 0.935-μm band. We were particularly interested in comparing ozone amounts derived from the Chappuis band with those derived by the Dobson.

The remaining two instruments were both absolute cavity radiometers: a Willson ACR and a Kendall Mark VI. Our main purpose in bringing the absolute cavities to MLO was to intercompare them, taking advantage of the nearly ideal atmospheric conditions at MLO.

During our 1-wk stay we were able to make measurements on 4 clear days. The mean aerosol optical depth at 0.5011 μm for the 4 days was 0.030. The ozone values derived from the Chappuis band were on the average 17% lower than the corresponding Dobson values. The cause for this difference is being studied.

We made 24 intercomparisons of the Willson and Kendall absolute cavities at a variety of different air masses on the 4 days. The cavities remained constant with respect to each other with a standard deviation of 0.1. The Willson yielded values consistently higher than the Kendall by 0.6%.

Table 31.--Stations in sunburn ultraviolet meter network

Stations	Period in continuous operation
Gainesville, Fla.	Aug 1973-present
Bismarck, N. Dak.	Oct 1973-present
Tallahassee, Fla.	Sep 1973-present
Oakland, Calif.	Oct 1973-present
Fort Worth, Tex.	Sep 1973-present
Minneapolis, Minn.	Oct 1973-present
Des Moines, Iowa	Oct 1973-present
Albuquerque, N. Mex.	Sep 1973-present
El Paso, Tex.	Sep 1973-present
Mauna Loa, Hawaii	Dec 1973-present
Philadelphia, Pa.	Sep 1973-present
Honeybrook, Pa.	Nov 1974-present
Detroit, Mich.	Sep 1977-present
Seattle, Wash.	Sep 1977-present
Salt Lake City, Utah	Oct 1977-present
New Orleans, La.	Sep 1977-present
Atlanta, Ga.	Oct 1977-present
Tucson, Ariz.	Jun 1975-present
Belsk, Poland	May 1975-present
Warsaw, Poland	Jun 1975-Sep 1976
Aspendale (Melbourne), Australia	Jun 1974-present
Brisbane, Australia	May 1974-present
Davos, Switzerland	Oct 1974-present
Hamburg, Germany	Feb 1976-present
Panama	Nov 1978-present
Point Barrow, Alaska	Oct 1978-present
Rockville, Md.	Sep 1978-present
Hamilton, New Zealand	May 1980-present
Basle, Switzerland	Mar 1980-present

5.9 Satellite Determination of Ozone

W. G. Planet
National Environmental Satellite Service, NOAA

and

A. J. Miller
National Weather Service
Washington, D.C. 20233

The National Environmental Satellite Service continues to receive total ozone records from 11 Dobson stations either operated directly by GMCC or associated with it. The data records begin in November 1978 and will continue through the operational lifetime of the TIROS-N series of operational environmental satellites into the late 1980's.

The atmosphere sounder on TIROS-N has spectral channels whose measured radiances are correlated with the total ozone amount. A multichannel regression scheme has been established whereby total ozone on a global scale can be deduced from the satellite measurements. To establish and upgrade the individual regression coefficients, coincident Dobson measurements and satellite observations are required. The regression coefficients are generated and implemented in the TIROS-N data processing system. Regression coefficients are latitudinally stratified and changed seasonally. The ozone amounts derived from the satellite measurements continue to be evaluated by comparisons with a selected subset of Dobson measurements for determining the accuracy of our retrieval process.

The same Dobson data set is also being used for the verification of ozone values determined by the Nimbus-7 SBUV/TOMS system. These efforts are under way in the Analysis and Information Branch, National Meteorological Center, Asheville, N.C.

Preliminary results of these efforts were presented in the fall 1979 AGU meeting and at the XVII General Assembly of IUGG, 1979.

5.10 Daily Sunspot Count, American Association of Variable Star Observers

W. R. Winkler
National Geophysical and Solar-Terrestrial Data Center, EDIS
Boulder, CO 80303

When weather and official duties permit, daily sunspot number is observed and reported monthly to the American Association of Variable Star Observers, Cambridge, Mass. Each daily observation is combined with others to determin R_A, the "American sunspot number." This index closely follows Rz, the "Zurich sunspot number." Both are published by the National Geophysical and Solar-Terrestrial Data Center in Solar-Geophysical Data--Part I, which appears monthly. Sunspot number, the only long term index of solar activity, dates from about 1750.

Visual counts of sunspots are made using a filtered 4-in reflecting telescope located in the fifth floor dome of RB-3 in Boulder, Colo. Figure 71 shows the form used by observers to report their data.

AAVSO – SOLAR DIVISION

SUNSPOT REPORT FOR JULY 1980
(MONTH / YEAR)

OBSERVER'S NAME AND COMPLETE ADDRESS
William Winkler
31 Valentine Lane
Longmont, Colo. 80501

☐ REFRACTOR X REFLECTOR APERTURE (4) in. FOCAL LENGTH (44) in.
X OBSERVATIONS DIRECT
☐ HERSCHEL WEDGE X objective FILTER FOCAL LENGTH OF EYEPIECE (18) mm
☐ OBSERVATIONS BY PROJECTION
FOCAL LENGTH OF PROJECTION LENS ( ) in. mm DIAMETER OF PROJECTED IMAGE ( ) in. mm
X APERTURE STOP USED DIAMETER OF STOP (3½) in.

DAY	c-d SEEING AND CLOUDINESS	e UNIVERSAL TIME	f NUMBER OF GROUPS	g NUMBER OF SPOTS	R_i SUNSPOT NUMBER	j NORTHERN GROUPS	k SOUTHERN GROUPS	l NORTHERN SPOTS	m SOUTHERN SPOTS	*= 3" F/5 refractor 18mm eyep. REMARKS
1	G-3	1800	5	14	64	2	3	3	11	
2	G-3	1800	5	19	69	2	3	8	11	
3	G-5	1800	5	20	70	2	3	11	9	
4	G-1	2130	5	24	74					*
5	G-0	2230	6	33	93					*
6										
7										
8	G-1	1800	4	28	68	3	1	13	15	
9	G-0	1800	5	16	66	3	2	11	5	
10	G-0	1800	4	13	53	2	2	8	5	
11	G-1	1800	5	17	67	1	4	3	14	
12										
13										
14										
15	G-1	1800	9	47	137	4	5	15	32	
16	G-0	1800	11	61	171	5	6	19	42	
17										
18										
19	G-3	2330	11	44	154					*
20	G-0	2245	13	56	186					*
21										
22	G-0	1845	12	44	164	5	7	15	29	
23										
24										
25	G-1	1800	8	21	101	3	5	8	13	
26										
27										
28										
29	G-1	1800	7	12	82	4	3	7	5	
30	G-4	1800	5	7	57	3	2	5	2	
31	G-2	1800	5	7	57	3	2	4	3	
		Σ								

INSTRUCTIONS

FILL IN THE MONTH, YEAR, AND COMPLETE MAILING ADDRESS IN THE SPACES PROVIDED ABOVE. GIVE INFORMATION ON YOUR INSTRUMENT AND OBSERVING METHODS BY PUTTING AN "X" IN THE BOXES WHICH APPLY, AND BY FILLING IN APERTURE, FOCAL LENGTH, ART DIAMETER IN THE SPACES PROVIDED. BE SURE TO CROSS OUT THE UNIT OF MEASURE WHICH DOES NOT APPLY TO YOUR DATA.

IN THE "c-d" COLUMN, SEEING QUALITY IS INDICATED BY A LETTER: E-POOR, F-FAIR, G-GOOD, AND E-EXCELLENT. SEEING QUALITY SHOULD BE RATED BY THE OBSERVER'S JUDGMENT FOR HIS INSTRUMENT AND FOR HIS AVERAGE SEEING CONDITIONS. 2 WILL INDICATE AVERAGE TO ABOVE AVERAGE VISIBILITY OF DETAIL ON THE SUN'S DISC. 1 WILL BE ASSIGNED FOR THOSE DAYS WHEN EXCEPTIONAL DETAIL CAN BE SEEN. F WILL INDICATE BELOW-AVERAGE SEEING AND P WILL INDICATE SEVERE CONDITIONS WHICH MAKE THE OBSERVATIONS OF SUNSPOTS FALSE. IN DETERMINING THE SEEING RATING, THE OBSERVER SHOULD CONSIDER SCINTILLATION, EVALUATION OF THE SUN'S DISC BY THEIR CLARITY OR HAZE, AND ANY OTHER CONDITIONS WHICH LIMIT THE VISIBILITY OF DETAIL ON THE DISC.

IF THE ACCURACY OF THE SUNSPOT COUNT IS LIMITED BY CONDITIONS OTHER THAN SEEING, SUCH AS HAZE OR INTERRUPTED COURTS DUE TO CLOUDS OR OTHER ADVERSE CONDITIONS, THE REASON SHOULD BE NOTED IN THE "REMARKS" COLUMN, AND A DIAGONAL LINE SHOULD BE DRAWN IN CORNER OF THE "c-d" BOX.

EXAMPLE: G-8

THE NUMBER FOLLOWING THE SEEING-QUALITY LETTER IN THE "c-d" COLUMN INDICATES THE FRACTION OF THE WHOLE SKY WHICH IS COVERED BY CLOUDS, 0 INDICATING A COMPLETELY CLEAR SKY AND 10 INDICATING 100% CLOUD COVER. 8 WOULD INDICATE 80% CLOUD COVER.

COLUMN "e" WILL CONTAIN THE UNIVERSAL TIME WRITTEN WITH FOUR DIGITS; EXAMPLE: 0400 = 4 HOURS U. T. NOTICE THAT WITH UNIVERSAL TIME BEING USED, THE OBSERVATIONS ARE RECORDED IN THE DATE LINE WHICH WOULD BE CORRECT IN GREENWICH, ENGLAND, AND THIS DATE MAY DIFFER FROM THE OBSERVER'S LOCAL CIVIL DATE.

COLUMN "f" CONTAINS THE TOTAL NUMBER OF SUNSPOT GROUPS OBSERVED. COLUMN "g" CONTAINS THE TOTAL NUMBER OF SUNSPOTS COUNTED IN THESE GROUPS. THE INDIVIDUAL OBSERVER'S RELATIVE SUNSPOT NUMBER FOR THE DAY IS COMPUTED BY ADDING THE TOTAL NUMBER OF SPOTS TO TEN TIMES THE NUMBER OF GROUPS. THIS VALUE IS RECORDED IN THE "R_i" COLUMN.

IN COLUMNS "j", "k", "l", AND "m", THE GROUPS AND SPOTS ARE RECORDED BY HEMISPHERE. THE OBSERVER SHOULD LEAVE THESE COLUMNS BLANK IF HE DOES NOT HAVE MEANS FOR DETERMINING THE POSITION OF SUNSPOTS.

WHEN THE OBSERVATION FOR THE LAST DAY OF THE MONTH HAS BEEN RECORDED, THE REPORT SHOULD BE SENT IMMEDIATELY TO THE SOLAR DIVISION CHAIRMAN BY AIRMAIL. IT IS IMPORTANT THAT THE MONTHLY SUNSPOT REPORT BE RECEIVED PROMPTLY.

Figure 71.--Typical sunspot report form.

5.11 Precipitation Chemistry at Samoa and Mauna Loa

Donald C. Bogen, Stuart J. Nagourney, and Camille C. Torquato
Environmental Measurements Laboratory
U.S. Department of Energy, New York, NY 10014

Monthly samples of wet, dry, and total deposition are collected at SMO and MLO. The samples are sent to the Environmental Measurements Laboratory (EML) for physical and chemical measurements.

The average monthly deposition values and range of results at SMO and MLO for April 1978 to March 1979 are presented in tables 32 and 33.

Table 32.--Chemical analyses of total, wet, and dry deposition at SMO, April 1978 through March 1979

	Total Collector		Wet collector		Dry collector	
	Mean	Range	Mean	Range	Mean	Range
Volume (ℓ)	7.88	0-14.0	10.0	1.96-14.4	-	-
pH	6.01	5.49-6.48	5.81	5.45-6.26	-	-
Conductivity ($\mu S\ cm^{-1}$)	69.4	19-115	25.9	9.6-63.5	-	-
Cl^- ($mg\ mo^{-1}$)	112	63-191	52	20-89	69	38-98
SO_4^{-2} ($mg\ mo^{-1}$)	20	10-31	9.9	3.7-16	10.9	6.6-15
NO_3^- ($mg\ mo^{-1}$)	3.8	ND*-41	0.02	ND*-0.28	0.01	ND*-0.08
Na^+ ($mg\ mo^{-1}$)	70	38-120	33	18-120	42	23-61
Mg^{+2} ($mg\ mo^{-1}$)	8.9	4.7-16	4.0	1.6-7.3	5.1	2.7-7.7
Ca^{+2} ($mg\ mo^{-1}$)	3.2	2.0-5.3	1.6	0.8-3.0	1.8	1.1-2.6
K^+ ($mg\ mo^{-1}$)	3.1	1.7-5.5	1.4	0.6-2.5	2.0	1.0-2.8
Total cations / Total anions	1.12 ± 0.06		1.15 ± 0.08		1.11 ± 0.06	

*ND-not detectable

Table 33.--Chemical analyses of total, wet, and dry deposition at MLO, April 1978 through March 1979

	Total Collector		Wet collector		Dry collector	
	Mean	Range	Mean	Range	Mean	Range
Volume (ℓ)	2.44	0-11.7	3.55	0-9.8	-	-
pH	5.13	4.77-5.56	5.48	5.01-5.85	-	-
Conductivity ($\mu S\ cm^{-1}$)	5.74	2.5-8.8	3.68	2.2-6.2	-	-
Cl^- ($mg\ mo^{-1}$)	0.21	0.02-0.58	0.19	0.03-0.43	0.07	0.02-0.28
SO_4^{-2} ($mg\ mo^{-1}$)	1.32	0.15-3.99	0.80	0.03-2.09	0.47	0.09-0.95
NO_3^- ($mg\ mo^{-1}$)	0.09	ND*-0.48	0.11	ND*-0.56	0.04	ND*-0.21
Na^+ ($mg\ mo^{-1}$)	0.39	0.04-2.51	0.20	0.02-0.55	0.13	0.04-0.32
Mg^{+2} ($mg\ mo^{-1}$)	0.07	0.01-0.22	0.07	ND*-0.19	0.02	0.01-0.04
Ca^{+2} ($mg\ mo^{-1}$)	0.09	ND*-0.35	0.08	ND*-0.23	0.05	0.01-0.06
K^+ ($mg\ mo^{-1}$)	0.02	ND*-0.05	0.02	ND*-0.09	0.01	ND*-0.03
Total cations / Total anions	0.93 ± 0.16		1.02 ± 0.32		0.98 ± 0.17	

*ND-not detectable

5.12 Drifting Snow at Barrow

G. Wendler
Geophysical Institute, University of Alaska
Fairbanks, AL 99701

On the Antarctic continent snow is redistributed, blown off, or evaporated. It is influential for all practical operations, since zero visibility is frequently experienced during periods of blowing snow. We are studying the katabatic wind in the French sector of Antarctica, an area where high winds are frequent. A maximum windspeed of 196 m h^{-1} was measured at Dumont d'Urville, but the whole austral winter is windy.

Schmidt developed an instrument that measures the size distribution of particles as well as frequency of blowing snow particles. We obtained a sensor from Schmidt but built our own electronics along lines described by Schmidt. Before

building three more instruments and installing them in Antarctica, we are testing one sensor including electronics at BRW. In contrast to Fairbanks where the winds are light in winter, BRW is more exposed and drifting snow is a common occurrence. Testing was sucessfully completed during spring 1980.

5.13 Recalibration of the Pollak Counter at the 680-mb Level

A.W. Hogan
State University of New York at Albany
Albany, NY 12222

The Pollak-Nolan photoelectric nucleus counter has been used as an aerosol detector by the GMCC program since its inception. The actual instruments in use are replicas of the last Dublin version, using a 2.5-cm unglazed ceramic fog tube and convergent light beam, constructed from Pollak's drawings by R. Gussman. The intrinsic calibration for this instrument has been used to convert observed values of light transmission through the fog tube to initial aerosol concentration.

The intrinsic calibration was established at sea level; Emmanuel and Squires (1969) repeated the calibration of Pollak's counter near the 850-mb level and concluded that the sea level calibration was sufficiently accurate for field studies. When the Pollak counter was installed at Mauna Loa, A.W. Hogan compared the instrument with an Aitken counter and found their measurements to generally agree over the range of concentrations expected to be observed. Since both Mauna Loa and South Pole have average station pressures of around 700 mb, a comparison of the Pollak with the photo recording Aitken counter of Winters, Barnard, and Hogan (1977) was conducted at Mauna Loa to confirm the numerous data collected at these stations.

5.13.1 Preliminary Calculations

The Pollak photoelectric nucleus detects particles smaller than a wavelength of light by Aitken's method of forcing them to grow into visible drops in a supersaturated environment. The calibration is based on the amount of change in light transmission caused by the formation of these drops on the initial particles; if more or less water vapor is made available to the growing particles, then in theory, the amount of light transmission at a given concentration may be altered, invalidating the calibration. Sensitivity of an Aitken counter does not depend on the size of the drops formed, as long as the drop grows to visible size; it can then be used as a reference instrument at the higher altitude.

The saturation in the Pollak counter is produced by raising the pressure in the aerosol filled fog tube with filtered air, allowing the sample to come into humidity equilibrium with the moist walls, and then expanding the air by venting the chamber to ambient pressure. The saturation produced is then calculable from adiabatic considerations:

$$T_F = T_o \left(P/P_o\right)^{.286}$$

At sea level an expansion of 160 mm Hg is used;

$$\frac{P_o + \Delta P}{P_o} = \frac{760 + 160}{760} = 1.21 \ .$$

The same expansion ratio can be achieved at Mauna Loa and South Pole by adjusting the overpressure accordingly:

$$\frac{P_o + \Delta P}{P_o} = \frac{511 + \Delta P}{511} = 1.21, \quad \Delta P \approx 105 \text{ mm Hg.}$$

If the ambient temperatures is assumed to be 293K (20°C) at all stations, the adiabatic temperature change can be calculated from the pressure ratio, 15.6°C. The saturation can be calculated from values given in the Smithsonian Tables, or an adiabatic diagram:

Temp.	Pressure	Saturation mixing ratio	Supersaturation
293K	1013 mb	14.6 g kg^{-1}	2.81
277.4K	1013 mb	5.2 g kg^{-1}	
293K	681 mb	21.4 g kg^{-1}	2.78
277.7K	681 mb	7.7 g kg^{-1}	

At sea level, this would liberate 9.4 g kg^{-1} of water condensation, and at Mauna Loa it would release 13.7 g kg^{-1}. When this is converted to volume mixing ratio, we find 11.99 g m^{-3} available at sea level; at Mauna Loa 12.24 g m^{-3} are available. The ratio of the cube roots of these values indicates that the drops may be 0.7% larger at Mauna Loa, which should not greatly influence the calibration.

5.13.2 Results of Experiments

The theoretrical considerations above indicate that no real discrepancy should exist between a sea level calibration of the Pollak counter and one at approximately 700 mb. The experimental results (fig. 72) indicate that this is true, since there is little or no systematic difference between the number of particles measured by the Aitken and Pollak techniques. Ambient aerosol was used for these comparisons, and the two instruments were operated in close time and space proximity.

Although there is little systematic difference through the calibration range, there is extreme variation when individual readings are compared. For example, 26 individual determinations of aerosol concentration were made, over a period of 5 days, when the Pollak counter indicated transmission of 93.5 to 94.5, a typical Mauna Loa value. The mean of these was 93.9, which corresponds to 156 $^{n}/cm^3$; the extreme values of 93.5 and 94.5 correspond to 170 $^{n}/cm^3$ and 137 $^{n}/cm^3$, respectively. The simultaneous observations of concentration made with the Aitken counter have a mean value of 164 $^{n}/cm^3$, which is in good agreement, but the individual values determined by the Aitken counter ranged from 42 to 301 $^{n}/cm^3$. This variation is apparently random error, since the sensitive volume of the Pollak counter contains 7,300 particles at this concentration, whereas the Aitken counter contains only 21 as a mean value. Since the particles are 2 mm apart at this concentration, a sensitive volume 1 mm thick would be subject to extreme concentration variation during instantaneous determinations. The six plotted points near this value in fig. 72 are the means of determinations during six

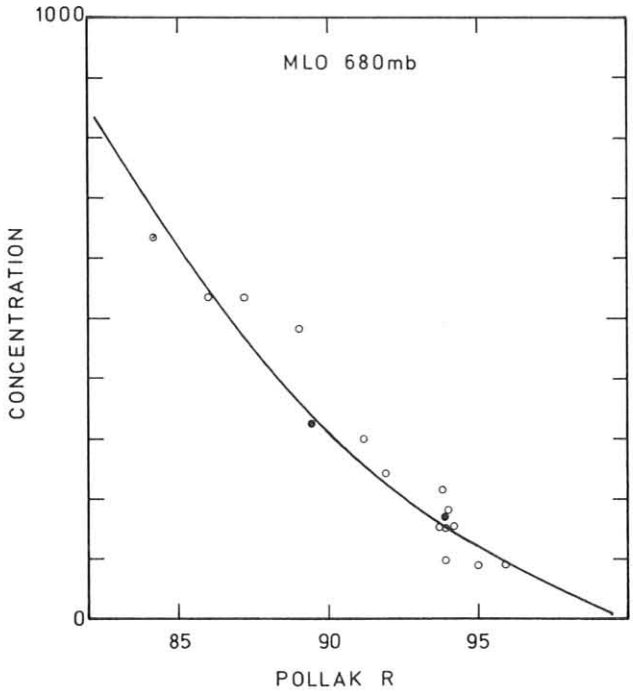

Figure 72.--Scale reading of Pollak replica PG13 at MLO (station pressure 681 mb) and coincident concentration determinations made with a photographic Aitken counter. The plotted curve is the Metnieks Pollak 1960 calibration. Solid circles are means of 10 or more determinations at the same Pollak reading, open circles single values.

periods. This wide range of Aitken values corresponding to a narrow range of Pollak values is a strong argument in favor of the Pollak as a prime instrument for obtaining climatological aerosol data.

An experiment was conducted at Mauna Loa, during a period of very stable natural aerosol concentration, to determine the sensitivity change of the instrument at several expansion ratios. The results of this experiment (fig. 73) indicate that the extinction in the fog tube is a linear function of water made available by the expansion up to the established (1.21) Aitken expansion ratio. At greater expansions the response flattens, probably because the relative radius change in the drops formed is diminishing. There are no discontinuities in the curve, which might be expected if additional particles were activated at some supersaturation rather than the additional available water causing existing drops to become larger. The minimum overpressure used was 15 mm Hg, which would produce a supersaturation of 1.20, sufficient to cause growth on 6×10^{-7} cm radius particles. It would seem reasonable to conclude that the Mauna Loa aerosol on this day consisted of particles larger than this, which is in agreement with past work with diffusion batteries.

5.13.3 Conclusion

The Pollak 1962 intrinsic calibration of the photoelectric nucleus counter is valid for climatological aerosol determinations at 700-mb station pressure.

Slightly exceeding the optimum (Aitken) expansion at altitudes above sea level has little influence on the value of concentration observed. Failure to achieve the Aitken saturation results in severe loss of sensitivity.

Acknowledgment

This work was supported by NOAA/ERL/ARL/GMCC under contract NA79RAD00023.

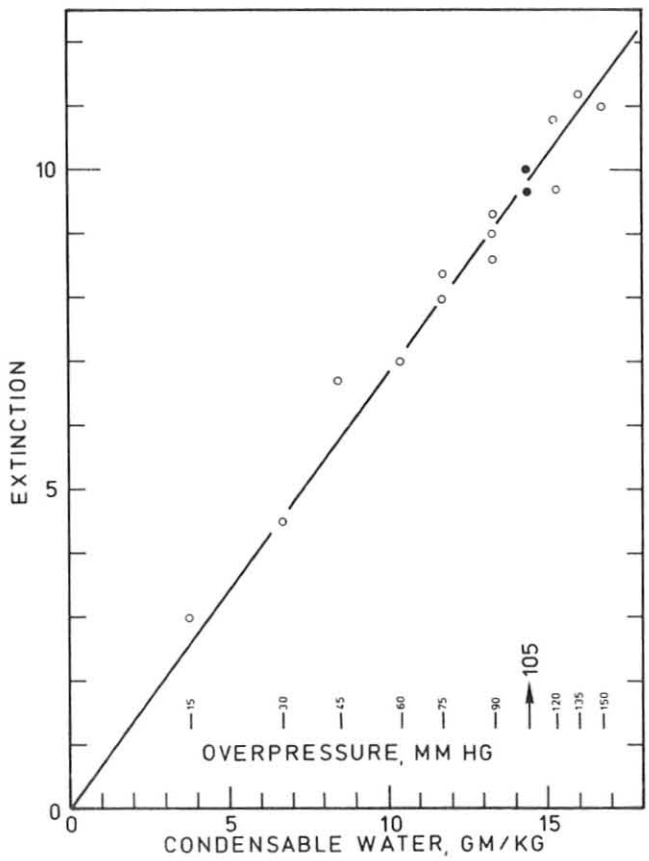

Figure 73.--Variation in extinction (100% reading) observed with the Pollak counter when varing the initial overpressure. The extinction appears to be a linear function of the amount of water made available for condensation. Increasing the overpressure causes less change in sensitivity per unit pressure than decreasing the overpressure. The smallest overpressure used (15 mm Hg) produced a supersaturation of 1.2, which should cause growth of particles larger than 6×10^{-7} cm radius.

5.14 Measurement of SO_2 and TSP at Mauna Loa Observatory

Richard Sasaki, Mavis Kadooka, and Wilfred Ching
Department of Health, State of Hawaii
Honolulu, Hawaii 96801

The cooperative program between the Department of Health, State of Hawaii, and NOAA is nearing completion of its third year of data collection. All raw data are being checked for accuracy, along with all required quality assurance data to ensure final data validity. Final computation and assessment have been delayed by late receipt of computer programs and equipment. Evaluation and assessment and all data will not be available until later this year.

6. INTERNATIONAL ACTIVITIES

Under the U.S.A.-U.S.S.R. Agreement on Cooperation in the Field of Environmental Protection, Working Group VIII, Soviet scientist Alexander Shashkov visited the NOAA Air Resources Laboratory, Boulder, Colo., from 9-28 October 1979, to study techniques and apparatus used in the NOAA/ERL/ARL Geophysical Monitoring for Climatic Change (GMCC) program for measuring carbon dioxide. During the visit, Dr. Shashkov studied procedures and equipment used in CO_2 flask sampling; practiced collecting CO_2 flask samples at Niwot Ridge, Colo.; studied instrumentation and methods employed in analysis of atmospheric CO_2 using nondispersive infrared analyzers; and participated in the analysis of the air samples collected at Niwot Ridge. Dr. Shashkov also had opportunity to study details of construction of nondispersive infrared CO_2 analyzer apparatus for continuous CO_2 measurements, manual CO_2 flask sample analysis instrumentation, and a newly developed semiautomatic apparatus used for analyzing CO_2 flask air samples.

While in Boulder, the Soviet scientist had an opportunity to become familiar with other GMCC programs concerning monitoring of atmospheric trace gases, including Freons, nitrous oxide, and ozone. He made a presentation at a GMCC seminar on techniques, instrumentation, and some results of the spectroscopic method developed in the U.S.S.R. for measuring the average CO_2 mixing ratio in a vertical column of the atmosphere. Useful discussions were held concerning spectroscopic instrument and nondispersive analyzer measurements of atmospheric CO_2 and CO_2 monitoring in general.

In October, 1979, K. Hanson traveled to Tblisi, U.S.S.R., to participate in the fifth annual meeting of Working Group VIII under the U.S.-U.S.S.R. Agreement on Protection of the Environment.

At the request of the World Meteorological Organization (Global Ozone Research and Monitoring Project) R. Grass participated in the Europian regional Dobson spectrophotometer intercomparison held in Potsdam, German Democratic Republic, in June 1979. The primary reason for the intercomparison was to ensure the compatibility of ozone measurements with Dobson ozone spectrophotometers for research purposes by comparing them with the regional standard instrument, which had been calibrated by the world standard at Boulder, Colo., in August 1977. While at Potsdam the Czechoslovakia Dobson no. 74, Hungarian Dobson no. 110, and the Romanian Dobson no. 121 were modified with the U.S. solid state circuits. Optical alignments were made on these three instruments as well as the French Dobson no. 11 and the German Federal Republic Dobson no. 44. Wedge calibrations were performed on Dobson no.'s 44, 74, 84, and 110. A training session was also conducted to teach the participants the procedures for performing certain tests and the techniques for making optical adjustments on the instruments.

In September 1979, B. Mendonca traveled to Chile, Peru, Ecuador, and Brazil to aid in initiating CO_2 monitoring sites at Easter Island, Chile; Cosmos, Peru; and Galapagos Islands, Ecuador. Initial government contacts were made. The scope of the CO_2 measurement program was explained as well as the techniques of flask sampling at remote sites.

B. Mendonca made a brief visit to Brazil to follow up on the solar radiation calibration facility that was started in 1979 at the national meteorological center in Brasília. The National Meteorological Institute there has initiated a national solar radiation monitoring network with the headquarters at the Solar Radiation Calibration Center in Brasília. All data are forwarded to the center for processing and evaluation. On the invitation of the University of Belém in Pará, Brazil, B. Mendonca conducted a seminar on the GMCC program. Informal talks were held with the university staff to explore possible cooperative programs between the GMCC program and the University of Belém. Interest was expressed in acid precipitation and carbon dioxide measurements.

7. 1979 PUBLICATIONS AND PRESENTATIONS BY GMCC STAFF

Bodhaine, B. A. Aerosol monitoring at Barrow, Mauna Loa, American Samoa, and the South Pole: instrumentation and results. Proceedings, WMO Technical Conference on Regional and Global Observations of Atmospheric Pollution Relative to Climate, 20-24 August 1979, Boulder, Colo.

Bodhaine, B. A. A modified General Electric condensation nuclei counter and its operation at baseline sites. Presented at 53rd Colloid and Surface Science Symposium, 11-13 June 1979, Rolla, Mo.

Bodhaine, B. A. GMCC Aerosol Chemistry Workshop summary and recommendations, March 8-9, 1979. Bull. Am. Meteorol. Soc. 60(11):1337-1339.

Bodhaine, B. A. Measurement of the Rayleigh scattering properties of some gases with a nephelometer. Appl. Opt. 18:121-125.

Bodhaine, B. A. Nephelometer light scattering measurements at baseline monitoring sites. Presented at 53rd Colloid and Surface Science Symposium, 11-13 June 1979, Rolla, Mo.

Cram, R. S., and H. R. Tatum. Record torrential rainstorms on the island of Hawaii, Jan.-Feb. 1979. Mon. Weather Rev. 107(12):1653-1662.

Dave, J. V., J. J. DeLuisi, and C. L. Mateer. Results of a comprehensive theoretical examination of the optical effects of aerosols on the Umkehr measurement. Proceedings, WMO Technical Conference on Regional and Global Observations of Atmospheric Pollution Relative to Climate, 20-24 August 1979, Boulder, Colo.

DeLuisi, J. J. Shortened version of the Umkehr method for observing the vertical distribution of ozone. Appl. Opt. 18:3190.

DeLuisi, J. J. Umkehr vertical ozone profile errors caused by the presence of stratospheric aerosols. J. Geophys. Res. 84(C4):1766-1770.

DeLuisi, J. J., K. J. Hanson, and B. G. Mendonca. Estimation of changes in the albedo and relative temperature due to stratospheric aerosols from Agung and subsequent volcanic activity. Proceedings, WMO Technical Conference on Regional and Global Observations of Atmospheric Pollution Relative to Climate, 20-24 August 1979, Boulder, Colo.

DeLuisi, J. J., C. L. Mateer, and D. F. Heath. Comparison of seasonal variations of upper stratospheric ozone concentrations revealed by Umkehr and Nimbus 4 BUV observations. J. Geophys. Res. 84(C7):3728-3732.

Dutton, E. G., W. D. Komhyr, and T. M. Thompson. Global baseline concentrations of selected fluorocarbons and nitrous oxide. Proceedings, WMO Technical Conference on Regional and Global Observations of Atmospheric Pollution Relative to Climate, 20-24 August 1979, Boulder, Colo.

Fegley, R. W. Practical comments on the Lidar monitoring of stratospheric and tropospheric aerosols. Proceedings, WMO Technical Conference on Regional and Global Observations of Atmospheric Pollution Relative to Climate, 20-24 August 1979, Boulder, Colo.

Hanson, K. J. Book reviews: Carbon Dioxide, Climate and Society, J. Williams (ed.), Pergamon, New York, N.Y., 1978. Clim. Change 2(2):194-195.

Hanson, K. J., J. T. Peterson, B. G. Mendonca, and W. D. Komhyr. Some examples of atmospheric dynamical effects on atmospheric trace constituents. Proceedings, 4th Annual Climate Diagnostics Workshop, 16-18 October 1979, Madison, Wis., Inst. for Environ. Studies, Madison, Wis., 246-265.

Harding, D., and J. M. Miller. Studies of acid rain on the big island. Proceedings, Second Conference on Natural Sciences, 217-219.

Harris, J. M., J. R. Jordan, and G. A. Herbert. Automation of GMCC's CO_2 Laboratory operations using microprocessors. Proceedings, WMO Technical Conference on Regional and Global Observations of Atmospheric Pollution Relative to Climate, 20-24 August 1979, Boulder, Colo.

Herbert, G. A., J. M. Harris, M. S. Johnson, and J. R. Jordan. Data acquisition and processing in GMCC. Proceedings, WMO Technical Conference on Regional and Global Observations of Atmospheric Pollution Relative to Climate, 20-24 August 1979, Boulder, Colo.

Hoyt, D. V. Atmospheric transmission from the Smithsonian Astrophysical Observatory pyrheliometric measurements from 1923 to 1957. J. Geophys. Res. 84(C8):5018-5028.

Hoyt, D. V. Pyrheliometric and circumsolar sky radiation measurements by the Smithsonian Astrophysical Observatory from 1923 to 1954. Tellus 31(3):217-229.

Hoyt, D. V. Theoretical calculations of the true solar noon atmospheric transmission. In SOLMET, vol. 2 (TD-9724), Dept. of Energy, Asheville, N.C., 119-163.

Hoyt, D. V. Variations in sunspot structure and climate. Clim. Change 2:79-92.

Hoyt, D. V. Variations in the solar constant caused by changes in the active features on the Sun. In Solar-Terrestrial Influences on Weather and Climate, B. M. McCormac and T. A. Seliga (eds.), Reidel, Dordrecht, Holland, 65-68.

Komhyr, W. D. An aerosol and gas sampling apparatus for observatory use. Proceedings, WMO Technical Conference on Regional and Global Observations of Atmospheric Pollution Relative to Climate, 20-24 August 1979, Boulder, Colo.

Komhyr, W. D., and T. B. Harris. NOAA CO_2-in-air calibration gas standards. Proceedings, WMO Technical Conference on Regional and Global Observations of Atmospheric Pollution Relative to Climate, 20-24 August 1979, Boulder, Colo.

Komhyr, W. D., W. R. Taylor, and T. B. Harris. A semi-automatic flask sample CO_2 analyzer. Proceedings, WMO Technical Conference on Regional and Global Observations of Atmospheric Pollution Relative to Climate, 20-24 August 1979, Boulder, Colo.

Mateer, C. L., J. J. DeLuisi, and C. C. Porco. On the development of the short Umkehr method for estimating the vertical distribution of ozone. Proceedings, WMO Technical Conference on Regional and Global Observations of Atmospheric Pollution Relative to Climate, 20-24 August 1979, Boulder Colo.

Mendonca, B. G. (ed.). Geophysical Monitoring for Climatic Change--No. 7. Summary report 1978. NOAA/ERL, 131 pp.

Mendonca, B. G., J. J. DeLuisi, K. J. Hanson, and J. T. Peterson. Signatures in atmospheric transmission variations at Mauna Loa Observatory, Hawaii. Proceedings, WMO Technical Conference on Regional and Global Observations of Atmospheric Pollution Relative to Climate, 20-24 August 1979, Boulder, Colo.

Miller, J. M. The monitoring of acid rain. Proceedings, American Society of Civil Engineers meeting, Boston, Mass., 95-103.

Miller, J. M., and A. Yoshinaga. The acidity of Hawaiian precipitation. Presented at Committee on Atmospheric Chemistry and Global Pollution Symposium on Budget and Cycles of Trace Gases and Aerosols in the Atmosphere, Boulder, Colo.

Miller, J. M., H. L. Volchok, D. C. Bogen, H. W. Feely, and R. J. Thompson. Evaluation of the U.S. baseline and regional precipitation chemistry program. Proceedings, WMO Technical Conference on Regional and Global Observation of Atmospheric Pollution Relative to Climate, 20-24 August 1979, Boulder, Colo.

Miller, J. M. The acidity of Hawaiian precipitation as evidence of long-range transport of pollutants. Proceedings, WMO Symposium on Long-Range Transport of Pollutants and Its Relation to General Circulation Including Stratospheric/Tropospheric Exchange Processes, 1-5 October 1979, Sofia, Bulgaria.

Miller, J. M. National Atmospheric Deposition Program: Analysis of data from the first year. In Atmospheric Sulfur Deposition, D. S. Shriner (ed.). Proceedings, Symposium on Potential Environmental and Health Effects of Atmospheric Deposition, 14-18 October 1979, Gatlinburg, Tenn.

Nimira, J. K., and J. J. DeLuisi. On the validity of the aerosol correction methods used in the Dobson ozone measurements. Proceedings, WMO Technical Conference on Regional and Global Observations of Atmospheric Pollution Relative to Climate, 20-24 August 1979, Boulder, Colo.

Oltmans, S. J. Near surface ozone measurements in clean air. Proceedings, WMO Technical Conference on Regional and Global Observations of Atmospheric Pollution Relative to Climate, 20-24 August 1979, Boulder, Colo.

Osborn, J. C., Jr. Geophysical Monitoring for Climatic Change (GMCC) at South Pole, 1978. Antarct. J. U. S., annual rev. issue, fall 1979.

Peterson, J. T. Effects of air pollution on solar radiation in the Los Angeles Basin. Fourth Symposium on Turbulence, Diffusion, and Air Pollution, 15-18 January 1979, Reno, Nev. Preprints, American Meteorological Society, Boston, Mass., 283-286.

Peterson, J. T., and V. Kovalyev. Cooperative U.S.A.-U.S.S.R. atmospheric transparency measurements. Bull. Am. Meteorol. Soc. 60(9):1084-1085.

Peterson, J. T., and T. L. Stoffel, 1979. Urban-rural solar radiation measurements in St. Louis, Missouri. NOAA Tech. Memo. ERL ARL-76, 51 pp.

Peterson, J. T., W. D. Komhyr, T. B. Harris, T. E. DeFoor, and L. S. Waterman. On the within-year variability of ambient CO_2 measurements at Barrow, Alaska. Proceedings, WMO Technical Conference on Regional and Global Observations of Atmospheric Pollution Relative to Climate, 20-24 August 1979, Boulder, Colo.

8. REFERENCES

Barrie, L. A., R. M. Hoff, and S. M. Duggupaty, 1980. The influence of mid-latitudinal pollution sources on the haze in the Canadian Arctic. Atmos. Environ. (accepted for publication).

Bischof, W., 1967. Preliminary report of flask sample analysis equipment for CO_2. NOAA/ARL, unpublished manuscript.

Bodhaine, B. A., 1979. Measurement of the Rayleigh scattering properties of some gases with a nephelometer. Appl. Opt. 18:121-125.

Bodhaine, B. A., and M. E. Murphy, 1980. Calibration of an automatic condensation nuclei counter at the South Pole. J. Aerosol Sci. 11:305-312.

Bodhaine, B. A., and J. C. Bortniak, 1981. Four wavelength nephelometer measurements at South Pole. Geophys. Res. Lett. (submitted for review).

Bodhaine, B. A., J. M. Harris, and G. A. Herbert, 1981. Aerosol light scattering and condensation nuclei measurements at Barrow, Alaska. Atmos. Environ. (accepted for publication).

Brinkman, R. T., 1968. Rotational Ramen scattering in planetary atmosphere. Astrophys. J. 154:1087.

Brosset, C., 1979. Long distance transport of carbonaceous matter. Proceedings, Conference on Carbonaceous Particles in Atmosphere. Rep. LBL-10735, Lawrence Berkeley Laboratory, Berkeley, Calif., p. 95.

Craig, R. A., 1965. The Upper Atmosphere: Meteorology and Physics. Academic Press, New York, 509 pp.

Cunningham, W. C., 1979. The composition, sources and sinks of South Polar aerosols. Ph.D. thesis, University of Maryland, College Park, Md.

Dave, J. V., 1978. Effect of aerosol on estimation of total ozone in an atmospheric column from the measurement of its ultraviolet radiance. J. Atmos. Sci. 35:899-911.

Dave, J. V., J. J. DeLuisi, and C. L. Mateer, 1980. Results of a comprehensive theoretical examination of the optical effects of aerosols on the Umkehr measurement. Proceedings, WMO Technical Conference on Regional and Global Observations of Atmospheric Pollution Relative to Climate, 20-24 August 1979, Boulder, Colo., WMO Publ. 549, Spec. Environ. Rep. 14, 15-22.

DeLuisi, J. J., 1975. Measurement of the extraterrestrial solar radiant flux from 2981 to 4000 A and its transmission through the earth's atmosphere as it is affected by dust and ozone. J. Geophys. Res. 80:345.

Dod, R., et al., 1980. Application of thermal analysis to the characterization of nitrogenous aerosol species. Rep. LBL-10735, Lawrence Berkeley Laboratory, Berkeley, Calif.

Draper, N. R., and H. Smith, 1966. Applied Regression Analysis. Wiley and Sons, N.Y., 407 pp.

Duce, R. A., C. K. Unni, B. J. Ray, J. M. Prospero, and J. T. Merrill, 1980. Long-range atmospheric transport of soil dust from Asia to the tropical north Pacific: Temporal variability. Science 209:1522-1524.

Ellis, H. T., and R. F. Pueschel, 1971. Solar radiation: Absence of air pollution trends at Mauna Loa. Science 172:845-846.

Emmanuel, M. B., and P. Squires, 1969. Absolute calibration of a photoelectric condensation nucleus counter at low values of nucleus concentration. Pure Appl. Geophys. 72:268-283.

Feely, H. W., H. L. Volchok, E. P. Hardy, Jr., and L. E. Toonkel, 1978. Worldwide deposition of ^{90}SR through 1976. Environ. Sci. and Tech. 12:808-809.

Flowers, E. C., R. A. McCormick, and K. R. Kurfis, 1969. Atmospheric turbidity over the United States, 1961-1966. J. Appl. Meteorol. 8:955-962.

Gladney, E. S., J. S. Small, G. E. Gordon, and W. H. Zoller, 1976. Composition and size distribution of in-stack particulate material at a coal-fired power plant. Atmos. Environ. 10:1071-1077.

Greenberg, R. R., W. H. Zoller, and G. E. Gordon, 1978. Composition and size distributions of particles released in refuse incineration. Environ. Sci. and Technol. 12:566-573.

Harris, J. M., J. R. Jordon, and G. A. Herbert, 1980. Automation of GMCC's CO_2 Laboratory operations using microprocessors. Proceedings, WMO Technical Conference on Regional and Global Observations of Atmospheric Pollution Relative to Climate, 20-24 August 1979, Boulder, Colo., WMO Publ. 549, Spec. Environ. Rep. 14, 103-108.

Hefter, J. L., A. D. Taylor, and G. J. Ferber, 1975. A regional-continental scale transport, diffusion, and deposition model. NOAA Tech. Memo. ERL ARL-50, 29 pp.

Kadowski, S., 1979. Silicon and aluminum in urban aerosols from characterization of atmospheric soil particles in the Nagoya area. Environ. Sci. and Technol. 13:1130-1133.

Komhyr, W. D., 1980. Dobson spectrophotometer systematic total ozone measurement error. Geophys. Res. Lett. 7(2):161-163.

Komhyr, W. D., and R. D. Evans, 1980. Dobson spectrophotometer total ozone measurement errors caused by interfering absorbing species in polluted air, such as SO_2, NO_2, and photochemically produced O_3. Geophys. Res. Lett. 7(2):157-160.

Komhyr, W. D., and T. B. Harris, 1976. Measurement of atmospheric CO_2 at the U.S.A. GMCC baseline stations. Proceedings, WMO Air Pollution Measurement Techniques Conference, 11-15 October 1976, Gothenburg, Sweden, WMO Publ. 460, Spec. Environ. Rep. 10, 9-19.

Komhyr, W. D., W. R. Taylor, and T. B. Harris, 1979. A semi-automatic flask sample CO_2 analyzer. Proceedings, WMO Technical Conference on Regional and Global Observations of Atmospheric Pollution Relative to Climate, 20-24 August 1979, Boulder, Colo., WMO Publ. 549, Spec. Environ. Rep. 14, 67-71.

Komhyr, W. D., T. M. Thompson, and E. G. Dutton, 1980. Chlorofluorocarbon-11, -12, and nitrous oxide measurements at the U.S. GMCC baseline stations (16 September 1973 to 31 December 1979). Submitted for consideration as a NOAA Tech. Rep.

Kowalczyk, G. S., C. E. Choquette, and G. E. Gordon, 1978. Chemical element balances and identification of air pollution sources in Washington, D. C. Atmos. Environ. 12:1143-1153.

Lockhart, L. B., Jr., 1962. Natural radioactive isotopes in the atmosphere at Kodiak and Wales, Alaska. Tellus 14:350-355.

Maenhaut, W., W. H. Zoller, R. A. Duce, and J. L. Hoffman, 1979. Concentration and size distribution of particulate trace elements in the south polar atmosphere. J. Geophys. Res. 84:2421-2431.

Mateer, C. L., and H. U. Dütsch, 1964. Uniform evaluation of Umkehr observations from the world ozone network. Part I: Proposed standard Umkehr evaluation technique. National Center for Atmospheric Research, Boulder, Colo., 105 pp.

Mateer, C. L., J. J. DeLuisi, and C. C. Porko, 1980. On the development of the short Umkehr method for estimating the vertical distribution of ozone. Proceedings, WMO Technical Conference on Regional and Global Observations of Atmospheric Pollution Relative to Climate, 20-24 August 1979, Boulder, Colo., WMO Publ. 549, Spec. Environ. Rep. 14, 23-28.

Mendonca, B. G. (ed.), 1979. Geophysical Monitoring for Climatic Change No. 7, Summary Report 1978. NOAA/ARL, Boulder, Colo., 131 pp.

Mendonca, B. G., J. J. DeLuisi, and K. J. Hanson, 1978. Volcanically related secular trends in atmospheric transmission at Mauna Loa Observatory, Hawaii. Science 202:513-515.

Mitchell, M., 1956. Visual range in the polar regions with particular reference to the Alaskan Arctic. J. Atmos. Terr. Phys. (Special Suppl.), p. 195.

Murphy, M. E., and B. A. Bodhaine, 1980. The South Pole automatic condensation nuclei counter: Instrument details and five years of observations. NOAA Tech. Memo. ERL ARL-82, 91 pp.

Ottar, B., et al., 1980. The transfer of airborne pollutants to the Arctic region. Atmos. Environ. (accepted for publication).

Parungo, F., B. A. Bodhaine, and J. Bortniak, 1981. Analysis of the winter Antarctic aerosol. Atmos. Environ. (submitted for review).

Pearman, G. I., 1977. Further studies of the comparability of baseline atmospheric carbon dioxide measurements. Tellus 29:171-181.

Pearson, E. S., and H. O. Hartley, 1966. Biometrika Tables for Statisticians. Cambridge Univ. Press, Cambridge, England, 519 pp.

Peterson, J. T., E. C. Flowers, G. J. Berri, C. L. Reynolds, and J. H. Rudisill, 1981. Atmospheric turbidity over central North Carolina. J. Appl. Meteorol. (in press).

Peterson, J. T., K. J. Hanson, B. A. Bodhaine, and S. J. Oltmans, 1980. Dependence of CO_2, aerosol, and ozone concentrations on wind direction at Barrow, Alaska, during winter. Geophys. Res. Lett. 7:349-352.

Pollok, L. W., and A. L. Metnieks, 1960. Intrinsic calibration of the photoelectric nucleus counter, model 1957, with convergent light beam. Tech. Note 9, Contract AF61, (052)-26, School of Cosmic Physics, Dublin Institute for Advanced Studies, Dublin, Ireland, 62 pp.

Rahn, K. A., and R. J. McCaffrey, 1980a. Long-range transport of pollution aerosol to the Arctic: A problem without borders. Proceedings, WMO Symposium on Long-Range Transport of Pollutants and its Relation to General Circulation, Including Stratospheric/Tropospheric Exchange Processes, 1-5 October 1979, Sofia, Bulgaria, WMO Publ. 538, 25-35.

Rahn, K. A., and R. J. McCaffrey, 1980b. On the origin and transport of the winter Arctic aerosol. Ann. New York Acad. Sci. 338:486-503.

Rosen, H., A. D. A. Hansen, R. L. Dod, and T. Novakov, 1978. Identification of the optically absorbing component in urban aerosols. Appl. Opt. 17:3859.

Shaw, G. E., and K. Stamnes, 1980. Artic haze: Perturbations of the polar radiation budget. Proceedings, Conference on Aerosols: Anthropogenic and Natural--Sources and Transport, 9-12 January 1979, N. Y. Acad. Sci., New York (in press).

Waggoner, A. P., and R. E. Weiss, 1980. Comparison of fine particle mass concentration and light scattering extinction in ambient aerosol. Atmos. Environ. 14:623-626.

Winters, W., S. Barnard, and A. Hogan, 1977. A portable photo recording Aitken counter. J. Appl. Meteorol. 16:992-996.

Yamamoto, G., M. Tanaka, and K. Arao, 1968. Hemispherical distribution of turbidity coefficient as estiamted from direct solar radiation measurements. J. Meteorol. Soc. Japan 46(4):278-300.

Zoller, W. H., W. C. Cunningham, and R. A. Duce, 1979. Trends in the composition of atmospheric aerosols from South Pole Station Antarctica. Proceedings, WMO Technical Conference on Regional and Global Observations of Atmospheric Pollution Relative to Climate, 20-24 August 1979, Boulder, Colo., WMO Publ. 549, Spec. Environ. Rep. 14, 245-250.

9. GMCC STAFF

Director's Office

*Kirby J. Hanson, Director
*Bernard G. Mendonca, Deputy Director
Helen Cook, Secretary
Gail M. Phillips, Secretary
*Dale A. Gillette, CIRES
John E. Hay, CIRES
Bill Hiscox, Lt. (jg) NOAA Corps
Jerome K. Nimira, CIRES
*John Osborn, Lt. NOAA Corps
Graeme I. Pearman, CIRES
Constance Shilvock, Jr. Fellow

Acquisition and Data Management Group

*Gary A. Herbert, Chief
Connie Carla, Secretary
*Joyce M. Harris, Computer Programmer
Lee Johnson, Computer Programmer
Milton S. Johnson, Electronic Technician
James Jordan, Electronic Engineer
Steven Waas, Jr. Fellow

Monitoring Trace Gases Group

*Walter D. Komhyr, Chief
Connie Carla, Secretary
Patricia Angel, Clerk Typist
*Robert D. Grass, Physicist
*Thomas B. Harris, Meteorological Technician
*Samuel Oltmans, Physicist
Frank Polacek III, Meteorological Technician
*Lee Waterman, Chemist
*Ellsworth Dutton, CIRES
Robert Evans, CIRES
Kent Leonard, CIRES
*William Taylor, CIRES

Aerosols and Radiation Monitoring Group

*John J. DeLuisi, Chief
Gail Phillips, Secretary
Bonnie Hill, Secretary
*Barry A. Bodhaine, Meteorologist
Richard Cram, Meteorologist
*Ronald W. Fegley, Physicist

Analysis and Interpretation Group

*James T. Peterson, Chief
Gail Phillips, Secretary
Bonnie Hill, Secretary
Douglas V. Hoyt, Physicist
Cheryl Reynolds, Jr. Fellow
Thomas Stoffel, CIRES
Thayne Thompson, Physicist

Mauna Loa Observatory

*Kinsell L. Coulson, Director
Judith B. Pereira, Secretary
*John F. S. Chin, Physicist
*Howard Ellis, Physicist
Mamoru Shibata, Electronic Technician
*Alan M. Yoshinaga, Analytical Chemist

Barrow Observatory

*Thomas DeFoor, Lt. NOAA Corps, Station Chief
*Dave Smith, Physical Scientist
Bradley C. Halter, Electronic Technician
Robert Hanby, Electronic Technician

Samoa Observatory

*Donald W. Nelson, Station Chief
Roger A. C. Williams, Electronic Technician

South Pole Observatory

*John Bortniak, Lt. (jg) NOAA Corps, Station Chief
Charles Smythe, Electronic Technician

---

*Contributors to Summary Report

☆ U. S. GOVERNMENT PRINTING OFFICE 1980 - 777-002/1236 Reg. 8